Laboratoire de Mécanique, Matériaux et Structure

Laboratory of Mechanics, Materials and Structure

NONLINEAR DYNAMICS AND SPATIAL NONHOMOGENEITY IN ENTOMOPATHOGENIC FUNGI GROWTH ON INSECT PEST

A Thesis submitted in partial fulfillment of the requirements for the degree of Doctor of Philosophy (PhD) in Physics,

Specialty: Fundamental Mechanics and Complex Systems

By

DJOUDA SONKOUE Byliole

Registration number: 11W0174

Master of Science in Physics

Under the supervision of

TCHAWOUA Clément

Professor

University of Yaoundé 1
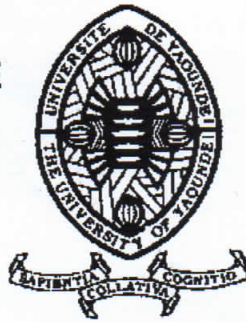
MOUKAM KAKMENI François Marie

Professor

University of Buéa

©Year 2022

ATTESTATION DE CORRECTION DE LA THÈSE DE DOCTORAT/Ph.D

Nous, Professeur **SIEWE SIEWE Martin** et Professeur **WOAFO Paul**, respectivement Examinateur et Président du jury de soutenance de la Thèse de Doctorat/PhD de Madame **DJOUDA SONKOUE Byliole**, Matricule **11W0174**, préparée sous la direction des Professeurs **MOUKAM KAKMENI François Marie** (Université de Buéa) et **TCHAWOUA Clément** (Université de Yaoundé 1), intitulée : « **NONLINEAR DYNAMICS AND SPATIAL NON HOMOGENEITY IN ENTOMOPATHOGENIC FUNGI GROWTH ON INSECTS' PEST**», soutenue le Jeudi, **05 Mai 2022, en vue de** l'obtention du grade de Docteur/PhD en Physique, Spécialité **Mécanique, Matériaux et Structures**, option **Mécanique Fondamentale et Systèmes Complexes** attestons que toutes les corrections demandées par le jury de soutenance ont été effectuées.

En foi de quoi, la présente attestation lui est délivrée pour servir et valoir ce que de droit.

Fait à Yaoundé, le **3 0 MAI 2022**

Examinateur   Le Président du jury   Le Chef de Département de Physique

Pr SIEWE SIEWE Martin   Pr WOAFO Paul   Pr NDJAKA Jean-Marie

University of Yaoundé I

Faculty of Sciences

Department of Physics

NONLINEAR DYNAMICS AND SPATIAL NON HOMOGENEITY IN ENTOMOPATHOGENIC FUNGI GROWTH ON INSECTS' PEST

Submitted in Fulfillment of the Requirements for the Degree of Doctor of Philosophy/PhD in Physics
Option: Fundamental Mechanics and Complex Systems

By

Djouda Sonkoué Byliole
Registration number: 11W0174
Master in Physics

Director

Pr. Moukam Kakmeni François Marie

Professor, University of Buéa (Cameroon)

Supervisor

Pr. Clément Tchawoua

Professor, University of Yaoundé I (Cameroon)

Laboratory of mechanics, Materials and Structures

Dedications

I dedicate this thesis to:

- My father, who was a great support of me.

- My Lovely family: My husband NOUME NZONTCHA and my son NOUME DJOUDA.

- My siblings, and my mother Odette DJOUDA.

For their unconditional love, encouragement, support and prayers.

Acknowledgements

First and foremost I thank God for giving me this wonderful opportunity to do a PhD. I owe a lot to him who controls everything and I say thank you God.

Secondly, the accomplishment of this thesis would not be possible without the assistance and the help of numerous individuals and institutions.

A particular acknowledgement is addressed to my supervisor, Professor TCHAWOUA Clément of the University of Yaoundé I. His goodwill toward me since my master thesis beyond purely academic matters is deeply appreciated. I consider him not only as a supervisor, but also as a father who is always available to provide me guidance and to share experience in many aspects of life.

I am indebted to my main supervisor Professor MOUKAM KAKMENI François Marie of the University of Buéa for his support and guidance throughout the conduct of this study since my Master degree. Working with him has allowed me to grow as a researcher and to explore my potential as a graduate student. I am grateful for his tireless dedication, encouragements and help on every aspect of this work along the way.

I would like to thank the hole Department of Physics at the Faculty of Science at the University of Yaoundé I.

I would like also to acknowledge Doctor TONNANG ZEFACK Henri Edouard. He has been as a mentor who taught me ecological modeling. My vision of the field has been deeply shaped through our interactions.

I express my deepest gratitude to Doctor Frank NDJOMATCHOUA of the (IRRI), for his contribution into this work. He had also helped me to understand the entomology and some biological aspects of this thesis related to insect pests and Biological control.

I also thank Professor CHEMBO Yanne (CNRS Research Scientist) and Professor WOAFO Paul (University of Yaoundé I) for their valuable contribution to this work.

I acknowledge in advance the scientists for accepting to examine this thesis, the President of Jury Professor WOAFO Paul and others members of jury:Professor SIEWE SIEWE Martin and Professor DJUIDJE KENMOE Germaine at the University of Yaoundé I, and Professor YAMAPI Réné at the University of Douala.

I am very grateful for the scholarship provided by the Volkswagen Foundation under the scame Funding Initiative Knowledge for Tomorrow-Cooperative Research Projects in Sub- Saharan on Resources, their Dynamics, and Sustainability-Capacity Development in Comparative and Integrated Approaches ($Project number : VW - 89362 and 94362$).

I cannot end without appreciating the encouragement and the various help from all my friends and fellow course mates that I encountered throughout this thesis.

ii

My deep gratitude is also addressed to my family and my in-law for the encouragement and financial support.

List of Abbreviations

EPF: EntomoPathogenic Fungi
BC :   Biological Control
PLM :   Population Level Model
RDM :   Reaction- Diffusion Model
IPM :   Integrated Pest Management
RK4 :   Fourth-order Runge-Kutta
SA :   Sensitivity Analysis
MC :   Monte- Carlo Method
LHS :   Latin Hypercube Sampling
PRCC :   Partial Rank Correlation Coefficient
PCC :   Partial Correlation Coefficient
CC Pearson :   **Pearson** Correlation Coefficient
CC spearman or RCC :   **spearman** Correlation or **R**ank Correlation Coefficient
CC :   Correlation Coefficient
PGF :   Probability Generating Functions
Pdfs :   Probability density Functions
PSD :   Power Spectrum density
mCGL :   modified Complex Ginzburg-Landau
MI :   Modulational Instability
FORTRAN :   FORmula TRANslation
MATLAB :   MATrix LABoratory

Contents

List of Figures

Abstract

Biological control is the beneficial application of natural enemies such as pathogens, predators and parasites in managing insects pests and their damage. Entomopathogenic fungi (EPF) have a crucial role in natural ecosystems and have been developed as an environmentally friendly alternative to the use and application of chemical insecticides against insect pests. However, the dynamics of the entomopathogenic fungi within the insect host is still not well understood; due to the complexity behind the interaction between EPF, insects and their living environment which is really fluctuating.

To study the dynamics of this system, we subdivided our work in three main points: in the first point host pathogen model is using to describe the intra-host dynamics of entomopathogenic fungi growth inside its host. The model is coupled with a nonlinear dependence of the consumption of insect resources by the host, described by the Holling and Powell type II functional responses. In the second point, a stochastic demography model (often called individual based model) defining as a random variation originating from the discrete nature of individuals is proposed to mimic the outbreak of EPF within insect's pests population; the model includes stochastic character of events like birth, death, infection and migration. Finally, the modified complex Ginzburg Landau equation (mGLCE) is used to model and to investigate the horizontal transmission between infectious insects and susceptible one. These studies show that the behavior of such system is rich in dynamics. Because the EPF growth is related to the instability of the system, particular attention is given to the stability analysis in this study.

In the first part, the stability of system around the steady states is conducted without taking the diffusion into account. When considering a small perturbation of the stable singular point due to nonlinear diffusion, the conditions for Turing instability occurrence are deduced. It is observed that the absence of the regeneration feature of insect resources prevents the occurrence of such phenomena. The long time evolution of our system enables us to observe both spot and stripe patterns. Moreover, when the diffusion of mycelia is slightly modulated by a weak periodic perturbation, the Floquet theory and numerical simulations allow us to derive the conditions in which diffusion driven instabilities can occur.

In the second part of our study, the stability analysis shows that the system dynamics is strongly affected by the contagion rate between infectious insects and the susceptible hosts, where as the bifurcation analysis lead to a transcritical bifurcation when the basic reproduction number is greater than one in local dynamics. When migrations

of species are considered, Hopf-damped Turing behavior can occur for a threshold contagion rate. However, sensitivity analysis of the extinction probability shows that the persistence of EPF depends to the proportion of spores collected from insect cadavers as well as their ability to be reactivated and create new infect insects.

Lastly, the Anderson-may model is modified by taking in account the migration of infectious host. The model is transformed to a modified complex Ginzburg Landau equation (mGCLE) using the multiple scale method. The effect of environmental conditionS is modeled in the infectious rate and the modulation instability (MI)of the wave plane is investigated. The linear stability analysis allows observing two types of modulation instabilities: Diffusion-driven instability or Turing instability and Parametric instability observed when environmental condition influence the infection rate. The Floquet theory used in the latter case shown parametric resonance via the exhibition of Arnold tongues. However, the increase of the proportion of insect which pass from latent to infectious class increases the gain of the nonlinear instability and induced irregular behavior of MI in the case of constant and periodic infection.

Keywords: Entomopathogenic fungi (EPF), Biological Control (BC), insect pests, individual-based models (IBM), demographic stochasticity, bifurcation analysis,mean field theory, multiple scale method, modified complex Ginzburg-landau equation, modulation instability, Floquet theory, Turing Pattern, parametric resonance.

Résumé

La lutte biologique est l'application bénéfique d'ennemis naturels tels que les agents pathogènes, les prédateurs et les parasites dans la gestion des insectes ravageurs de culture et leurs degâts. Les champignons entomopathogènes (EPF) jouent un rôle crucial dans les écosystèmes naturels et ont été développés comme une alternative écologique à l'utilisation et à l'application d'insecticides chimiques contre les insectes nuisibles. Cependant, la dynamique des champignons entomopathogènes au sein de l'insecte hôte et de la population d'insecte n'est pas encore bien comprise; dû à la complexité des interactions entre les EPF, les insectes et leur habitat qui est très influencé par les conditions environmentales fluctuantes.

Pour mener à bien l'étude de la dynamique de ce système, nous avons segmentés ce travail en trois pticipaux points: Au premier point nous utilisons un modèle d'hôte pathogène couplé pour etudier la dynamique intra-hôte du champignon entomopathogènes. Le model est couplée avec une dépen-dance non-linéaire de la consommation des ressources de l'insecte par l'hôte, décrite par les réponses fonctionnelles de Holling et Powell de type II. Au second point, nous developons un model individuel qui prend en compte la stochasticité démographique (souvent appelée bruit démographique) pour mimer l'évolution du champignons entomopathogènes au sein d'une population d'insectes nusibles; ce modèle définit comme une variation aléatoire provenant de la nature discrète des individus et du caractère stochastique d'événements tels que la naissance, la mort, l'infection et la migration. Enfin, l'équation complexe de Ginzburg Landau modifiée est utilisée pour modeliser et analyser la transmission horizontal de l'infection fongique d'un insecte infecté à un insecte susceptible. L étude de ces systèmes montre qu'ils exhibent une dynamique riche. Etant donné que la croissance de l'EPF est liée à l'instabilité du système, une attention particulière est accordée à l'analyse de la stabilité le long de cette étude.

La première partie de ce travail porte sur l' étudié de la stabilité de l'état d'équilibre sans tenir compte de la diffusion. En considérant une petite perturbation du point singulier stable, les conditions d'apparition de l'instabilité de Turing qui ici, provient du terme de diffusion non-linéaire ont été déduites. Il est observé que l'absence de la régénération des ressources chez l'insecte empêche l'apparition de tels phénomènes. Une simulation de ce système au déla du temps transistoire montre différent formes de motifs (circulaires et en bandes). De plus, lorsque la diffusion du mycélium est légèrement modulée par une faible perturbation périodique, la théorie de Floquet et

les simulations numériques nous permettent de déduire les conditions pour lesquelles l'instabilité dû à la diffusion se produit.

Dans la deuxième partie de notre étude, l'analyse de stabilité du système en absence des termes de diffusion montrent que la dynamique du système est fortement influencée par le taux de contagion des insectes susceptibles par des insectes infectés, tandis que l'analyse de la bifurcation prevoit la bifurcation transcitique lorsque le nombre d'infections secondaires dû à une première infection est supérieure à 1 . Lorsque l'on considère la migration de chaque espèce dans un ensemble de sites, les modes de Hopf-Turing amortis peuvent apparaître pour un seuil de valeur du taux de contagion. Cependant, l'analyse de sensibilité de la probabilité d'extinction montre que la persistance d'un agent de lutte biologique dépend de la proportion de spores collectées sur les cadavres d'insectes ainsi que de leur capacité à être réactivés et crée de nouvelles infections.

Dans la dernière partie de ce travail, le modèle Anderson-May est modifié en tenant compte de la migration de l'hôte infectieux, puis transformé en une équation modifiée de Ginzburg - Landau complexe en utilisant la méthode des echelles à temps multiples. L'effet des conditions environnementales est consideré sur le taux d'infection et par la suite, une analyse de l'instabilité de modulation (MI) de l'onde plane est menée. L' analyse de la stabilité linéaire permet d'observer deux types d'instabilités de modulation: L'instabilité due à la diffusion ou l'instabilité de Turing et l'instabilité paramétrique observée lorsque les conditions environnementales influencent le taux d'infection. La théorie de Floquet prévoit une résonance paramétrique via l'apparution des langues d'Arnold. L'augmentation de la proportion d'insectes qui passent de la classe latente à la classe infectieuse augmente le gain de l'instabilité non-linéaire et induit une dynamique irrégulière de l'IM.

Mots clés: Champignons entomopathogènes (EPF), lutte biologique (BC), insectes nuisibles, modèles individuelles (IBM), stochasticité démographique, théorie des champs moyens, analyse de la bifurcation, méthode d'expansion à échelle multiple, équation de Ginzburg-Landau complexe modifiée, instabilité de modulation, théorie de Floquet, instabilité de Turing, instabilité paramétrique.

General Introduction

With a rapidly expanding population, there is growing demand for food and simultaneous need for higher environmental sustainability[7]. However, agricultural production is facing several problems including the difficulty of controlling planting times due to climate change, poor seed quality, poor soil quality, crop pests and so on. [8, 9, 10, 11, 12]. Insect pests are responsible for a loss of 18–26% of worldwide annual crop production, which corresponds to an estimated value of 470 Dollars billion [13]. The greatest part of the losses (13–16%) occurs in the field, before harvest [13]. Furthermore, post-harvest pests constitute a major part of storage losses of agricultural products. About 50–60% of stored grains can be lost during the storage period due to insufficient control measures [14]. The intense use of chemicals has led to more than 500 species of arthropod pests becoming resistant to one or more insecticide classes [14]. Additionally, environmental and food regulations represent a barrier for the development of new insecticides, in terms of both time and cost.

Crop protection by agrochemicals has been responsible for maintaining and increasing the quality and quantity of crop production worldwide. However, their extensive and often irresponsible use has resulted in pest resistance, resurgence of secondary pests and a disruption or elimination of natural enemy complexes, thus reducing the efficacy of natural control processes. These factors, coupled with concerns about the impact on environment and human safety, have provided the momentum to develop more environmentally safe strategies that are both cost-effective and reliable.

Assistance to realize this goal may, unexpectedly for many, come from biological control of insect's pests in agriculture. Empirical data suggest the utilization of bio control agents in integrated pest management (IPM) can foster sustainable yields in agricultural systems at lower costs than alternative non-sustainable methods based on chemical pesticides [7], which can result in the build up of persistent chemicals in the

environment or development of pesticide resistance. It is hoped that through a combination of theoretical and empirical studies. Biological control may provide an economically sustainable solution to pest control.

Despite the development of many mathematical models that have examined the use of microorganisms as control agents. The role of entomopathogenic fungi has not been investigated fully [15]. It surprising as these EPF have great potential as biological controls agent of insects pest [15]. The aims of this thesis are then to develop mathematical models describing the EPF-host system in order to optimize their use as bio control agents.

The present thesis is structured in three parts described as follows:

In the first chapter, we conducted a review of the scientific literature around the theme of this thesis. We begin by presenting the infectious cycle of entomopathogenic fungi, the different challenges faced by EPF by infecting it host. The chapter presents subsequently the biology and ecology of the entomopathogenic fungi, a brief outlook on insect pests and the impact of their damage in the field as well as the scientific problems related to the study of this biological control agent. Furthermore, different methods and concepts of modelling used in the literature to simulate the growth of entomopathogenic fungi insight insect pests as well as their inadequacies are presented. Finally, methods for coupling the spread, conidia dynamics and insect's dynamics adopted in the past are presented.

In Chapter 2, this thesis presents the approaches used to solve the problems mentioned in Chapter 1 and how they will be used in order to obtain the results. A reaction diffusion system with a cross-diffusion term in the resource consumption has employed to describe the intra-host (insect pests)-pathogen (entomopathogenic fungi (EPF)) interactions. Assuming that the diffusion rate of mycelia depends on the diffusion rate of the insect resource and time, the interaction between the resources from the insect pest and the mycelia of EPF is represented by the Holling and Powell type II functional responses. The stability analysis and Floquet theory were used respectively to generate the spatially localized Turing modes and to study the effect of temperature on the EPF growth and spread using a reaction-diffusion model(RDM). In order to study the propa-

gation and the persistence of EPF within insect's host population, this chapter continues with the presentation of advanced methods that are used to investigate epidemiological model. The first sequence of analyzes consists of the construction of the mathematical models (Individual based model (IBM) and it corresponding deterministic model called Population level model (PLM)), the IBM which is inherently stochastic, is formulated as a continuous time Markov's process, which is then, decomposed into a deterministic dynamics using stochastic corrections and system size expansion. In order to evaluate the temporal evolution and the spatial distributions of the global systems (insect susceptible to be infected, infected insects and spores collected on insects cadavers), and deduce the mechanisms behind its dynamics; we compare both obtained models and to better understand the interplay between deterministic and stochastic forces. The Latin hypercube sampling (LHS) on combination with a partial rank correlation coefficient (PRCC) is used to find the keys parameters for successful outbreak of EPF with insect pests population. We finally, estimate the power spectral density (PSD) which describes the stochastic fluctuations affecting each systems variable. The last part of this chapter, focus on the transmission of the EPF disease between insects. Since EPF undergo latent period within insect before beginning to produce infectious conidium (transmission stage), we choose the susceptible, infected and infectious Anderson-May's model and then modified by incorporating one dimensional spatial diffusion. Reaction-Diffusion model is known to exhibit traveling wave behavior [16]. That means the disease outbreak within insect population involve like wave across the field. The well know model describing the evolution of the modulated wave is the Complex Ginzburg-Landau (CGL) equation, which is well applied in the biological system [17, 18, 19]. We used the multiple scale method to transform the reaction-diffusion model to a modified Complex Ginzburg-Landau (mCGL) equation. By taking into account the periodic modulation on the infection rate due to the abiotic conditions, we investigate the modulational instability. The modulational instability is a ubiquitous phenomenon causing by the interplay between complex nonlinear process. From a mathematical point of view, the underlying phenomenon refers also to the mechanism where a weak periodic perturbations of an continuous wave (CW) grow exponentially [20, 21, 22, 23]

The Chapter 3 is devoted to the presentation of the key obtained results and their discussions.

The document ends up by a general conclusion summarizing the main findings add, provides the futures directions.

LITERATURE REVIEW AND BIOLOGICAL BACKGROUND

I.1 Introduction

This chapter presents a brief overview on the biological systems and physical phenomena studied in this thesis. It is organized as follows: section I.2 deals with the overview on Entomopathogenic fungi (EPF), section I.4 is devoted to the advantages and disadvantages of the use of EPF as biological control agents, in section I.5 the overview on modelling EPF growth on insect pest is presented. Followed by a brief description of key existing models investigating the Entomopathogenic fungi dynamics. The motivation of this research is given in Section I.7 and the last section concludes this chapter.

I.2 Overview on Biological control: case of Entomopathogenic fungi (EPF)

I.2.1 Generalities on insects pests and their damage

An arthropod pest is any species of arthropod that can be considered harmful to humans, by being a pest of plants, plant products or animals [10]. Insects attacking crops has been a problem since agriculture began. Crop pests can damage the plant above or below the ground, through chewing, sucking, tunnelling, causing galls, removing parts of the plant or by increasing the susceptibility to viral, bacterial or fungal pathogens [24]. These insects are then cause significant damages during their immature and mature life stages. Young larvae of some species climb plants and feed mainly on leaves, while older larvae eat into the stems and often sever them. In fields with small hills or knolls, damage may first appear in the highest areas of the field. Others inflict their damage on stored products mainly by direct feeding, causing loss of weight and

quality [8, 9, 11, 12]. To keep damage low, fields should be examined regularly and applied the controls when insect populations reach economic threshold levels. As mentioned above, crop devastators are responsible for an average of 20 Percent of lost in agriculture [13], adding to the part losses during harvest. Furthermore, post-harvest pests constitute a major part of storage losses of agricultural products. About 50–60% of stored grains can be lost during the storage period due to insufficient control measures [14]. Therefore, it becomes necessary to set up appropriate pest management programs to control these insect pest populations. The harmfulness of chemical insecticides to humans and to the environment has motivated the development of biological mechanisms with pathogenic organisms that only target the insect [25].

I.2.2 Generalities on EPF

Entomopathogenic fungi (EPF) have a key role in natural ecosystems and are being developed as environmentally friendly alternatives to chemical insecticides for pests control [4]. They causes many insect diseases and play important roles by regulating insect populations in nature [25]. Those belonging to the Beauveria and Metarhizium have been widely used for the control of various agricultural insect pests and vectors of human diseases [26]. More than 700 species of fungi are entomopathogenic, making them the most common insect pathogen [27, 28]. EPF are found in the divisions Zygomycota, Ascomycota, Deuteromycota, Chytridiomycota and Oomycota [27]. Some of these fungi have a restricted host range while others have a wide host range with different isolates being more specific to certain pests [27, 29]. Species and even isolates within a species can act very differently in terms of their host range, infectivity, rate of germination and optimum temperature [25, 30]. They have large potential as biopesticides unlike bacteria and viruses they infect hosts through direct penetration of the cuticle, allowing them to act as contact insecticides [4]. EPF possesses the ability to infect the host by ingestion or by simple contact, therefore making insects vulnerable at any of their life stages [27, 28]. The penetration process is the most important step in pathogenesis [31]. In contact with the insect's cuticle, conidia (the infectious fungus unit) germinates if conditions of temperature and humidity are favorable (high humidity) [32], and penetrates through the integument of the insect by combining mechanical and enzymatic pressures [25, 33]. After penetration, it proliferates as hyphae (branching filamentous cell of a fungus collectively called "mycelium") into the insect hemocoel, absorb nutrients, produce toxins, destroy host cells, and eventually kill the insect; and

produce new infective spores, which are ejected toward the insect cuticle for immediate transmission if the environmental conditions are favorable. These infectious spores are subsequently dispersed in the environment by natural phenomena such as wind and rain, which then favor their propagation to susceptible insects. In addition, this infection can be transmitted by a simple contact between infected and susceptible insects [3, 9, 29, 32] . However, the efficiency of this method is good when the densities of the targeted insect populations are very high, thus enhancing contamination by abundant production and dissemination of spores in the saprophyte phase. The insect immune system, the lack of recognition between the host and the pathogen, and the inability of the spores to exploit resources from the insect cuticle can strongly influence the pathogenicity of these natural enemies [33, 34]. To the best of our knowledge, the change of morphology and components can reveal the connection between spores and mycelia (group of hyphae), and provide a systems-level understanding of the cell. Despite its importance, only a limited number of methodologies have been developed for morphology and species analysis [4].

I.2.3   Infection life cycle and morphology of entomopathogenic fungi

Infection process

Entomopathogenic fungi have a complex life cycle. The later can be divided in two main parts (see Fig.1): a parasitic cycle where fungi growth on insect and use the insect body resource, this part start from the attached on insect cuticle to the insect death or for some species to the maturation of mycelia (agglomeration of hyphae body) and the saprophytic cycle which corresponds to the sporulation after insect death (for some species since insects are infected, in that specific case the resource extracted is under the harmful threshold) [1]. However, for a successful infection, the fungi have to meet several host challenges in order to produce enough new infectious spores. Firstly, successful transmission often requires the release of massive spore numbers and/or sticky spore surfaces or substances that maximize adhesion in other ways [27]. Secondly, spores should germinate and initiate penetration of the solid insect exoskeleton relatively quickly or survive digestion after oral uptake[35]. Third, fungal cells must proliferate within the hemocoel, muscles, or other tissues of the host's body to collapse the host's immune system so that its subsequently dies [35]. Fourth, the fungal pathogen should manage the host (or cadaver) to optimize spore production and dispersal under prevailing environmental conditions [3]. Thus, entomopathogenic fungi display several steps in the development of fungal infections.
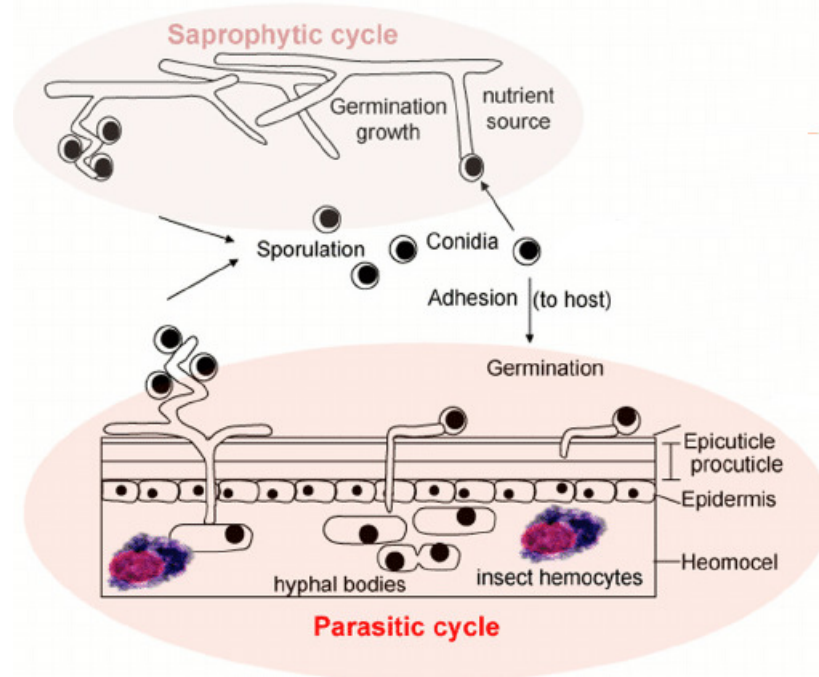
Figure 1: life cycle of Entomopathogenic fungi, illustrating the saprophytic and parasitic cycles [1, 2]

- Spore attachment to the host cuticle

    Pathogenicity starts with the attachment of the spore to the host (Fig.2(1a)) [3]. Although some entomopathogenic fungi enter the gut or respiratory tract, the majority invade their host through the external cuticle [25, 36]. The spore attachment process has two stages, the initial absorption of the conidia to the cuticle surface by passive interactions involving charged groups on both surfaces, followed by more specific attachment involving a short-range stereo chemical interaction [27]. The process of adhesion appears to be strengthened after germination with the production of more mucoid substances, presumably secreted by the appressoria cells [27].

- Spore germination

    The conditions on the cuticle surface determine whether or not germination will occur. Some researchers reported that spore germination (see fig.2(1b)) is mostly dependent on the environmental conditions, especially temperature and humidity [35, 37]. Fungal spores require saturating humidity for germ tube development and its germination also dependents on exogenous nutrients [28], which are obtained from cuticle and as a result of the process of penetration [33]. Furthermore successful germination does not always lead to
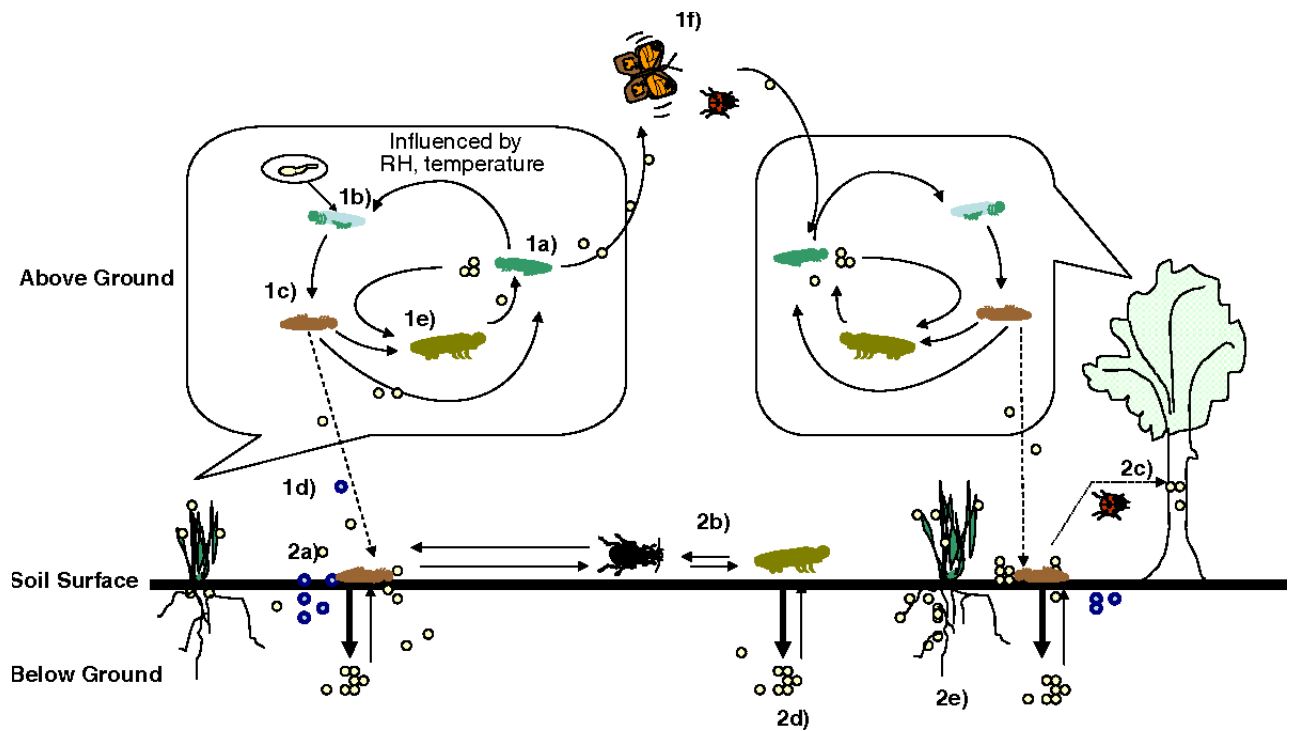
Figure 2: Infection cycle of entomopathogenic fungi [3]. Arrow size indicates the direction of interaction that is likely to be greatest in semi-natural habitats.

infection [25, 33]. EPF use a combination of physical and enzymatic processes to degrade the cuticle and enter the haemocoel, after a period of growth on the host surface, EPF produce appressoria which permanently attaches the EPF to the insect [3]. Appressoria develop penetration plugs which secrete a range of enzymes to facilitate cuticle penetration. Invasion of the host body and hemolymph occurs when the EPF passes through the cuticle via germ tubes, appressoria and penetration plugs; EPF like Beauvaria and Metarhizium secrete a variety of enzymes to aid this invasion [28].

• Penetration of the cuticle

For the infection to be successful, the EPF must penetrate the insect cuticle. Making the penetration of the cuticle (process from Fig.2(1b)) very important for virulence [38]. The insect procuticle consists of chitin fibrils embedded in a protein matrix and penetration appears to involve both mechanical and enzymatic components (which involved in cuticle degradation) [31]. St Leger suggests that many enzymes are important determinants of virulence by enabling the pathogen to exist with the changing metabolic processes associated with the host's disease state [33]. Thus, successful penetration of the cuticle depends on the ability of spore to adhere to the cuticle, to germinate and to penetrate [35]. The cuticle

is divided into three sections: the envelope, underneath the envelope is the epicticle, fol-lowed by the procuticle (Fig.1). The epidermal cells are found at the base of the proticule and hemocoel is underneath the epidermal cells (Fig.1). The way in which EPF penetrate the insect depends also on the properties of the cuticle, such as thickness, sclerotization and the presence of antifungal and nutritional substances. In addition to invading the insect via cuticle areas and intersegmental membranes, fungal entomothogens have been reported to invade insects through sense organs and spirales [39]. In that way, because higher humid-ity is not a problem in digestive tract, spores can germinate rapidly in this environment, although the digestive fluids can destroy them or degrade germination hyphae.

- Growth in the hemocoel and immune response of the host

    Knowledge of the immune response of insects induced by fungal pathogens contributes to the understanding of both insect defenses and the fungal pathogenicity that defeats it. Ultimately uncovering fungal virulence determinants gives rise to opportunities to manip-ulate these virulence factors to improve the success of biocontrol agents [4]. Growth of penetrating EPF through the cuticle appears to vary. In many cases, the first reaction of the insect to the invading fungus is a melanisation of the cuticle (see Fig. 2) [2, 28, 40]. This reaction could be effective against pathogenic organisms, but it appears to occur too late or in insufficient magnitude to stop highly pathogenic fungi [40]. More clearly, the main immune reaction in the host tissue is the cellular encapsulation and phagocytosis of the fungal propagules (see Fig.3), which are immediately melanised upon penetration into the hemocoel [3]. Host defenses also include a phenoloxidase system which deposits oxidized phenols (melanin) and protease inhibitors in the cuticle, and which may restrict pathogen enzyme activity [3]. Many entomopathogenic fungi produce toxins to overcome the im-munodefensive mechanism of the insect [29]. Destruxins, afrapeptins and oosporein are compounds that were isolated and identified from cultures of Beauveria, Fusarium, Go-liocladium, Cordyceps, Entomophthora, Verticillium, Metarhizium and Paecilomyces [28]. Destruxins are the only fungal toxins that have been detected in insects in sufficient quan-tities to cause death [28]. However, after reaching the hemocoel, EPF develop it vegetative form (commonly call hyphae) which change to yeast (entomophthorales)[32], and produce blastospores (3), avoid recognition by circulating hemocytes in hemocoel [4]. The advan-tages of this cellular form are probably the increase in nutrient acquisition rates and fungal

cells can mutiply in the hemocoel without being detected by the insect immune system, which uses cell wall as detectors [2, 25].
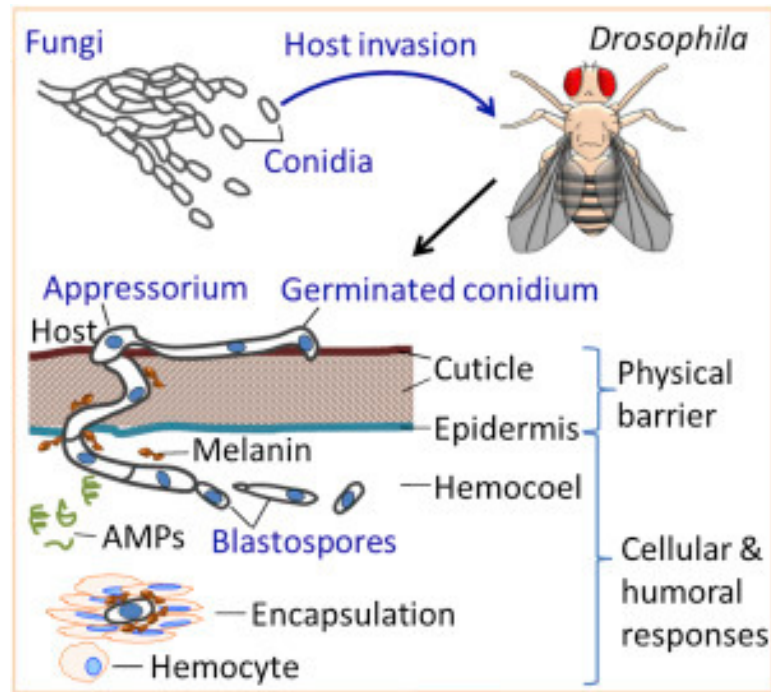
Figure 3: Insect immune system against fungal growth [4].

- Death and saprophytic development

    When the hyphae attempt the insect hemolymph, the next step in the lifecycle is hyphal differentiation into blastospores/hyphal bodies in the hemolymph of the host [3]. EPF's blastospores circulate inside the insect hemolymph producing toxins (see Fig.3) [3]. Growth of EPF within the host hemolymph is linked with secretion of toxins by the fungus. Host colonization is associated with the ability to overcome the host immune defenses and the extraction of nutrients from the host [3, 27, 28]. Furthermore fungi overcome host defenses and extract nutrients from the host body [4]. The insect dies from toxicosis or obstruction of organs. Once the hyphae have exhausted the nutrients available in the host environment they penetrate out to the host cadaver surface (see Fig. 2(1e)) [3]. When temperature and humidity conditions are favorable, the hyphae can cross the integument of the insect again from insight, occuring to the emergence of the fungus towards the outside. Generally, emergence occurs in the less sclerotic regions of the integument: such as the integumental membrane or spiracles depending to the host's stage of development. Hyphae crossing the integument can remain in the vegetative phase and begin the sporulation pro-

cess within $24 - 48h$ [28]. The hyphae from conidiospores, giving rise to asexuel spores that are infective units with dissemination function [27]. Sporulation normally occurs in cadavers but can also occurs in live insects [41]. Conidia dispersal is passive, relying principally on wind but other factors such as rain and interspecific competitions between species, can play a role in dissemination [25, 42].

Morphology of entomopathogenic fungi

Fungal bodies are made up by filaments called hyphae. Hyphae that have walls between the cells are called septate hyphae; hyphae that lack walls and cell membranes between the cells are called nonseptate or coenocytic hyphae (Fig.4). The life cycle of EPF starts with the production of spores which are infectious agents that germinate to form hyphae threads. Given that most of these fungi are sessile, apical extension/growth of the hyphae ultimately results in the formation and growth of the mycelia (hyphae network). Note that mycelia are a collection/bundle of hyphae; they are more visible compared to hyphae that may not be visible. Mycelium (plural mycelia) plays an important role in reproduction, it's corresponds to the vegetative parts of fungi. So after reaching the hemocoel, EPF carry out a dimorphic transition, since they have more than one appearance during their life cycle. This dimorphic character is very important for infectivity. They are capable of changing their appearance in response to environmental changes such as nutrient availability or fluctuations in temperature. This ability helps EPF to survive in diverse environments [9].

I.2.4 Transmission of entomopathogenic fungi between insects and spatially heterogeneous environments

The key parameter that determines the rate of spread of entomopathogenic fungi within host populations is called transmission. It defines the potential of pathogen to be use as a microbial control agent [29]. This process can be view as the dispersal of infective propagules from an infected host to a new host and is the most "perilous" part of the lifecycle of a fungal pathogen [25]. Transmission can occurs in a vertical or a horizontal process. The horizontal transmission is when an infected insect contaminated a susceptible one, here it is important to increase interactions between insects by manipulating the density of the target pests population and thus facilitate the dispersal of conidia. While the vertical transmission refers to the process where an
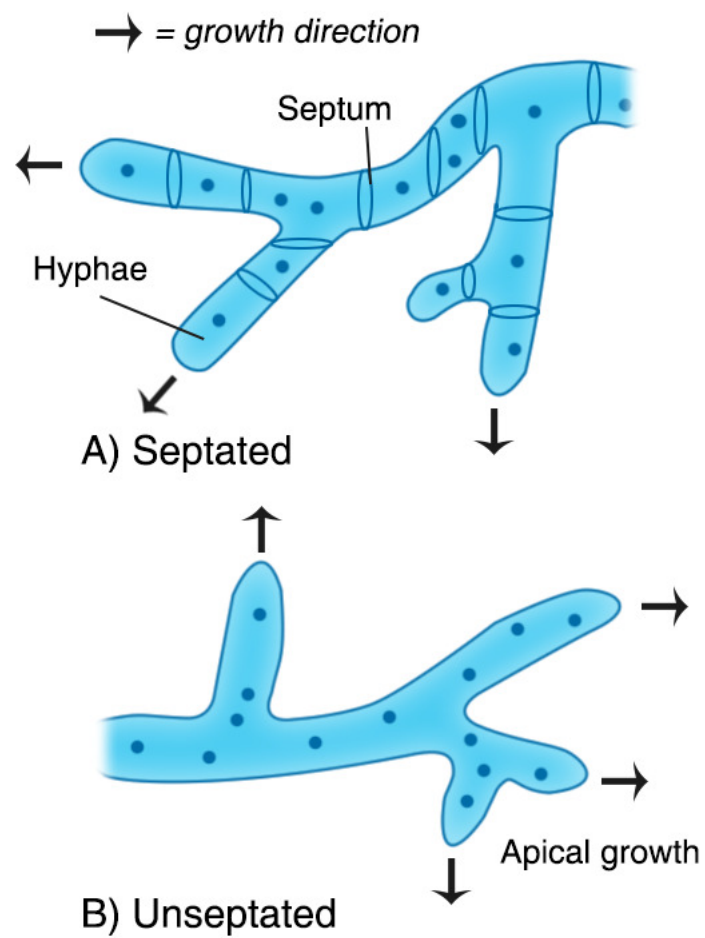
Figure 4: fungal growth within the insect's hemocoel [2].

infected organism contaminates its offspring; In this specific case, some fungi species corrupt their hosts' sexual behaviors to increase their odd of transmissions [28, 29, 43, 44, 45, 46]. Movement of entomopathogenic fungi by host and non-host invertebrates to susceptible hosts is one of the most important mechanisms for transmitting to new habitats [3]. It is noteworthy that, horizontal transmission between individuals of the same species (autodissemination) can occur through direct contact between contaminated and uncontaminated individuals or indirectly via conidia that have been deposited on the substrate [39]. However, direct transmission between infected and susceptible insects is less variable and more efficient than indirect transmission via conidia that have been deposited on the substrate, and can lead to high mortality rates even when the number of contaminated individuals is low. Nevertheless, indirect transmission is important to vector infective stages to new hosts and habitat at the soil surface through epigeal predators which remove inoculum by consoming cadavers [3, 28, 29]. Some researchers proposed patched model based on direct transmission between infected and susceptible hosts [30, 47]. Although, we have explored similar models based on pathogens such as baculoviruses and many fungal entomopathogens which infect by means of free-living infective stages, the conclusions are not qualitatively different. They shown that, EPF-infected hosts have the ability to disperse and to spread disease into new colonies as documented for aphid species [3]. Some specialist fungi such as Strongwellsea spp. Sporulate from one or two holes on living hosts and conidia are dispersed in this way [47].

I.2.5 Factors affecting the efficacy of fungi as bio-control agents

Biotic Factors

1. The Pathogen

   The ability of entomopathogens to infect by producing epizootics on the host is influenced by factors such as pathogen density, host range, genetics, dispersal, latency, virulence and persistence [3, 34, 48]. For the fungus to kill the host, it is presumed that a threshold number of propagules are necessary. High propagule density in the field increases the chances of an insect coming in contact with enough or adequate number of propagules that exceed the inoculum threshold [34]. The ability of EPF species to remain effective for a longer time in an environment increases the probability of an insect coming into contact with propagules to cause disease. Generally, EPF gain entry through penetration of the

host cuticle using a combination of hydrolytic enzymes and mechanical force [27]. After penetration to the hemocoel, the host dies due to a combination of toxin, obstruction of blood circulation, nutrient depletion and invasion of organs [39].

2. The insect host

Most arthropods are hosts of fungi although host spectra vary widely, depending on fungal species. Most studies have shown that B. bassiana and M. anisopliae have much wider host ranges within the Arthropoda [12, 38]. The susceptibility of the insect pest to entomopathogenic fungus is influenced by both physiological and morphological factors [4]. Host population density and distribution, pest population growth characteristics, host behavior and population composition are keys factors. It has also been reported that inadequate nutrition increases the susceptibility of the pest insect to the fungus [1]. Increased host density, increases contact between the infected and uninfected populations hence favors infection and also increases availability of substrate and nutrients for pathogen growth and reproduction. This increases the quantity of inoculum available in the habitat to further cause infection [29]. After the insect pests have been exposed to the fungus, some insects tend to behave differently. For example, flies and locusts elevate body temperatures to a level that is averse to the entomopathogenic fungus in the hemocoel. There is also grooming in termites and summit disease syndrome in grasshoppers [42]. The cuticle of some pests possess physicochemical properties that affect the infection process either negatively or positively. As a defence mechanism, a range of immune responses are initiated once the fungus reaches the hemolymph [4]. However, species M. anisopliae and B. bassiana have shown capability of avoiding encapsulation in the hemocoel [33, 34].

Environmental factors

Environmental conditions are key component influencing the virulence, the persistence in the soil surface or into foliar environments and the outbreak of EPF (Fig.2(2c-2e)).

1. Temperature

Furthermore, the impact of temperature, determined by environmental conditions and insect thermoregulation, is probably the main factor affecting the performance of bio insecticides based on fungal entomopathogens, potentially reducing and/or delaying insect

mortality [30, 49, 50, 51]. Temperature can affect the virulence of entomopathogenic fungi at different phases of the infection process, with inter- and intra-specific variations in thermal requirements mainly related to habitat, geographical origin, and even insect host (see Fig.2 (2a)) [27]. Their hyphal growth and conidial germination under constant and fluctuating temperature regimes, and virulence when insects can thermo regulate remain unknown [52].

2. Relative humidity

This is also an important environmental factor influencing the potential of EPF. This is because moisture stress can limit conidia germination and vegetative growth of the fungus hence reducing the ability of the fungus to penetrate into the host [30, 49]. Many studies showed that daily high humidity is among the most crucial climatic constraints for EPF. Although higher relative humidity (RH) is required for effective colonization, Some of the techniques used to increase the RH are by using an appropriate formulation and application of irrigation water as it improves the microclimate. For example, there was a successful infection in desert locust at $20 - 30\%$ RH under field condition using oil-based conidial formulation [28].

3. Rainfall

Conidia/resting spore distribution and persistence at the soil surface are influenced by abiotic factors such as rainfall that influence horizontal transmission by promoting conidium formation on cadavers, mechanically dispersing conidia and potentially increasing vectoring by other invertebrates (see Fig.2 (2a)). However, There are few studies showing that rainfall affects the persistence of fungus on insects and on foliage, this could be because it is difficult to study rainfall as a single factor due to available interaction from other factors like solar radiation, which also affect the persistence of fungus. Rainfall has positive implications towards fungal epizootics since it can dislodge and disperse conidia from substrates .

I.3 Biological pest control

In nature the majority of living species are attacked by natural enemies such as parasites, predators and pathogens which may regulate their population levels [53]. This is utilised in bio-

logical pest control where the application of natural enemies, or their products, is used to reduce the damage caused by pests to tolerable levels [3]. Biopestides used include microbial pesticides such as bacteria, fungi, viruses and protozoans, entomopathogenic nematodes, carnivorous insects and parasites [42]. Utilizing natural enemies, and their products, for the reduction of crop and plant damage allows maintenance of biodiversity and protection of both farming and human health [10, 42].

I.4   EPF as biological control agents

There are many advantages of using EPF for biological pest control, including their specificity, absence of undesirable effects on food chains and on human health, reduced probability of insects developing resistance and they may persist for long periods in some environments which could provide long term control effects [27]. Disadvantages of using EPF include that it takes longer to kill insects with fungi than with chemical insecticides and application needs to be timed for high relative humidity, low temperature and low pest numbers; Fungal isolates vary in virulence towards different hosts. Virulent strains generally express spore-bound proteases, produce and release exoenzymes during penetration of the cuticle and produce toxins during colonization of target hosts [3]. Furthermore environmental conditions and insect behavior influence fungal activity and these factors need to be taken into account when selecting suitable strains and inoculums for biological control [28]. To resume:

1. Benefits of using entomopathogenic fungi

    (a) Their residues have no known adverse effects on the environment.

    (b) EPF are little or non-toxic to non-target organisms.

    (c) They have narrow area of toxic action, mostly specific to a single group or few species.

    (d) They can be used in combination with synthetic chemical insecticides.

    (e) They are self-perpetuating under ideal environmental conditions.

    (f) Reduce chemical insecticide use.

    (g) Protects biodiversity in managed ecosystem.

    (h) Potential development of pest resistance to EPF is less common or may develop more slowly due to unique mode of action.

2. Limitations of entomopathogenic fungi

   (a) They need specific environmental conditions to germinate and cause infection.

   (b) Can be very costly to produce for commercial use.

   (c) They have short shelf life

   (d) The pest must be present before the pathogen can be usefully applied thus making preventive treatment difficult.

   (e) Lack of persistence and low rate of infection under challenging environmental conditions.

   (f) Often slow acting and require high application rate and thorough spray coverage.

3. Methods for persistence of EPF

   When host numbers are low and/or environmental conditions are not favourable, most EPF species produce resting spores which can arise from asexual reproduction and persist in soil for long periods of time. For insure a successful control, EPF can be employed under three broad biological control strategies, namely classical biological control, augmentation or conservation [27, 28].

   (a) Classical biological control

      Classical biological control is generally accepted to be the use of natural enemies against a host which is exotic in an area and has established without its full guild of natural enemies. Surveys are made in the centre of origin of the insect pest to identify suitable candidate natural enemies which are then released in its newly expanded range [41]. The aim of classical biological control is to provide long-term sustainable and economic control of a target insect pest [41]. Often natural enemies of the target pest are present at too low a level to limit crop damage, in this instance natural enemies can be augmented by either inoculation or inundation.

   (b) Augmentation

      In many situations natural enemies are present in indigenous pest populations, but they are either too few or active too late to limit crop damage. In these cases the natural enemies can be augmented. There are two approaches to augmentation; inoculation and inundation. In an inoculative approach the fungus is applied, often

in small amounts, early in the season of the crop, with the expectation that it will repeatedly cycle (i.e. establish epizootics) in pest populations and spread over a period of time, thereby maintaining the pest population below the economic threshold. Inundative augmentation involves applying the fungus, often in large amounts, for rapid short-term control with no expectation of secondary infection [41]. In this way, the fungus is used in a similar way to a chemical insecticide. The terms "mycopesticide" or "mycoinsecticide" have been used to describe this approach. For fungi, augmentation usually involves adding in vitro-produced mycelia or conidia in aqueous suspensions to a field or glasshouse crop, often in combination with synthetic materials, which are formulation components to enhance persistence and/or infectivity [27, 28, 41]. Hyphomycete fungi have great potential as inundative biocontrol agents, since they are relatively easy to massproduce and formulate for use with conventional spray application equipment. Several commercial products are available for insect control in different agricultural operations [41].

Three examples are given on the use of commercial or semi-commercial products containing isolates of hyphomycete fungi. Verticillium lecanii is used in Europe for control of aphids and related insects in glasshouses; Beauveria bassiana is available for use against a wide range of insect pests and largely sold in North America; finally, Metarhizium anisopliae var. acridum has recently gained approval for use against locust and grasshopper pests in Africa[27, 28, 41].

(c) Conservation

This strategy involves the modification of farming practices to enhance the activity of an entomopathogen population [27, 41]. Biological control through conservation seeks to identify effective indigenous natural enemies and adopt management practices which conserve and promote them in the field. Management practices which favor entomopathogenic fungi may include provision of increased moisture, e.g. by irrigation, reduction in pesticide use and provision of overwintering sites of alternative hosts. In a looser definition, we can also include the development of " inaction thresholds " which determine the population size of the fungus in addition to the pest to determine whether the fungus can control the pest population without the requirement for insecticides [41].

I.5   Overview on modelling EPF growth on insect Pest

I.5.1   Review of literature

Entomopathogenic fungi (EPF) play a vital role in insect population dynamics making it the earliest insect pests control agents. Earliest farmers rely on the actions of predators, pathogens and host plant resistance for the control of insect pests until the discovery of insecticide. The first groundbreaking field trials with EPF started with a Russian microbiologist, Elie Metchnikoff in 1888, who later became a Nobel Prize winner and named Metarhizium anisopliae [54]. Metchnikoff mass produced fungal conidia on sterilized brewer's mash and combine cultures with sand granules for spreading on field crops. Though results were inconsistent, the work of Metchnikoff ignited curiosity around the world and led to programs in Europe and United States for experimentation with fungi against insect pests [55]. Boverin, a Beauveria bassiana-based mycoinsecticide for the control of Colorado potato beetle and codling moth in the former USSR, was developed in 1965 [56]. The first formal and published proposal for microbial control came with John LeConte's suggested use of microsporidia to control grape phylloxera, Daktulosphaira vitifoliae (Fitch). The study presented visionary ideas for an effective and economic alternative method of pest control and paved the way for future scientists to study EPF. Studies on EPF was quiet after the World War II when affordable synthetic chemical insecticides became available for insect pests control. Recent developments on EPF show that they can serve as an integral part of integrated pest management strategy. Many insect pathogenic fungi based bioinsecticides have been formulated and commercially manufactured [57]. The application of EPF in biological control is increasing largely because of greater environmental awareness, food safety concerns and the failure of conventional chemicals due to an increasing number of insecticide resistant species [58]. These "ready to use" formulations are available in many developed and developing countries of Europe, Asian, Africa and the West.

The behavioral response of an insect to a fungal pathogen has a direct effect on the efficacy of the fungus as a biological control agent. In this thesis we take into account two processes that have a significant effect on the interactions between insects and entomopathogenic fungi: (a) the ability of target insects to detect and avoid fungal pathogens and (b) the transmission of fungal pathogens between host insects. The behavioral interactions between insects and entomopathogenic fungi are described for a variety of fungal pathogens ranging from commer-

cially available bio-pesticides to non-formulated naturally occurring pathogens. The artificial manipulation of insect behavior using dissemination devices to contaminate insects with entomopathogenic fungi have been described [9]. Models were used in the literature to study the density dependence and spatial structure in the dynamics of insect pathogens [9]. A simplest theoretical models describing pathogen dispersal within a host population are based on the process of diffusion and provide a moderately good description of dispersal at small spatial scales has be proposed by G. Dwyer and collaborators [59]. The spread analysis of the contagious disease caused by Beauveria bassiana (EPF) in pest (Russian Wheat Aphid) population, and the study of the effect of conidial dispersal of fungal pathogen on the survival of its host have been carried out [32]. A recent study has proposed a model to explain the dynamical evolution of EPF on insects by addressing simple life history questions such as the allocation of resources to either mycelia growth or spore production [1]. The authors assumed that the insect was under a nutritive stress, and their analysis ignored the spatial aspects of the population dynamics and EPF propagation [1]. However, the results of the nonspatial analysis are usually applied to the case of spatially homogeneous and well-mixed populations, which implies that the corresponding habitat is sufficiently small, and the impact of spatial dimensions is, therefore, ignored in a somewhat more exotic case where the individuals of a given species are assumed to remain fixed in space at any time and in any generation [60, 59]. Spatial simulation can overcome such limitations via the link of process and scales [61]. Neglecting the spatial component in such an ecological problem is misleading and thus limits the understanding of ecological relationships which are essential for the occurrence of spatial patterns, and are also inevitable for studying contagious processes [62, 48]. In contrast to the experimental literature on viral entomopathogens [16], there are no studies directly examining heterogeneity in transmission of fungal entomopathogens. Heterogeneity in transmission is expected; however, due to individual differences in host susceptibility observed in the laboratory [3], and the heterogeneous distribution of infective conidia in the field [38]. Such heterogeneity in natural-enemy attack rates is strongly stabilizing [63], and produces stable cycles for a range of parameter values in host-pathogen models [24]. However, Hess developed a host-pathogen model from the classical Levins metapopulation model to explore the conditions under which hosts and pathogens may persist in a fragmented landscape [64]. In this paper, they concluded that host dispersal between patches enhanced the spread of disease and thus could lead to host extinction. Fungus-infected hosts are then, able to disperse and to

spread disease into new colonies. This is possible for some special fungi such as Strongwellsea spp. which sporulate from one or two holes on living hosts and disperse conidia. In previous studies, a framework to consider a generalist pathogen, the abundance of which is maintained in a second host species which acts as a reservoir has been developed [3]. In contrast to Hess [64], they concluded that greater landscape connectance enhanced the stability of the host-pathogen interaction. Habitat corridors allow host species to disperse and escape pathogens, effectively creating a form of refuge. However, complete connectance is equivalent to a homogenous habitat; and a degree of habitat partitioning actually promotes coexistence of host species by, for example, relaxing apparent competition mediated by a shared natural enemy. A general principle that emerges from these and other studies is that the spatial complexity of population structure is a source of heterogeneity that can promote the coexistence of hosts and pathogens.

However, the precise dynamics will depend upon the spatial distribution of hosts, the productivity of patches (in terms of host growth rates), the life history characteristics of the pathogens and the mobility patterns of hosts and pathogens [3]. Consequently, the response of fungal entomopathogens to habitat fragmentation would be best explored in specific host populations using models of intermediate complexity that have been adapted to incorporate species specific information.

Furthermore, In previous experimental studies, external infectious stages ensured that the fungi persists during periods of low host population density when the horizontal transmission is insufficient to maintain the prevalence in the host population [3]. This hypothesized that EPF could potentially regulate, and cause cycles in insect's pest's population. In order to address important issues about the biological control and pest eradication problems in applied ecology, numerous mathematical models were suggested [62, 41, 65].

Referring to preview researches, this contagious phenomenon (transmission) among infectious insects and susceptible one are essential for successful of biological control [28, 29, 43, 44, 45, 46]. The movement of entomopathogenic fungi is really important mechanisms for transmitting to new habitats. This movement is regulating by host and non-host invertebrates to susceptible hosts [28, 29]. Although, the transmission from infectious insects to susceptible one is less variable, it is more efficient than indirect transmission via conidia deposited on the substrate [29, 25]. Even when the number of infected individuals is low, transmission by contagion is sufficient to insure the EPF outbreak and lead to high insect mortality [28, 29]. This can be explain by the

density dependent nature of transmission, high host density lead to high contact rates between individuals and by then give rise to high number of secondary infection R_0 [25, 28].

There is a large body of research shown in the one side that vertical transmission occurs in very few case and on other side that high vertical transmission rate might make the condition for efficient EPF growth less rigorous [28, 29, 43]. In addition, it has been shown that horizontal transmission (auto-dissemination) and dispersal are essential for long-term management of destructive insects, such that investigate the EPF transmission become really interesting since, it raises questions about dispersion and pathogen outbreak within insects population [66]. This explained our focus on the horizontal transmission. Previous researches evaluate the effects of various factors such as temperature, relative humidity, and UV light exposure on the effectiveness of entomopathogenic fungi and underlying the fact EPF efficiency is strongly influences by environmental fluctuations [53].

Many theoretical and/or experimental models exploring the potentials of EPF to regulate insects pests population has been proposed: a patched model investigating the best strategy for EPF to manage the resource extracted from insect [67], spatial heterogeneity in EPF outbreak within insect host population [68, 16]. Recently, a model describing the interaction between EPF and insect immune response has been proposed [69]. The latter model show the impact of abiotic conditions on the fungi growth within insect body, and have also through Turing pattern formation show the different morphological state that EPF can take insight the host according to the allocation of the resource extracted and the ability of insect immune system to protect itself against the pathogen. Previous researchers shown the interplay between species and/or their habitat; and predicted the dynamics, the extinction and the persistence of individuals by using bifurcation and stability analysis theory [70, 71, 72, 73, 74, 75, 76, 77]. The underlying theories demonstrated relevant results in the context of predators-prey models [70, 71, 72, 73, 74, 75, 76, 77, 78, 79], in context of disease transmission [65, 80], in population dynamics [81] and so on.

Anderson et Al [82], proposed a general host-pathogen model showing the impact of the pathogenic microorganisms on the dynamics of insects populations. Authors assumed that the models can be used for all host-pathogen system with minor modification [82]. But this model cannot well used in the context of biological control (BC) since it only describe the temporal evolution of host density. This is not stringent for the biological control, which aims to spatially spread the disease with pest population and then, the transmission. It is also demonstrated in

previous experimental research that, transmission of EPF to hosts is affected by environmental conditions [29]. However, there is no mathematical model investigating this point.

Since Reaction-Diffusion model is known to exhibit traveling wave behavior [16]. Previous studies show that the well know model describing the evolution of the modulated wave is the Complex Ginzburg-Landau (CGL) equation. It has been shown that this kind of equation through the nonlinear instability can be used in a large variety of physical systems such as biological system [17, 18, 19], nonlinear optics, plasma physics, fluid mechanics, nerves cells and so on [17, 18, 19, 20, 83]. Previous work show in context of nonlinear optics that the periodic modulation in MI give rise to the parametric instability which is opposed to the Turing instability observed in absence of the periodic perturbations of the parameters [84, 22, 85, 86]. Theoretical and experimental investigation on the MI carried out in dispersion oscillating fiber ring cavities [23, 84, 22, 85, 86].

I.5.2   Stochasticity in epidemiological system

Entomopathogenic Fungi (EPF) are convenient for use in biological control (BC) and in integrated pest management to reduce crop devastators damages, because it can generate a secondary infection after the initial spray via the production of spores by first infected individuals during their interactions, depending on temperature, humidity degree and dispersion by natural phenomenon such as wind, rain, and interspecific competitions between species [28, 68]. As mentioned above, the infection of a pest occurs in two ways: (1) direct contamination by spores, (2) contamination by infected insects (contagious phenomenon) giving an epidemiological propagation [29]. For such diseases, theory has shown that pathogen persistence time in the environment is an important determinant of whether an epidemic will occur [87], but applications of the theory require estimates of persistence probability. Estimating persistence probability from observations of disease spread in insect population is difficult, on the one side because losses due to pathogen breakdown may be outweighed by gains due to pathogen particles produced from new infections [81], making it hard to distinguish persistence from infectiousness. In the second side due to the stochastic demography (often called demographic noise), defined as a random variation originating from the discrete nature of individuals and stochastic character associated to birth, death, infection, immigration, and emigration of insects assuming the physical environment constant.

However, in experimental studies accurate measurement of prevalence of the fungi without biased sampling of either susceptible or diseased insects can be difficult and some challenges are specific to fungal entomopathogens [3]. A truly accurate assessment of prevalence can only be achieved by sampling all stages of the host in a life table analysis but this is rarely possible. Two methods are usually employed to estimate prevalence (1) sampling living individuals only, followed by laboratory incubation until death when infection can be confirmed by phenotypic characteristics and (2) sampling both living, dead and dying individuals, followed by laboratory incubation and identification [3].

An important approach to model this is individual-based models (or individual level models (ILMs)) which include demographic noise effects. This is a useful approach to understand how biological and ecological systems evolve over time while considering the behavior and the interactions among species and, deduct the associated emerging patterns when the population is well mixed [78, 88]. This approach was successfully applied in predicting: rift valley fever inter-epidemic activities and outbreak patterns [65], predator-prey cycles from resonant amplification from demographic stochasticity [89, 90, 91], stochastic amplification in epidemics [91], demographic noise and resilience in a semi-arid ecosystem [80], impact of human mobility on the periodicity and mechanisms underlying diseases dynamics [92], demographic stochasticity and heterogeneity in transmission of infection [93], and stochastic Turing's patterns [90, 94]. Clearly any model which hopes to capture these epidemic dynamics needs to include stochasticity. Formulating a stochastic model with random variation is straightforward and depending on assumptions can qualitatively capture the correct dynamics of both entomopathogenic fungi and crop devastators. The ILM approach is promising and it was hypothesized that it can provide good insight when applied in the context of biological control modeling.

I.5.3 Individual based models

Challenge in epidemic modeling is to form a model which captures the observed dynamics but also elucidates the mechanisms behind them [95, 96, 97]. There are many different approaches which can capture the dynamics, but they offer little understating of the mechanisms. A major factor in the debate over the role of stochasticity in recurrent epidemics is the dominant modeling paradigm which exists in the field and to a large extent in theoretical ecology in general. The most popular approach tends to have two steps: first to create a suitable pop-

ulation level model (PLM), usually in terms of ordinary or partial differential equations which are deterministic. Next the corresponding individual based model (IBM) is formed, and then simulated, to investigate any stochastic properties [98, 95]. In this thesis, logically the procedure should be reversed: real populations are finite and the PLM is always an approximation to the underlying IBM [96, 99]. Usually it is assumed that the PLM will be accurate in the limit of large populations, but what is meant by large must first be defined [99]. Clearly the IBM, rather than the PLM, should be adopted as the starting point of an investigation. Once an IBM has been defined, it is usually studied using computer simulations. However simulations are still inferior in at least one respect to the analysis that can be carried out on PLMs: general results valid over a wide range of models and parameters cannot in general be established. In addition, many insights and a deeper understanding can frequently be obtained from analytical studies than can be found from computer simulation. Knowledge of the mathematics required to analyze stochastic models has lagged behind that used to study non-linear differential equations. Recently, more effort has been put into this area [90, 82, 100], although the lack of analytical studies of IBMs has held back the study of stochastic, and other effects, in models of epidemics. We take the IBM approach in this thesis, but as well as simulating the models we also use an analytic approach to derive the emergent population level dynamics. The novel aspect of this work is that we applied this method in the context of biological control, to predict the behavior of the EPF insight crop devastator's population, and calculate the power spectrum of the oscillations analytically and compare the results with stochastic simulations. We do this by formulating the model as a master equation which can then be studied using van Kampen's expansion in the inverse system size [99]. The macroscopic dynamics can then be viewed as a sum of a deterministic and a stochastic part. The value of the analytic approach is that we can more easily deduce the mechanisms behind the dynamics and better understand the interplay between the deterministic and stochastic forces.

I.6 Existing models describing the Entomopathogenic Dynamics

I.6.1 General Model of Fungal Growth within a Patch [1]

- The model description

    Gilchrist and collaborators [1] formulated the within-patch model by first assuming that

every patch has the same initial density of resources, r_0 and that each spore germinates and leads to the same initial density of mycelial cells, m_0. In addition, they assumed that: (1) The density of fungal mycelium m decays at a constant rate γ.

(2)The fungus extracts resources from the patch at a rate proportional to its own size, m, and the resource density of the patch, r.

Resources extracted from the patch by the fungus can be allocated to the production of either spores (Z in the patch array model) or mycelium cells m which form the hyphae within the patch. Whereas spore production leads to a direct contribution to the expected spore production of a patch, p increasing mycelium density, m can lead to an indirect contribution to p via greater future resource extraction and, subsequently, greater spore production. The resource allocation level, $u(a)$, describes the proportion of extracted resources which are allocated to spore production. Because $u(a)$ is a proportion, it is constrained to be between zero and one. The model is given by following coupled equations:

$$
\begin{aligned}
\frac{dm}{da} &= m\left(c_1 \varepsilon r\left(1-u\right)-\gamma\right), \\
\frac{dr}{da} &= -\varepsilon mr.
\end{aligned}
\tag{1}
$$

Where a is the fungal age, ε represent the resource extraction rate and c_1 is the conversion rate for resources into mycelia biomass. Assuming that the spore production rate of the fungus p is proportional to the amount of resources allocated to spore production by the fungus provides a link between this within patch model and the expected spore production of a fungus. It follows that, $p = uc_2\varepsilon mr$, c_2 defined the conversion rate for resources into spore biomass.

- A brief description of limit around this model

    Although this model is well described the fungi and resource patch dynamics, we find a number of limitations. It is not close to the reality to assume that after infection, insect is under a nutritive stress [28]. The model is derived from the epidemiology literature, the spread and persistence of a saprophytic fungus within an array of resource patches, the spread and persistence of a disease within a population of hosts should be consider. In this model, space scale is not taking into account, forgetting that successful growth appears when fungi colonize the insect hemocoel. So, neglecting space means there is a critical

density of uncolonized patches required for a fungal strain to be able to establish itself within an array of resource patches.

I.6.2 Model of EPF outbreaks

- The model description

  To model changes in insect populations whose densities may be driven by disease outbreaks, Anderson and May [82] used a system of ordinary differential equations based on standard epidemiological models. In traditional epidemiological models, the host population is divided into infected and susceptible classes, with one differential equation representing each class [59, 24]. What made Anderson and May's model innovative was the introduction of an additional class representing the population of infectious pathogen particles in the environment. These particles are found in widely divergent taxa of invertebrate pathogens, including viruses, fungi, and microsporidia [82], and they allow pathogens to survive in the environment for several decades [28]. Anderson and May's presented one of the first simple mathematical models for the dynamics of insect pathogens [82]. Their model is:

$$
\begin{aligned}
\frac{dS}{dT} &= r\,(S+I) - \nu PS, \\
\frac{dI}{dT} &= \nu PS - \alpha I, \\
\frac{dP}{dT} &= \lambda I - (\mu + \nu\,(S+I))\,P,
\end{aligned}
\tag{2}
$$

  where S is the density of susceptible hosts, I is the density of infected hosts, P is the density of pathogen particles, r is the reproductive rate of the host, ν is the transmission coefficient, α is the rate of disease-induced mortality, λ is the rate of production of pathogen particles by infected hosts, μ is the decay rate of the virus, and T is time.

- A brief description of limit around this model

  This model includes only a small number of processes: host density-independent reproduction and death, host disease-induced death, pathogen production by infected hosts, the breakdown of the pathogen in the environment, consumption of the pathogen by the host, vertical disease transmission and no horizontal disease transmission (contagious process which is a key transmission in epidemiological disease). The model thus ignores much of what biologists have discovered can influence the course of a virus or pathogen disease in

an individual host. For example, contagion affects the susceptibility and the disease outbreak within individual hosts [39]. Moreover, temperature can affect the time between host infection and death [28, 29]. Since, for insect pathogen, transmission occurs either when the host accidentally consumes the pathogen on contaminated foliage, or when the host probably hit infected host; the transmission must be affected by host behavior or migration.

I.7 Motivation

Agriculture is one of the pillars of the economy of sub-Saharan Africa and particularly of Cameroon. It is mostly practiced at a small scale and depends largely on family's labor, with about 70 Percent of the active population of this country engaged in it. This sector is responsible for providing food security to both the rural and urban populations of this country via local production [101]. One can note the high involvement in agriculture in Cameroon especially the culture of maize and bean which are widely grown crop and one of the most affordable cereals in terms of market price and cost of seeds in sub-Saharan Africa and the culture of vegetable crops such as cabbage, carrots, tomatoes, celery, pepper and onions [101, 102]. The cultivation of these crops usually based in countryside of Cameroon, has brought an increase in agricultural production used to feed families and the nation. Among various economic and social benefits, market gardening has a vital and multifaceted role in providing food security, meeting the demands of consumer markets, utilizing labor and generating income. The income generated from market gardening also provides indirect socio-economic benefits for market gardeners, such as greater access to household items (televisions, chairs, school fees, health care) and other goods. Yield and quality are central to sustainable agricultural production. If not properly managed, pests and diseases can dramatically reduce crops (see Fig.5) [101, 102]. However, when evade crop devastators in the field, people also face problem of preserving harvested food due to the post-harvest insect-pests some of these stored product insects are acquired from the field to storage where their populations rapidly build up during storage period. Post-harvest food insect-pests which include the "field-to-store" and the "store" pests are a major constraint to food security and income generation in Sub-Saharan Africa in general; they cause significant post-harvest losses in quantity and grain quality degradation [101, 102]. To reduce the damage inflicted by these different pests, farmers have resorted to using various methods, using an integrated pest's

management. However, most farmers in sub-Saharan Africa have limited resources, coupled with low education and therefore do not have the means or skills and knowledge to obtain and handle pesticides appropriately. For instance most farmers in most areas of Cameroon when using insecticides often do not use appropriate protective clothing, nose masks and do not respect pre-harvest interval stipulated by manufacturers. Farmers need to resort to safe and more environmentally friendly methods of managing pre- and post-harvest pests. This gave reason for this work to be carried out to develop a mathematical model to better understand the entomopathogenic fungi growth on insect, improve its use and give practical strategies to the farmers.
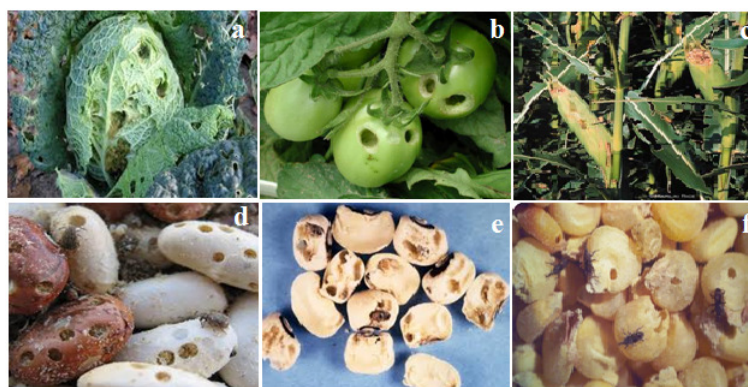
Figure 5: The first line represent the pre-harvest pests damage on culture: a) Cabbages, b) Tomatoes, c) maize. The second line illustrates the crop devastators harmful on stored grains: d)-e) beans, f) and dry maize.

I.8 Conclusion

This chapter has set the biological background for the rest of this thesis, and the existing literature on the models mimicking the interaction between insects and EPF. Its different limits and highlight of our contributions have been provided. Moreover, we gave an appearance of the damage and lost cause by the insect pest, the importance of EPF as biological control agents. The challenges related to the modeling of the EPF growth insight insect pest in general have been presented. Finally, we highlighted the problems and challenges encountered in coupling the insect pest dynamic and epidemiological models. In the next chapter, we presented the different analytic and numerical approaches used to investigate these different problems in this study.

MODELING AND MATHEMATICAL

METHODS

II.1 Introduction

The entomopathogenic fungi (EPF) regulate insect population as well as their abundance and the persistence in the surrounding environment [3]. The first challenge is to accurately understand how fungi (EPF) are in both hosts and the surrounding environment. This chapter present a brief overview on the techniques used to investigate the dynamics of EPF. It is structured in two main parts: the intra host dynamics of EPF based on a Reaction-diffusion models and on it epidemiological outbreak within a host population. The chapter is closed by a conclusion.

II.2 Within host dynamics of EPF

II.2.1 Model description

The model presented by Gilchrist et al. [1] was reformulated by introducing functional responses, logistic growth on resources, and spatial inhomogeneity using the phenomenon of diffusion to characterize the mobility of species. Consideration was given to the most important morphological states of the fungus, which are the mycelia (M) and the spores (S) [1], while taking into account the magnitude and characteristics of the quantity of resources (R) that the insect contains. The system can, thus, be described by the following set of coupled partial differential equations (PDE):

$$
\begin{aligned}
R_t &= D_R \nabla^2 R - F(R)\ M + \alpha R \left(1 - \frac{R}{K}\right), \\
M_t &= D_M \nabla^2 M + C_1 (1 - q) F(R) M - \gamma M + D_{MR} \nabla (M \nabla R).
\end{aligned}
\tag{3}
$$

where t is simply the independent time variable and ∇ is the Nabla operator. α corresponds to the linear birth regeneration rate of resources and K is defined to be the carrying capacity [103]. D_R and D_M are the diffusion rates of resources and mycelium, respectively, on the one hand, D_{MR} is the nonlinear diffusion rate on the other hand. It is assumed that the density of mycelium (M) can decay naturally at $\gamma \cdot dt$ between the instants t and $t + dt$ and that resources extracted from the insects by fungi are allocated to the mycelium growth and spore production. The coefficient C_1 represents the conversion rate of the resources into mycelium [1], and $q \cdot dt$ is defined as the probability that the extracted resources are allocated to the sporulation in the presence of the mycelium between the instants t and $t + dt$. The spore production density of the fungus S, is assumed to be proportional to the amount of resources allocated to spore production by the fungus, and can be written as:

$$S = C_2 q F(R) M.$$

where, C2 defines the conversion rate of the resources into spores. The infestation function is represented by a Holling and Powell type-II functional responses defined by [89, 104, 105, 106]

$$F(R) = \frac{AR}{B + R}. \tag{4}$$

This function $F(R)$ has been considered to model the nonlinear interaction between species, and more clearly, it is worth the amount of resources extracted per insect's cell per unit time. Here, B is the quantity of resources that leads the functional response to half-saturation, and A is the maximum amount of resources that can be extracted per cell and per unit time. A corresponds also to the value of $F(R)$ when R is very large. In reality, mycelia are switching to resources at different moments with different efficiencies. As most of the mycelia usually switch to resources that are significantly abundant [107], mycelia pressure is expected to increase more than linearly with resource density over the initial range. Therefore, the nonlinear diffusion term $D_{MR}\nabla(M\nabla R)$ is applied for modeling the tendency of resources congregation (immune system) R to protect itself from the attack of the mycelia M. In order to predict with a good accuracy the behavior of insects during EPFs' infestation or the efficiency of EPF, this switching behavior of the mycelia is modeled by a time-periodic function [107, 108, 109, 110, 111].

It is worth mentioning that, in the case of insect–fungi interaction, daily environmen-

tal conditions such as temperature, relative humidity, and solar radiation affect the insect thermoregulation, mycelia growth, and the virulence strategy of fungus entomopathogens [3, 25, 28]. Thus, it becomes obvious that they equally affect the multiplication and the dispersal of infectious propagules within an insect's body [3]. It has been demonstrated that the diffusion coefficient of cells' biology changes with temperature shifts. Because of our focus on mycelia growth, we neglect the influence of this temperature variation on the resource of insects. A rough analogy with the transmembrane proteins diffusion coefficient in bacteria dynamics shows that diffusion coefficient is proportional to temperature and, consequently, time [112, 113]. Such that,

$$D = D_0 T \tag{5}$$

where, T is temperature, and D_0 is function of the number of transmembrane domains, the fluid viscosity, the Boltzmann constant, the membrane thickness, the membrane viscosity and so on. In view of the fact that living organisms maintain their membranes in a fluid state, diffusion coefficient can be made time dependent [112, 113]. Since, To study the effect of fluctuating temperatures on insect development, often some researchers have shown that, diurnal temperature can be approximated by a periodic time dependent function where time is a fractional part of the day [114, 105]. So, temperature can be modeled as a sinusoidal curve with a period of 24 hours of the form

$$T(t) = T_{mean} + \frac{(T_{max} - T_{min})}{2} sin\left(\frac{2\pi}{24}t\right) \tag{6}$$

here, T_{mean}, T_{max} and T_{min} are mean, maximal and minimal daily temperature, respectively. t is time in hours. This allow to write diffusion coefficient as potentially vary with respect to time. A typical example of this is oceanic diffusion [115]. This important phenomenon has also been taken into account in an ecological model for predator–prey planktonic species, and in a population pathogen model, in order to study the impact of constant and time varying diffusion terms on the disease dominated ecological population [115, 116]. In these studies, a sinusoidal variation of diffusion with respect to time was employed to represent seasonal and daily variation, environmental factors and various intrinsic factors that are inherently internal in nature [116]. In our case, the diffusion coefficient of the resources, D_R is assumed to be a constant

and, D_M and D_{MR} are functions of time t and are given by the expressions:

$$D_M = D_R \left(d + b \sin \left(\omega t \right) \right),$$
$$D_{MR} = D_R \left(D_{21} + B_{21} \sin \left(\omega t + \phi \right) \right),$$

$$(7)$$

where $d > 1, d > |b|, D_{21} > 1, D_{21} > |B_{21}|$. The model is defined in a bounded fixed domain. The following dimensionless quantities are introduced in order to simplify the equation:

$$\frac{\partial}{\partial \tau} = \gamma^{-1} \frac{\partial}{\partial t}, M = \gamma \frac{B}{A} m, R = \gamma \frac{B}{C_1 A} r, S = \gamma^2 \frac{C_2 B}{C_1 A} s, b_{21} = \gamma \frac{B_{21} B}{C_1 A}, \beta = \frac{\alpha}{\gamma},$$
$$a = \gamma \frac{1}{C_1 A}, d_{21} = \gamma \frac{D_{21} B}{C_1 A}, x = \sqrt{\frac{\gamma}{D_R}} x', \Omega = \frac{\omega}{\gamma}.$$

$$(8)$$

and the master equations (3) become

$$\dot{r} = \beta r \left(1 - \frac{r}{\varepsilon} \right) - \frac{mr}{1+ar} + \nabla'^2 r,$$
$$\dot{m} = (1-q) \frac{mr}{1+ar} - m + (d + b \sin(\Omega \tau)) \nabla'^2 m + (d_{21} + b_{21} \sin(\Omega \tau + \phi)) \nabla' \left(m \nabla' r \right).$$

$$(9)$$

with

$$s = q \frac{mr}{1+ar}.$$

The homogeneous Neumann boundary conditions are used, assuming that no external input is imposed on the system.

II.2.2 Stability analysis and Turing instabilities (case $b = b_{21} = 0$)

It was considered that, there exists a set of stationary, spatially uniform solutions of (9). This allowed us obtain three singular points. The only endemic equilibrium point is

$$(r_0, m_0) = \left(\frac{1}{1-q-a}, \frac{(-1+q)\beta \left(\varepsilon \left(a + q - 1 \right) + 1 \right)}{\varepsilon (a+q-1)^2} \right),$$

which has a biological relevance only if $(q + a) < 1, \varepsilon (1 - a - q) > 1$, conditions that will be applied throughout the rest of this section. Linearizing the system of (9) in the neighborhood of the steady state (r_0, m_0) [117, 118], the following equation is obtained:

$$\mathbf{w}_t = \mathbf{J}\mathbf{w} + \mathbf{D}\nabla^2 \mathbf{w},$$

$$(10)$$

where

$$\mathbf{w} = \begin{pmatrix} r - r_0 \\ m - m_0 \end{pmatrix},$$

$$\mathbf{J} = \begin{pmatrix} -\dfrac{\beta \left(a^2 \varepsilon + (1 + \varepsilon(-1 + q)) a - q + 1\right)}{((-1 + q) \varepsilon (a + q - 1))} & \dfrac{1}{-1 + q} \\ -\dfrac{\beta (\varepsilon (a + q - 1) + 1)}{\varepsilon} & 0 \end{pmatrix},$$

and

$$\mathbf{D} = \begin{pmatrix} 1 & 0 \\ d_{21} m_0 & d \end{pmatrix}.$$

Since $\det \mathbf{J} = \dfrac{\beta (\varepsilon (a + q - 1) + 1)}{\varepsilon (-1 + q)}$ is always negative, the only way for the endemic singular point to become unstable if $tr(\mathbf{J}) > 0$. The parameter space (a, q) shows the zone where the steady state is stable and, thus, diffusion-driven instability can develop. To find Turing instability with spatial wavenumber k, we search eigenvalues λ of the matrix λ of the matrix $\mathbf{A}(k) = \mathbf{J} - k^2 \mathbf{D}$ (the expressions of $\mathbf{J}$ and $\mathbf{D}$ are given in above). When the real part of the dominant eigenvalue λ crosses the imaginary axis for some $k \neq 0$, the spatially homogeneous equilibrium is destabilized by a periodic perturbation of wavelength $2\pi/k$, and the perturbations will exponentially grow with time. If each eigenvalue has a negative real part ($\mathrm{Re}(\lambda_i(k)) < 0, \forall k, i = 1, 2$), the homogeneous state is stable: every perturbation will eventually die out and no pattern will develop. Turing bifurcation happens at the critical value

$$d_{21}^c = \frac{(a + q - 1)^2}{(1 - q) \det \mathbf{J}} \left(-tr(\mathbf{J})d + 2\sqrt{\det \mathbf{D} \det \mathbf{J}}\right),$$

which corresponds to the critical wavenumber

$$k_c^2 = \sqrt{\frac{\det \mathbf{J}}{d}}.$$

II.2.3 Time-dependent diffusivities (case $b \neq 0$ and $b_{21} \neq 0$)

This section analyzes the time-dependent diffusivities using Eq.11 that admits a periodic solution. The stability of the system is studied by superimposing a small perturbation of the form $a_j(t) \exp(ikx), (j = 1, 2)$ and by then applying the theory of Floquet [109]. In this expression, k corresponds to the wavenumber. By spatially linearizing the inhomogeneous system in the

neighborhood of the endemic equilibrium point, we obtained the following first order system:

$$\mathbf{a_t} = A(k,t)\mathbf{a}, \tag{11}$$

where $\mathbf{a} = (a_1, a_2)^T$ represents the amplitude of the perturbation affecting r and m respectively; $(.)^T$ stands for a transposed vector, $A(k,t)$ is a 2-dimensional matrix defined by

$$\mathbf{A}(k,t) = \begin{pmatrix} a_{11} - k^2 & a_{12} \\ a_{21} - m_0 k^2 (d_{21} + b_{21} \sin(\Omega t + \phi)) & a_{22} - k^2 (d + b \sin(\Omega t)) \end{pmatrix} \tag{12}$$

where the coefficients $a_{ij}, (i, j = 1, 2)$ are the elements of the Jacobian matrix given above in subsection (II.2.2). $A(k,t)$ is periodic with a minimal period of $2\pi/\Omega$, Ω being the frequency of the perturbation. The stability of this system is defined by the eigenvalues of the monodromy matrix. According to the Floquet theory [119, 120], the solutions of this system $\mathbf{a}(t)$ obey the formula

$$\mathbf{a}(t) = \mu \mathbf{a}\left(t + \frac{2\pi}{\Omega}\right),$$

where μ is any eigenvalue of the constant matrix $\mathbf{E}$ transforming a fundamental matrix $\Phi(t)$ of the system into its translate $\Phi\left(t + \frac{2\pi}{\Omega}\right)$. The stability of this system is defined by the eigenvalues of the monodromy matrix $\mathbf{E}$. If $\mu = 1$ then, the system has periodic solutions. For $\mu < 1$ the system has a stable solutions; and if any eigenvalue μ is such that $\mu > 1$, then an unstable behavior appears. It is known that the product of characteristic multipliers is given by:

$$\mu_1 \mu_2 = \exp\left(\int_0^{2\pi/\Omega} tr\mathbf{A}(k,t)\, dt\right) = b, \tag{13}$$

with $b = \exp\left\{\frac{2\pi}{\Omega}\left(tr(\mathbf{J}) - k^2(1+d)\right)\right\} < 1$. Considering the Cardano's relationship, the characteristic multipliers of the monodromy matrix are solutions of the equation:

$$\mu^2 - h(k,\Omega)\mu + b = 0.$$

Based on the fact that $b \in [0, 1]$, the form of $h(k, \Omega)$ is not required, only their interval of variations are needed [109]. However, it exists in the (k, Ω) - plane curves that separate zones

where the amplitudes have different qualitative behaviors (see Appendix A). Because the function $h(k, \Omega)$ is not explicitly defined, we searched for the (k, Ω) - couples of values describing these variations by using Fourier series. Let's assumed that:

$$\begin{pmatrix} a_1 \\ a_2 \end{pmatrix} = \sum_{n=-\infty}^{+\infty} \begin{pmatrix} A_n e^{a_n t} \\ B_n e^{b_n t} \end{pmatrix}. \tag{14}$$

By substituting (Eq.14) into (Eq.9), and using the identity $\sin\theta = \left(e^{i\theta} - e^{-i\theta}\right)/2i$, we get

$$\begin{aligned} &\sum_{n=-\infty}^{n=+\infty} \left(k^2 - a_{11} + a_n\right) A_n e^{a_n t} - a_{12} \sum_{n=-\infty}^{n=+\infty} B_n e^{b_n t} = 0, \\ &\sum_{n=-\infty}^{n=+\infty} \left(k^2 d + b_n\right) B_n e^{b_n t} + \sum_{n=-\infty}^{n=+\infty} \left(k^2 m_0 d_{21} - a_{21}\right) A_n e^{a_n t} - i\frac{k^2 m_0 b_{21}}{2} e^{i\phi} \sum_{n=-\infty}^{n=+\infty} A_n e^{a_{n+1} t} \\ &+ i\frac{k^2 m_0 b_{21}}{2} e^{-i\phi} \sum_{n=-\infty}^{n=+\infty} A_n e^{a_{n-1} t} - i\frac{k^2 b}{2} \sum_{n=-\infty}^{n=+\infty} B_n e^{b_{n+1} t} + i\frac{k^2 b}{2} \sum_{n=-\infty}^{n=+\infty} B_n e^{b_{n-1} t} = 0. \end{aligned} \tag{15}$$

For nontrivial solutions, the determinant of the matrix obtained from Eq.15 must be null. Since the determinant is infinite, the first and second sections of Eq.15 are divided by $\left(k^2 - a_{11} - 4m^2\right)$ and $\left(k^2 d - 4m^2\right)$ respectively, for the convergence. By considering the lower-order Hill determinant (six rows and six columns) and setting it equal to zero, the following nonlinear algebraic equation is obtained

$$\Delta_H = F_4(k)\,\Omega^4 + F_3(k)\,\Omega^3 + F_2(k)\,\Omega^2 + F_1(k)\,\Omega + F_0(k) = 0, \tag{16}$$

where the coefficients $F_i(k)\ (i = 0, .., 4)$ are given in Appendix B. This equation can be solved numerically by the bisection method or by the Newton-Raphson algorithm.

II.3 EPF outbreaks within host population

II.3.1 Model description

In this section, an individual-based stochastic model, which considers all essential features of the interactions between EPF and insect pests, is formulated. This model investigates a biological control using entomopathogenic fungi to target insect pests population when their size is large

but finite. This work focused solely on the pathogen particle populations, assuming that they are implicitly dispersed in the environment by natural phenomena such as wind or rain. An additional transmission pathway is simple contacts between infected and susceptible insects dependent to the species of entomopathogenic fungi [29, 51], assuming this can be ignored in the particular case where spores are produced by insect's cadavers. It is assumed that insect's individuals exist in two discrete states: susceptible, or infected. To simplify the analyses, it was supposed that for same specie every individual has identical probability for birth, death, migration or acquiring infection. New insects produced at a birth rate b_1 are susceptible to be infected. They undergo natural death at the rate d_1. A susceptible insect is infected by a previous infected insect or by pathogen particle at probabilities I_1 and I_2 respectively. Infected insects die and product either more infective conidia with the probability b_2. if environmental conditions are not favorable spores become inactivate at the rate d_3. The carrying capacity N, defined the maximum number of individuals allowed per site is kept constant. In this framework, n denotes the number of insects susceptible to be infected S, m the number of infected insects species I, l the number of pathogen particle species C. A fourth class, E denoting empty (describe the possibility to receive new individual in the patch) is introduced. It is supposed that the population dynamics of the system can be essentially described by four processes:
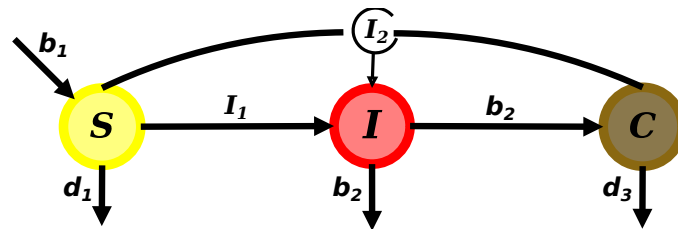
Figure 6: Flow diagram of BC model using EPF on insects pests

1. Infection:

   A spore species may come into contact with a susceptible insect giving rise to one infected pests. This is assumed to take place at a rate I_2. A susceptible insect may also be infected by an infected (that is, from the environment, reproduction) for certain species of entomopathogenic fungi at the rate I_1 giving rise to two infected pest. So, to generalize this study, there are two mechanisms written as: $CS \rightarrow CI$ and $IS \rightarrow II$. The case where spores emerge on their host cuticle only after insect death, correspond to the case the second mechanisms does not exist.

2. Death:

   To describe more realistic epidemiological model, it is assumed that each of the three types of individuals has its specific death rate. These are represented by $S \rightarrow E$ and $C \rightarrow E$ at the rate d_1 and d_3 respectively. The death of spore means the resting process (inactive stage). The death of infected insect is affected to the case 4.

3. Birth:

   In regards of the potential of EPF to rapidly kill their host, it is assumed here that there is not offspring for infected insects. Their only give rise to the new spores generation. Thus, the mechanisms $SE \rightarrow SS$ occurs for susceptible insects at the rate b_1.

4. Death / Conidia production:

   Each death of infected insects give rises to the sporulation. This transition is represents by $I \rightarrow C$ and occurs at the rate b_2.

II.3.2   Local dynamics

Small population size

The transition probability, per unit time step of the local system of individuals from state $\sigma = (n, m, l)$ to the state $\sigma' = (n', m', l')$ is noted $T(\sigma' | \sigma)$. The process occurring in this framework is conceptualized by the following events:

1. Birth

$$T(n+1, m, l \,|\, n, m, l) = 2b_1 \frac{n}{N}(N - n - m - l), \tag{17}$$

2. Infection

$$T(n-1, m+1, l \,|\, n, m, l) = \frac{2I_1 nm}{N} + \frac{2I_2 nl}{N}, \tag{18}$$

3. Death

$$T(n-1, m, l \,|\, n, m, l) = d_1 n,$$
$$T(n, m, l-1 \,|\, n, m, l) = d_3 l. \tag{19}$$

4. Death/ Conidia production

$$T\left(n, m - 1, l + 1 \,|\, n, m, l\right) = b_2 m. \tag{20}$$

The factor of 2 in Eqs.(17-18)come from the fact that the choices AB and BA are identical; A,B illustrate different species. The rate of occurrence (transition rate) depends only on the present state and could be for a species A defined as the number of this type at the time t divided by the total number of possibility to draw individuals, Thus the coefficients b_1 and I_i *(with $i = 1, 2$)* are scaled by a factor $(N - 1)$, b_2 and d_i by a factor N. The system (17)-(20) is simulated using Gillespie Algorithm [6].

System size expansion

The master equation describing the time evolution of the system is defined to be a sum of transition probabilities giving rise to change in the probability distribution function $P\left(n, m, l, t\right) = P\left(\sigma, t\right)$ with time, take the following form [99, 121, 122]

$$dP\left(\sigma, t\right) / dt = \sum_{\sigma \neq \sigma'} \left(T\left(\sigma \,|\, \sigma'\right) P\left(\sigma', t\right) - T\left(\sigma' \,|\, \sigma\right) P\left(\sigma, t\right)\right), \tag{21}$$

where t represent the time since the first infection, for more details the reader is referred to Appendix C. This equation is too complicated to solve exactly and as proposed in previous research [97, 99, 123, 124], it can be analyzed in the limit of large system size. Van Kampen's approximation transforms the system to a deterministic equations associated with its stochastic corrections [97, 99, 123]. Defined in terms of the populations $\phi = \lim_{N \to \infty} n/N, \varphi = \lim_{N \to \infty} m/N, \psi = \lim_{N \to \infty} l/N$, these equations are explicitly given by

$$\begin{aligned}
\dot{\phi} &= r\phi(1 - \tfrac{\phi}{k}) - \alpha_1 \phi\varphi - \beta_1 \phi\psi, \\
\dot{\varphi} &= \alpha_2 \phi\varphi + \theta \phi\psi - b_2 \varphi, \\
\dot{\psi} &= b_2 \varphi - d_3 \psi.
\end{aligned} \tag{22}$$

in these equations, the dot above the average state variable represents the first order derivative with respect to the time, and the coefficients are given by: $r = 2b_1 - d_1, k = 1 - \dfrac{d_1}{2b_1}, \alpha_1 = 2\left(b_1 + I_1\right), \beta_1 = 2\left(b_1 + I_2\right), \alpha_2 = 2I_1$ and $\theta = 2I_2$.

Stability analysis

It was considered that there exists a set of stationary, spatially uniform solutions of (22). This system has to be analyzed with the set of initial conditions $\phi > 0$, $\varphi > 0$ and $\psi > 0$. This system possesses three different equilibrium points: (i) $E^0 = (\phi = 0, \varphi = 0, \psi = 0)$ species free equilibrium, (ii) $E^1 = (\phi = k, \varphi = 0, \psi = 0)$ infected insects and spores free equilibrium, and (iii) and the only endemic equilibrium point is $E^{SIC} = (\phi^s, \varphi^s, \psi^s)$, which has a biological relevance if and only if $k(\theta b_2 + \alpha_2 d_3) - b_2 d_3 > 0$. This biological relevance condition is thus giving the threshold for the basic reproduction number defined the expected number of secondary infection caused by a single infection such that $R_0 - 1 > 0$ where

$$R_0 = \frac{k(\theta b_2 + \alpha_2 d_3)}{b_2 d_3}, \tag{23}$$

obtained from the existence of the endemic equilibrium method. According to previous researches, there exist many analytical methods for evaluating the basic reproduction number. Such as the next generation method, the survival function [125, 126], the eigenvalues of the jacobian matrix around the free-disease equilibrium [65], the constant term of the characteristic polynomial of the free-disease equilibrium, the existence of the endemic equilibrium [125, 126], the number of susceptible at the endemic steady state, the average age of infection, the final size equation and the intrinsic growth rate [80]. However, the same results can be obtained when using the constant term of the characteristic polynomial around the free-disease equilibrium, the average life time. By using the latter method, the basic reproduction number can be decomposed as follows:

$$R_0 = R_0^{in\,sec\,ts} + R_0^{spores}, \tag{24}$$

, where $R_0^{in\,sec\,ts}$ is the number of secondary infections from infected insects and R_0^{spores} corresponds to the number of secondary infections cause by a single spore. The average number of insects that can be infected by a single infected insect during its life period $(1/b_2)$ is $\alpha_2 k$. So a single infected insect will give rise to an average $R_0^{in\,sec\,ts} = \alpha_2 k/b_2$. Similarly a new generated spore will give rise an average new infections $R_0^{spores} = \theta k/d_3$ during its life period $(1/d_3)$ time units. Adding both expression, lead to expression Eq.(23). So the equilibrium E^{SIC} can be rewrite as $\phi^s = \dfrac{k}{R_0}, \varphi^s = \dfrac{d_3 r(R_0 - 1)}{R_0(\alpha_1 d_3 + b_2 \beta_1)}, \psi^s = \dfrac{b_2 r(R_0 - 1)}{R_0(\alpha_1 d_3 + b_2 \beta_1)}.$

- The species free equilibrium point E^0: The jacobian matrix is triangular matrix with eigenvalues $(r, -d_3, -b_2)$. Because $(r > 0, d_3 > 0, b_2 > 0)$. E^0 is always a saddle point, so its stability does not change.

- The infected insects and conidia free equilibrium E^s: This point is stable if and only if
  $$0 < -\mathrm{r}\left(k\theta\mathrm{b}_2 + k\alpha_2\mathrm{d}_3 - b_2 d_3\right),$$
  $$0 < -k\alpha_2 + b_2 + d_3 + r, \text{ and}$$
  $$0 < -\mathrm{r}\left(k\alpha_2 - b_2 - d_3\right) - k\theta\mathrm{b}_2 - k\alpha_2\mathrm{d}_3 + b_2 d_3 + \mathrm{r}\left(k\theta\mathrm{b}_2 + k\alpha_2\mathrm{d}_3 - b_2 d_3\right) / \left(-k\alpha_2 + b_2 + d_3 + r\right).$$

  or we restrict the analysis here to the case where $0 < \left(k\theta\mathrm{b}_2 + k\alpha_2\mathrm{d}_3 - b_2 d_3\right)$ holds true in condition to the property that all parameter values are positive. Because $r > 0$, the first condition can not be satisfy then E^s is also a saddle point for the three dimensional equilibrium point. However the characteristic polynomial obtained from the Jacobian matrix around the free-disease steady state is a cubic polynomial with coefficient $1, A, B, C$, where
  $$A = -k\alpha_2 + b_2 + d_3 + r, B = (A - r)\,r - (R_0 - 1)\,, C = -\left(R_0 - 1\right)rb_2d_3 \cdot$$
  Such that for $C = 0$ meaning that $R_0 = 1$ the system exhibits transcritical bifurcation and is stable for $R_0 < 1$.

- The epidemic equilibrium: The characteristic polynomial obtained from the Jacobian matrix around the endemic steady state is a cubic polynomial with coefficient $1, A, B, C$. So, for $A > 0, B > 0$ and $C > 0$ for $R_0 > 1$ the steady state exists. Thus the polynomial equation has no root which is positive or zero (Descartes' rule of sign). This equation will only have negative roots or complex roots with negative real part if and only if $AB - C > 0$ according to the (Routh-Hurwitz criteria). Thus the system is stable about the infectious equilibrium point E^{SIC} whenever it exists and $AB - C > 0$ (condition we plot to obtain the stability diagram), with $A = d_3 + \dfrac{k\theta b_2 + d_3 r}{d_3 R_0} > 0$, for $R_0 > 1$
  $$B = \frac{r}{R_0}\left(\frac{\alpha_1 b_2 d_3\left(R_0 - 1\right)}{\alpha_1 \mathrm{d}_3 + b_2\beta_1} - \frac{b_2 d_3\alpha_2}{\theta\mathrm{b}_2 + \alpha_2\mathrm{d}_3} + b_2 + d_3\right),$$
  $$C = \frac{rb_2d_3\left(R_0 - 1\right)}{R_0} \text{ for } R_0 > 1. \text{ If } C = 0 \text{ thus } R_0 = 1, \text{ the system exhibits transcritical}$$
  bifurcation and the endemic point is stable for $R_0 > 1$.

In our model, in addition to $AB - C > 0$. when $R_0 < 1$, the endemic equilibrium point do not have a biological relevance and the EPF population density will die out with time and cannot reduce the pest population; whereas for $R_0 > 1$, the introduction of EPF can lead to a targeted

spread, the endemic equilibrium point exists and can be stable/unstable. Because R_0 and I_1 are proportional, R_0 can be sufficient to describe dynamics of the systems [47]. The sensitivity analysis of the basic reproduction number R_0, is conducted by a Latin hypercube sampling (LHS) on combination with a partial rank correlation coefficient (PRCC) [127]. This method is useful to identify parameters that affect the quantity . The input models parameters k, θ, α_2 or I_1, b_2, d_3 from which R_0 depends are randomly and uniformly distributed between their lower and higher values into Q-equal probability intervals and subsequently used to compute the LHS matrix of five (number of input parameters) columns with Q lines. The basic reproduction number R_0 is evaluated as a corresponding output matrix. These matrices are rank - transformed to calculate the partial rank correlation coefficient (PRCC) which gives the sensitive index of R_0 associated to each parameter [127]. The parameters which have the sensitivity indexes closer to, ± 1 should significantly affect R_0. The more a parameter is tending to minus one, the more it has a reductive effect on R_0 and the parameters for which the PRCC is close to one increase the basic reproduction number.

Probability of extinction and coexistence

In epidemic models, the main concern is to find conditions under which a pathogen agent introduced into a community will develop into a large outbreak, while coexistence of populations was never observed [5]. It has been shown that the epidemic outbreak is not always guaranteed by having R_0 greater than one: stochastic extinction can occur during the period immediately following the introduction, when there are few infectious individuals within the system [93, 6]. Rather than the major outbreak that would be expected based on the behavior of the deterministic model, only a minor outbreak might occur. During this early period after EPF introduction, little depletion of susceptible insect will have occurred and so invasion probabilities can be derived using the linear model that arises by assuming that the populations are entirely susceptible [93, 122]. A more challenging question is to calculate the probability that the infection persists or extinct through the trough that follows the initial epidemic [5]. It is noteworthy to mention that, infection of insect pest occurs in two range: one is the transmission of infection by direct contact between infected and susceptible insects [29]. The other is refers to the transmission from pathogen particle (spore) to susceptible individuals. In many disease models, it is assumed that a constant rate of death for the hosts and a constant death rate for resting spore, leading

to the duration of infection, for both hosts and pathogen, being exponentially distributed [122]. Assuming the secondary infections arise independently at a constant rate over these infectious periods [93, 122], extinctions probabilities taken as s_1 and s_2 for host and EPF respectively, start from a single individual of the same type, is found by calculating the smallest positive root of the equation $G_1(G_2(s_1)) = s_1$ and $G_2(G_1(s_2)) = s_2$, respectively. Where G_i, (*with i=1,2*) denotes the probability generating functions (PGF). The subscript 1 is used for insect species and 2 for pathogen particle. Their distributions of secondary infections of each type can be summarized by the two generating functions, $G_i(s_1, s_2) = \sum\limits_{k_1, k_2} s_1^{k_1} s_2^{k_2} P(X_{i1} = k_1, X_{i2} = k_2)$. Here, i is equal to 1 or 2 and X_{ij} is the random variable giving the number of secondary infections of the type j that arise from an individual of type i.

Assuming that the number of spores it very small, thus $l = 1$; A spore only infects healthy insects according to a Poisson process with the intensity θ during their on life period $1/d_3$ in which it exponentially distributed. In this case, the probability of generating function offspring producing by a single spore during on infectious period t is estimated as:

$G_2(s_1, s_2) = \sum\limits_{k_1, k_2} s_1^{k_1} s_2^{0} P(X_{21} = k_1, X_{22} = 0)$ since there is not a transmission between spores.

This given: $G_2(s_1) = \sum\limits_{k_1} s_1^{k_1} P(X_{21} = k_1) = \sum\limits_{k_1} s_1^{k_1} \int\limits_0^{+\infty} d_3 e^{-d_3 t} \left(\dfrac{(\theta t)^{k_1} e^{-\theta t}}{k_1!} \right)$,

$= d_3 \int\limits_0^{+\infty} e^{-(d_3 + \theta)t} \left(\sum\limits_{k_1=0}^{+\infty} \dfrac{(s_1 \theta t)^{k_1}}{k_1!} \right) dt$,

$= d_3 \int\limits_0^{+\infty} e^{-(d_3 + \theta - s_1 \theta)t} dt$.

$$G_2(s_1) = \frac{1}{1 + R_{12}(1 - s_1)}, \tag{25}$$

with $R_{12} = \dfrac{\theta}{d_3}$.

In addition, an infected pest infects a susceptible and also give rise to new propagules according to a Poisson process at the intensity α_2 and b_2 respectively, within it infectious period $1/b_2$. Take a single infected insect in their exponential distributions, we have found the probability of generating function as:

$$G_1(s_1, s_2) = \sum\limits_{k_1, k_2} s_1^{0} s_2^{k_2} P(X_{11} = 0, X_{12} = k_2),$$

rearranging the latter, the following expression is obtained:

$$G_1(s_2) = \frac{1}{1 + R_{21}(1 - s_2)}, \tag{26}$$

where $R_{21} = \dfrac{b_2 + \alpha_2}{b_2}$.

In stochastic models the terms R_{12} and R_{21} denoted the distributions of secondary infections for EPF-to-insect and insect-to-EPF transmission respectively. The probability of extinction following introduction of a single spore is found by calculating the positive roof of equation $G_1(G_2(s_1)) = s_1$, which corresponds to

$$s_1 = \frac{1}{1 + R_{21}\left(1 - \dfrac{1}{1 + R_{12}(1 - s_1)}\right)}, \tag{27}$$

that lead to

$$(1 - s_1)\left[1 + R_{12} - R_{12}(1 + R_{21})s_1\right] = 0,$$

which is a square polynomial in s_1, note that $s_1 = 1$ is always a solution. The other solution is always positive and is smaller than 1 if and only if $R_{12}R_{21}$ is greater than 1. Estimation of the extinction probability following the introduction of a single spore required to find the smallest non-negative root of $G_1(G_2(s_1)) = s_1$ after rearranging the above equation and solving, we obtained two positive solutions, $s_1 = 1$ is always a solution. The other solution is given by

$$s_1 = \frac{1 + R_{12}}{R_{12}(1 + R_{21})}, \tag{28}$$

Sensitivity analysis

Sensitivity analysis (SA) is a method for quantifying uncertainty in any type of complex model. The objective of SA is to identify critical inputs (parameters and initial conditions) of a model and quantifying how input uncertainty impacts model outcome(s). When input factors such as parameters or initial conditions are known with little uncertainty, we can examine the partial derivative of the output function with respect to the input factors. This sensitivity measure can easily be computed numerically by performing multiple simulations varying input factors around a nominal value. This technique is called a local SA because it investigates the impact on model output, based on changes in factors only very close to the nominal values. In

biology, input factors are often very uncertain and therefore local SA techniques are not appropriate for a quantitative analysis; instead global SA techniques are needed. These global techniques are usually implemented using Monte-Carlo(MC) simulations and are, therefore, called Sampling-based methods. In this study sensitivity analysis is performed with LHS and partial rank correlation coefficient (PRCC) methods, The LHS method assumes that the sampling is performed independently for each parameter, although a procedure to impose correlations on sampled values has also been developed [5]. The sampling is done by randomly selecting values from each pdf (Fig. 7(A)). Each interval for each parameter is sampled exactly once (without replacement), so that the entire range for each parameter is explored (Fig. 7(A)). A matrix is generated (which we call the LHS matrix) that consists of N rows for the number of simulations (sample size) and of k columns corresponding to the number of varied parameters (Fig. 7(B)). The LHSmatrix (X) is then built by assembling the samples from each pdf. Each row of the LHS matrix represents a unique combination of parameter values sampled without replacement. The hypothetical model (in our case a parameter) is then evaluated, the corresponding output generated and stored in the matrix (Y). Each matrix is then rank transformed (X_R and Y_R). N model solutions are then simulated, using each combination of parameter values (each row of the LHS matrix, (Fig. 7(B))). The rank-transformed LHS matrix (X) and the output matrix (Y) are used to calculate the CCPearson, Spearman or rank correlation coefficient (RCC) and the partial rank correlation coefficient (PRCC)(Fig7(C)). Correlation provides a measure of the strength of a linear association between an input and an output. A CC between x_j and y is calculated as follows:

$$r_{x_j,y} = \frac{Cov\left(x_j,y\right)}{\sqrt{Var\left(x_j\right)Var\left(y\right)}} = \frac{\sum\limits_{i=1}^{N}\left(x_{ij}-\bar{x}\right)\left(y_i-\bar{y}\right)}{\sqrt{\sum\limits_{i=1}^{N}\left(x_{ij}-\bar{x}\right)^2\sum\limits_{i=1}^{N}\left(y_i-\bar{y}\right)^2}}, \tag{29}$$

with $j = 1, 2..., k$ and $r_{x_j,y}$ varies between -1 and 1, $Cov\left(x_j,y\right)$ represents the covariance between x_j and y while $Var\left(x_j\right)$ and $Var\left(y\right)$ are respectively the variance of x_j and y. If the data x_j and y have not been analyzed, then the coefficient r is called sample or Pearson CC (Fig7(C)). If the data are rank transformed, thus the result is a Spearman or rank correlation coefficient (also refers to Fig7(C)). Partial correlation characterizes the linear relationship between input x_j and output y after the linear effects on y of the main inputs are discounted. note that, the PCC between x_j and y is the CC between the two residuals $\left(x_j - \widehat{x}_j\right)$ and $\left(y - \widehat{y}\right)$, where $\widehat{x}_j$ and $\widehat{y}$

A

Mathematical model   **Output**

$$\dot{\mathbf{x}} = g\left(\mathbf{x}, \boldsymbol{\theta}\right), \mathbf{x} \in \mathbb{R}^2$$

$$\boldsymbol{\theta} \in \mathbb{R}^3, \boldsymbol{\theta} \equiv \left\{a, b, c\right\} \longrightarrow \quad y = f\left(\mathbf{x}; \boldsymbol{\theta}\right)$$

Latin Hypercube Sampling - LHS   **Sample size N=5**
Uniform and Normal pdfs

$$a \sim Unif\left(a_{\min}, a_{\max}\right)$$

$$b \sim Unif\left(b_{\min}, b_{\max}\right)$$

$$c \sim Normal\left(\mu_c, \sigma_c\right)$$

B

LHS MATRIX   **OUTPUT MATRIX**

$$X = \begin{bmatrix} a_1 & b_1 & c_1 \\ a_2 & b_2 & c_2 \\ a_3 & b_3 & c_3 \\ a_4 & b_4 & c_4 \\ a_5 & b_5 & c_5 \end{bmatrix} \longrightarrow Y = \begin{bmatrix} y_1 = f\left(a_1, b_1, c_1\right) = 5.2 \\ y_2 = f\left(a_2, b_2, c_2\right) = 7.9 \\ y_3 = f\left(a_3, b_3, c_3\right) = 3.1 \\ y_4 = f\left(a_4, b_4, c_4\right) = 6.4 \\ y_5 = f\left(a_5, b_5, c_5\right) = 0.8 \end{bmatrix}$$

Ranking   **Ranking**

$$X_R = \begin{bmatrix} 2 & 3 & 4 \\ 5 & 1 & 3 \\ 4 & 5 & 2 \\ 1 & 2 & 5 \\ 3 & 4 & 1 \end{bmatrix} \qquad Y_R = \begin{bmatrix} 3 \\ 5 \\ 2 \\ 4 \\ 1 \end{bmatrix}$$

C

Sampling-based sensitivity indexes

$$CC_{Pearson}\left(X, Y\right)$$

$$CC_{Spearman}\left(X_R, Y_R\right)$$

$$PRCC\left(X_R, Y_R\right)$$

Figure 7: Scheme performed for sensitivity analysis with LHS and PRCC methods [5],(A) Mathematical model specification (dynamical system, parameters, output) and the corresponding LHS scheme. Probability density functions (pdfs) are assigned to the parameters of the model (e.g. a, b, c). We show an example with sample size N equal to 5. Each interval is divided into five equiprobable subintervals, and independent samples are drawn from each pdf (uniform and normal)The subscript represents the sampling sequence.

are the following linear regression models:

$$
\begin{cases}
\widehat{x}_j = a_0 + \sum_{p=1}^{k} a_p x_p, \\
\widehat{y} = b_0 + \sum_{p=1}^{k} b_p x_p.
\end{cases}
\tag{30}
$$

with $p \neq j$

similarly to PCC, partial rank correlation (PRC) performs a partial correlation on rank-transformed data: x_j and y are first rank transformed, and then the linear regression models defined $\widehat{x}_j$ and $\widehat{y}$ are built. PRCC is a robust sensitivity measure for nonlinear but monotonic relationships between x_j and y, as long as little to no correlation exists between the inputs.

Periodicity and stochastic amplification

As mentioned previously, the ILM model discussed here lead to the existence of stochastic cycles (also called quasi-cycles) because it does not have a single period, but a distribution of period centered on an average value corresponding to the maximal amplitude of fluctuations. Therefore, a power spectrum density (PSD) of frequency distribution is essential for adequately capture the quasi-periodicity. A description of the stochastic fluctuations of the system requires consideration of higher-order terms in the Van Kampen expansion. In particular, a very good approximation is obtained only if the next to leading order is considered. In this way, we obtain linear Fokker-Planck equations given by:

$$
\frac{\partial \Pi}{\partial t} = - \sum_{i,j=1}^{3} a_{ij} \frac{\partial (\zeta_j \Pi)}{\partial \zeta_i} + \frac{1}{2} \sum_{i,j=1}^{3} b_{ij} \frac{\partial^2 \Pi}{\partial \zeta_i \partial \zeta_j}.
\tag{31}
$$

The coefficients a_{ij} and b_{ij} are given in appendix. The corresponding Langevin's equations for the temporal evolution of the normalized fluctuations of susceptible, infectious individuals and pathogen particle around equilibrium values (ξ, η, ϑ respectively) are

$$
\frac{d\zeta_i}{dt} = \sum_{j=1}^{3} a_{ij} \zeta_j + \lambda_i(t), (i,j = 1,2,3).
\tag{32}
$$

Where ζ_i $(i = 1,2,3)$ denotes the random deviation of system from the mean fields and $\lambda_i(t)$ $(i = 1,2,3)$ the Gaussian white noise with zero mean and a correlation function given by $\langle \lambda_i(t) \lambda_j(t') \rangle = b_{ij} \delta(t - t')$.

By Fourier transformation of these Langevin's equations, we are able to analytically calculate the power spectral densities (PSD) corresponding to the normalized fluctuations, which, is no longer dependent on the community size N. After averaging, the three expected forms of these PSD of susceptible pests, infected pests and spores around endemic equilibrium are given by

$$
\begin{aligned}
P_\phi(\omega) &= \left\langle |\xi(\omega)|^2 \right\rangle = \frac{b_{11}\omega^4 + \Gamma_\phi\omega^2 + \kappa_\phi}{|D(\omega)|^2}, \\
P_\varphi(\omega) &= \left\langle |\eta(\omega)|^2 \right\rangle = \frac{b_{22}\omega^4 + \Gamma_\varphi\omega^2 + \kappa_\varphi}{|D(\omega)|^2}, \\
P_\psi(\omega) &= \left\langle |\vartheta(\omega)|^2 \right\rangle = \frac{b_{33}\omega^4 + \Gamma_\psi\omega^2 + \kappa_\psi}{|D(\omega)|^2}.
\end{aligned}
\tag{33}
$$

The complete derivations of these PSDs and detailed descriptions about the functions $\kappa_i, b_{ij}, \Gamma_i$ and $D(\omega)$ depend on model parameters and defined in appendix C.

II.3.3   Spatial dynamic

Here, It is supposed that the population dynamics of the system cannot be only described in a local space. Thus to make the model more realistic we also suppose that individuals are allowed to migrate to nearest-neighbor patches if space is available. In addition to the processes describe in the non-spatial model, an individual is moved from the patch i to another patch label j at the constant rate as:

- Susceptible pest: $S_iE_j \rightarrow E_iS_j, E_iS_j \rightarrow S_iE_j$ at the rate μ_1.

- Infected pest: $I_iE_j \rightarrow E_iI_j, E_iI_j \rightarrow I_iE_j$ at the rate μ_2.

- A given spore can be displaced by rain, wind,or spray by another insect, animal: $C_iE_j \rightarrow E_iC_j, E_iC_j \rightarrow C_iE_j$ at the rate μ_3.

Small population size

In this section, we proposed a spatial stochastic version of the model. The mechanisms corresponding to birth, death, and infections describe above are assumed to be local that is only involved in a particular site, here the possibility of migration between nearest-neighbor patches is taken into consideration. It is also assumed that the inhabited patches, labeled by $i = 1, ..., \Omega$, and are defined as sites of a d-dimensional hypercubic lattice [121]. For applications, we are

interested in the case of a square lattice in two dimensions but we prefer to work with general d. One reason is that it is not any more complicated to do so, another justification is because our stochastic simulations have been carried out in $d = 1$ in order to achieve higher accuracy. Each patch possesses a finite carrying capacity, N which is the maximum number of individuals allowed per site. The number of susceptible, infected pests and spores in the patch i will be denoted by n_i, m_i and l_i respectively. There are therefore $(N - n_i - m_i - l_i)$ empty or vacant spaces, E, in the patch i. The transitions rate is given in two groups: the local part, corresponds to the transition probability given in Eqs. (17)-(20) adding a subscription i and scaled by Ω. And the migratory part is given by:

$$
\begin{aligned}
T\left(n_i + 1, n_j - 1 \,|\, n_i, n_j\right) &= \frac{\mu_1 n_j \left(N - n_i - m_i - l_i\right)}{z\Omega N}, \\
T\left(n_i - 1, n_j + 1 \,|\, n_i, n_j\right) &= \frac{\mu_1 n_i \left(N - n_j - m_j - l_j\right)}{z\Omega N}, \\
T\left(m_i + 1, m_j - 1 \,|\, m_i, m_j\right) &= \frac{\mu_2 m_j \left(N - n_i - m_i - l_i\right)}{z\Omega N}, \\
T\left(m_i - 1, m_j + 1 \,|\, m_i, m_j\right) &= \frac{\mu_2 m_i \left(N - n_j - m_j - l_j\right)}{z\Omega N}, \\
T\left(l_i + 1, l_j - 1 \,|\, l_i, l_j\right) &= \frac{\mu_3 l_j \left(N - n_i - m_i - l_i\right)}{z\Omega N}, \\
T\left(l_i - 1, l_j + 1 \,|\, l_i, l_j\right) &= \frac{\mu_3 l_i \left(N - n_j - m_j - l_j\right)}{z\Omega N}.
\end{aligned}
\tag{34}
$$

Here, z denotes the coordination number of the lattice that is the number of nearest neighbors of any given site. It needs to be included since it represents the choice of nearest neighbor j, once a patch i has been chosen.

System size expansion and stochastic amplification

The master equation is rewritten in two main contributions: the first part defined local mechanisms which correspond to the form given in non-spatial case adding a subscript i with a scaled Ω calling T_i^{loc} and the second one take migration into consideration T_{ij}^{mig}.

$$
\begin{aligned}
T_{ij}^{mig} &= \left(\varepsilon_{x_i}^{-1}\varepsilon_{x_j} - 1\right) T\left(n_i + 1, n_j - 1 \,|\, n_i, n_j\right) + \left(\varepsilon_{x_i}\varepsilon_{x_j}^{-1} - 1\right) T\left(n_i - 1, n_j + 1 \,|\, n_i, n_j\right) \\
&+ \left(\varepsilon_{y_i}^{-1}\varepsilon_{y_j} - 1\right) T\left(m_i + 1, m_j - 1 \,|\, m_i, m_j\right) + \left(\varepsilon_{y_i}\varepsilon_{y_j}^{-1} - 1\right) T\left(m_i - 1, m_j + 1 \,|\, m_i, m_j\right) \\
&+ \left(\varepsilon_{z_i}^{-1}\varepsilon_{z_j} - 1\right) T\left(l_i + 1, l_j - 1 \,|\, l_i, l_j\right) + \left(\varepsilon_{z_i}\varepsilon_{z_j}^{-1} - 1\right) T\left(l_i - 1, l_j + 1 \,|\, l_i, l_j\right).
\end{aligned}
\tag{35}
$$

Such that

$$\frac{dP_{n,m}(t)}{dt} = \sum_{i=1}^{\Omega} \left(T_i^{loc} P_{n,m}(t) + \sum_{j\in i} T_{ij}^{mig} P_{n,m}(t) \right), \tag{36}$$

where the notation $j \in i$ means that j is the nearest neighbor of i. The deterministic models is written as the 3Ω macroscopic equations given by

$$\dot{\phi} = r\phi(1 - \frac{\phi}{k}) - \alpha_1\phi\varphi - \beta_1\phi\psi + \mu_1 \left(\nabla^2\phi + \phi\nabla^2\varphi - \varphi\nabla^2\phi + \phi\nabla^2\psi - \psi\nabla^2\phi \right),$$

$$\dot{\varphi} = \alpha_2\phi\varphi + \theta\phi\psi - b_2\varphi + \mu_2 \left(\nabla^2\varphi + \varphi\nabla^2\phi - \phi\nabla^2\varphi + \varphi\nabla^2\psi - \psi\nabla^2\varphi \right), \tag{37}$$

$$\dot{\psi} = b_2\varphi - d_3\psi + \mu_3 \left(\nabla^2\psi + \psi\nabla^2\phi - \phi\nabla^2\psi + \psi\nabla^2\varphi - \varphi\nabla^2\psi \right).$$

where $i = 1, ..., \Omega$ and the symbols $(.)$ and ∇^2 denote the time derivation (scaled $\tau = t/\Omega$) and Laplacian operator (see appendix E for more details). The power spectral density is obtained by replacing a_{ij} by $\alpha_{k,ij}$, and b_{ij} by $B_{k,ij}$ in Eq.33, Details on $\alpha_{k,ij}$ and $B_{k,ij}$ are given in appendix E.

II.4 Transmission of disease between hosts (for some specific EPF)

II.4.1 Model description

The model presented by Anderson and May [82] describe the temporal changes in host and disease transmission based on the fact that, many pathogens undergo latent period within host before starting to produce transmission stage for horizontal transmission or infect their unborn offspring (vertical transmission) [82]. In our case where the vertical transmission is neglected, the new born is count in susceptible class. By adding spatial spread of infectious host the model can be rewrite as

$$\frac{\partial X}{\partial t} = a(X + M + Y) - bX - \beta XY,$$

$$\frac{\partial M}{\partial t} = \beta XY - (b + v)M, \tag{38}$$

$$\frac{\partial Y}{\partial t} = vM - (\alpha + b)Y + \mu\frac{\partial^2 Y}{\partial x^2}.$$

Where $M(t, x)$ denotes the latent class (infected but not yet infectious) at the time t in the location x, $Y(t, x)$ represents the number of infected insects spreading the infection. Insects are assumed to pass from latent into infectious class at a constant rate v. Susceptible Insects $X(t, x)$ become infected at the rate β, the birth process whereby new born are recruited in susceptible class occurs at the rate a, note that the offspring of infected hosts pass directly into infected class if

it is infected. Natural death are also assumed to die at the rate b, whereas μ is the spreading coefficient of infectious insects see Fig.(8). With some transformation Eq.38 takes the form
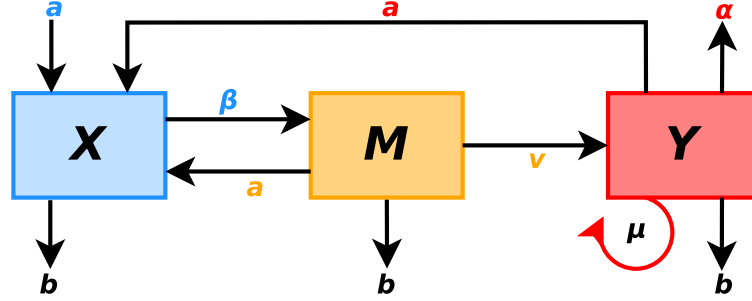
Figure 8: Flow diagram of disease transmission between insects pests

$$\frac{\partial^2 Y}{\partial t^2} - (\lambda_1 X + \lambda_2) Y - \lambda_3 \frac{\partial^2 Y}{\partial x^2} - \lambda_4 X - \lambda_5 \frac{\partial X}{\partial t} - \mu \frac{\partial^3 Y}{\partial x^2 \partial t} = 0,$$
$$\frac{\partial^2 X}{\partial t^2} + (\gamma_1 X + \gamma_2) Y + (\beta Y + \gamma_3) \frac{\partial X}{\partial t} + \left(\beta \frac{\partial Y}{\partial t} + \gamma_4 \right) X - a \frac{\partial Y}{\partial t} = 0. \tag{39}$$

where
$$\lambda_1 = \frac{\beta v \left(a - \alpha - 2b - v \right)}{a}, \lambda_3 = -\left(\alpha + b \right) \mu, \gamma_2 = -a \left(b + v \right), \lambda_5 = -\frac{v \left(\alpha + 2b + v \right)}{a},$$
$$\lambda_4 = \frac{v \left(a\alpha + 2ab + av - \alpha b - 2b^2 - bv \right)}{a}, \gamma_4 = -ab - av + b^2 + bv,$$
$$\gamma_1 = -\beta \left(a - b - v \right), \gamma_3 = -a + 2b + v, \lambda_2 = \alpha^2 + 2\alpha b + \alpha v + b^2 + 2bv + v^2.$$

Global analysis is really difficult by using linear methods or direct numerical simulation. To better analyze this equation, we need to transform and make some simplification to obtain a most useful and manageable equation. This can be done using multiple scale method [17, 18, 19, 128]. The idea is to introduce fast and slow variables into the equation Eq.39. In order to find solution in a weakly dissipation medium, the parameters $\lambda_2, \lambda_5, \mu, a,$ and γ_3 are also considered to be perturbed at the order ε^2 such that

$$\frac{\partial^2 Y}{\partial t^2} - \left(\lambda_1 X + \varepsilon^2 \lambda_2 \right) Y - \lambda_3 \frac{\partial^2 Y}{\partial x^2} - \lambda_4 X - \varepsilon^2 \lambda_5 \frac{\partial X}{\partial t} - \varepsilon^2 \mu \frac{\partial^3 Y}{\partial x^2 \partial t} = 0,$$
$$\frac{\partial^2 X}{\partial t^2} + (\gamma_1 X + \gamma_2) Y + \left(\beta Y + \varepsilon^2 \gamma_3 \right) \frac{\partial X}{\partial t} + \left(\beta \frac{\partial Y}{\partial t} + \gamma_4 \right) X - \varepsilon^2 a \frac{\partial Y}{\partial t} = 0. \tag{40}$$

Let assume a low-amplitude oscillation of the density of the individuals, such that

$$Y \to \varepsilon \varphi, X \to \varepsilon \psi. \tag{41}$$

Where, $\varepsilon << 1$ is a small perturbation. Using Eq.41, Eq.40 becomes

$$
-\psi\varphi\varepsilon\lambda_1 - \varphi\varepsilon^2\lambda_2 - \varepsilon^2\lambda_5\frac{\partial\psi}{\partial t} - \varepsilon^2\mu\frac{\partial^3\varphi}{\partial x^2\partial t} - \lambda_4\psi - \lambda_3\frac{\partial^2\varphi}{\partial x^2} + \frac{\partial^2\varphi}{\partial t^2} = 0,
$$
$$
\left(\frac{\partial\varphi}{\partial t}\right)\psi\beta\varepsilon - \varepsilon^2 a\frac{\partial\varphi}{\partial t} + \psi\varphi\varepsilon\gamma_1 + \varphi\left(\frac{\partial\psi}{\partial t}\right)\beta\varepsilon + \left(\frac{\partial\psi}{\partial t}\right)\varepsilon^2\gamma_3 + \psi\gamma_4 + \varphi\gamma_2 + \frac{\partial^2\psi}{\partial t^2} = 0.
$$
$$(42)$$

II.4.2 Multiple scale expansion

In order to study the modulation of a wave plane caused by nonlinear effects, we apply the method of multiple scale expansion to transform Eq.42. In this method one proceeds further by making a change of variables according to the new time and space scales $X_i = \varepsilon^i x$ and $T_i = \varepsilon^i t$, ε is a small perturbation, thus we obtain a perturbation series of operators from independent variables:

$$
\frac{\partial}{\partial t} \to \frac{\partial}{\partial T_0} + \varepsilon\frac{\partial}{\partial T_1} + \varepsilon^2\frac{\partial}{\partial T_2},
$$
$$(43)$$

$$
\frac{\partial}{\partial x} \to \frac{\partial}{\partial X_0} + \varepsilon\frac{\partial}{\partial X_1}.
$$
$$(44)$$

We look for modulated wave solution of the form

$$
\varphi = Ae^{i\theta} + A^*e^{-i\theta} + \varepsilon\left(C + Be^{2i\theta} + B^*e^{-2i\theta}\right) + O\left(\varepsilon^2\right),
$$

$$(45)$$

$$
\psi = Ee^{i\theta} + E^*e^{-i\theta} + \varepsilon\left(D + Fe^{2i\theta} + F^*e^{-2i\theta}\right) + O\left(\varepsilon^2\right).
$$

Where the amplitudes A, B, E, F as well as their respective corresponding complex conjugates A^*, B^*, E^*, F^* and C, D are functions of (T_1, T_2, X_1); and $\theta = (kX_0 - \omega T_0)$, where k is the wave vector and ω is the frequency of the wave. Substituting Eqs. (43),(44), and (45) into Eq. (42) and grouping terms in order of perturbation $\varepsilon^0, \varepsilon^1$ and ε^2, we obtain the following results:

At the zeroth-order of approximation ε^0, annihilation of terms in $e^{\pm i\theta}$ gives the dispersion relation of the form

$$
\omega^4 + \left(-k^2\lambda_3 - \gamma_4\right)\omega^2 + k^2\gamma_4\lambda_3 + \lambda_4\gamma_2 = 0,
$$
$$(46)$$

and

$$
E = \frac{\gamma_2 A}{\omega^2 - \gamma_4}.
$$
$$(47)$$

The dispersion relation gives the form in Fig. 9 if and only if $k^2\left(\alpha + b\right)\mu < v\left(\alpha + 2b + v\right)$.
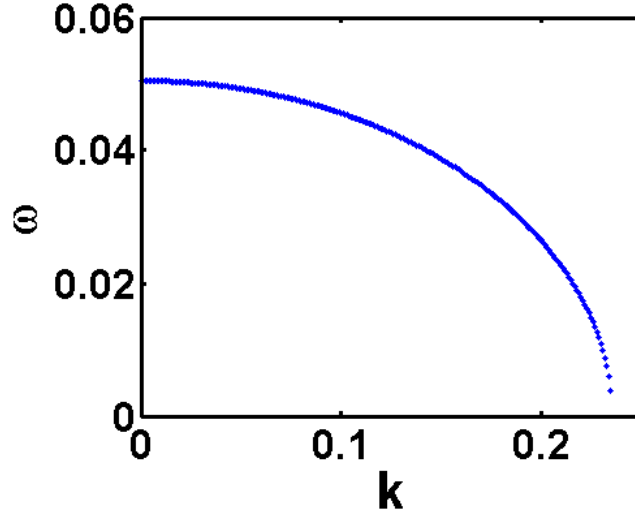
Figure 9: Dispersion relation. Using the parameters values:$a = 0.5, b = 0.02, v = 0.01, \mu = 0.5, \alpha = 0.25, \beta = 0.25$.

The first order of approximation ε^1, annihilation of terms in $e^{\pm i\theta}$ and $e^{\pm 2i\theta}$ gives respectively,

$$C = -2\,\frac{A^* A\,(\gamma_1\lambda_4 - \gamma_4\lambda_1)}{(\omega^2 - \gamma_4)\,\lambda_4}, \tag{48}$$

$$D = -2\,\frac{\lambda_1\gamma_2 AA^*}{(\omega^2 - \gamma_4)\,\lambda_4}, \tag{49}$$

$$\frac{\partial A}{\partial T_1} + \left(\frac{k\lambda_3}{\omega}\right)\frac{\partial A}{\partial X_1} = 0, \tag{50}$$

$$\frac{\partial E}{\partial T_1} = 0, \tag{51}$$

$$B = -\frac{\gamma_2 A^2\,\left(2\,i\beta\,\omega\,\lambda_4 - 4\,\omega^2\lambda_1 - \gamma_1\lambda_4 + \gamma_4\lambda_1\right)}{(16\,k^2\omega^2\lambda_3 - 4\,k^2\gamma_4\lambda_3 - 16\,\omega^4 + 4\,\omega^2\gamma_4 - \gamma_2\lambda_4)\,(\omega^2 - \gamma_4)}, \tag{52}$$

and

$$F = -\frac{\gamma_2 A^2\,\left(8\,i\beta\,k^2\omega\,\lambda_3 - 8\,i\beta\,\omega^3 - 4\,k^2\gamma_1\lambda_3 + 4\,\omega^2\gamma_1 - \lambda_1\gamma_2\right)}{(16\,k^2\omega^2\lambda_3 - 4\,k^2\gamma_4\lambda_3 - 16\,\omega^4 + 4\,\omega^2\gamma_4 - \lambda_4\gamma_2)\,(\omega^2 - \gamma_4)}. \tag{53}$$

At the second order of perturbation, the terms $e^{\pm i\theta}$ gives the following relation

$$iAk^2\mu\omega - iE\omega\lambda_5 + CE\lambda_1 + \lambda_1 DA + A^* F\lambda_1 + E^* B\lambda_1$$
$$+\lambda_2 A + \frac{\partial^2 A}{\partial X_1{}^2}\lambda_3 + 2i\omega\frac{\partial A}{\partial T_2} - \frac{\partial^2 A}{\partial T_1{}^2} = 0. \tag{54}$$

Using the new scales $\xi_i = X_i - v_g T_i$ and $\tau_i = T_i$, with velocity v_g and the above relation (Eq.54),

we get the modified complex Ginzburg–Landau equation.

$$i\frac{\partial A}{\partial \tau_2} + \frac{P}{2}\frac{\partial^2 A}{\partial \xi_1^2} + Q|A|^2 A + \frac{1}{2}iRA = 0 \tag{55}$$

where the coefficients P, Q and R are given by

$$P = -\frac{\lambda_3\left(k^2\lambda_3 - \omega^2\right)}{\omega^3}, Q = Q_r + iQ_i, R = R_r + iR_i \tag{56}$$

Q_r, Q_i, R_r and R_i represent the real and imaginary parts of the non-linearity coefficient and the dissipation coefficient respectively.

$$Q_r = \left(-\frac{\left(-\delta\gamma_4 + \rho\lambda_4\right)\gamma_2\delta}{\omega\left(\omega^2 - \gamma_4\right)^2\lambda_4} - \frac{\delta^2\gamma_2}{\omega\left(\omega^2 - \gamma_4\right)\lambda_4}\right)\beta^2$$
$$+\frac{\beta^2\delta\gamma_2\left(2k^2\omega^2\rho\lambda_3 - 2k^2\rho\gamma_4\lambda_3 - 2\omega^4\rho + 5/2\delta\omega^2\gamma_2 + 2\omega^2\rho\gamma_4 - \delta\gamma_2\gamma_4 + 1/2\rho\gamma_2\lambda_4\right)}{\left(\omega^2 - \gamma_4\right)^2\left(16k^2\omega^2\lambda_3 - 4k^2\gamma_4\lambda_3 - 16\omega^4 + 4\omega^2\gamma_4 - \lambda_4\gamma_2\right)\omega},$$

$$Q_i = -\frac{\gamma_2\beta^2\delta\left(4\,k^2\omega^2\lambda_3 - 4\,k^2\gamma_4\lambda_3 - 4\,\omega^4 + 4\,\omega^2\gamma_4 + \lambda_4\gamma_2\right)}{\left(\omega^2 - \gamma_4\right)^2\left(16\,k^2\omega^2\lambda_3 - 4\,k^2\gamma_4\lambda_3 - 16\,\omega^4 + 4\,\omega^2\gamma_4 - \lambda_4\gamma_2\right)}, \tag{57}$$

$$R_r = \mu\,k^2 - \frac{\lambda_5\gamma_2}{\omega^2 - \gamma_4},$$

$$R_i = \frac{\lambda_2}{\omega}.$$

Without loss the generality, Eq.55 can be rewritten as Eq.58.

$$i\frac{\partial A}{\partial \tau_2} + \frac{P}{2}\frac{\partial^2 A}{\partial \xi_1^2} + \beta\left(\tau_2\right)Q|A|^2 A + \frac{1}{2}iRA = 0, \tag{58}$$

where $\beta\left(\tau_2\right)$ is periodic time dependent infection rate defined by the following equation

$$\beta\left(\tau_2\right) = \beta_{av} + \beta_m \sin\left(\frac{2\pi}{T}\tau_2\right) \tag{59}$$

The periodic modulation modeled the impact of daily environmental condition on the EPF growth, germination, virulence and infection [29, 25, 3]. The variations of constants P/Q_r and PQ_r with respect to the wave vector k are represented in Fig. 10. Since the dispersion coefficient is real, if the infection rate (β_2) is constant or positive, the modulation instability depends on the sign

of PQ_r. The system is then stable for negative values of PQ_r, while it is unstable for positive values.
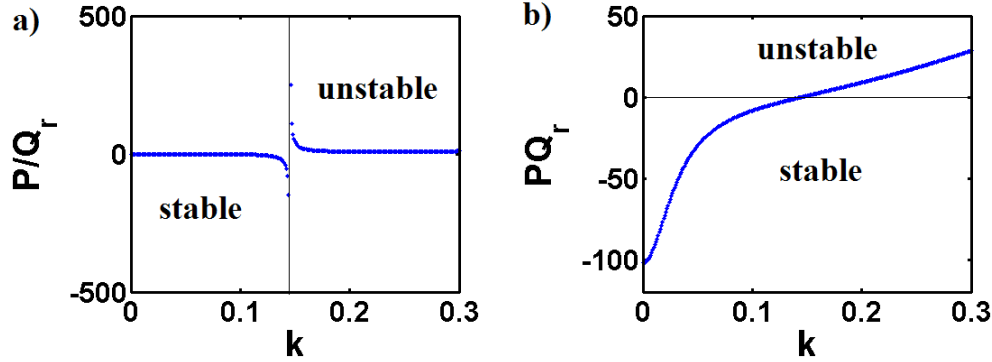
Figure 10: Modulational instability According to Benjamin-Feir instability criterion (a) P/Q_r, (b) PQ_r. Using the parameters values in Fig. 9 with $\omega = 0.2612$.

II.4.3 Linear stability analysis

The steady states of Eq. (58) can be destabilize through the exponential growth $\propto \exp\left(g\left(k\right)\xi_1\right)$ of the periodic modulations where k defined the spatial frequency. This perturbation can lead to parametric instability or Turing instability. We thus distinguished two cases meaning two types of modulation instability, in one side uniform transmission for all insects; this case is characterized by Turing instability. The other case refers to the parametric instability links to the parametric resonance due to the seasonal forcing.

For both case we considered the evolution of the perturbed solution $A\left(\xi_1, \tau_2\right) = A_0 + \eta\left(\xi_1, \tau_2\right)$, with the assumption $|\eta| << |A_0|$ and writing $\eta = p + iq$ with p and q real functions, we obtain the following linear system:

$$
\begin{cases}
-\dfrac{\partial q}{\partial \tau_2} + \dfrac{P}{2}\dfrac{\partial^2 p}{\partial \xi_1^2} - \left(\beta\left(\tau_2\right)Q_i A_0{}^2 + \dfrac{R_r}{2}\right)q + \left(3\beta\left(\tau_2\right)Q_r A_0{}^2 - \dfrac{R_i}{2}\right)p = 0, \\[2mm]
\dfrac{\partial p}{\partial \tau_2} + \dfrac{P}{2}\dfrac{\partial^2 q}{\partial \xi_1^2} + \left(\beta\left(\tau_2\right)Q_r A_0{}^2 - \dfrac{R_i}{2}\right)q + \left(3\beta\left(\tau_2\right)Q_i A_0{}^2 + \dfrac{R_r}{2}\right)p = 0.
\end{cases}
\tag{60}
$$

Defining the perturbations as

$$\tilde{p}\left(\xi_1, \tau_2\right) = \frac{1}{\sqrt{2\pi}}\int p\left(\xi_1, \tau_2\right)e^{ik\xi_1}d\xi_1, \quad \tilde{q}\left(\xi_1, \tau_2\right) = \frac{1}{\sqrt{2\pi}}\int q\left(\xi_1, \tau_2\right)e^{ik\xi_1}d\xi_1.$$

and using the Fourier transform of this system in the space variable ξ_1, we obtain the following

ordinary differential equation in frequency domain:

$$\frac{\partial}{\partial \tau_2} \begin{pmatrix} \tilde{p} \\ \tilde{q} \end{pmatrix} = \begin{pmatrix} -h_1(\tau_2) & -h_2(\tau_2) \\ g_1(\tau_2) & -g_2(\tau_2) \end{pmatrix} \begin{pmatrix} \tilde{p} \\ \tilde{q} \end{pmatrix},$$ (61)

with $h_1(\tau_2) = 3\beta(\tau_2) Q_i A_0{}^2 + 1/2 R_r$, $h_2(\tau_2) = \beta(\tau_2) Q_r A_0{}^2 - 1/2 R_i - 1/2 Pk^2$, $g_1(\tau_2) = 3\beta(\tau_2) Q_r A_0{}^2 - 1/2 R_i - 1/2 Pk^2$, and $g_2(\tau_2) = \beta(\tau_2) Q_i A_0{}^2 + 1/2 R_r$.

The case of uniform disease infection $(\beta_m = 0)$

In the case of uniform disease transmission $(\beta_2(\tau_2) = \beta_{av}$ and $\beta_m = 0)$. The underlying case refers to the situation where the impact of environmental conditions on the EPF development is neglected, meaning that the infection rate is the same at each time. Here, Eq.(61) is similar to a damped harmonic oscillator. And the eigenvalues with respect to the time variations is given by

$$\lambda_{1,2} = -2\beta_{av} Q_i A_0{}^2 - 1/2 R_r \pm i\Omega_{av}$$ (62)

where
$$\Omega_{av} = \left(\left(\frac{Pk^2}{2} - 2\beta_{av} Q_r A_0{}^2 + \frac{R_i}{2} \right)^2 - \beta_{av}{}^2 A_0{}^4 \left(Q_i{}^2 + Q_r{}^2 \right) \right)^{1/2},$$
is the average angular frequency. This expressions are used to determine the condition for the modulation instability. When Q_r is sufficiently high Ω_{av} can become imaginary for certain range of k. In this case if $|\Omega_{av}| > 2\beta_{av} Q_i A_0{}^2 + 1/2 R_r$ the perturbations grow exponentially with the growth rate

$$g(k) = -2\beta_{av} Q_i A_0{}^2 - 1/2 R_r + \Omega_{av}$$ (63)

The case of periodically modulated disease infection $(\beta_m \neq 0)$

We now consider the impact of all environmental fluctuations of EPF infection, such that the infection rate $\beta(\tau_2)$ is modulated by periodical forcing referring to the temperature fluctuations. The stability analysis corresponds here, to the stability analysis of Eq.(61) based on Floquet Theory since the system is τ_2-periodic with the period T. Thus, the stability depends on the so-called characteristic exponents or Floquet multipliers. The later are obtained by constructing the fun-

damental matrix $\mathbf{M}$ defined by

$$\begin{pmatrix} \tilde{p}(T) \\ \tilde{q}(T) \end{pmatrix} = \mathbf{M} \begin{pmatrix} \tilde{p}(0) \\ \tilde{q}(0) \end{pmatrix}, \tag{64}$$

using identity matrix as initial conditions. According to this theory, the dynamics is unstable only if there is one eigenvalue of the matrix $\mathbf{M}$ (Floquet multipliers) satisfying $|\lambda| > 1$. However, the equation (Eq. 61) cannot be solved analytically and some approximated results can be found, and provide an overview on the stability for small variation of β_m which, is necessary holds valid regardless of the specific shape of the forcing [129]. To do so, we considered the unperturbed case ($\beta_2(\tau_2) = \beta_{av}$, $\beta_m = 0$), When switching on the periodic infection rate (for small β_m) the eigenvalues are close to the eigenvalues in the unperturbed case. Remark that, (Eq. 61) is similar to the damped harmonic oscillator. By using an adequate change of variables, after integration, we obtained the eigenvalues of the Floquet map

$$\lambda_{av} = e^{\pm iT\Omega_{av}}, \tag{65}$$

Under resonant condition, $\Omega_{av} = m\pi/T$ and the corresponding spatial frequency is given by

$$k_m = \left(\frac{1}{P}(4A_0{}^2 Q_r \beta_{av} - R_i + 2(\beta_{av}{}^2 A_0{}^4 \left(Q_i{}^2 + Q_r{}^2\right)) + \frac{\pi^2 m^2}{T^2})^{1/2})^{1/2}, \tag{66}$$

and defined the condition for parametric resonance. We then distinguished two case: on the one side the resonant case ($\Omega_{av} = m\pi/T$), the system has two equal eigenvalues ($\lambda_{av}^+ = \lambda_{av}^- = \pm 1$), the lower and upper sign holds for m odd or even respectively. Both lie on the real axis. Under small perturbation, two eigenvalues can be obtained, one greater than one, one less than one in absolute value, meaning that the system (Eq.61) remains unstable. However, under very peculiar perturbations, the eigenvalues might also move along the circle. This imply that the system remains stable. whereas for($\Omega_{av} \neq m\pi/T$), the system is under off-resonance. we obtained two distinct and complex conjugate eigenvalues ($\lambda_{av}^+ = (\lambda_{av}^-)^*$), both lie on the unit circle, away from the real axis. Under small perturbation they remain on the unit circle, since they cannot move into the complex plane away from the unit circle, implying that the system remains stable. To resume when the infection rate is periodically modulated, the perturbation grow under resonant

condition. Returned to the original equation (Eq.61), the Floquet multipliers is giving by

$$\delta_{av} = \exp\left(T\left(-4\beta_{av}Q_iA_0{}^2 - R_r\right)/2\right)\lambda_{av}. \tag{67}$$

The eigenvalues (λ) of (Eq.61) might either moves inside the unit circle if

$$\exp\left(T\left(-4\beta_{av}Q_iA_0{}^2 - R_r\right)/2\right) < 1, \tag{68}$$

or outside if not. The blue colored region of Fig. 11 gives the couples (α, v) for which this
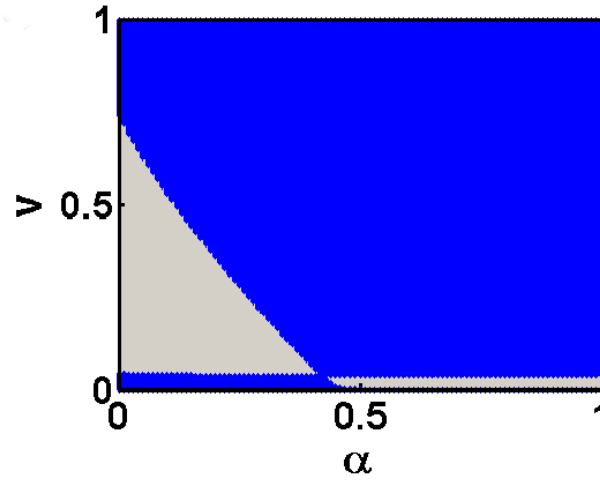
Figure 11: (a)Parameter space giving the stability analysis, the blue region corresponds to couples of points satisfying the condition given by Eq.68.

condition is satisfying. The eigenvalues lie on the circle of radius $r = e^{T\left(-4\beta_{av}Q_iA_0{}^2 - R_r\right)/2}\lambda_{av}$. In order to study the effect of the modulation β_m on the system stability, we considered through the rest of this paper the case (Eq.68) is satisfied. Then, the unperturbed eigenvalues (δ_{av}) lie in the complex plane either on the circle of radius $e^{T\left(-4\beta_{av}Q_iA_0{}^2 - R_r\right)/2} < 1$ (in off-resonance) or are two equal eigenvalues $\delta_{av}^+ = \delta_{av}^- = \pm\exp\left(T\left(-4\beta_{av}Q_iA_0{}^2 - R_r\right)/2\right)$ (on-resonance).

In this specific case the unstable wave number can lead to parametric modulation instability with the growth rate or gain $G(k)$ is given by

$$G(k) = \frac{\ln\left(\max|\lambda^{\pm}|\right)}{T} \tag{69}$$

II.5 A bref comment with related work

This thesis modeled species in an ecological or biological system where the interaction between individuals of species is of the predator-prey type. Furthermore, both individuals based models and deterministic models we have proposed are type of reaction-diffusion equation which have been extensively explored in chemical reaction [130], semiconductor transport [131], and in condensed matter physics which study the interaction of discrete entities for example, atoms, molecules or spins [121]. In these different studies, the model is a two-component reaction-diffusion equation of activator -inhibitor type displaying rich dynamics as well as spatiotemporal chaos, Turing instability and Hopf-Turing bifurcation [121, 130, 131]. However, In our knowledge the underlying mechanisms involving concepts such as nonlinear dynamics, instabilities can be view as a link between biology and physical sciences.

II.6 Numerical simulations

II.6.1 Nonlinear differential and partial differential equation

Considering a set of initial values, we can use an iterative scheme for approaching numerically the solution of the systems of nonlinear differential equations; to do so, we used the following generic form:

$$\dot{x}(t) = f(x, t),$$
$$x = (x_1(t),\ x_2(t), ..., x_n(t)) \tag{70}$$

and, determine the solution over the time interval $[0, T]$. In this study, we used the 4th Runge-kutta method to solve this equation. It reposes on the following numerical scheme:

$$x^{(k+1)} = x^{(k)} + \frac{h}{6}\left(L_1 + 2L_2 + 2L_3 + L_4\right) \tag{71}$$

with

$$L_1 = f(x, t),$$
$$L_2 = f\left(x + \frac{L_1}{2}, t + \frac{h}{2}\right),$$
$$L_3 = f\left(x + \frac{L_2}{2}, t + \frac{h}{2}\right),$$
$$L_4 = f\left(x + L_3, t + h\right). \tag{72}$$

Note that h is the time step and k is the index related to the temporal increment. Once the set of initial values $x^{(0)}$ are provided, the solutions are deduced from the iterative scheme given in Eq. (71). The other nonlinear partial differential Equations Eq. (9) and Eq. (37) have been solved using the RK4 method with a finite-difference approach on space. In this thesis, the algorithms were written in MATLAB or FORTRAN.

II.6.2   Monte-Carlo simulation / Gillespie algorithm

In 1976 Daniel T. Gillespie proposed an algorithm to exactly simulate the stochastic dynamics of chemical reactions [6, 132]. To describe this method, let us defined by $P\left(\tau, j \mid \mathbf{n}, t\right) d\tau$ the probability that the next event or reaction will occur in the interval $(t + \tau, t + \tau + d\tau)$ and will be of type j [6, 132]. We defined the propensity function for each mechanism as,

$$a_k\left(\mathbf{n}\right) = T\left(\mathbf{n} + \mathbf{v_k} \mid \mathbf{n}\right) \tag{73}$$

Where $\mathbf{v_k}$ is a vector representing the change in state caused by the k'th process. So for example for infection process (Eq. 18) $a_3\left(n, m\right) = \dfrac{2 I_1 n m}{N} + \dfrac{2 I_2 n l}{N}$ and $v_3 = (-1, +1)$. Assuming there are a total of q events (processes/ mechanisms), the probability that no event will happen by time τ is $\exp\left(-\sum\limits_{k} a_k\left(\mathbf{n}\right)\tau\right)$ [6, 132], then

$$P\left(\tau, j \mid \mathbf{n}, t\right) = a_j\left(\mathbf{n}\right) \exp\left(-\sum_{k=1}^{q} a_k\left(\mathbf{n}\right)\tau\right) \tag{74}$$

From this one can then use Monte-Carlo methods to generate a random pair (τ, j) according to the distribution $P\left(\tau, j \mid \mathbf{n}, t\right)$, which gives the time to the next event and the type. The simplest scheme for this is called Gillespie's direct method or the stochastic simulation algorithm [6, 132]. One step of the algorithm involves drawing a pair of uniform $[0, 1]$ random numbers, (r_1, r_2). The time to the next reaction is then given by

$$\tau = \frac{1}{a_0}\ln(1/r_1) \tag{75}$$

where $a_0 = \sum\limits_{k} a_k(\mathbf{n})$. Next we find $j \in [1, ..., q]$ from,

$$\sum_{k=1}^{j-1} a_k < r_2 a_0 \leq \sum_{k=1}^{j} a_k \tag{76}$$

Finally, at $t = t + \tau$ and the state $\mathbf{n}$, and propensities are updated to reflect the chosen event. This method is sufficient for simulating the stochastic model defined in the section I.4. The algorithm can be summed up as:

Step 0: Define each transition probability and the corresponding propensity.

Step 1: Calculate putative waiting times, $t_k = (1/a_k)\ln(1/r_k)$, for each reaction, where r_k is a uniform random number $]0, 1]$. This is essentially drawing times from an exponential distribution.

Step 2: Let j be the event whose putative time is least and set $\tau = \min\{t_k\}$.

Step 3: Update $t \to t + \Delta t_j$, update $\mathbf{n}$, recalculate $a_k(\mathbf{n})$.

Step 4: If $t < t_{stop}$ repeat from step 1, otherwise terminate the calculation.

II.7 Conclusion

In this chapter, first of all, we established and proposed nonlinear equations and a stochastic model which can well describe the dynamics of entomopathogenic fungi on the one side within insect host and, on the other side, within a pest population. After that, we gave different theoretical and numerical methods used for the analysis of both case studies. And the results obtained by using all these mathematical and numerical techniques are presented in chapter 3 and subsequently discussed.

RESULTS AND DISCUSSIONS

III.1   Introduction

This chapter present the main results obtained in this thesis. It is subdivided in three parts based on the intra-host dynamics of EPF, the temporal and spatio-temporal modelling of the EPF dynamics within a given host population with demographics noise effects. And finally analyze the interaction between infected pest population dynamic and disease growth dynamics.

III.2   within host dynamics of EPF

III.2.1   Spatiotemporal dynamics (1D simulations)

Figs.12(b)-(d) present the Turing instability parameter regions. For $d_{21} > d_{21}^c$, the unstable wavenumber resides between two critical values. This linear analysis of the homogeneous state enables us to determine whether the resulting wave is steady or oscillatory when we look at the imaginary part of the eigenvalues $\mathrm{Im}\,(\lambda_i\,(k))$. Steady patterns correspond to $\mathrm{Im}\,(\lambda_i\,(k)) = 0$ for all unstable modes k, in which case the instability is called Turing instability. However, when $\mathrm{Im}\,(\lambda_i\,(k)) \neq 0$ for an unstable mode at a nonzero k, the system is said to undergo wave instability, and the resulting pattern consists of traveling waves, but this behavior does not occur in this system.   The system was numerically solved using a fully explicit Euler method with a finite-difference approach on space and a temporal step size of $0.01t.u.$ (time units). No-flux boundary condition and positive random initial condition with amplitude of 0.01 over the endemic steady state were employed. The nonlinear diffusion term was approximated by a second-order finite difference algorithm. Spatiotemporal patterns were observed during simulations. The system shows stationary Turing patterns. This behavior is presented in Figs. 13. In panel (a) of this figure, the dispersion relation is plotted and it shows diffusion-driven instability. This behavior is modulated by stationary waves, whereas the space-time structures displayed in Figs. 13(b) are regular stationary stripes. The density of resources oscillates over time and it is reported in
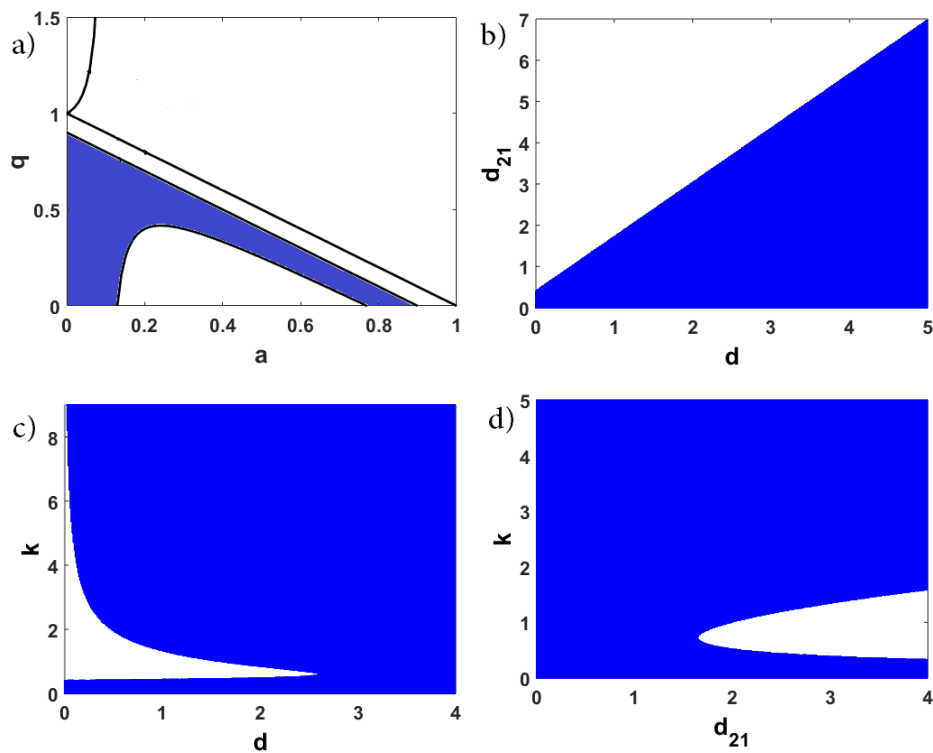
Figure 12: a) Stability diagram of the homogeneous steady state. The colored zone corresponds to stable region where $tr\left(\mathbf{J}\right) < 0$ according to the biological relevance conditions and thus, Turing instability can occurs in this region when diffusion are taken into consideration. Others panels show Turing instability parameters regions in the three parameters spaces b) $k = 1$; c) $d_{21} = 2.5$; d) $d = 1.2$. Here, colored zone is also stable regions obtained from a coupled of point with satisfy stability condition. Parameters values are $\varepsilon = 10.0, \beta = 0.47, a = 0.05; q = 0.5;$ for each case

Fig. 13(c) at two different points of space. The amplitude of the density of resources oscillates periodically in space (see Fig. 13(d)). In order to observe the role of the term of the birth regeneration rate of the resources on the system, the dynamics of the endemic equilibrium point was simulated in the absence of the logistic growth rate of resources. It can be noted that, when $\beta = 0$ (see Figs. 13(a),(e)-(f)), the resource density decreases and there is no pattern formation over time, whereas if $\beta \neq 0$, the species density varies at each site of space as t evolves, as shown in Fig. 13(b).
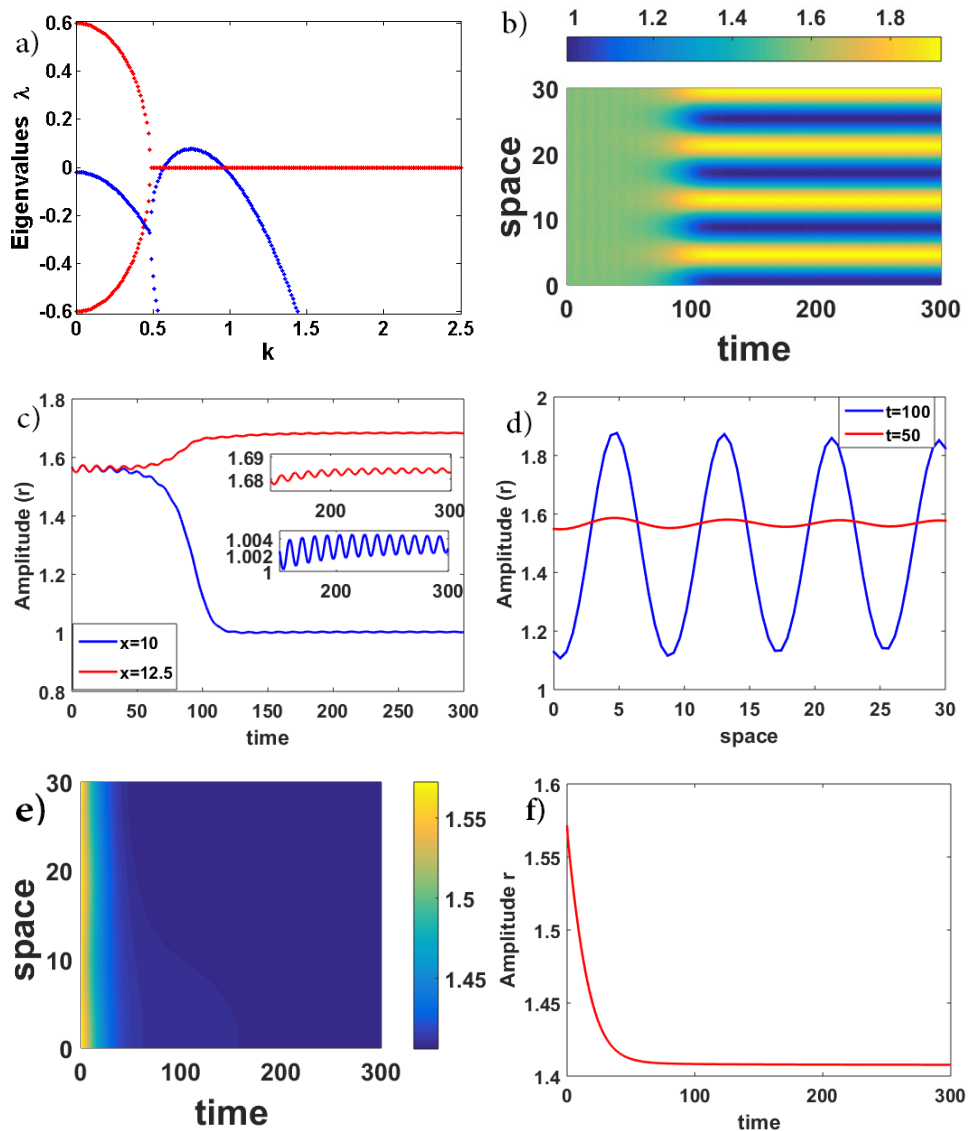
Figure 13: (a) stability analysis showing the complex part (red) and the real part (blue) of the eigenvalues. (b) 1D Turing pattern formation, the parameters values chosen is $\varepsilon = 10.0, \beta = 0.47, a = 0.06, q = 0.3, d = 1.2, d_{21} = 2.5$(c) blue and red curves are two oscillations located at space $x = 10$ and $x = 12.5$. (d) Displays the spatial amplitude modulation at the time given in the legend; (e),(f) show the influence of the regeneration rate of the EPF during growth ($\beta = 0$ in these case)

III.2.2   Spatial evolution of fungi within insects hemocoel (2D simulations)

In this section, the dynamics of EPF within their host is explored. The numerical simulations by using the fourth-order Runge–Kutta scheme in a two-dimensional grid with a grid spacing of 0.0625 and a time step of 0.001 were considered. Fig. 14 shows the temporal transients of the regular Turing pattern of the mycelia population at different evolution times. In Fig. 14(a), the oscillatory instability seems to emerge after perturbation of the steady state. After a few iterations, the formation of stripes was observed, but hot spots (isolated zones with a high density of mycelia) also occur (Figs. 14(b) and (c)). For a large number of iterations, we observed a formation of interlaced stripes with a high and low density of mycelia population (see Figs. 14(d) and (e)). The panel (f) of Fig. 14 shows more regular patterns with hot spots (isolated zones with a high density of mycelia) and cold stripes (isolated zones with a low population density of mycelia). This means that at a point in space, the density of species fluctuates in time. It was noticed that when the density of the spores is stationary, the density of mycelia and resources are also stationary but not equal; so the EPF impose their dynamics on the insect. After discarding the transients subsequent to a long time evolution of their dynamical systems, we could reach some specific Turing structures that are effectively heterogeneous stationary pattern (with permanent or fixed, or non evolving spatial profiles).   Fig. 15 shows the stationary spatial pattern of resource density. Fig. 15(a) shows double spots connected two by two with stripes, whereas an increase in the cross diffusion coefficient gives in Fig. 15(b) a pattern composed by single spots (see Fig. 15(b)). But Figs. 15(c) and (d) give the Turing pattern of resource density for two different values of probability that the extracted resources are allocated to the sporulation in the presence of the mycelium such that the panel (Fig. 15(c)) has regular structures composed by hot spots showing a hexagonal form. But by increasing the probability , high stripes connecting cold spots occurs (see Fig. 15(d)).

III.2.3   Time-dependent diffusivities (case $b \neq 0$ and $b_{21} \neq 0$)

This section analyzes the time-dependent diffusivities using Eq.9 that admits a periodic solution. To analyze the stability, we first plot in Fig. 16(b) the sum of the floquet's characteristic multipliers as a function of their products. In this figure the colored zone give the stability zone. By using the Newton–Raphson algorithm, we solve the polynomial equation in and thus plot the stability boundaries in the (Ω, k)- plane for the sets of the system parameters represented in Fig. 16(b),
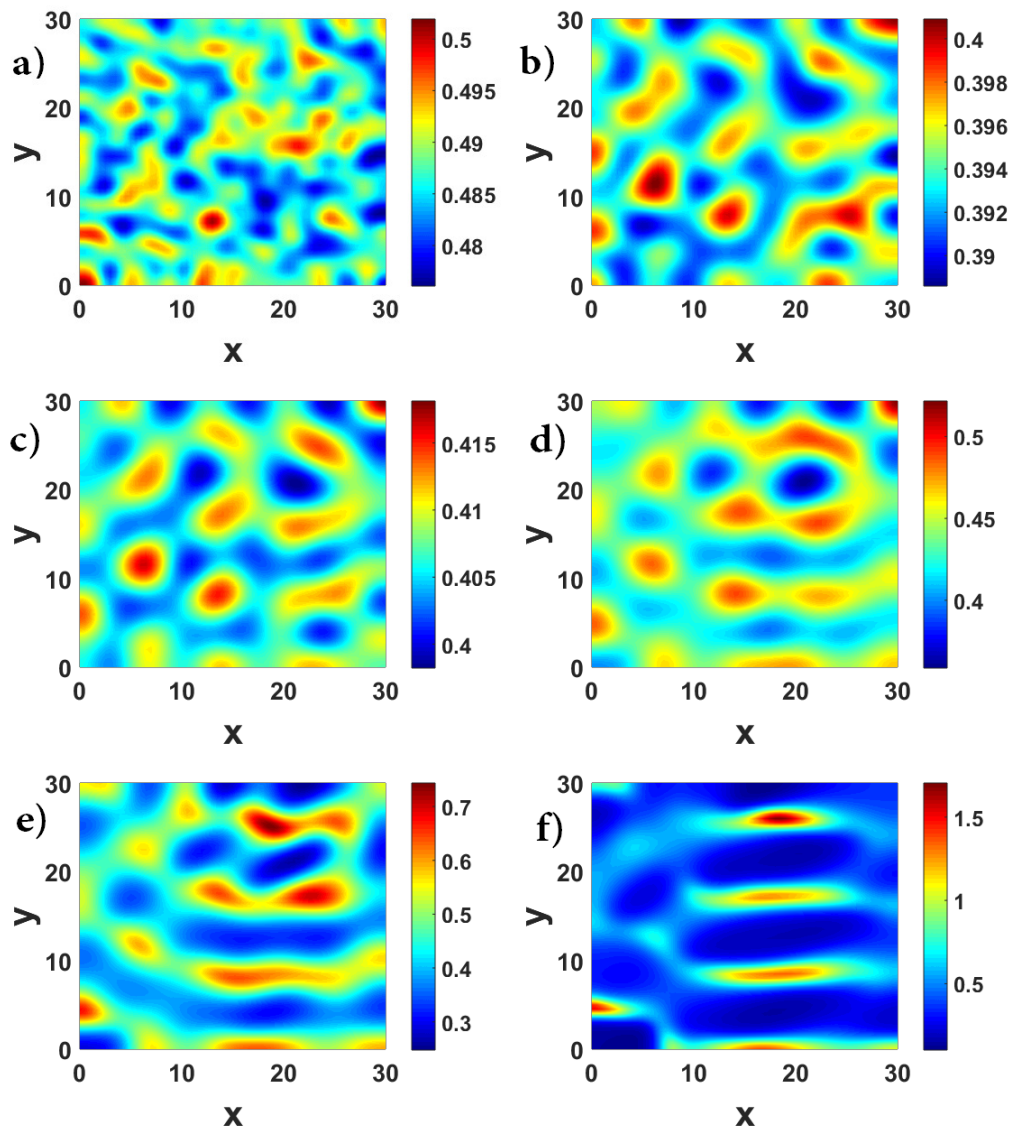
Figure 14: The processes of pattern formation of mycelia with parameters values chosen identical as in Fig. 13. Times iterations: (a)100, (b)500, (c)1500, (d) 4500, (e) 6500, (f) 8000. The colorbar shows the magnitude of the population density of mycelia.
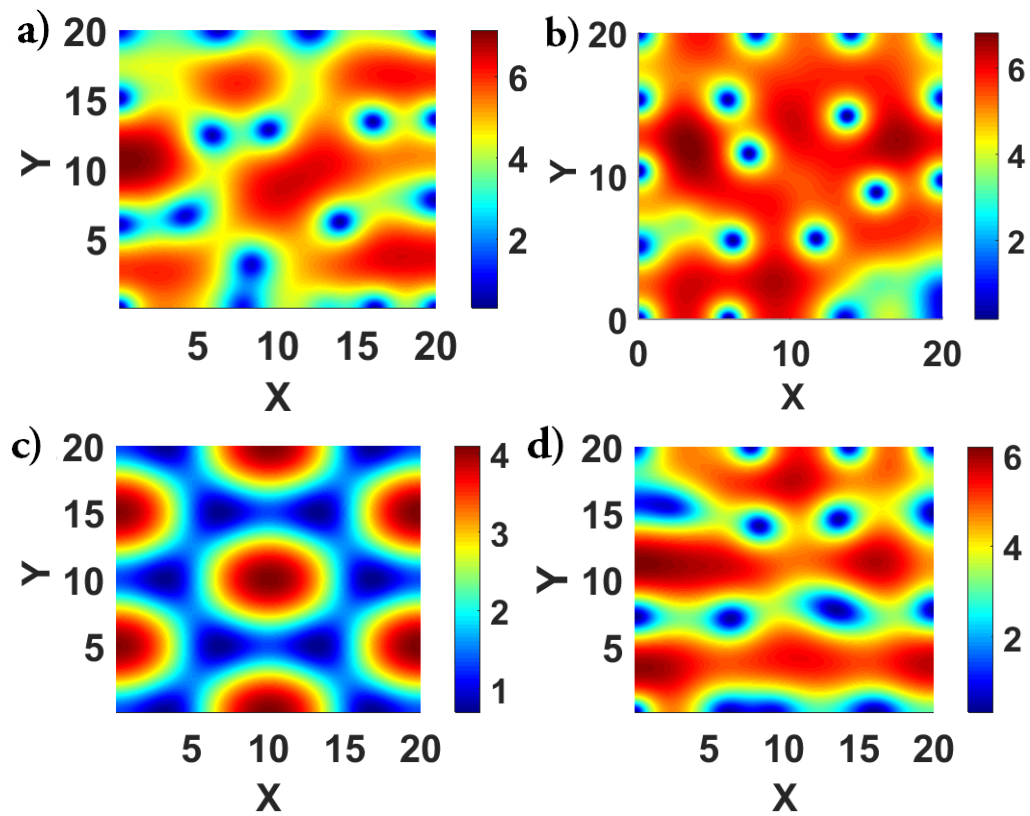
Figure 15: Stationary spatial patterns of resources density obtained through simulation of model Eq.9 on a squared spatial grid with no−flux boundary conditions for non-temporal diffusion. Gives Pattern formation of resources with parameters values (a) $\varepsilon = 10.0, \beta = 0.47, a = 0.05; q = 0.5; d = 1.2; d_{21} = 2.2$; (b) $\varepsilon = 10.0, \beta = 0.47, a = 0.05; q = 0.5; d = 1.2; d_{21} = 2.35$. Others panels give comparison patterns of the resources between two probabilities q with parameters values: $\varepsilon = 10.0, \beta = 0.47, a = 0.06; d_{21} = 2.25; d = 1.2.(c)q = 0.3$, (d)$q = 0.4$. The colorbar shows the magnitude of the population density of resources.

where I and III regions are stable domains. At first, the values are chosen and then, with the same parameter values used to derive Figs. 16(b) and fig11(c)shows that the perturbation is inhibited because both amplitudes of perturbation are tending to zero, and modulation by the diffusion periodicity can easily be observed. Second, if are taken in region II with the same parameter values, there is an increase in the amplitude of the perturbation. The system then exhibits diffusion driven instability (Fig. 16(d)), with the modulation through the periodicity of the diffusive coefficients. Our main objective here was to indicate via a stability analysis approach that, even in the case of periodic driven system, diffusion-driven instabilities can occur. This study enables us to say that in these conditions, Turing patterns could possibly occur. The occurrence of these patterns is not systematic. However, the diffusion-driven instability conditions, as obtained in Fig. 16(b) provide necessary but not sufficient conditions for these Turing profiles to emerge.
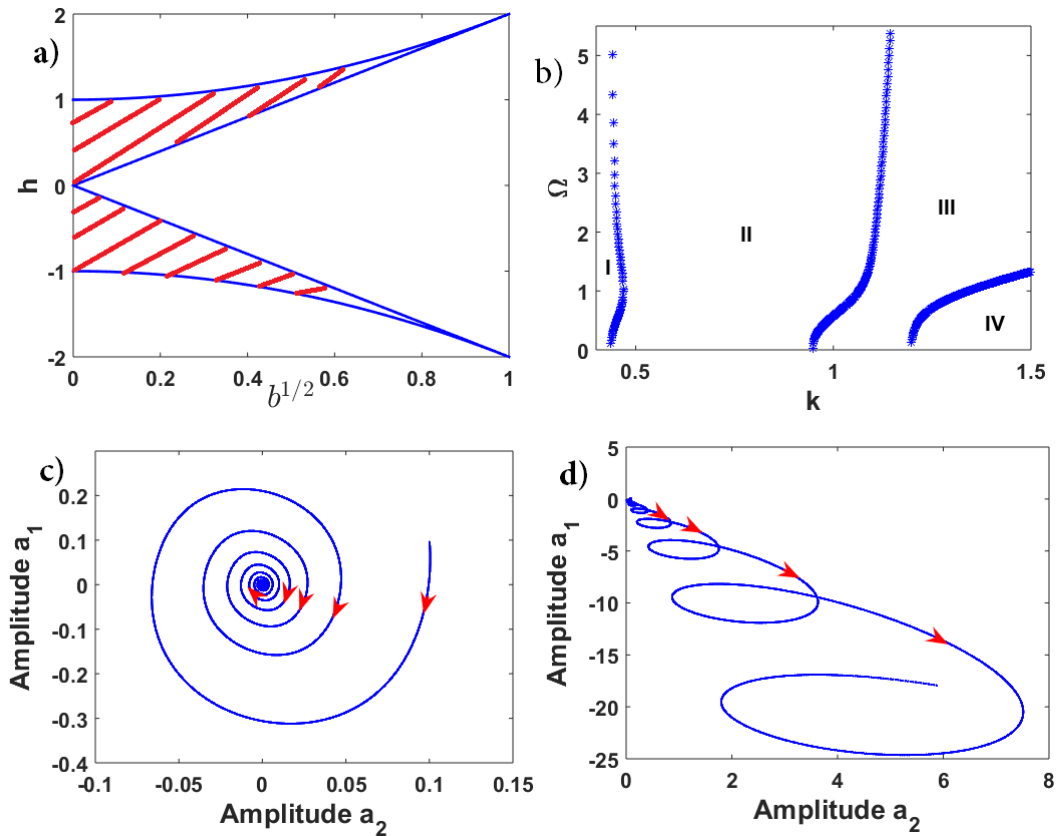
Figure 16: (a) stability boundaries region , (b) Transition curve between stability and Turing instability with parameters values: $\varepsilon = 10.0, \beta = 0.47, a = 0.05, q = 0.5, d_{21} = 2.5, b_{21} = 2, d = 1.2, b = 0.8, \theta_1 = \theta_2 = 0$; (c) Inhibition of Turing instability (both amplitude of perturbation tending to zero) ; (d) Turing instability (both amplitude of perturbation grow).

III.2.4 Discussions

A mathematical model (patch array model) based on the age of the resource allocation matrix to evaluate the effectiveness, in the biological control, of a group of fungi exploiting discrete resource spots in their hosts using the bang-bang resource allocation strategy with the assumption that the insect undergoes a nutritive stress has been developed [1]. studying the fitness of the spores, it was possible to establish that there is a link between the propagation and the persistence of the entomopathogenic fungus [1].The study proved that the success of the employed method depends on the types of fungus and the host species. The literature has revealed some established conditions in which the fungi behave like parasites in their host [1].

However, the study did not account for the interactions between the fitness of components. To improve the model presented in Ref. [1], a functional response, birth regeneration terms, constant, and time dependent diffusion terms were included in both insect and EPF evolution equations. The proposed model exhibits Turing instability. The nonlinear cross-diffusion term describes the tendency of the mycelia to move in response to a spatially decreasing resource density to maximize resource suppression. As presented in Ref. [133], Turing pattern can occur when cross-diffusion is taken into account.Note that its nonlinear diffusion rate must verify the threshold condition.

In the past, biological control models assumed that either only the spores disperse or the host population (infected and susceptible larvae) change their state [24, 134]. However, these studies show that the simplifications underlying the discrepancy between some of their theoretical results and the experimental results were mainly due to the presence of the diffusion coefficient on a certain species [24, 134]. To illustrate this, in ecology, when a species invades the territory of another species, the invader interacts with the native species and moves in response to external influences or the medium crowding;there is, therefore, a natural displacement of each species [62]. This is the reason why we asked ourselves the following question: " what would happen if mycelia (m) and the resources (r) are able to disperse simultaneously?" In order to investigate possible outcomes of such a situation, the proposed model took into account not only the reaction between these species but also the dissemination into the insect hemocoel.

In the presence of nonlinear diffusion, the models analyzed here show a destabilization of the homogenous distribution of mycelia and resources, and Turing pattern formation, which have important biological significance. In previous studies, similar phenomena were observed

in reaction–diffusion models applied to predator–prey dynamics [135, 136, 90, 137]. However, the proposed model presents additional features with three equilibrium points. When the endemic point is stable and the terms of spatial in-homogeneity are introduced,two cases can be distinguished: the case in which the system remains stable, and the situation in which the diffusion drives the instability. Such results corroborate well with what is found in the literature [98, 136].

Previous studies have shown that varying the key parameters of a system can induce the formation of rich patterns. In predator–prey models, increasing the value of prey growth rate generates similar behavior [90]. This is unlike our case, where PDE (Eq.9, $b_i = 0$) exhibits Turing structures only in the presence of a nonzero intrinsic growth rate (of resource) such that the system changes from a stable to an unstable steady state when the regeneration rate (β) passes through zero. A numerical simulation of the system shows the space and space-time plot of density for $\beta = 0$, which indicates a stable behavior of the resource species. For $\beta \neq 0$, the graph exhibits the oscillations of the species populations arising out of instability. It has also been shown that as time evolves, the spatial dynamics of fungus presents more regular structures. Some studies have shown that temporally periodic perturbations introduced in the diffusion rate have a weak stabilizing effect.Since such a phenomenon has been observed in predator–prey systems(with two species), it shows that the interval of the dispersal rate in which instability occurs is reduced when the variability is included in the diffusion coefficient [108, 116]. On the contrary, the developed model always exhibits stable and unstable regions, but both amplitudes of perturbation do not rapidly tend to zero in the case of stability. Furthermore, it can be noticed that varying the diffusion coefficient has a strong stabilizing effect. The temporal forcing parameters k and Ω in the problem provide a transition zone for the occurrence of Turing instability. It appears that in addition to destabilizing the equilibrium points, a periodic perturbation of the diffusion coefficient provides a better optimization of biological control in the sense that it could be better oriented from this new variation. Therefore, it is possible that the reaction–diffusion models between infected and uninfected larvae and spores are insufficient to determine more precisely the conditions for the success of this spatio-temporal biological control [24, 134], because optimizing the spatial growth of the EPF ensures good control.

Turing instability corresponds to the growth of the EPF and,therefore, to the death of the insect host. Naturally, if the regeneration rate of the insect's resources is nil, the density of

resources decreases to a threshold, but does not necessarily induce the death of insects. However, the inability of mycelia to use these resources can lead to a failure of biological control [42], thus explaining why in the situation where the mycelia density decreases, there is no intra-host growth. In the case of the two-dimensional spatial domain,different behaviors of the system are observed at different times when parameters are varied in Turing regions. In particular, it is proved that the presence of the nonlinear diffusion term produces instability in cases only where there is space and time modulation.

III.3 EPF outbreaks within host population

III.3.1 Extinction probability of insects pests and persistence of EPF

It was considered that there exists a set of stationary, spatially uniform solutions of (17)-(20). This allowed us to obtaining three singular points. The only endemic equilibrium point is $E^{SIC} = (\phi^s, \varphi^s, \psi^s)$ which has a biological relevance only if $k(\theta b_2 + \alpha_2 d_3) - b_2 d_3 > 0$ conditions that will be applied throughout the rest of this study.
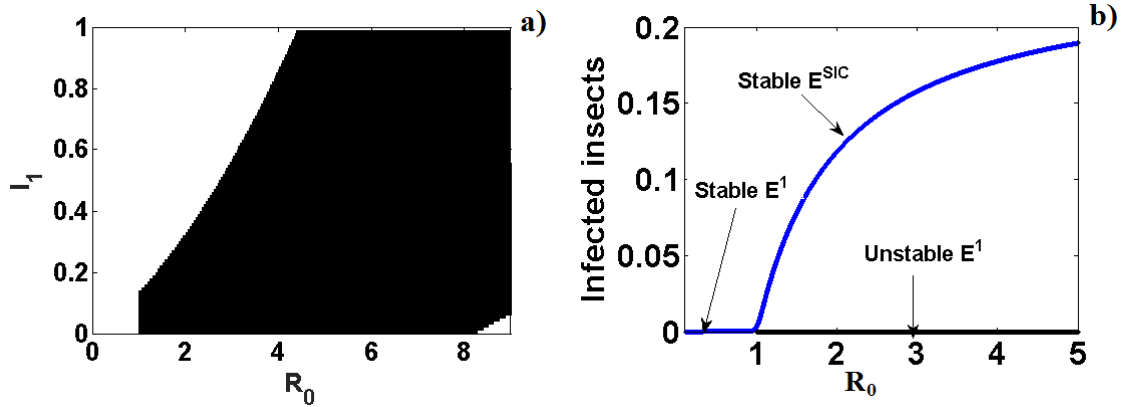
Figure 17: Stability diagram of the endemic steady state, the colored zone corresponds to stable region according to the biological relevance conditions and the coupled of point with satisfy stability condition in the parameters spaces. b) Transcritical bifurcation at R_0. Parameters values are $d_1 = 0.05, b_1 = 0.25, b_2 = 0.15, d_3 = 0.1, I_2 = 0.05$; for each case

To make this analysis more easy, the basic reproduction number R_0 defining the expected number of secondary infections caused by a single infected case, is introduced from the relevance biological conditions(see details in Appendix A). In our model, when $R_0 < 1$, the endemic equilibrium point do not have a biological relevance and the EPF population density will die out with time and cannot reduce the pest population; whereas for $R_0 > 1$, the introduction of EPF

can lead to a targeted spread, the endemic equilibrium point exists and can be stable/unstable. The color zones of Fig17 (a) display stability region of the steady state according to the relevance of the conditions given above. The parameter space (R_0, I_1) show the zone where the steady state exists and are unstable, so that EPF can invade insects pest population. Fig17 (c) shows that, transcritical bifurcation occurs at $R_0 = 1$ and changes the stability from the trivial steady state (disease free equilibrium E^1) to the endemic equilibrium. More clearly when $R_0 < 1$, E^1 is stable. The underlying steady state becomes unstable for $R_0 > 1$ corresponding to the black colored area of panel (a). At threshold basic reproduction number $R_0 = 1$ the infected insect population can invade the susceptible population, and the resulting free disease equilibrium system becomes unstable. Because R_0 and I_1 are proportional, R_0 can be sufficient to describe dynamics of the systems [?]. Therefore, the fundamental question here is: ***How to maintain*** R_0 ***always greater than one?*** To answer this question, the sensitivity analysis of the basic reproduction number R_0, is conducted by a Latin hypercube sampling (LHS) on combination with a partial rank correlation coefficient (PRCC) [5]. This method is useful to identify parameters that affect the quantity R_0. The input models parameters $k, \theta, \alpha_2 or I_1, b_2, d_3$ from which R_0 depends are randomly and uniformly distributed between their lower and higher values into Q - equal probability intervals and subsequently used to compute the LHS matrix of five (number of input parameters) columns with Q lines. The basic reproduction number R_0 is evaluated as a corresponding output matrix. These matrices are rank - transformed to calculate the partial rank correlation coefficient (PRCC) which give the sensitive index of R_0 associated to each parameter [5]. The parameters which have the sensitivity indexes closer to, ± 1 should significantly affect R_0. The more a parameter is tending to minus one, the more it has a reductive effect on R_0 and the parameters for which the PRCC is close to one increase the basic reproduction number. So, the resting rate of spore d_3 decrease the basic reproduction number Fig18(a). It is also easy to see that, the carrying capacity and the fraction of susceptible insect pest have the most important augmentative effect on the basic reproduction number. This affects the logistic growth of others species in this BC systems. This is in agreement with the investigation [60], where it is showed that in the BC using entomopathogenic against nematodes pests can be efficiently used to control the host population only if the host's reproductive rate is also regulated in a density-dependent manner. A comparison between ILM and deterministic systems equations obtain in van Kampen approximation, shown through a numerical simulation, sustained oscillations of all species

(Fig.18 red line). Whereas the deterministic equations models showed damped oscillations (see Fig18(dark and blue dotted line)), similar result was observed [65, 81, 138, 87]. It is the expected long-term behavior for host- vectors models [65].
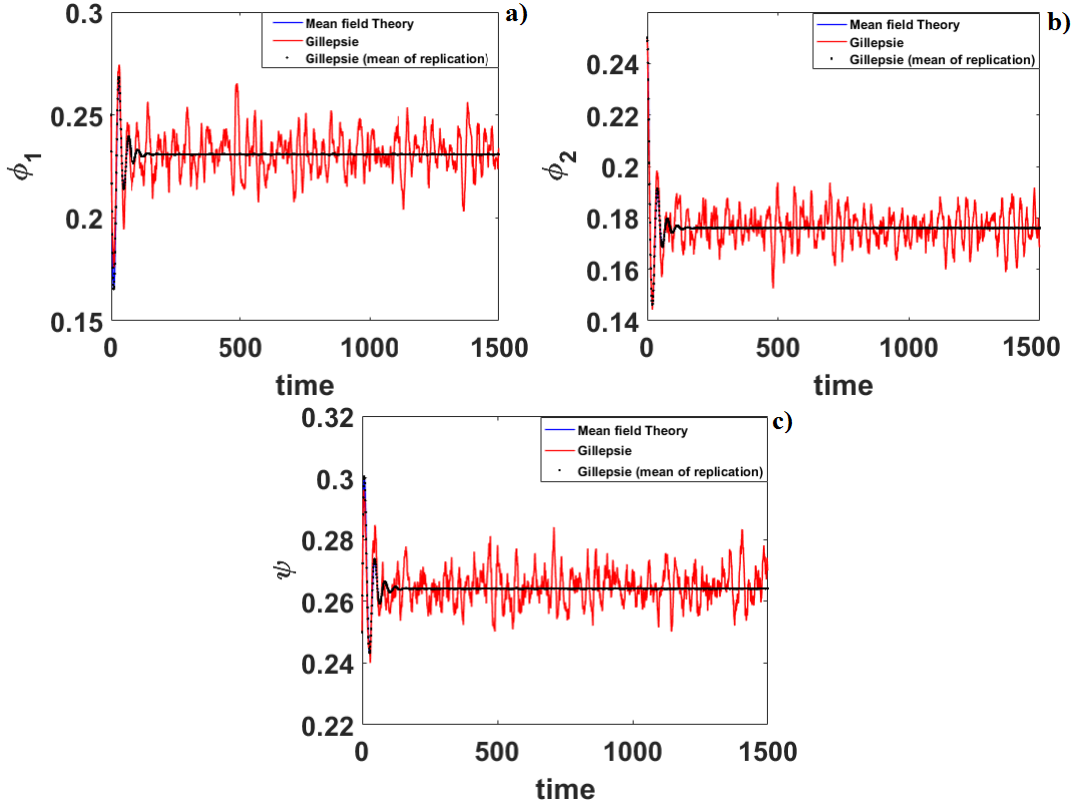
Figure 18: These panels show susceptible (ϕ), infected pest (φ) and pathogen (ψ) population densities as a function of time ((a), (b) and (c) respectively) for $N = 10000$. The red line is the average of time series of 100 replications generated from the ILM (Eq.(17) to (Eq.20)) using Gillespie Algorithm [6], the dashed dark line is the average of the species density time series from 10000 replicates generated from the ILM and is almost indistinguishable with the continuous blue line which corresponds to the deterministic equations from mean-field approximation simulated with a classical Runge-Kutta algorithm. The parameters used in the simulations are:$b_2 = 0.15$, $d_3 = 0.1$, $I_1 = 0.25$, $d_1 = 0.05$, $b_1 = 0.25$, $I_2 = 0.05$.

In order to find required conditions under which the pathogen agent goes to large outbreak within insect population, we make the sensitivity analysis of the basic reproduction number R_0 and the extinction probability of EPF I_1. The Parameters which have the sensitivity indexes closer to, ± 1 should significantly affect the main parameter (R_0 or/and I_1). The more a parameter is tending to minus one, the more it has a reductive effect on the main parameter and the parameters for which the PRCC is close to one increase R_0/I_1. So, the resting rate of spore d_3 decrease the basic reproduction number Fig. 19(a). It is also easy to see that, the carrying capacity and the fraction of susceptible insect pest have the most important augmentative effect

on the basic reproduction number. This affects the logistic growth of others species in this BC systems. This is in agreement with the investigation [62], where it is showed that in the BC using entomopathogenic nematodes pests can be efficiently used to control the host population only if the host's reproductive rate is also regulated in a density-dependent manner. However, the sensitivity analysis of the probability of pest extinction is given in Fig. 19(b). In contrast to other parameters, the sensitivity indexes for α_2, θ are negative; meaning that they are decreasing on s_1. It is easy to remark that the proportion of infected pest's death b_2 and the rate d_3 of spore become resting stage have a large effect on increasing extinction probability because these spores have ability to be reactivate when conditions are favorable.

III.3.2 stochastic fluctuations

A description of the stochastic fluctuations of the system requires analyzing the power spectrum density. In Fig. 19(c), one can remark a very large amplification of these stochastic fluctuations for the infected host species. The system has tendency to oscillate at greater amplitude at some frequencies rather than at others. Internal noise arises from demographic stochasticity contained in the individual's processes and leads to the resonant effect. By using the expression for the PSD for the infected insects, the basic reproduction number effects on the periodicity of the pest's outbreaks is examined. The Fig. 19(d) shows that as R_0 moves from unity, the amplitude of PSD decrease whereas the width increases. The width is important as it shows how coherent the cycles are: the smaller the width is, the longer cycles remain in phase. So, for R_0 tending to one the power spectra present a large peak at a preferred frequency different to zero corresponding to the irregular dynamics. In Fig19 (c), the very large amplification of these fluctuations is remarkable and almost exceptionally important for the infected host species. The system has tendency to oscillate at a greater amplitude at some frequencies rather than at others. Internal noise arises from demographic stochasticity contained in the individual's processes and leads to the resonant effect. By using the expression for the PSD for the infected insects, the basic reproduction number effects on the periodicity of the pest's outbreaks is examined. The Fig19(d) and (e) shows that as R_0 moves from unity, the amplitude of PSD decrease whereas the width increase. The width is important as it shows how coherent the cycles are: the smaller the width is, the longer cycles remain in phase. So, for R_0 tending to one the power spectra present a large peak at a preferred frequency different to zero which corresponds to the irregular dynamics. This
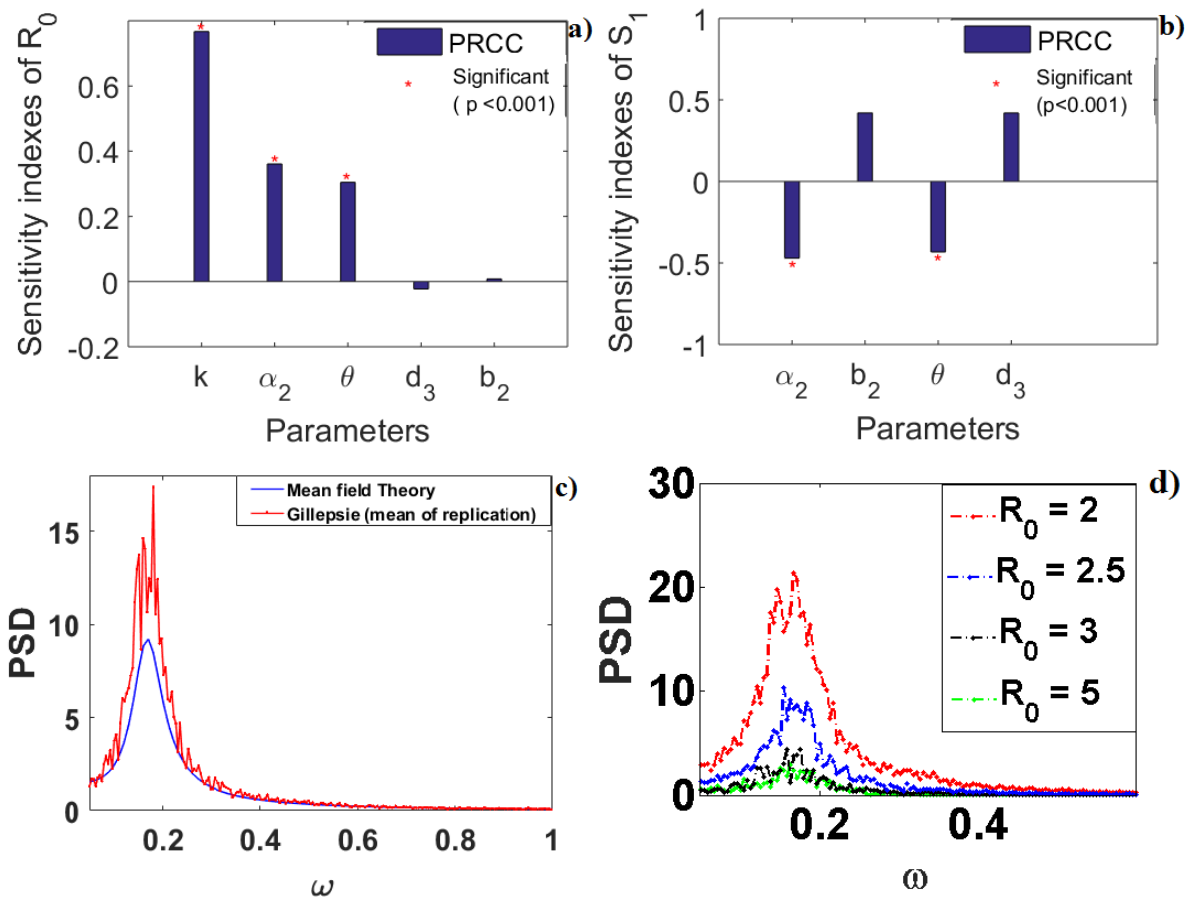
Figure 19: a) Sensitivity analysis of the number of secondary infections (R_0) results, b) Sensitivity analysis of the number of secondary infections (S_1) results. Sample size $Q = 1000$. The symbol ($*$) denotes PRCCs that the p-values are significantly different from zero, c)numerical and theoretical predictions of the power spectral density of infected insects Eq.**??** for a total number of species using the same parameters values five in Fig. 18, d)effect of the basic reproduction number on the power spectral density of infected insects

increase stochasticity in the smaller systems, but also the fade-out boundary, where extinction and re-colonization events start to have an impact on the dynamics [87]. However, the PSD of the deterministic case show that when R_0 increases the amplitude of the power spectral density decreases. And a light shift of resonant frequency is observed.

III.3.3   Influence of Spatial dynamics on the EPF dynamics

When migration of species is considered, we first make the stability analysis to anticipate on the system dynamic. The linear analysis of the homogeneous state is also able to determine whether the resulting wave is steady or oscillatory by looking at the imaginary part of the eigen-values $\mathrm{Im}\,(\lambda_i\,(q))$. Steady patterns correspond to $\mathrm{Im}\,(\lambda_i\,(q)) = 0$ for all unstable modes q, the case in which the instability is called a Turing instability. When $\mathrm{Im}\,(\lambda_i\,(q)) \neq 0$ for an unstable mode at a nonzero q, the system exhibit a wave instability as the resulting pattern will consist of traveling waves, or at the zero q, this conditions leads to bifurcation [88, **?**]. The present study also suggests that the total size of the population can have a relevant effect in the oscillation features. The dispersion relation is shown in Fig20. The Fig20(a) show that adding the migration processes lead the systems to go over three possible dynamics. Region (I), at zero wave number the eigenvalues is positive and thus is above the threshold $\mathrm{Re}\,(\lambda\,(q=0)) = 0$. The system exhibits Hopf bifurcation mode. In region II, the real part of the dominant eigenvalues is negative and defined a stable dynamics. With oscillation frequency defining by $\mathrm{Im}\,(\lambda\,(q)) \neq 0$. The region III pass through the condition for Turing instability but with $\mathrm{Re}\,(\lambda\,(q)) < 0$ describing damped Turing modes. From region I to II, there is a bifurcation point satisfying the condition $\mathrm{Re}\,(\lambda\,(q)) = 0$ and $\mathrm{Im}\,(\lambda\,(q)) \neq 0$ with $q \neq 0$. The latter condition gives the threshold of Hopf-Turing bifurcation. These unstable modes occur for selected parameter values (see Fig.20(b)). Unlike to the temporal model (17)-(20) Hopf-damped Turing bifurcation dynamics occurs for the contagion rate threshold $I_1 = 0.305$. By using Gillespie algorithm mentioned above and the fully explicit Euler method with a three-point approximation with no-flux boundary conditions, we compare numerically the stochastic model (17)- (20) and (22) and the deterministic model (37). As shown in Fig.21, the same phenomenon of sustained oscillations and damped oscillations observed above in local dynamics occurs here, from mathematical perspective the similar behavior appear in the [90]. The discrete version seems to exhibit slower dynamic compared to its continuous analog.

These space components also have a large influence on the power spectral density. It is clear that the migration contributions make a significant different in the both spectra. It is observed that in infected insects pest's spectra especially, there are a large peak at a nonzero value of ω depending to the k-values as shown in Fig. 22. So, resonant behavior still occurs in this spatial model just as it did in the non-spatial case. The more k increases, the peak decreases although the migration rate differs among all the three species. The present study also suggests that the total size of the population can have a relevant effect in the oscillation features. When varying the total number of population, it is observed in Fig. 23 that, there exists a spatial amplification; secondly, when the population's size increases, the pathogenesis period is shifted to lower central frequencies. It is observed that in infected insects pest's spectra especially, there are a large peak at a nonzero value of ω depending to the q-values as shown in Fig22. So resonant behavior still occurs in this spatial model just as it did in the non-spatial case. The more q increases, the peak increases although the migration rate differs among all the three species.

The results presented in Fig23 and Fig24 aim to show the effect of total population size on the power spectra and it spatial distribution respectively. These figure show the PSD of infected insects pests obtained from direct analytic calculations with $N = 500, 1000, 5000$ and $N = 15000$. The population size has an effect on the power spectra in two ways: at first, the existence of a spatial amplification; second, when the population size increase, the pathogenic period is shifted to lower central frequencies. This means that the frequency of oscillation depends on the total number of individuals.

III.3.4 Discussions

This study proposed a model to understand the entomopathogenic fungi outbreak within insect population. Based to the fact that demographic processes are inherently random, an individual level model is proposed here, in comparison to the deterministic model, in order to determine the most appropriate or useful approach which better mimic the dynamic occurs between the both species. In addition, because the outbreak of EPF is related to the instability and the persistence of EPF within the insect habitat, stability conditions and the extinction probability are investigated.

Natural population dynamic is controlled by random fluctuations. These fluctuations among individuals within populations are often caused by birth and death events and usually
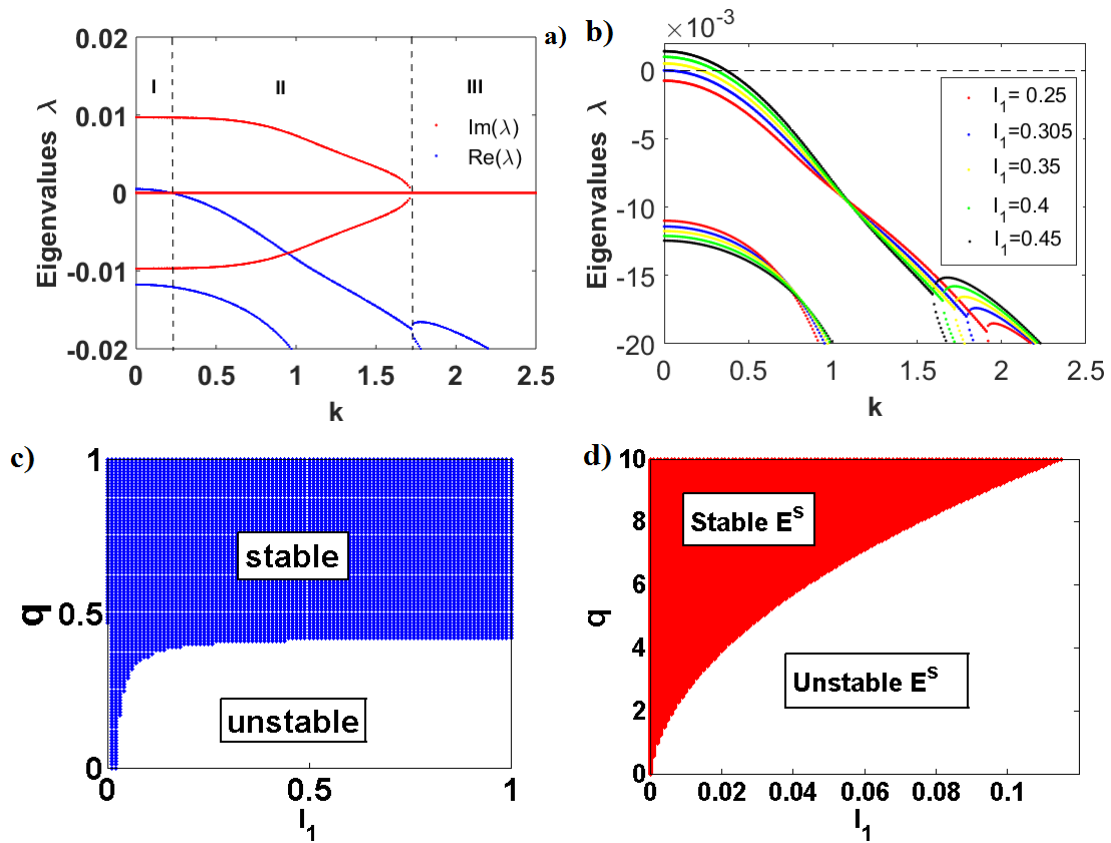
Figure 20: Linear stability analysis showing (a) the complex part (red) and the real part (blue) of the eigenvalues. H: Hopf-bifurcation with $\mathrm{Re}\left(\lambda\left(q\right)\right) > 0$ and $\mathrm{Im}\left(\lambda\left(q\right)\right) > 0$ at $q = 0$, DT: damped Turing with $\mathrm{Re}\left(\lambda\left(q\right)\right) < 0$ and $\mathrm{Im}\left(\lambda\left(q\right)\right) = 0$ at $q \neq 0$ (b) the real part of the eigenvalues for five different values of I_1. (c) Linear stability analysis around the endemic steady state. (d) Linear stability analysis around the free-disease steady state. Using the same parameters values:$\Omega = 500$, $N = 15000$, $b_2 = 0.15\Omega$, $d_3 = 0.1\Omega$, $I_1 = 0.31\Omega$,$I_2 = 0.05\Omega$,$d_1 = 0.05\Omega$, $b_1 = 0.25\Omega$, $\mu_1 = 0.6\Omega$,$\mu_2 = 0.4\Omega$, $\mu_3 = 0.2\Omega$.
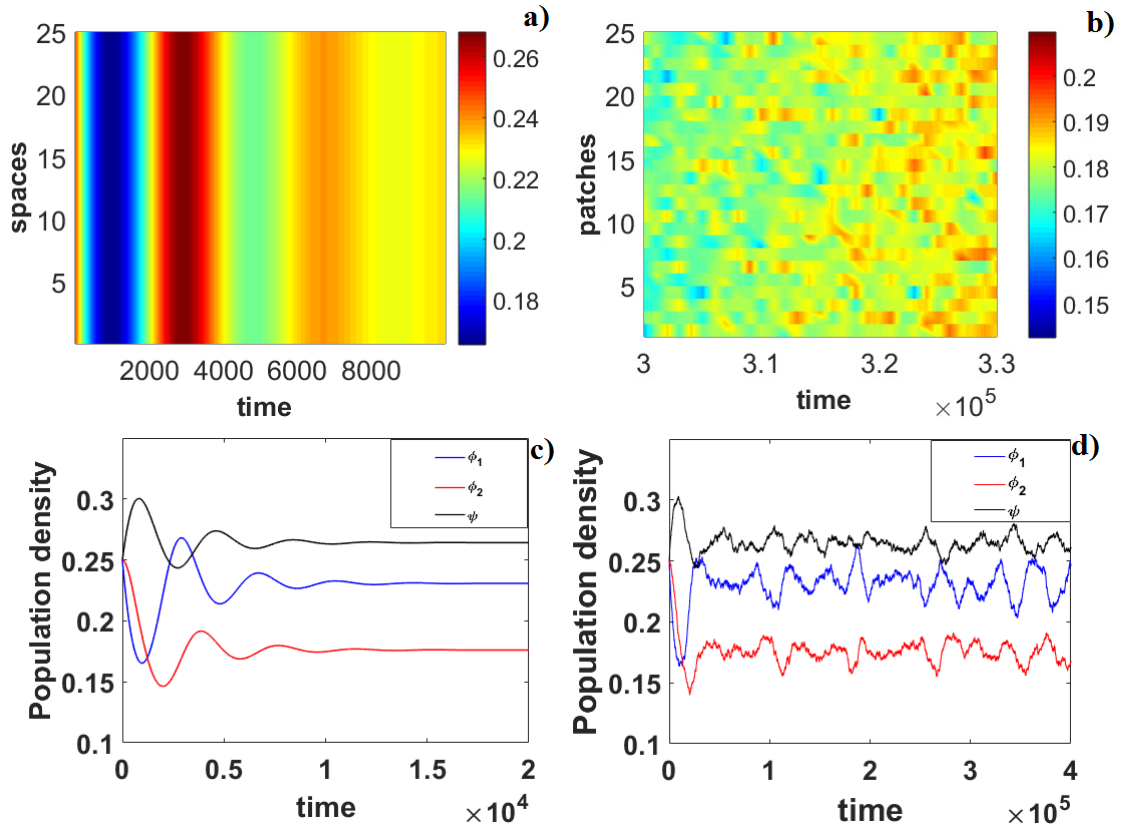
Figure 21: Comparison of the spatio-temporal dynamics of the species density in the stochastic model (panel b) with that in the corresponding deterministic approximation (panel a) for the line patches defined as a continuous space in mean-field approximation. A comparison of the temporal dynamics of the species density in the stochastic model (panel d)) with that in the corresponding deterministic approximation (panel c)) at the same selected patch. The uninfected insect pest (ϕ), infected pest (φ) and pathogen (ψ) are plotted in green, blue and red respectively. The zoomed curves are purposely displayed for highlighting oscillation persistence. While the deterministic approximation leads to stabilization, the full stochastic model recovers. The color bar gives the density of infected insects. The capacity and the number of patches were $N = 10000$ and $\Omega = 100$. The parameters used in the simulations are:$b_2 = 0.15\Omega$, $d_3 = 0.1\Omega$, $I_1 = 0.25\Omega$, $I_2 = 0.05\Omega$, $d_1 = 0.05\Omega$, $b_1 = 0.25\Omega$, $\mu_1 = 0.6\Omega$,$\mu_2 = 0.4\Omega$, $\mu_3 = 0.2\Omega$.
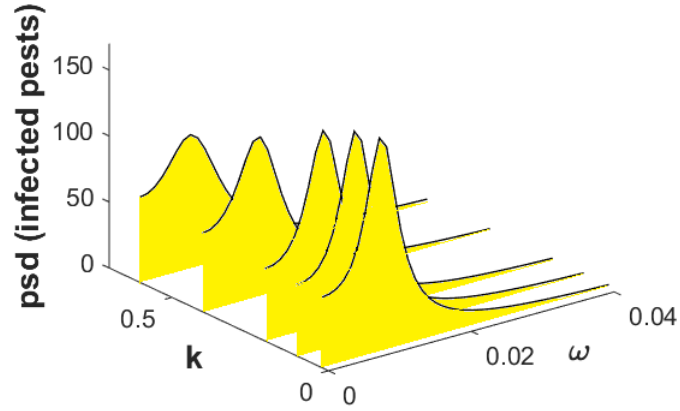
Figure 22: Theoretical predictions of the power spectral density (PSD) for a system composed of $\Omega = 500$ sites occupied by $N = 15000$ species for different size populations using the same parameters values:$b_2 = 0.15\Omega$, $d_3 = 0.1\Omega$, $I_1 = 0.25\Omega$,$I_2 = 0.05\Omega$,$d_1 = 0.05\Omega$, $b_1 = 0.25\Omega$, $\mu_1 = 0.6\Omega$,$\mu_2 = 0.4\Omega$, $\mu_3 = 0.2\Omega$.
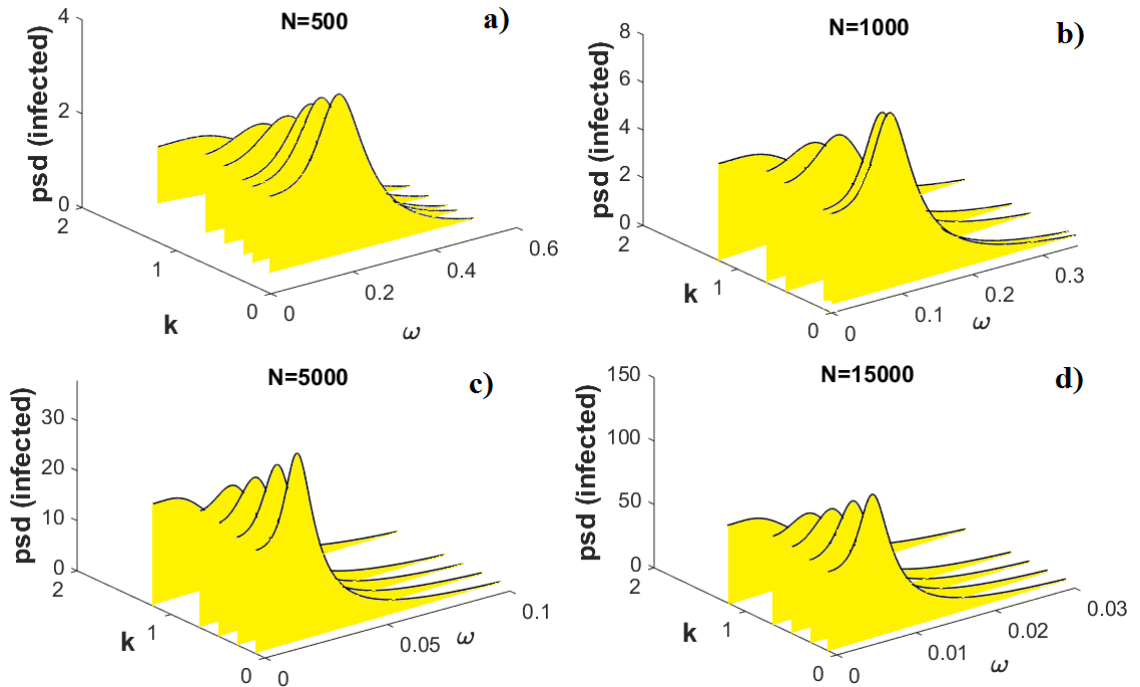
Figure 23: Theoretical predictions of the power spectral density (PSD) for a system composed of $\Omega = 500$ sites occupied by a) $N = 500$, b) $N = 1000$, c) $N = 5000$, d) $N = 15000$ species for different size populations using the same parameters values:$b_2 = 0.15\Omega$, $d_3 = 0.1\Omega$, $I_1 = 0.25\Omega$,$I_2 = 0.05\Omega$,$d_1 = 0.05\Omega$, $b_1 = 0.25\Omega$, $\mu_1 = 0.6\Omega$,$\mu_2 = 0.4\Omega$, $\mu_3 = 0.2\Omega$.
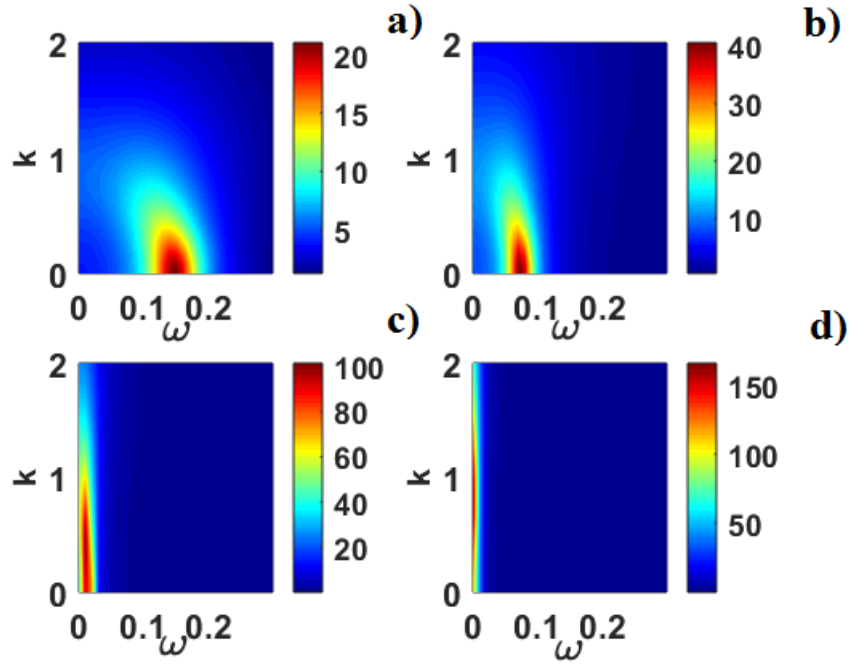
Figure 24: Spatial distributions of the power spectral density (PSD) for a system composed of $\Omega = 500$ sites occupied by a) $N = 500$, b) $N = 1000$, c) $N = 5000$, d) $N = 15000$ species for different size populations using the same parameters values:$b_2 = 0.15\Omega$, $d_3 = 0.1\Omega$, $I_1 = 0.25\Omega$,$I_2 = 0.05\Omega$,$d_1 = 0.05\Omega$, $b_1 = 0.25\Omega$, $\mu_1 = 0.6\Omega$,$\mu_2 = 0.4\Omega$, $\mu_3 = 0.2\Omega$.

called demographic stochasticity [78, 139]. This latter occurs independently among individuals and lead the population growth in large populations or to reduce in size. Understanding the processes that influence demographic stochasticity and its potential effect of the pathogen is therefore important when attempting to explain patterns of extinction of pest and success of biological control method.

A large body of biological research was devoted to the biological control using EPF to target crop devastators [78, 140]. The mechanism identified as most important in this interaction is the contagiousness among pest individuals, which permits propagation of the EPF within the insect population. In order to understand this mechanism, we begun by the investigation of the dynamics between EPF and insects pests in the local patch, following by the interaction on a larger collection of patches. The approach is totally different from what is found in the literature as majority of studies focused only on either individual level [62], or on a well-mixed populations [78, 140]. Most existing models on the population dynamics of host/parasitoid or predator/prey include a type II functional response. It used experimental data to describe relationship between the host density and number of host attacked per natural enemy per unit of time; and showed that the parasitoid/pathogen does not really create a stable pest enemy equi-

librium during the growing season of a crop, but that it suppresses the insect population and subsequently prevent the pest from causing yield losses [62]. However, the same phenomena are observed here without any functional response. A number of models described how insects and their fungal pathogens could be used in a framework to exploring metapopulation theory [28]; in addition, they lack realism because all ecological and biological phenomenon are inherently random [88, 97]. The challenge in modeling the complexity of fungal entomopathogens in populations of insects is thoroughly discussed in [28], these authors emphasize on the heterogeneity of individuals should be incorporated; they further demonstrated the explicit consideration of stochastic demography is crucial. In order to provide a framework for evaluating different ensembles of life history and demographic properties favoring the success of biological control based EPF, the present study complements experimental and theoretical approaches through the use and application of individual-level model (ILM). The model assumed that insect hosts do not acquire immunity to their pathogens and therefore do not include a resistant class of hosts immune to further infection [28], insect is also assumed to be infected only by a single spore, multiple infection are not considered in this model.

By comparing the IBM and it corresponding population level model (PLM), it observed that most of the existing models for EPF-pest interactions which are mean-fields, failed to adequately capture the resilience and oscillations sustainability of the pathogenesis without any external reservoir [1, 24, 133, 134]. Our analytical results pertain to self-maintained of species (pest and the pathogen population) dynamics in the absence of seasonality, thus reflecting the role of individual (discrete) behaviors of EPF in regulating the populations of insect's pests and vice-versa.

In previous studies, external infectious stages ensured that the fungi persists during periods of low host population density when the horizontal transmission is insufficient to maintain the prevalence in the host population [28]. It was hypothesized that EPF could potentially regulate, and cause cycles in each species [16, 28], which corroborates the quasi-cycles persistence predicted by our model. By assuming that naturals selections drive the rates of transmission through altered host susceptibility [16, 81, 141, 142] , it was found that stochasticity induces cycles even at a high rate of heterogeneity during transmission. By considering natural selection as a pure demographic stochasticity, we were able to characterize the quasi-cycle amplitudes and frequency distribution which is not the case in the literature [16, 81, 141, 142]. It was demon-

strated that the control ability of EPF is strongly dependent on the average number of secondary infections produced by a single infectious unit of EPF (conidia) [62].

With the aims to maintain R_0 greater than one, a sensitivity analysis is performed in order to determine which parameters can make the basic reproductive number growth. We also assess the relative importance of different factors responsible for pests and EPF growth to better determine how to reduce the harmfulness of insect devastator. In contrast to the present study, the basic reproduction number reported in previous epidemiological researches describing insect-EPF dynamics, but did not highlighted the relevance on the degree self-limitation of the susceptible insects on the proportion of spore entering in the inactive stage and their important effects on EPF invasion [138, 140]. If the population grows according to a birth and death process, then BC agents might survive forever and the number of spores increases at a slower speed than the population does, so the fraction of infected individuals goes to zero. It is also possible that the pest population and conidia reach equilibrium and the fraction of infectious individuals converges to a constant as defined by BC. However, although EPF may suppress a pest below its carrying capacity, most systems could show prolonged oscillations[81]. The fraction of susceptible insect exposed to be contaminated by infected insects, therefore, the contagious event is primordial [133]. So, in this study where the desired results is to obtain an important number of infected pests for a successful BC (increases of the basic reproductive number), the suggested strategy must be to increase the carrying capacity, apply the EPF in large area to optimize the chance for infecting a large number of insect pest host. Some models are proposed to investigate this density dependence and spatial pattern dynamics of EPF [24], to investigate the spread of infections through dispersion of conidia by considering the behavior of susceptible and infected host [9, 32, 134]. The potential of fungi to regulate insect populations will depend on their abundance in the host population (prevalence) as well as their abundance and persistence in the surrounding environment. Because this abundance is strongly controlled by the contagion phenomenon another suggested strategy would be to develop a control method by increasing the host individual to get the propensity of having more physical contacts.

However, one of the most powerful tools for analyzing such oscillations is the power spectrum. This determines how the periodicity of the stochastic system that makes up the time-series is distributed. We derived the PSD of the fluctuations around equilibrium using a large N expansion method due to Van Kampen.

In the case, where pest was not influenced by any external regulation, pathogens could be responsible for population cycles [28, 142]. However, the largely sustained oscillations, which replace the deterministic predictions of damped oscillations behavior, have a single preferred frequency at which resonant stochasticity occurs.

The results obtained show that coexistence or extinction probabilities of species can have a complex relationship when spreading parameters are varied. It is demonstrated that the extinction probability of host is strongly susceptible to be amplified by the death rate of insect pest during the infectious period. Furthermore, the proportion of spores entering in inactivate stage reduces the number of susceptible hosts, by their potential to survive in the soil and on dormant or mummified pest [62]. These spore control the persistence of BC, by their ability to be reactivated, alternatively infected hosts and produce another conidium [62]. Unfortunately, EPF takes a lot of time to suppress pest populations whereas chemical pesticides provide immediate results [15]. Moreover, this BC agent is used to reduce the population density but not often give rise to total extinction. Another limit is that sometimes it needs to be sprayed more than one time in the field [65].

Entomopathogenic fungi are relatively immobile compared with the hosts but could be migrated by water, wind, rain and so on, thus any spatial refuge may be vital in allowing hosts to escape parasitism [28]. So, populations may regularly pass through a series of localized extinctions and re-colonize from neighboring populations shown that, increasing the spatial wavelength of perturbation gives rise to the large possible oscillation frequency that increases the maximal infectious period. In order to illustrate the role of the non-local interaction term, the temporal evolution of each species is computed at a single patch for the stochastic and deterministic approach, this model verify as assumed in the intra-host dynamic that a nonlinear diffusion is well appropriate to describe biological systems. It is observed that with diffusion coefficient system start to exhibit chaotic behavior for the contagions rate smaller than in the homogeneous case.

The phenomenon of sustained oscillations observes in the stochastic approach remain when patches interact. Many researchers compared the stochastic model and the deterministic analog in spatial-temporal dynamics, and shown in certain case that deterministic system predict an extinction [80]; here it is observed a discrete behavior slows evolution of dynamics and predict self-maintained oscillations.

Reilly and collaborators [143], showed that depending on the threshold of insect population size and amount of bio control, the system may display large-amplitude cycles, steady states or a range of intermediate behaviors. The present study further complements previous results by illustrating that an increase of the possibility of having contact between host populations reduces the width of the PSD and consequently, the extension of the infection period for the EPF persists to large periods. The interest in this result stems from observed epidemic oscillations in EPF and insects pests. Despite sustained oscillations could be produced in deterministic models by introducing various complications (external seasonal forcing or nonlinear dissipation for instance), in contrast to what is reported in the literature on insect pest–BC interactions [16, 81, 141, 142]., here it is shown that cycles result from coherence between random variations and damped oscillations [78]. The oscillations of stochastic model presented here have a frequency distribution, evidenced by the power spectral density of infected insects and stochastically varying amplitude. This phenomenon, in which random fluctuations sustain nearly periodic oscillations in a system which has a stable constant equilibrium in the deterministic limit, has been called coherence resonance or autonomous stochastic resonance [91]. From numerical study, we can understand that the mobility of the species within their habitat increase the possibility of disease transmission and lead to a chaotic behavior. When increase the infection rate, the magnitude of the onset of instability through Hopf-bifurcation increase

III.4   Transmission of disease between host

III.4.1   Modulation instability: case of uniform disease infection

Figure. 25 shows how the modulation instability involves. In order to have the right appreciation of the kind of MI occurring here, the stability diagram is reported in Fig.26 (c). One can remark that the MI generates mechanism of the Turing pattern but only in a subset of the unstable region $(\mathrm{Re}\,(\lambda) > 0)$; since the real part of the dominant eigenvalue is positive for some $k \neq 0$, and the imaginary part is null. In Fig. 26 (a)-(b), the range of values for which the later occurs are illustrated for the parameter space (v, a) with $(a > b)$. Fig.26 (e) show the grow of perturbation and local form corresponding to spatio-temporal Turing pattern formation, that means that the waveform is the almost same for all stationary dynamics (see Fig. 26 (f)). Numerical simulations were carried out using a fully explicit Euler method with a finite-difference approach with No-

flux boundary condition. The initial conditions were taken in the form of the CW to which a small periodic perturbation was added

$$A\left(\xi_1, 0\right) = A_0 + a_0 \cos\left(\omega_0 \xi_1\right) \tag{77}$$

where a_0 and ω_0 defining a small perturbation and its frequency respectively.
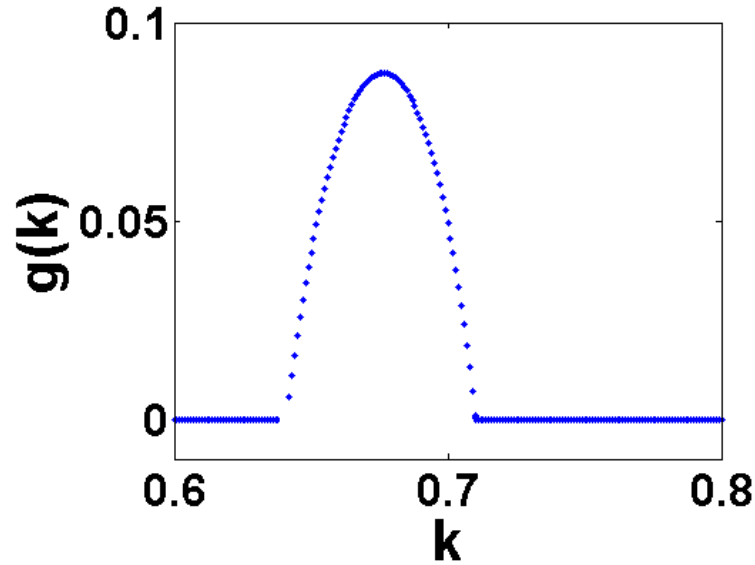
Figure 25: The MI gain spectra:case of uniform transmission. Using the parameters values $a = 0.5$, $b = 0.02$, $v = 0.01$, $\mu = 0.2$, $\alpha = 0.25$, $\beta_{av} = 0.25$.

III.4.2 Modulation instability: case of periodic disease infection

The unstable dynamic still occurs under resonant conditions, but only if the amplitude of the seasonal forcing β_m is sufficiently large to push the maximal eigenvalues in absolute value outside the unit circle (see Fig. 28 (a)). In this specific case the unstable wave number can lead to parametric modulation instability with the growth rate or gain $G\left(k\right)$ is given by

$$G\left(k\right) = \frac{\ln\left(\max\left|\lambda^{\pm}\right|\right)}{T} \tag{78}$$

Figure27(b) shows Floquet multiplier spectra showing instability due to on-resonance. In Fig.27(c) the parametric gain spectrum as a function of the modulation of infection rate (β_m) and the spatial frequency, obtained numerically on one period $(T = 1)$ is given. This figure show many branches of MI, usually called Arnold tongues [84, 23, 129], which in general are characteristic
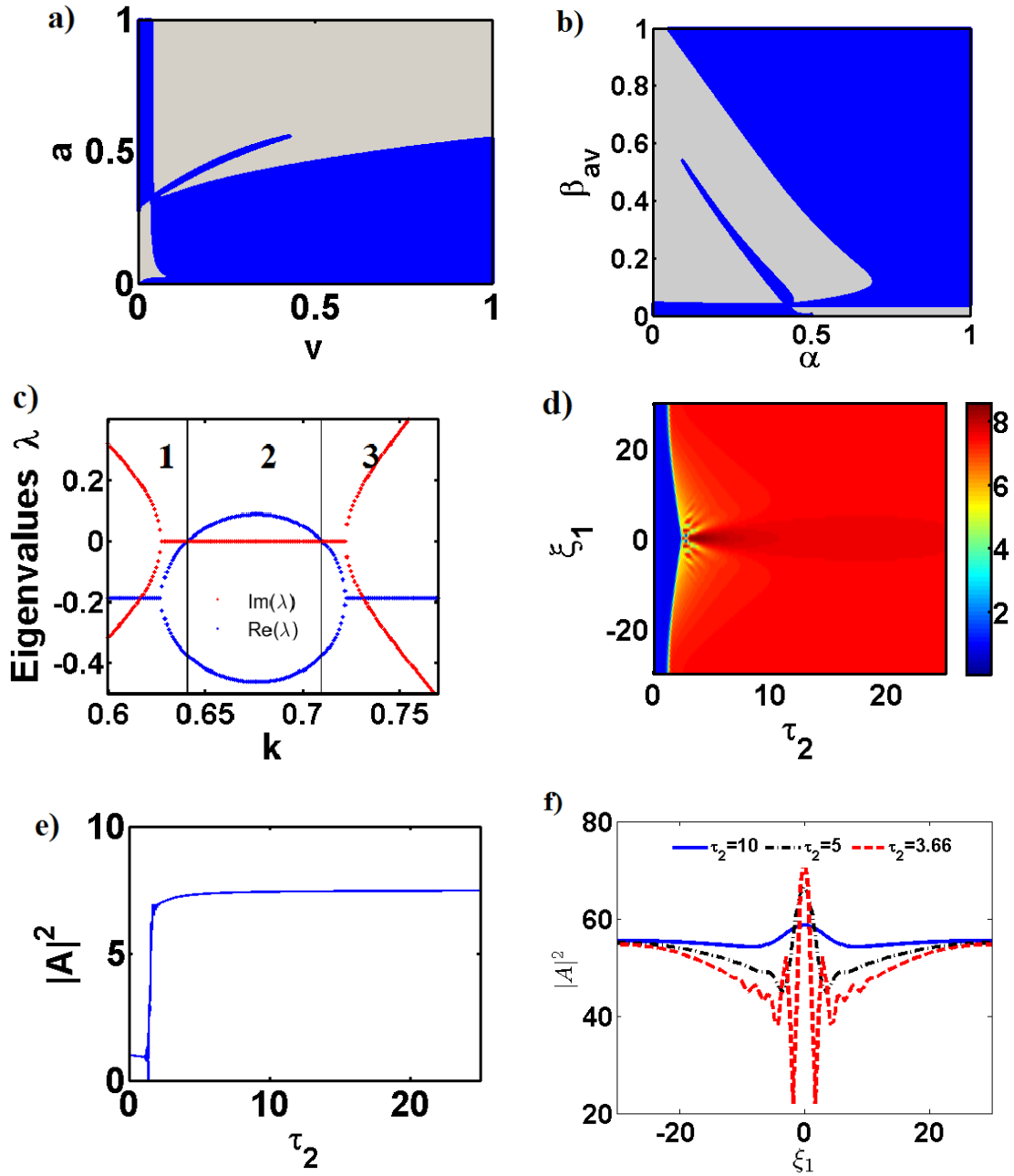
Figure 26: (a)-(b)Parameter space giving the stability analysis, the blue region corresponds to couples of points satisfying the stability condition. (c) Stability analysis showing the complex part (red) and the real part (blue) of the eigenvalues. (d) Turing pattern formation (in one space dimension) originated from MI, the color bar give the magnitude of $|A|^2$. (e) $|A|^2$ evolution of a localize wave form for $\xi_1 = 18$. And (f) $|A|^2$ space profile for $\tau_2 = 5$. Using the parameters values $a = 0.5$, $b = 0.02$, $v = 0.01$, $\mu = 0.2$, $\alpha = 0.25$, $\beta_{av} = 0.25$.
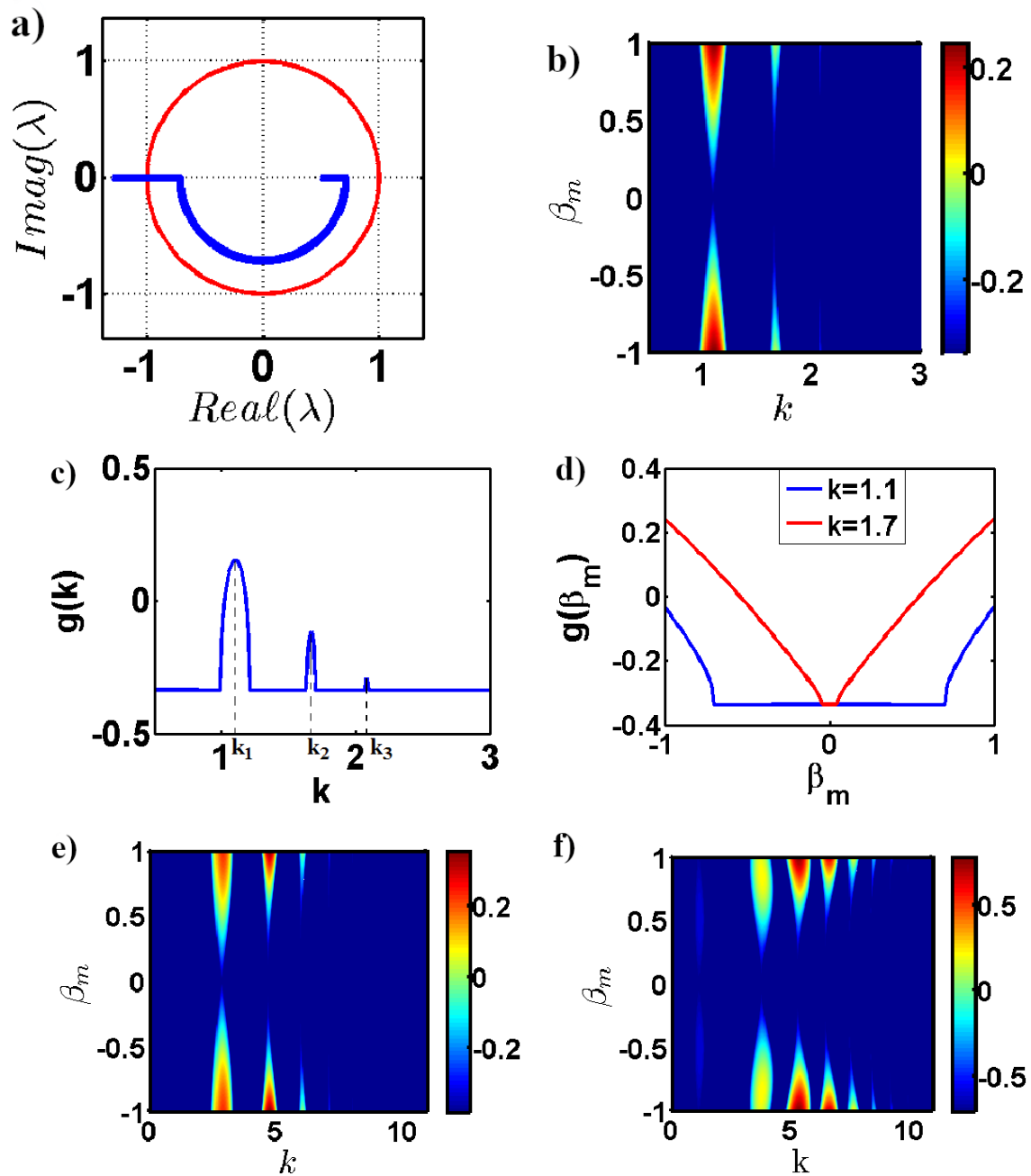
Figure 27: (b) Floquet multiplier spectra (in red the unit circle and the blue point gives Floquet multipliers). (c) Color level plot of modulation instability (MI) gain in the plane (k, β_m) of spatial frequency and infection rate shift. (d) MI gain for $\beta_m = 0.9$. (e) MI gain for some k. (e) and (f) MI gain for $\alpha = 0.03$ and $v = 0.0155$ Using the same parameters values.

of parametric instability sustained by periodic modulation unlike to Turing-type of MI observed in subsection III.3.2. Fig.27(e) gives the evolution of gain when (β_m) change for the three Arnold tongues spatial frequency (corresponding to the On-resonance case) whereas the evolution profile of the gain with respect to the wavenumber for $\beta_m = 0.9$ is given in Fig.27(d). Fig.27(f) and (g) show the effect of the infected mortality rate (α) and the change class rate (the probability to pass from latent into infectious class) v. When α decreases the third Arnold tongues is amplify and a fourth tongues occurs but instability appears for more large spatial frequency (Fig.27(f)). However, when v increases the number of Arnold tongues increase considerably (Fig.27(g)). Contrary to the spatio-temporal waveform observed in the Turing mechanism, the spatio-temporal pattern when the modulation is switched on, show hot and cold vertical stripes (Fig.28(a)). The system dynamic is better observed in Fig.28(c), one can observed the modulated waveform, the great difference is observed in the temporal evolution where periodic modulation is observed (Fig.28(b)). When β_m increases only the amplitude of oscillation increase (see Fig.28(d), (e)). Lastly, increasing v leads the MI evolution to a chaotic state, as shown in Fig. 29

III.4.3 Discussions

Anderson and May provide a simple mathematical including: susceptible, infected (but not yet infectious) and infectious species. In the present study, we modified the anderson-May model by including host displacement. For some simplification, we only add the spatial spread of infectious insects. According to previous researches, spatial spread allows to understand long-term insect disease dynamics [16, 68, 69]. The resulting Reaction-Diffusion model is then transformed to the modified complex Ginzburg-Landau equation using multiple scale method. The modified complex Ginzburg-Landau equation appear in various area of research, in nonlinear optics [21, 20], nerves networks [18, 128, 19], biomembres and nerves [17, 18] . This study show that the modified complex Ginzburg-Landau equation can be apply in the domain of Biological control and is able to describe the bio control agent outbreak in general, and the EPF spread in particular. The spread of EPF is then associated to the system instability here called modulation instability. In the aims to make the model more realistic, the influence of environmental condition on the infection rate is considered. And consequently lead us to a modified CGL equation with periodic cubic term. We then observed two types of modulation instability: the modulation instability due to diffusion (also called Turing mechanism) and the parametric instability
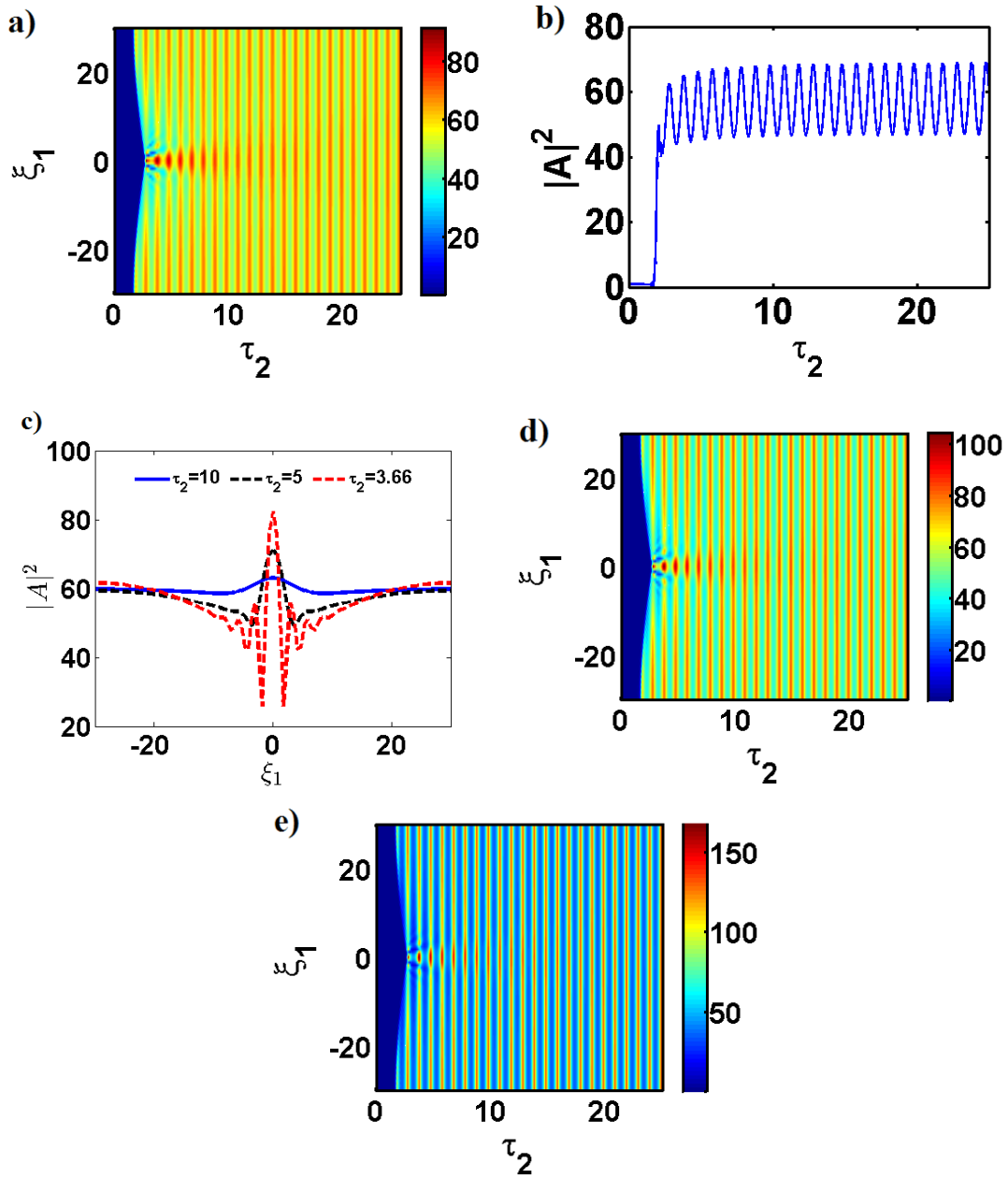
Figure 28: (a) Spatio-temporal evolution illustrating the parametric instability (in one space dimension) for $\beta_m = 0.05$, the color bar give the magnitude of $|A|^2$. (b) $|A|^2$ temporal evolution for $\xi_1 = 18$. (c) $|A|^2$ spatial evolution for $\tau_2 = 5$. Spatio-temporal evolution for: (d) $\beta_m = 0.08$ and (e) $\beta_m = 0.15$.
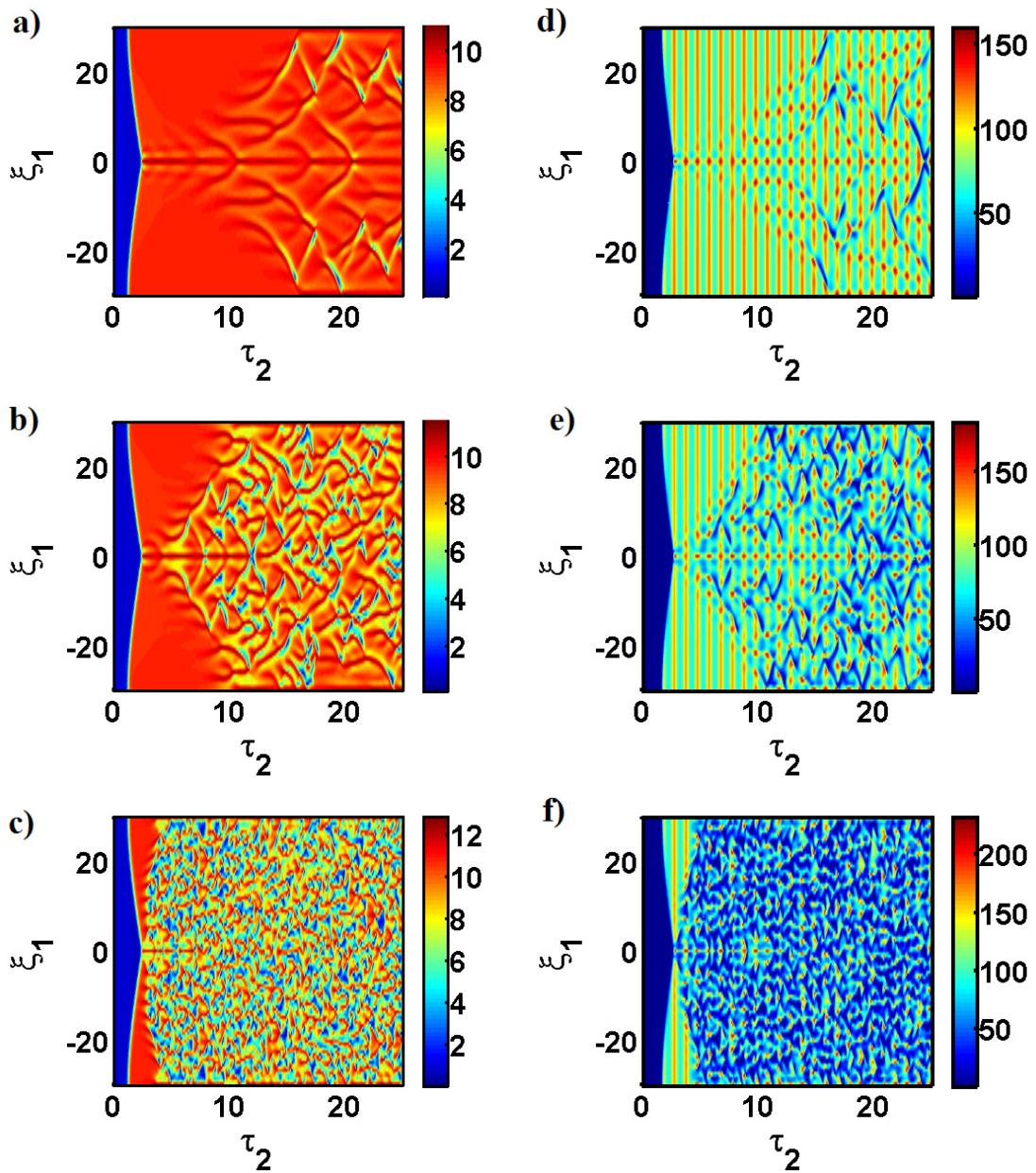
Figure 29: Creation of spatio-temporal irregular evolution by the modulation instability, the color bar give the magnitude of $|A|^2$. The first line corresponds to the case $\beta_m = 0$ and the second line for $\beta_m \neq 0$, the column is obtained for $v = 0.01528$, $v = 0.0155$ and $v = 0.016$ respectively. For $\beta_m = 0.15$.

due to parametric resonance. Similar results have been observed in fibers optics particularly in oscillating fibers ring [22, 84, 86]. By apply the concept of linear stability analysis, we verified the occurrence of the modulation instability (MI) shown by the Benjamin-Feir instability analysis and computed the MI gain spectrum. The Floquet theory allow to determine with good precision the position of multiple MI sidebands. Although there is a threshold of β_m from which the parametric resonance appears, no explicit expression of gain can be derived due to the fact that the value of the threshold differs for each resonant condition. In the limit of uniform infection rate $(\beta_m = 0, \beta(\tau_2) = \beta_{av})$ the system exhibit Turing instability. This observation is a proof of disease spread through the field and by then underlying the importance of including diffusion or migration in host-pathogen models when aiming to improve the use of EPF in biological control. Most ecological or diseases models are local and no adequately mimic the population dynamic [3, 15, 32], since arthropod species move naturally to new habitat with climate change or to feed. Many mathematical model describing pathogen spread in host population based on the diffusion of species, have provided good insights [16, 68, 51] All these studies show that spatial distribution promote heterogeneity and coexistence of species. However, the underlying dynamics is known to be strongly affected by abiotic factors [3, 15, 32]. We explored a wide spectrum of theoretical host-EPF models but any one included thermal conditions and consequently are not the full appropriate analytically framework to mimic the EPF outbreak. [16, 68, 51]. Including the effects of abiotic conditions on the disease spread lead us to obtain a periodically modulated infection rate. In this situation, the EPF outbreak within a host population is related to the parametric instability due to parametric resonance. The latter can be shows on the gain spectra which contrary to the uniform infection case is periodically modulated. When varying key parameters (as v), the form of pattern, the magnitude and the pattern periodicity change. The gain spectrum which accurately predicts the spontaneous growth of MI bands change considerably, similar results are observed in biomenbranes and nerves [19]. Increasing the probability (v) of insect to pass from latent class to infectious class increases the number of spatial frequency for which the parametric resonance occurs. This can be explained by the fact that, when (v) increases the number of infectious host growth; it is noteworthy to mention that each infectious host can be consider as a focal point of disease transmission making the number of secondary infection important. However, the number of spatial resonant frequency reduces when the dead rate of infected insects increases; since the number of focal point of disease transmission decreases. And

can be extend to other epidemiological disease outbreak

General Conclusion

Main results

In summary, this study attempted to improve the use of entomopathogenic fungi a bio control agent use to reduce insect pest in agriculture. This work led to conclude that the EPF outbreaks within pest's population could be achieved by a wave plane among the insects habitat. The approach used here has the potential to be generalized to any type of pathogen-host physical system.

The generalities on EPF, its interaction with the insects pests and the existing models dynamics were presented in the first chapter. Much attention was devoted to the behavioral dynamics within host and host habitat, affected by environmental change, particularly the arrival of new species (either host or fungus), climate change, habitat fragmentation and/or alteration will have differential effects across this community.

In chapter two, we first of all, make a mathematical modeling of EPF dynamics in three steps:

- The intra-host growth of the EPF by considering some physical hypothesis of hemocoel dynamics.

- The EPF growth within a pest population based on the demographic stochasticity.

- The epidemiological aspect of EPF within host population underlying by the contact between infectious insect and susceptible insect. By integrating the latent category.

And we end with three types of nonlinear equations. In the intra-host dynamics, the effects of temperature on the diffusion rate considered, and we end with a reaction-diffusion model. The second model was based on the markov process including demographic random variations and lead to the ILM, then by using a mean field theory, we obtain a PLM representing by an ODE in the local dynamics and by A PDE when migration of species is taking into account. The last model is the modified complex Ginzburg-Landau equation meaning that the contagions process

between insect can involve as a solitonic wave. To end, we presented the materials and both numerical and theoretical methods that permit to analyze these models.

The third chapter is devoted to the presentation of different results obtained in our work. The results we have presented were mainly based on analytical calculations and numerical simulations of the three models mentioned above.

• The proposed model differs from others by including the functional response to describe nonlinear interactions between the host and the EPF and also by introducing constant and time dependent diffusion and cross-diffusion terms in both the insect and EPF, in one hand to adequacy capture the effect of environmental conditions on the fungi growth and on the other side to model the ability of insect immune system to protect itself against the pathogen. The study started by analyzing the stability of the system, establishing conditions for the diffusion driven instability of an in-homogeneous distribution system, and understanding the type of perturbations of the system that lead to equilibrium states and can allow the occurrence of Turing instability. It was observed that cross-diffusion has a remarkable impact on Turing patterns, clearly the Turing patterns appears only for a threshold values of the cross-diffusion. The results showed that the birth regeneration rate is an important parameter that leads to the occurrence of patterns (diffusion driven instability). According to the fact that, the growth of EPF is related by the instability, we can say that the model assuming that after infection the insects undergoes a nutritive stress failed to adequacy capture the within host dynamics of EPF. The Floquet theory permits us to predict and determine the transition curves in the parameter space that demarcate the region's leading to stable and unstable solutions when diffusion and cross-diffusion are described as temporal periodic functions. This study is important for understanding and obtaining the Turing instability in biological control using EPF, which describe the different morphological states of fungus growth within their host. The obtained outcomes help to better understand the spatial structures of the mycelia relative to the spatial distribution of the insect resources and their persistence while manipulating the quantity of insect resource used by fungus and the ability of host to protect itself.

• This model describes biological control developed in order to understand EPF persistence mechanism in a pest's population by taking into consideration the random variation of demographic parameter. It is shown that, when increase the contagions rate, the system exhibit transcritical bifurcation in local and Hopf-damped Turing bifurcation in spatial dynamics.

Meaning that, the optimal control strategy depends on the success of establishing more contact between infected and susceptible host. This remark is also underlying by the sensitivity analysis of the basic reproduction number. The assumption made in the experimental studies that, the EPF is more efficient in for large host population size, has been verify by this study. The model predicted the existence one endemic equilibrium when the basic reproduction number (R_0) is greater than unity. The present study leads us to conclude that R_0 should be maintained above this threshold to guaranty fungi invasion into the insect host population. The cost-effective strategy for performing the spread of infection unit is also determined. By the application of Van Kampen approximation, the deterministic analysis of the proposed model is performed. It allowed examining the period of the cycle occurrence in the biological system by the power spectrum in both nonspatial and spatial considerations. For control variables to be handled in order to maximize the number of infected hosts by then, the total number of pathogen collected on insect's cadavers: (1) carrying capacity on host population, (2) the contagions rate, (3) the number of pest death and/or (4)the number of resting conidia.

●In summary, the last model investigate the development of different kinds of instabilities in biological control (case study of EPF) with periodic variation of the infection transmission rate. We presented an improve version of the well known of Anderson-May model adapted for the description of EPF within insects pest populations. Quite remarkably, we demonstrated that this equation can lead to a modified Complex Ginzburg-Landau equation using the multiple scale method. We reviewed the theory of Turing (modulation) and Faraday (parametric) instability by means of Floquet theory. We reported the numerical demonstration of the generation of stable Turing and Faraday patterns in the same device, which can be controlled by changing the disease transmission rate and/or the latent period $\left(\dfrac{1}{v}\right)$. It is also observed that Turing and Parametric instabilities not only differ by their characteristic frequency but also by their dynamical behavior.

In summary, this work can serve as a tool for understanding the complexity of the fungus developmental processes and growth dynamics that take place in insects as well as in insect's population and that can be generalized to other microorganism with appropriate modulation.

Perspectives

Like future work based in this thesis,

It is noteworthy to remember that, although the entomopathogenic fungi are important agents

to reduce the negative harmful less of crop's devastators. High humidity and low temperature are main factors limiting the use of entomopathogenic fungi. However, the required conditions strongly depend to the high degrees of pluviometry. It is important to note that, rain have a negative impact on the adherence of conidia on pest and also cause their loss. The effects of certain factors on the viability of conidia have been extensively studied as temperature, the effect of humidity and the effect of solar radiation on the inactivation of the infective inoculums [3, 29, 30, 32]. In a future work, One could study:

• The dynamics of entomopathogens with predatory insect to reduce pest's populations.

• Including allee effect on the insect population and may be the delay between EPF and insects predators.

• Use systems Thinking techniques to adequately capture all agents which impact the systems dynamics.

Appendix

Appendix A: Temporal diffusion case

The polynomial equation

$$\mu^2 - h\left(k, \Omega\right)\mu + \eta = 0$$

have for solutions

$$\mu = \frac{1}{2}\left(h \pm \sqrt{h^2 - 4\eta}\right)$$

. For distinct values of μ (Eq.11) has two linearly independent solutions of the form $\varsigma_i = p_i\left(\tau\right)\exp\left(\rho_i\tau\right)$, $(i = 1, 2)$ where $\exp\left(\rho_i T\right) = \mu_i (i = 1, 2)$, and p_i are function of period T. The general solution of (Eq.11)(the first component of ς) is given by

$$a_1 = p_1\left(\tau\right)e^{\rho_1\tau} + p_2\left(\tau\right)e^{\rho_2\tau} \tag{79}$$

The stability or otherwise of the periodic solution of (Eq.11) will be determined by the behavior of **a** in (Eq.11). The system is stable if $\mathrm{Re}\left(\rho_1\right) < 0$ and $\mathrm{Re}\left(\rho_2\right) < 0$. This is equivalent to $\mu_1 < 1$ and $\mu_2 < 1$. Analysis can be split in three cases.

1. $h^2 > 4\eta$, μ_1 and μ_2 are both real and positive, or both real and negative according to the sign of h: in both cases $\mu_2 < \mu_1$. If they are both positive, then the periodic solution is stable if $\mu_1 = \left(h + \sqrt{h^2 - 4\eta}\right)/2 < 1$, or $h < 1 + \eta$. According to the fact that $\eta \in [0, 1]$, this lower bound is always greater than $2\sqrt{\eta}$. The region between $h = 1 + \eta$ and $h = 2\sqrt{\eta}$ (hatched region in $h > 0$ on Fig. 7(a)) are a stable region. Similarly if $h < -2\sqrt{\eta}$, then the stability boundaries are $h = -1 - \eta$ and $h = -2\sqrt{\eta}$.

2. $h^2 = 4\eta$, then there exists a unique double eigenvalue $\mu_1 = \mu_2 = h/2 = \pm\sqrt{\eta}$, stable solution arise. And are periodic for the negative eigenvalues.

3. $h^2 < 4\eta$, μ_1 and μ_2 are complex conjugates given by $\left(h \pm i\theta\right)/2$, where $\theta = \sqrt{4\eta - h^2}$. The

system is therefore stable if $|h| < 2$. In addition to the "natural oscillations" with frequency Ω, there appear new oscillations. By plotting this boundaries regions, Fig. 4(a) is obtained, a stable behavior occurs in a colored region.

Appendix B: Hill determinant

Equating each of the coefficients of the exponential functions to zero yields of (Eq.15), the following infinite set of linear, algebraic, homogeneous equations for A_m and B_m:

$$
\begin{aligned}
&\left(k^2 - a_{11} + a_m\right) A_m - a_{12} B_m = 0, \\
&\left(k^2 d + b_m\right) B_m + \left(k^2 m_0 d_{21} - a_{21}\right) A_m - i\frac{k^2 m_0 b_{21}}{2} e^{i\phi} A_{m-1} + i\frac{k^2 m_0 b_{21}}{2} e^{-i\phi} A_{m+1} \\
&- i\frac{k^2 b}{2} B_{m-1} + i\frac{k^2 b}{2} B_{m+1} = 0.
\end{aligned} \tag{80}
$$

For nontrivial solutions, the determinant of the matrix obtained from Eq.80 must be null. Since the determinant is infinite, the first and second sections of Eq.80 are divided by $\left(k^2 - a_{11} - 4m^2\right)$ and $\left(k^2 d - 4m^2\right)$ respectively, for the convergence. And thus, obtained the lower Hill's determinant given by,

$$
\Delta_H = \begin{vmatrix}
\Delta_{11} & \Delta_{12} & 0 & 0 & 0 & 0 \\
\Delta_{21} & \Delta_{22} & \Delta_{23} & \Delta_{24} & 0 & 0 \\
0 & 0 & \Delta_{33} & \Delta_{34} & 0 & 0 \\
\Delta_{41} & \Delta_{42} & \Delta_{43} & \Delta_{44} & \Delta_{45} & \Delta_{46} \\
0 & 0 & 0 & 0 & \Delta_{55} & \Delta_{56} \\
0 & 0 & \Delta_{63} & \Delta_{64} & \Delta_{65} & \Delta_{66}
\end{vmatrix}, \tag{81}
$$

where,

$$
\begin{aligned}
&\Delta_{11} = \frac{k^2 - a_{11} + \theta_1 - i\Omega}{k^2 - a_{11} - 4}, \Delta_{12} = -\frac{a_{12}}{k^2 - a_{11} - 4}, \Delta_{21} = -\frac{-m_0 k^2 d_{21} + a_{21}}{k^2 d - 4}, \Delta_{22} = \frac{k^2 d + \theta_2 - i\Omega}{k^2 d - 4}, \\
&\Delta_{23} = i\frac{k^2 m_0 b_{21} e^{(-i\phi)}}{2k^2 d - 8}, \Delta_{24} = i\frac{k^2 b}{2k^2 d - 8}, \Delta_{33} = \frac{k^2 - a_{11} + \theta_1}{k^2 - a_{11}}, \Delta_{34} = -\frac{a_{12}}{k^2 - a_{11}}, \Delta_{41} = -i\frac{m_0 b_{21} e^{(i\phi)}}{2d}, \\
&\Delta_{42} = -i\frac{b}{2d}, \Delta_{43} = -\frac{-m_0 k^2 d_{21} + a_{21}}{k^2 d}, \Delta_{44} = \frac{k^2 d + \theta_2}{k^2 d}, \Delta_{45} = i\frac{m_0 b_{21} e^{(-i\phi)}}{2d}, \Delta_{46} = i\frac{b}{2d}, \\
&\Delta_{55} = \frac{k^2 - a_{11} + \theta_1 + i\Omega}{k^2 - a_{11} - 4}, \Delta_{56} = -\frac{a_{12}}{k^2 - a_{11} - 4}, \Delta_{63} = -i\frac{k^2 m_0 b_{21} e^{(i\phi)}}{2k^2 d - 8}, \Delta_{64} = -i\frac{k^2 b}{2k^2 d - 8}, \\
&\Delta_{65} = -\frac{-m_0 k^2 d_{21} + a_{21}}{k^2 d - 4}, \Delta_{66} = \frac{k^2 d + \theta_2 + i\Omega}{k^2 d - 4}.
\end{aligned}
$$

By rearranging this determinant, the form following equation is obtained

$$\Delta_H = F_4\left(k\right)\Omega^4 + F_3\left(k\right)\Omega^3 + F_2\left(k\right)\Omega^2 + F_1\left(k\right)\Omega + F_0\left(k\right), \tag{82}$$

with $F_i\left(k\right)$ $(i = 0, .., 4)$ defined by,

$$F_4 = \frac{\left(dk^4 + \left(\left(-a_{11} + \theta_1\right)d + d_{21}m_0a_{12} + \theta_2\right)k^2 - a_{11}\theta_2 - a_{12}a_{21} + \theta_1\theta_2\right)}{(k^2 - a_{11} - 4)^2(k^2d - 4)^2\left(k^2 - a_{11}\right)k^2d},$$

$$F_3 = -\frac{1}{2(k^2 - a_{11} - 4)^2(k^2d - 4)^2\left(k^2 - a_{11}\right)d}\left(a_{12}bk^2m_0b_{21}\sin\left(\varphi\right)\right),$$

$$F_2 = \frac{1}{2(k^2 - a_{11} - 4)^2(k^2d - 4)^2\left(k^2 - a_{11}\right)k^2d}(m_0ba_{12}k^4b_{21}\left(\left(-d + 1\right)k^2 + \theta_1 - \theta_2 - a_{11}\right)\cos\left(\varphi\right)$$

$$+ \left(2d_{21}m_0(d-1)^2a_{12} + \left(2\theta_1 - 2a_{11}\right)d^3 + 6\theta_2d^2 - \left(b^2 - 6\right)\left(\theta_1 - a_{11}\right)d + \left(-b^2 + 2\right)\theta_2\right)k^6$$

$$+ (m_0{}^2\left(-4d_{21}{}^2 + b_{21}{}^2\right)a_{12}{}^2 - \left(4d - 4\right)\left(-d_{21}m_0a_{11} + \theta_1d_{21}m_0 - \theta_2d_{21}m_0 + \tfrac{1}{2}da_{21} - \tfrac{1}{2}a_{21}\right)a_{12}$$

$$+ 6\theta_2\left(\theta_1 - a_{11}\right)d^2 + \left(6\theta_2{}^2 + 6(\theta_1 - a_{11})^2\right)d - \theta_2\left(b^2 - 6\right)\left(\theta_1 - a_{11}\right))k^4 + (8d_{21}m_0a_{21}a_{12}{}^2$$

$$+ \left(2\theta_1 - 2\theta_2 - 2a_{11}\right)\left(-d_{21}m_0a_{11} + \theta_1d_{21}m_0 - \theta_2d_{21}m_0 + 2da_{21} - 2a_{21}\right)a_{12}$$

$$+ \left(2\theta_1 - 2a_{11}\right)\left(3\theta_2{}^2 + (\theta_1 - a_{11})^2\right)d + \left(2\theta_2{}^2 + 6(\theta_1 - a_{11})^2\right)\theta_2)k^2$$

$$+ \left(4a_{12}a_{21} + 2\theta_2{}^2 + 2(\theta_1 - a_{11})^2\right)\left(-a_{12}a_{21} + \theta_2\left(\theta_1 - a_{11}\right)\right)) + \left(-b^2d + 2d^3 + 2d\right)k^8$$

$$F_1 = \frac{\sin\left(\varphi\right)b_{21}bm_0k^2a_{12}\left(dk^4 + \left(\left(-a_{11} + \theta_1\right)d + d_{21}m_0a_{12} + \theta_2\right)k^2 - a_{11}\theta_2 - a_{12}a_{21} + \theta_1\theta_2\right)}{2(k^2 - a_{11} - 4)^2(k^2d - 4)^2\left(k^2 - a_{11}\right)d},$$

$$F_0 = -\frac{1}{2(k^2 - a_{11} - 4)^2(k^2d - 4)^2\left(k^2 - a_{11}\right)k^2d}\left(k^4d + \left(\left(\theta_1 - a_{11}\right)d + d_{21}a_{12}m_0 + \theta_2\right)k^2\right)$$

$$(\theta_2\left(\theta_1 - a_{11}\right) - a_{12}a_{21})(2bb_{21}k^4m_0a_{12}\left(k^2 - a_{11} + \theta_1\right)\cos\left(\varphi\right) + \left(b^2 - 2d^2\right)k^8$$

$$+ \left(\left(-4\theta_1 + 4a_{11}\right)d^2 + \left(-4d_{21}a_{12}m_0 - 4\theta_2\right)d + 2b^2\left(\theta_1 - a_{11}\right)\right)k^6$$

$$(-2(\theta_1 - a_{11})^2d^2 + \left(\left(-8\theta_1 + 8a_{11}\right)\theta_2 - 4a_{12}\left(-d_{21}m_0a_{11} + \theta_1d_{21}m_0 - a_{21}\right)\right)d - 2\theta_2{}^2 - 4\theta_2d_{21}m_0a_{12}$$

$$+ b^2a_{11}{}^2 - 2b^2\theta_1a_{11} + m_0{}^2\left(-2d_{21}{}^2 + b_{21}{}^2\right)a_{12}{}^2 + b^2\theta_1{}^2)k^4 - \left(-4a_{12}a_{21} + 4\theta_2\left(\theta_1 - a_{11}\right)\right)$$

$$((\theta_1 - a_{11})d + d_{21}a_{12}m_0 + \theta_2)k^2 - 2(-a_{12}a_{21} + \theta_2\left(\theta_1 - a_{11}\right))^2)$$

$$\tag{83}$$

Appendix C: Mean Field theory

In the beginning of this appendix, details of the mean-field versions of the stochastic models are given. In the second part, the stability analysis of the equilibrium state derived from the deterministic model. The master equation which completely defined time evolution of the non-spatial system is given by:

$$\frac{dP(n,m,l,t)}{dt} = T(n,m,l|n-1,m+1,l)\,P(n-1,m+1,l,t) + T(n,m,l|n-1,m,l)\,P(n-1,m,l,t)$$

$$+T(n,m,l|n+1,m,l)\,P(n+1,m,l,t) + T(n,m,l|n,m-1,l+1)\,P(n,m-1,l+1,t)$$

$$+T(n,m,l|n,m,l-1)\,P(n,m,l-1,t) - [T(n-1,m+1,l|n,m,l) + T(n-1,m,l|n,m,l)$$

$$+T(n+1,m,l|n,m,l) + T(n,m-1,l+1|n,m,l) + T(n,m,l-1|n,m,l)]P(n,m,l,t).$$

$$(84)$$

Using step operators $\varepsilon_x^{\pm 1}, \varepsilon_y^{\pm 1}$ and $\varepsilon_z^{\pm 1}$ defined in function of n, m and l such that:

$$\varepsilon_x^{\pm 1} f(n,m,l) = f(n \pm 1, m, l)$$

$$\varepsilon_y^{\pm 1} f(n,m,l) = f(n, m \pm 1, l) \qquad (85)$$

$$\varepsilon_z^{\pm 1} f(n,m,l) = f(n, m, l \pm 1)$$

Equation92 can be rewritten as follows:

$$\frac{dP(n,m,l,t)}{dt} = \left(\left(\varepsilon_x \varepsilon_y^{-1} - 1 \right) T(n-1,m+1,l|n,m,l) + (\varepsilon_x - 1)\,T(n-1,m,l|n,m,l) \right.$$

$$+ \left(\varepsilon_x^{-1} - 1 \right) T(n+1,m,l|n,m,l) + \left(\varepsilon_y \varepsilon_z^{-1} - 1 \right) T(n,m-1,l+1|n,m,l) \qquad (86)$$

$$+ \left. (\varepsilon_z - 1)\,T(n,m,l-1|n,m,l) \right) P(n,m,l,t).$$

By transforming stochastic variables $\sigma = (n,m,l)$ to a new stochastic variable $\zeta = (\xi, \eta, \vartheta)$ such that.

$$n = N\phi(t) + N^{1/2}\xi,$$

$$m = N\varphi(t) + N^{1/2}\eta, \qquad (87)$$

$$l = N\psi(t) + N^{1/2}\vartheta.$$

The probability distribution function defined by $P(n,m,l,t) = \Pi(\xi,\eta,\vartheta,t)$ is written as:

$$\frac{dP}{dt} = \frac{\partial \Pi}{\partial t} - N^{1/2}\frac{d\phi}{dt}\frac{\partial \Pi}{\partial \xi} - N^{1/2}\frac{d\varphi}{dt}\frac{\partial \Pi}{\partial \eta} - N^{1/2}\frac{d\psi}{dt}\frac{\partial \Pi}{\partial \vartheta}, \qquad (88)$$

with $\phi = \lim\limits_{N\to\infty} n/N, \varphi = \lim\limits_{N\to\infty} m/N, \psi = \lim\limits_{N\to\infty} l/N$ the step operators defined in Eq. (93) in terms involving the new variables is gives by:

$$
\begin{aligned}
\varepsilon_x^{\pm 1} &= 1 \pm N^{-1/2}\frac{\partial}{\partial \xi} + \frac{1}{2}N^{-1}\frac{\partial^2}{\partial \xi^2} + \cdots, \\
\varepsilon_y^{\pm 1} &= 1 \pm N^{-1/2}\frac{\partial}{\partial \eta} + \frac{1}{2}N^{-1}\frac{\partial^2}{\partial \eta^2} + \cdots, \\
\varepsilon_z^{\pm 1} &= 1 \pm N^{-1/2}\frac{\partial}{\partial \vartheta} + \frac{1}{2}N^{-1}\frac{\partial^2}{\partial \vartheta^2} + \cdots, \\
\varepsilon_x\varepsilon_y^{-1} &= 1 + N^{-1/2}\left(\frac{\partial}{\partial \xi} - \frac{\partial}{\partial \eta}\right) + \frac{1}{2}N^{-1}\left(\frac{\partial}{\partial \xi} - \frac{\partial}{\partial \eta}\right)^2 + \cdots, \\
\varepsilon_y\varepsilon_z^{-1} &= 1 + N^{-1/2}\left(\frac{\partial}{\partial \eta} - \frac{\partial}{\partial \vartheta}\right) + \frac{1}{2}N^{-1}\left(\frac{\partial}{\partial \eta} - \frac{\partial}{\partial \vartheta}\right)^2 + \cdots,
\end{aligned}
\tag{89}
$$

Replacing these expressions and transitions rates in Eq.(94), the follows list given contributions, at the order N^0 and N^2 is obtained:

1. $\left(\varepsilon_x\varepsilon_y^{-1} - 1\right)\left(\dfrac{2I_1 nm}{N} + \dfrac{2I_2 nl}{N}\right),$

   $N^0 : (I_1\phi\varphi + I_2\phi\psi)\dfrac{\partial^2}{\partial \xi^2}, (I_1\phi\varphi + I_2\phi\psi)\dfrac{\partial^2}{\partial \eta^2}, -2(I_1\phi\varphi + I_2\phi\psi)\dfrac{\partial^2}{\partial \xi\partial \eta}, 2I_1\phi\dfrac{\partial}{\partial \xi}\eta,$

   $(2I_1\varphi + 2I_2\psi)\dfrac{\partial}{\partial \xi}\xi, -(2I_1\varphi + 2I_2\psi)\dfrac{\partial}{\partial \eta}\xi, 2I_2\phi\dfrac{\partial}{\partial \xi}\vartheta, -2I_1\phi\dfrac{\partial}{\partial \eta}\eta, -2I_2\phi\dfrac{\partial}{\partial \eta}\vartheta,$

   $N^{1/2} : 2(I_1\phi\varphi + I_2\phi\psi)\dfrac{\partial}{\partial \xi}, -2(I_1\phi\varphi + I_2\phi\psi)\dfrac{\partial}{\partial \eta}.$

2. $(\varepsilon_x - 1)d_1 n,$

   $N^0 : d_1\dfrac{\partial}{\partial \xi}\xi, \dfrac{d_1}{2}\phi\dfrac{\partial^2}{\partial \xi^2},$

   $N^{1/2} : d_1\phi\dfrac{\partial}{\partial \xi}.$

3. $(\varepsilon_z - 1)d_3 l,$

   $N^0 : d_3\dfrac{\partial}{\partial \vartheta}\vartheta, \dfrac{d_3}{2}\psi\dfrac{\partial^2}{\partial \vartheta^2},$

   $N^{1/2} : d_3\psi\dfrac{\partial}{\partial \vartheta}.$

4. $\left(\varepsilon_x^{-1} - 1\right)2b_1\dfrac{n}{N}(N - n - m - l),$

   $N^0 : 2b_1\phi\dfrac{\partial}{\partial \xi}\xi, 2b_1\phi\dfrac{\partial}{\partial \xi}\eta, 2b_1\phi\dfrac{\partial}{\partial \xi}\vartheta, -2b_1(1 - \phi - \varphi - \psi)\dfrac{\partial}{\partial \xi}\xi, b_1\phi(1 - \phi - \varphi - \psi)\dfrac{\partial^2}{\partial \xi^2},$

   $N^{1/2} : -2b_1\phi(1 - \phi - \varphi - \psi)\dfrac{\partial}{\partial \xi}.$

5. $\left(\left(\varepsilon_y\varepsilon_z^{-1} - 1\right)b_2 m,\right.$

   $N^0 : b_2\varphi\dfrac{\partial^2}{\partial \eta^2}, b_2\varphi\dfrac{\partial^2}{\partial \vartheta^2}, -2b_2\varphi\dfrac{\partial^2}{\partial \vartheta\partial \eta}, b_2\dfrac{\partial}{\partial \eta}\eta, -b_2\dfrac{\partial}{\partial \vartheta}\eta,$

   $N^{1/2} : b_2\varphi\dfrac{\partial}{\partial \eta}, -b_2\varphi\dfrac{\partial}{\partial \vartheta}.$

Substituting these terms on Eq.(94) and identifying the terms of order $N^{1/2}$ on the resulting equation to the equation (88), we obtained macroscopic equation given by Eq.(28). The terms of

order N^0 lead to a Fokker-Planck equation for a fluctuations variables $\zeta = (\xi, \eta, \vartheta)$:

$$\frac{\partial \Pi}{\partial t} = -\sum_{i,j=1}^{3} a_{ij} \frac{\partial (\zeta_j \Pi)}{\partial \zeta_i} + \frac{1}{2} \sum_{i,j=1}^{3} b_{ij} \frac{\partial^2 \Pi}{\partial \zeta_i \partial \zeta_j} \tag{90}$$

the coefficients a_{ij} and b_{ij} are given by:

$$a_{11} = -2b_1\phi^s - d_1 + 2b_1 \left(1 - \phi^s - \varphi^s - \psi^s\right) - \left(2I_1\varphi^s + 2I_2\psi^s\right), a_{12} = -2\left(b_1 + I_1\right)\phi^s,$$

$$a_{13} = -2\left(b_1 + I_2\right)\phi^s, a_{21} = 2\left(I_1\varphi^s + I_2\psi^s\right), a_{22} = \left(-b_2 + 2I_1\phi^s\right),$$

$$a_{23} = 2I_2\phi^s, a_{31} = 0, a_{32} = b_2, a_{33} = -d_3, b_{11} = 2I_1\phi^s\varphi^s + 2I_2\phi^s\psi^s + d_1\phi^s \tag{91}$$

$$+2b_1\phi^s \left(1 - \phi^s - \varphi^s - \psi^s\right), b_{23} = -2b_2\varphi^s, b_{22} = 2I_1\phi^s\varphi^s + 2I_2\phi^s\psi^s + 2b_2\varphi^s,$$

$$b_{33} = 2b_2\varphi^s + d_3\psi^s, b_{12} = -4I_1\phi^s\varphi^s - 4I_2\phi^s\psi^s.$$

At the non-trivial steady state.

Appendix D: Power spectral analysis

The power spectra of the fluctuations in the neighborhood of the equilibrium state, is evaluated from the temporal Fourier transform of the Langevin equation which describes fluently the stochastic behavior of the system [65, 98, 121]. The latter corresponding to the Fokker-Planck equation (Eq.(90)) are

$$\frac{d\zeta_i}{dt} = \sum_{j=1}^{3} a_{ij}\zeta_j + \lambda_i\left(t\right), \left(i, j = 1, 2, 3\right) \tag{92}$$

Where ζ_i $(i = 1, 2, 3)$ denotes the random deviation of system from the mean fields and $\lambda_i\left(t\right)$ $(i = 1, 2, 3)$ the Gaussian white noise with zero mean and a correlation function given by $\langle \lambda_i\left(t\right) \lambda_j\left(t'\right) \rangle = b_{ij}\delta\left(t - t'\right)$. Taking the temporal Fourier transform $\tilde{\zeta}_i\left(\omega\right) = \int\limits_{-\infty}^{+\infty} e^{-i\omega t}\zeta_i\left(t\right) dt$ of Eq.(92) lead to

$$-i\omega\tilde{\zeta}_i\left(\omega\right) = \sum_{j=1}^{3} a_{ij}\tilde{\zeta}_j\left(\omega\right) + \tilde{\lambda}_i\left(\omega\right), \tag{93}$$

with $\left\langle \tilde{\lambda}_i\left(\omega\right) \tilde{\lambda}_j\left(\omega'\right) \right\rangle = b_{ij}\left(2\pi\right)\delta\left(\omega + \omega'\right)$. The obtained system corresponds now to a three coupled linear algebraic equations which can be used to derive a closed form expression for the power spectra. Therefore, solving equation Eq.(92) we obtain:

$\tilde{\xi}(\omega) = \frac{(a_{23}a_{32}-a_{22}a_{33})\tilde{\lambda}_1+(a_{12}a_{33}-a_{13}a_{32})\tilde{\lambda}_2+(a_{13}a_{22}-a_{12}a_{23})\tilde{\lambda}_3+\tilde{\lambda}_1\omega^2+i\omega\left(-(a_{33}+a_{22})\tilde{\lambda}_1+\tilde{\lambda}_2 a_{12}+\tilde{\lambda}_3 a_{13}\right)}{D(\omega)}$,

$\tilde{\eta}(\omega) = \frac{(a_{21}a_{33}-a_{23}a_{31})\tilde{\lambda}_1+(a_{31}a_{13}-a_{11}a_{33})\tilde{\lambda}_2+(a_{11}a_{23}-a_{13}a_{21})\tilde{\lambda}_3+\tilde{\lambda}_2\omega^2+i\omega\left(a_{21}\tilde{\lambda}_1-(a_{11}+a_{33})\tilde{\lambda}_2+\tilde{\lambda}_3 a_{23}\right)}{D(\omega)}$, where

$\tilde{\vartheta}(\omega) = \frac{(a_{22}a_{31}-a_{21}a_{32})\tilde{\lambda}_1+(a_{32}a_{11}-a_{12}a_{31})\tilde{\lambda}_2+(a_{12}a_{21}-a_{11}a_{22})\tilde{\lambda}_3+\tilde{\lambda}_3\omega^2+i\omega\left(a_{31}\tilde{\lambda}_1+a_{32}\tilde{\lambda}_2-(a_{11}+a_{22})\tilde{\lambda}_3\right)}{D(\omega)}$,

the denominator is given by

$D\left(\omega\right) = (i\omega)^3 + tr\mathbf{a}(i\omega)^2 + \Theta\left(i\omega\right) + \det\mathbf{a}$,

with $\quad tr\mathbf{a} = a_{11} + a_{22} + a_{33}$,

$\quad \Theta = a_{11}a_{22} + a_{11}a_{33} - a_{12}a_{21} + a_{22}a_{33} - a_{23}a_{32} - a_{13}a_{31}$,

and

$\det\mathbf{a} = a_{11}a_{22}a_{33} - a_{11}a_{23}a_{32} - a_{12}a_{21}a_{33} + a_{13}a_{21}a_{32} + a_{31}a_{12}a_{23} - a_{13}a_{22}a_{31}$.

We recall that the power spectra corresponds to the squared moduli average $\tilde{\zeta}_i\left(\omega\right)$. Using the expression

$$\left\langle \tilde{\lambda}_i\left(\omega\right)\tilde{\lambda}_j\left(\omega'\right)\right\rangle = b_{ij}\left(2\pi\right)\delta\left(\omega+\omega'\right)$$

, we obtained

$$
\begin{aligned}
P_\phi\left(\omega\right) &= \left\langle \left|\xi\left(\omega\right)\right|^2\right\rangle = \frac{b_{11}\omega^4 + \Gamma_\phi\omega^2 + \kappa_\phi}{\left|\left(\omega\right)\right|^2}, \\
P_\varphi\left(\omega\right) &= \left\langle \left|\eta\left(\omega\right)\right|^2\right\rangle = \frac{b_{22}\omega^4 + \Gamma_\varphi\omega^2 + \kappa_\varphi}{\left|D\left(\omega\right)\right|^2}, \\
&and \\
P_\psi\left(\omega\right) &= \left\langle \left|\vartheta\left(\omega\right)\right|^2\right\rangle = \frac{b_{33}\omega^4 + \Gamma_\psi\omega^2 + \kappa_\psi}{\left|D\left(\omega\right)\right|^2}.
\end{aligned}
\tag{94}
$$

Where

$$|D\left(\omega\right)|^2 = \left(\omega^3 - \Theta\omega\right)^2 + \left(\det \mathbf{a} - tr\mathbf{a}\omega^2\right)^2,$$

$$\Gamma_\phi = a_{12}{}^2 b_{22} + 2a_{12}a_{13}b_{23} - 2a_{12}a_{22}b_{12} - 2a_{13}a_{32}b_{12} - 2a_{12}a_{23}b_{13} + a_{13}{}^2 b_{33} - 2a_{13}a_{33}b_{13} + a_{22}{}^2 b_{11}$$

$$+2a_{23}a_{32}b_{11} + a_{33}{}^2 b_{11},$$

$$\kappa_\phi = a_{12}{}^2 a_{23}{}^2 b_{33} - 2a_{12}{}^2 a_{23}a_{33}b_{23} + a_{12}{}^2 a_{33}{}^2 b_{22} - 2a_{12}a_{13}a_{22}a_{23}b_{33} + 2a_{12}a_{13}a_{22}a_{33}b_{23}$$

$$+2a_{12}a_{13}a_{23}a_{32}b_{23} - 2a_{12}a_{13}a_{32}a_{33}b_{22} + 2a_{12}a_{22}a_{23}a_{33}b_{13} - 2a_{12}a_{22}a_{33}{}^2 b_{12}$$

$$-2a_{12}a_{23}{}^2 a_{32}b_{13} + 2a_{12}a_{23}a_{32}a_{33}b_{12} + a_{13}{}^2 a_{22}{}^2 b_{33} - 2a_{13}{}^2 a_{22}a_{32}b_{23} + a_{13}{}^2 a_{32}{}^2 b_{22}$$

$$-2a_{13}a_{22}{}^2 a_{33}b_{13} + 2a_{13}a_{22}a_{23}a_{32}b_{13} + 2a_{13}a_{22}a_{32}a_{33}b_{12} - 2a_{13}a_{23}a_{32}{}^2 b_{12}$$

$$+a_{22}{}^2 a_{33}{}^2 b_{11} - 2a_{22}a_{23}a_{32}a_{33}b_{11} + a_{23}{}^2 a_{32}{}^2 b_{11},$$

$$\Gamma_\varphi = a_{11}{}^2 b_{22} - 2a_{11}a_{21}b_{12} - 2a_{13}a_{21}b_{23} + 2a_{31}a_{13}b_{22} + a_{21}{}^2 b_{11} + 2a_{21}a_{23}b_{13} + a_{23}{}^2 b_{33}$$

$$-2a_{23}a_{31}b_{12} - 2a_{23}a_{33}b_{23} + a_{23}{}^2 b_{22},$$

$$\kappa_\varphi = a_{11}{}^2 a_{23}{}^2 b_{33} - 2a_{11}{}^2 a_{23}a_{33}b_{23} + a_{11}{}^2 a_{33}{}^2 b_{22} - 2a_{11}a_{13}a_{21}a_{23}b_{33} + 2a_{11}a_{13}a_{21}a_{33}b_{23}$$

$$+2a_{11}a_{13}a_{23}a_{31}b_{23} - 2a_{21}a_{23}a_{31}a_{33}b_{11} - 2a_{11}a_{13}a_{33}a_{31}b_{22} + 2a_{11}a_{21}a_{23}a_{33}b_{13}$$

$$-2a_{11}a_{21}a_{33}{}^2 b_{12} - 2a_{11}a_{23}{}^2 a_{31}b_{13} + 2a_{11}a_{23}a_{31}a_{33}b_{12} + a_{13}{}^2 a_{21}{}^2 b_{33} + a_{13}{}^2 a_{31}{}^2 b_{22}$$

$$-2a_{13}{}^2 a_{21}a_{31}b_{23} - 2a_{13}a_{21}{}^2 a_{33}b_{13} + 2a_{21}a_{13}a_{23}a_{31}b_{13} + 2a_{21}a_{13}a_{31}a_{33}b_{12}$$

$$-2a_{13}a_{23}a_{31}{}^2 b_{12} + a_{21}{}^2 a_{33}{}^2 b_{11} + a_{23}{}^2 a_{31}{}^2 b_{11},$$

$$\kappa_\psi = a_{11}{}^2 a_{22}{}^2 b_{33} - 2a_{11}{}^2 a_{22}a_{32}b_{23} + a_{11}{}^2 a_{32}{}^2 b_{22} - 2a_{11}a_{12}a_{21}a_{22}b_{33} + 2a_{11}a_{12}a_{21}a_{32}b_{23}$$

$$+2a_{11}a_{21}a_{22}a_{32}b_{13} + 2a_{11}a_{12}a_{21}a_{32}b_{23} + 2a_{11}a_{12}a_{22}a_{31}b_{23} - 2a_{11}a_{12}a_{31}a_{32}b_{22}$$

$$-2a_{11}a_{21}a_{32}{}^2 b_{12} - 2a_{11}a_{22}{}^2 a_{31}b_{13} + 2a_{11}a_{22}a_{31}a_{32}b_{12} + a_{12}{}^2 a_{21}{}^2 b_{33} - 2a_{12}a_{21}{}^2 a_{32}b_{13}$$

$$-2a_{12}{}^2 a_{21}a_{31}b_{23} + a_{12}{}^2 a_{31}{}^2 b_{22} + 2a_{21}a_{12}a_{22}a_{31}b_{13} + 2a_{21}a_{12}a_{31}a_{32}b_{12} - 2a_{12}a_{22}a_{31}{}^2 b_{12}$$

$$-2a_{21}a_{22}a_{31}a_{32}b_{11} + a_{22}{}^2 a_{31}{}^2 b_{11} + a_{21}{}^2 a_{32}{}^2 b_{11},$$

$$\Gamma_\psi = a_{11}{}^2 b_{33} - 2a_{11}a_{31}b_{13} + 2a_{12}a_{21}b_{33} - 2a_{12}a_{31}b_{23} - 2a_{21}a_{32}b_{13} + a_{22}{}^2 b_{33} - 2a_{22}a_{32}b_{23}$$

$$+a_{31}{}^2 b_{11} + 2a_{31}a_{32}b_{12} + a_{32}{}^2 b_{22}.$$

(95)

Appendix E: System size expansion in spatial dynamic

Now the master equation is written in two contributions: the first part defined local mechanisms which correspond to the form given in non-spatial case adding a subscript with a scaled

Ω calling and the second take migration into account T_{ij}^{mig}. The latter is given by:

$$T_{ij}^{mig} = \left(\varepsilon_{x_i}^{-1}\varepsilon_{x_j} - 1\right) T\left(n_i + 1, n_j - 1 \,|n_i, n_j\right) + \left(\varepsilon_{x_i}\varepsilon_{x_j}^{-1} - 1\right) T\left(n_i - 1, n_j + 1 \,|n_i, n_j\right)$$
$$+ \left(\varepsilon_{y_i}^{-1}\varepsilon_{y_j} - 1\right) T\left(m_i + 1, m_j - 1 \,|m_i, m_j\right) + \left(\varepsilon_{y_i}\varepsilon_{y_j}^{-1} - 1\right) T\left(m_i - 1, m_j + 1 \,|m_i, m_j\right) \quad (96)$$
$$+ \left(\varepsilon_{z_i}^{-1}\varepsilon_{z_j} - 1\right) T\left(l_i + 1, l_j - 1 \,|l_i, l_j\right) + \left(\varepsilon_{z_i}\varepsilon_{z_j}^{-1} - 1\right) T\left(l_i - 1, l_j + 1 \,|l_i, l_j\right).$$

To obtain its contribution on the master equation, we carry out the same procedures doing on the local contribution in subsection 1. So, the operator expressions listed below are required, for the other parameters change $u = (x, y, z)$ and $\zeta = (\xi, \eta, \vartheta)$

$$\varepsilon_{u_i}^{-1}\varepsilon_{u_j} - 1 = N^{-1/2}\left(\frac{\partial}{\partial\zeta_j} - \frac{\partial}{\partial\zeta_i}\right) + \frac{1}{2}N^{-1}\left(\frac{\partial}{\partial\zeta_i} - \frac{\partial}{\partial\zeta_j}\right)^2 + \cdots,$$
$$\varepsilon_{u_i}\varepsilon_{u_j}^{-1} - 1 = N^{-1/2}\left(\frac{\partial}{\partial\zeta_i} - \frac{\partial}{\partial\zeta_j}\right) + \frac{1}{2}N^{-1}\left(\frac{\partial}{\partial\zeta_i} - \frac{\partial}{\partial\zeta_j}\right)^2 + \cdots, \quad (97)$$

Replacing these expressions and transitions rates in T_{ij}^{mig}, the follows list given contributions, at the order N^0 and $N^{1/2}$ is obtained:

$\left(\varepsilon_{x_i}^{-1}\varepsilon_{x_j} - 1\right) T\left(n_i + 1, n_j - 1 \,|n_i, n_j\right)$:

N^0 :
$$-\phi_j\left(\frac{\partial}{\partial\xi_j} - \frac{\partial}{\partial\xi_i}\right)(\xi_i + \eta_i + \vartheta_i), (1 - \phi_i - \varphi_i - \psi_i)\left(\frac{\partial}{\partial\xi_j} - \frac{\partial}{\partial\xi_i}\right)\xi_j, \frac{1}{2}\phi_j(1 - \phi_i - \varphi_i - \psi_i)\left(\frac{\partial}{\partial\xi_j} - \frac{\partial}{\partial\xi_i}\right)^2$$
$$(98)$$

$N^{1/2}$:
$$\phi_j\left(1 - \phi_i - \varphi_i - \psi_i\right)\left(\frac{\partial}{\partial\xi_j} - \frac{\partial}{\partial\xi_i}\right) \quad (99)$$

The contributions of the terms are $\left(\varepsilon_{x_i}\varepsilon_{x_j}^{-1} - 1\right) T\left(n_i - 1, n_j + 1 \,|n_i, n_j\right)$ obtained by interchanging i and j. So adding the terms in order $N^{1/2}$ together and identified $\partial\Pi/\partial\xi_i$ for each i with the corresponding term on the left-hand side of the master equation, it lead to

$$-\frac{2\mu_1}{z\Omega}\left(\sum_j(\phi_j - \phi_i) + \sum_j(\phi_i\varphi_j - \phi_j\varphi_i) + \sum_j(\phi_i\psi_j - \phi_j\psi_i)\right)$$

Using the discrete Laplacian operator $\Delta f_i = (2/z) \sum\limits_{j \in i} (f_j - f_i)$, the following equation is obtained.

$$-\frac{\mu_1}{\Omega} \left(\Delta\phi_i + \phi_i\Delta\varphi_i - \varphi_i\Delta\phi_i + \phi_i\Delta\psi_i - \psi_i\Delta\phi_i \right) \tag{100}$$

A similar analysis may be carried out for the terms

$\left(\varepsilon_{y_i}^{-1}\varepsilon_{y_j} - 1 \right) T\left(m_i + 1, m_j - 1 \,|\, m_i, m_j \right)$, $\left(\varepsilon_{y_i}\varepsilon_{y_j}^{-1} - 1 \right) T\left(m_i - 1, m_j + 1 \,|\, m_i, m_j \right)$

and $\left(\varepsilon_{z_i}^{-1}\varepsilon_{z_j} - 1 \right) T\left(l_i + 1, l_j - 1 \,|\, l_i, l_j \right)$, $\left(\varepsilon_{z_i}\varepsilon_{z_j}^{-1} - 1 \right) T\left(l_i - 1, l_j + 1 \,|\, l_i, l_j \right)$

to obtain

$$-\frac{\mu_2}{\Omega} \left(\Delta\varphi_i + \varphi_i\Delta\phi_i - \phi_i\Delta\varphi_i + \varphi_i\Delta\psi_i - \psi_i\Delta\varphi_i \right) \tag{101}$$

and

$$-\frac{\mu_3}{\Omega} \left(\Delta\psi_i + \psi_i\Delta\varphi_i - \varphi_i\Delta\psi_i + \psi_i\Delta\phi_i - \phi_i\Delta\psi_i \right) \tag{102}$$

respectively. Identifying Eq.100, Eq.101, Eq.102 to the left-hand side of the master equation, lead to a deterministic equations defined by

The stochastic contributions of the terms $\left(\varepsilon_{x_i}^{-1}\varepsilon_{x_j} - 1 \right) T\left(n_i + 1, n_j - 1 \,|\, n_i, n_j \right)$ are given by the two first terms of N^0 :

$$\frac{\mu_1}{z\Omega} \sum_{i,j} \left(\frac{\partial}{\partial\xi_j} - \frac{\partial}{\partial\xi_i} \right) \left(-\phi_j \left(\xi_i + \eta_i + \vartheta_i \right) + \left(1 - \phi_i - \varphi_i - \psi_i \right) \xi_j \right) \tag{103}$$

Adding with the contributions from $\left(\varepsilon_{x_i}\varepsilon_{x_j}^{-1} - 1 \right) T\left(n_i - 1, n_j + 1 \,|\, n_i, n_j \right)$ lead to

$$-\frac{\mu_1}{\Omega} \sum_i \frac{\partial}{\partial\xi_i} \left(D_{i,11}\xi_i + D_{i,12}\eta_i + D_{i,13}\vartheta_i \right) \Pi \tag{104}$$

where

$$\begin{aligned} D_{i,11} &= \Delta - \left(\varphi_i + \psi_i \right) \Delta + \left(\Delta \left(\varphi_i + \psi_i \right) \right) \\ D_{i,12} &= D_{i,13} = \phi_i\Delta - \left(\Delta\phi_i \right) \end{aligned} \tag{105}$$

To obtain the stochastic contributions given from the terms concerning by the migration of in-

fected pests and spores just interchanging:

For infected pest: $\mu_1 \to \mu_2$, $\phi_i \to \varphi_i$ and $\xi_i \to \eta_i$

For spore: $\mu_1 \to \mu_3$, $\phi_i \to \psi_i$ and $\xi_i \to \vartheta_i$

So, this give respectively,

$$-\frac{\mu_2}{\Omega} \sum_i \frac{\partial}{\partial \eta_i} \left(D_{i,21}\xi_i + D_{i,22}\eta_i + D_{i,23}\vartheta_i \right) \Pi \tag{106}$$

and

$$-\frac{\mu_3}{\Omega} \sum_i \frac{\partial}{\partial \vartheta_i} \left(D_{i,31}\xi_i + D_{i,32}\eta_i + D_{i,33}\vartheta_i \right) \Pi \tag{107}$$

with

$$
\begin{aligned}
D_{i,21} &= D_{i,23} = \varphi_i \Delta - (\Delta \varphi_i), \\
D_{i,22} &= \Delta - (\phi_i + \psi_i) \Delta + (\Delta (\phi_i + \psi_i)), \\
D_{i,33} &= \Delta - (\varphi_i + \phi_i) \Delta + (\Delta (\varphi_i + \phi_i)), \\
D_{i,31} &= D_{i,32} = \psi_i \Delta - (\Delta \psi_i).
\end{aligned}
\tag{108}
$$

The deterministic models is written as the 3Ω macroscopic equations given by

$$
\begin{aligned}
\dot{\phi}_i &= r\phi_i(1 - \frac{\phi_i}{k}) - \alpha_1 \phi_i \varphi_i - \beta_1 \phi_i \psi_i + \mu_1 \left(\Delta \phi_i + \phi_i \Delta \varphi_i - \varphi_i \Delta \phi_i + \phi_i \Delta \psi_i - \psi_i \Delta \phi_i \right), \\
\dot{\varphi}_i &= \alpha_2 \phi_i \varphi_i + \theta \phi_i \psi_i - b_2 \varphi_i + \mu_2 \left(\Delta \varphi_i + \varphi_i \Delta \phi_i - \phi_i \Delta \varphi_i + \varphi_i \Delta \psi_i - \psi_i \Delta \varphi_i \right), \\
\dot{\psi}_i &= b_2 \varphi_i - d_3 \psi_i + \mu_3 \left(\Delta \psi_i + \psi_i \Delta \phi_i - \phi_i \Delta \psi_i + \psi_i \Delta \varphi_i - \varphi_i \Delta \psi_i \right).
\end{aligned}
\tag{109}
$$

where $i = 1, ..., \Omega$ and the symbols $(.)$ and Δ denote the time derivation (scaled $\tau = t/\Omega$) and discrete Laplacian operator $\Delta f_i = (2/z) \sum_{j \in i} (f_j - f_i)$. In this sum z corresponds to the total of first neighbors. the limit $\Omega \to \infty$ corresponds to shrink the lattice spacing d to zero and so leading to the continuum mean-field description. In this limit, the system (109)converge to

$$
\begin{aligned}
\dot{\phi} &= r\phi(1 - \frac{\phi}{k}) - \alpha_1 \phi\varphi - \beta_1 \phi\psi + \mu_1 \left(\nabla^2 \phi + \phi \nabla^2 \varphi - \varphi \nabla^2 \phi + \phi \nabla^2 \psi - \psi \nabla^2 \phi \right), \\
\dot{\varphi} &= \alpha_2 \phi\varphi + \theta \phi\psi - b_2 \varphi + \mu_2 \left(\nabla^2 \varphi + \varphi \nabla^2 \phi - \phi \nabla^2 \varphi + \varphi \nabla^2 \psi - \psi \nabla^2 \varphi \right), \\
\dot{\psi} &= b_2 \varphi - d_3 \psi + \mu_3 \left(\nabla^2 \psi + \psi \nabla^2 \phi - \phi \nabla^2 \psi + \psi \nabla^2 \varphi - \varphi \nabla^2 \psi \right).
\end{aligned}
\tag{110}
$$

The terms given in Eq. 108 are the diffusion contribution of the first terms of Fokker-Planck

equations, such that it can be defined by

$$\frac{\partial \Pi}{\partial t} = -\sum_{i=1}^{\Omega} \frac{\partial \left(A_i \left[\zeta \left(t \right) \right] \Pi \right)}{\partial \zeta_i} + \frac{1}{2} \sum_{i,j} \frac{\partial^2 \left[B_{ij} \left(t \right) \Pi \right]}{\partial \zeta_i \partial \zeta_j} \tag{111}$$

where, fluctuations variables $\zeta_i = (\xi_i, \eta_i, \vartheta_i)$ are introduced. The function $A_i \left(\zeta \right)$ is given by

$$
\begin{aligned}
A_{i,1} &= \alpha_{i,11} \xi_i + \alpha_{i,12} \eta_i + \alpha_{i,13} \vartheta_i, \\
A_{i,2} &= \alpha_{i,21} \xi_i + \alpha_{i,22} \eta_i + \alpha_{i,23} \vartheta_i, \\
A_{i,3} &= \alpha_{i,31} \xi_i + \alpha_{i,32} \eta_i + \alpha_{i,33} \vartheta_i.
\end{aligned}
\tag{112}
$$

where $\alpha_{i,jk}$ $(j, k = 1, 2, 3)$ are exactly the coefficients found adding element a_{ij} given in Appendix C (Eq.91) with subscript i with diffusion terms defined by Eq.105 and Eq.108 at an equilibrium state and can be also deduced from stability analysis of the spatial equation given by Eq. (110). The matrix B_{ij} is defined as follow:

$$
\begin{aligned}
B_{ij,11} &= \left(2I_1 \phi^s \varphi^s + 2I_2 \phi^s \psi^s + d_1 \phi^s + 2b_1 \phi^s \left(1 - \phi^s - \varphi^s - \psi^s \right) \right. \\
&\left. + 4\mu_1 \phi^s \left(1 - \phi^s - \varphi^s - \psi^s \right) \right) \delta_{ij} - \frac{4\mu_1}{z} \phi^s \left(1 - \phi^s - \varphi^s - \psi^s \right) J_{\langle ij \rangle}, \\
B_{ij,23} &= B_{ij,32} = -2b_2 \varphi^s, \\
B_{ij,22} &= \left(2I_1 \phi^s \varphi^s + 2I_2 \phi^s \psi^s + 2b_2 \varphi^s + 4\mu_1 \varphi^s \left(1 - \phi^s - \varphi^s - \psi^s \right) \right) \delta_{ij} \\
&- \frac{4\mu_2}{z} \varphi^s \left(1 - \phi^s - \varphi^s - \psi^s \right) J_{\langle ij \rangle}, \\
B_{ij,13} &= B_{ij,31} = 0, \\
B_{ij,12} &= B_{ij,21} = -4I_1 \phi^s \varphi^s - 4I_2 \phi^s \psi^s, \\
B_{ij,33} &= \left(2b_2 \varphi^s + d_3 \psi^s + 4\mu_1 \phi^s \left(1 - \phi^s - \varphi^s - \psi^s \right) \right) \delta_{ij} - \frac{4\mu_1}{z} \phi^s \left(1 - \phi^s - \varphi^s - \psi^s \right) J_{\langle ij \rangle},
\end{aligned}
\tag{113}
$$

This term is found by using the elements defined in equations Eq.89 and the third terms of Eq.98.

Bibliography

[1] M. A. Gilchrist, D. L. Sulsky, and A. Pringle, "Identifying fitness and optimal life-history strategies for an asexual filamentous fungus," *Evolution*, vol. 60, no. 5, pp. 970–979, 2006.

[2] A. Vilcinskas and P. Götz, "Parasitic fungi and their interactions with the insect immune system," in *Advances in parasitology*, vol. 43, pp. 267–313, Elsevier, 1999.

[3] H. Hesketh, H. Roy, J. Eilenberg, J. Pell, and R. Hails, "Challenges in modelling complexity of fungal entomopathogens in semi-natural populations of insects," *BioControl*, vol. 55, no. 1, pp. 55–73, 2010.

[4] S. Qu and S. Wang, "Interaction of entomopathogenic fungi with the host immune system," *Developmental & Comparative Immunology*, vol. 83, pp. 96–103, 2018.

[5] S. Marino, I. B. Hogue, C. J. Ray, and D. E. Kirschner, "A methodology for performing global uncertainty and sensitivity analysis in systems biology," *Journal of theoretical biology*, vol. 254, no. 1, pp. 178–196, 2008.

[6] D. T. Gillespie, "Exact stochastic simulation of coupled chemical reactions," *The journal of physical chemistry*, vol. 81, no. 25, pp. 2340–2361, 1977.

[7] J. Offenberg, "Ants as tools in sustainable agriculture," *Journal of Applied Ecology*, vol. 52, no. 5, pp. 1197–1205, 2015.

[8] S. J. Risch, D. Andow, and M. A. Altieri, "Agroecosystem diversity and pest control: data, tentative conclusions, and new research directions," *Environmental entomology*, vol. 12, no. 3, pp. 625–629, 1983.

[9] G. Knudsen and D. Schotzko, "Spatial simulation of epizootics caused by beauveria bassiana in russian wheat aphid populations," *Biological Control*, vol. 16, no. 3, pp. 318–326, 1999.

[10] E.-J. Scholte, K. Ng'Habi, J. Kihonda, W. Takken, K. Paaijmans, S. Abdulla, G. F. Killeen, and B. G. Knols, "An entomopathogenic fungus for control of adult african malaria mosquitoes," *Science*, vol. 308, no. 5728, pp. 1641–1642, 2005.

[11] H. Ranson, "N guessan r, lines j, moiroux n, nkuni z, corbel v. 2011," *Pyrethroid resistance in African anopheline mosquitoes: what are the implications for malaria control*, pp. 91–98.

[12] B. Ouafa, *Evaluation de Metarhizium anisopliae titre dagent de lutte biologique contre les larves de moustiques*. PhD thesis, thesis (University Constantine 1, 2015).

[13] D. Pimentel and M. Burgess, "An environmental, energetic and economic comparison of organic and conventional farming systems," in *Integrated Pest Management*, pp. 141–166, Springer, 2014.

[14] D. Kumar and P. Kalita, "Reducing postharvest losses during storage of grain crops to strengthen food security in developing countries," *Foods*, vol. 6, no. 1, p. 8, 2017.

[15] A. Fenton, R. Norman, J. P. Fairbairn, and P. J. Hudson, "Modelling the efficacy of entomopathogenic nematodes in the regulation of invertebrate pests in glasshouse crops," *Journal of Applied Ecology*, vol. 37, no. 2, pp. no–no, 2000.

[16] G. Dwyer, "Density dependence and spatial structure in the dynamics of insect pathogens," *The American Naturalist*, vol. 143, no. 4, pp. 533–562, 1994.

[17] A. Mvogo, A. Tambue, G. H. Ben-Bolie, and T. C. Kofané, "Localized modulated wave solutions in diffusive glucose–insulin systems," *Physics Letters A*, vol. 380, no. 25-26, pp. 2154–2159, 2016.

[18] F. M. Kakmeni, E. Inack, and E. Yamakou, "Localized nonlinear excitations in diffusive hindmarsh-rose neural networks," *Physical Review E*, vol. 89, no. 5, p. 052919, 2014.

[19] G. F. Achu, S. M. Tchouobiap, F. M. Kakmeni, and C. Tchawoua, "Periodic soliton trains and informational code structures in an improved soliton model for biomembranes and nerves," *Physical Review E*, vol. 98, no. 2, p. 022216, 2018.

[20] P. H. Tatsing, T. C. Kofane, A. Mohamadou, and C. G. L. Tiofack, "Modulational instability in oppositely doubled-doped directed couplers with a non-kerr-like nonlinear refractive-index change," *Optical and Quantum Electronics*, vol. 51, no. 12, p. 390, 2019.

[21] D. Zanga, S. I. Fewo, C. B. Tabi, and T. C. Kofané, "Modulational instability in weak non-local nonlinear media with competing kerr and non-kerr nonlinearities," *Communications in Nonlinear Science and Numerical Simulation*, vol. 80, p. 104993, 2020.

[22] M. Conforti, A. Mussot, A. Kudlinski, and S. Trillo, "Modulational instability in dispersion oscillating fiber ring cavities," *Optics letters*, vol. 39, no. 14, pp. 4200–4203, 2014.

[23] M. Conforti, A. Mussot, A. Kudlinski, S. R. Nodari, G. Dujardin, S. De Biévre, A. Armaroli, and S. Trillo, "Heteroclinic structure of parametric resonance in the nonlinear schrödinger equation," *Physical review letters*, vol. 117, no. 1, p. 013901, 2016.

[24] J. Bale, J. Van Lenteren, and F. Bigler, "Biological control and sustainable food production," *Philosophical Transactions of the Royal Society B: Biological Sciences*, vol. 363, no. 1492, pp. 761–776, 2008.

[25] A. Hajek and R. St. Leger, "Interactions between fungal pathogens and insect hosts," *Annual review of entomology*, vol. 39, no. 1, pp. 293–322, 1994.

[26] M. B. Thomas and S. Blanford, "Thermal biology in insect-parasite interactions," *Trends in Ecology & Evolution*, vol. 18, no. 7, pp. 344–350, 2003.

[27] R. A. Samson, H. C. Evans, and J.-P. Latgé, *Atlas of entomopathogenic fungi.* Springer Science & Business Media, 2013.

[28] H. E. Roy, F. E. Vega, D. Chandler, M. S. Goettel, J. Pell, E. Wajnberg, *et al.*, *The ecology of fungal entomopathogens.* Springer, 2010.

[29] J. Baverstock, H. E. Roy, and J. K. Pell, "Entomopathogenic fungi and insect behaviour: from unsuspecting hosts to targeted vectors," in *The ecology of fungal entomopathogens*, pp. 89–102, Springer, 2009.

[30] S. Blanford and M. B. Thomas, "Host thermal biology: the key to understanding host–pathogen interactions and microbial pest control?," *Agricultural and Forest Entomology*, vol. 1, no. 3, pp. 195–202, 1999.

[31] P. Ferron, J. Fargues, and G. Riba, "Les champignons agents de lutte microbiologique contre les ravageurs," *Dossiers de la Cellule Environnement*, vol. 5, pp. 65–92, 1993.

[32] R. M. Weseloh, "Effect of conidial dispersal of the fungal pathogen entomophaga maimaiga (zygomycetes: Entomophthorales) on survival of its gypsy moth (lepidoptera: Lymantriidae) host," *Biological Control*, vol. 29, no. 1, pp. 138–144, 2004.

[33] R. St Leger, "Parasites and pathogens of insects: biology and mechanisms of insect-cuticle invasion by deuteromycete fungal pathogens. vol. 2," 1993.

[34] R. I. Carruthers, Z. Feng, M. E. Ramos, and R. S. Soper, "The effect of solar radiation on the survival of entomophaga grylli (entomophthorales: Entomophthoraceae) conidia," *Journal of Invertebrate Pathology*, vol. 52, no. 1, pp. 154 – 162, 1988.

[35] T. J. Kurtti and N. O. Keyhani, "Intracellular infection of tick cell lines by the entomopathogenic fungus metarhizium anisopliae," *Microbiology*, vol. 154, no. 6, pp. 1700–1709, 2008.

[36] S. Wraight, R. Carruthers, S. Jaronski, C. Bradley, C. Garza, and S. Galaini-Wraight, "Evaluation of the entomopathogenic fungi beauveria bassiana and paecilomyces fumosoroseus for microbial control of the silverleaf whitefly, bemisia argentifolii," *Biological control*, vol. 17, no. 3, pp. 203–217, 2000.

[37] D. Boucias, J. Pendland, and J. Latge, "Nonspecific factors involved in attachment of entomopathogenic deuteromycetes to host insect cuticle," *Applied and environmental microbiology*, vol. 54, no. 7, pp. 1795–1805, 1988.

[38] N. V. Meyling and J. Eilenberg, "Ecology of the entomopathogenic fungi beauveria bassiana and metarhizium anisopliae in temperate agroecosystems: potential for conservation biological control," *Biological control*, vol. 43, no. 2, pp. 145–155, 2007.

[39] H. E. Roy and J. K. Pell, "Interactions between entomopathogenic fungi and other natural enemies: implications for biological control," *Biocontrol Science and Technology*, vol. 10, no. 6, pp. 737–752, 2000.

[40] I. Dubovskiy, M. Whitten, V. Kryukov, O. Yaroslavtseva, E. Grizanova, C. Greig, K. Mukherjee, A. Vilcinskas, P. Mitkovets, V. Glupov, *et al.*, "More than a colour change: insect melanism, disease resistance and fecundity," *Proceedings of the Royal Society B: Biological Sciences*, vol. 280, no. 1763, p. 20130584, 2013.

[41] P. Shah and J. Pell, "Entomopathogenic fungi as biological control agents," *Applied micro-biology and biotechnology*, vol. 61, no. 5-6, pp. 413–423, 2003.

[42] A. E. Hajek and J. Eilenberg, *Natural enemies: an introduction to biological control*. Cambridge University Press, 2018.

[43] H. K. Kaya and F. E. Vega, "Scope and basic principles of insect pathology," *Insect Pathology. Academic Press, London, United Kingdom*, pp. 1–12, 2012.

[44] Y. Sanjaya, V. R. Ocampo, B. L. Caoili, *et al.*, "Transmission effect of entomopathogenic fungi on population of tetanychus kanzawai (kishida)(tetranychidae: Acarina)," *Arthropods*, vol. 2, no. 1, pp. 36–41, 2013.

[45] G. Brown and R. Hasibuan, "Conidial discharge and transmission efficiency of neozygites floridana, an entomopathogenic fungus infecting two-spotted spider mites under laboratory conditions," *Journal of invertebrate pathology*, vol. 65, no. 1, pp. 10–16, 1995.

[46] A. Brooks and R. Wall, "Horizontal transmission of fungal infection by metarhizium anisopliae in parasitic psoroptes mites (acari: Psoroptidae)," *Biological Control*, vol. 34, no. 1, pp. 58–65, 2005.

[47] S. Arthurs and M. B. Thomas, "Effects of temperature and relative humidity on sporulation of metarhizium anisopliae var. acridum in mycosed cadavers of schistocerca gregaria," *Journal of Invertebrate Pathology*, vol. 78, no. 2, pp. 59–65, 2001.

[48] M. Hassell, *The spatial and temporal dynamics of host-parasitoid interactions*. OUP Oxford, 2000.

[49] J. I. Klass, S. Blanford, and M. B. Thomas, "Development of a model for evaluating the effects of environmental temperature and thermal behaviour on biological control of locusts and grasshoppers using pathogens," *Agricultural and Forest Entomology*, vol. 9, no. 3, pp. 189–199, 2007.

[50] P. Valverde-Garcia, C. Santiago-Alvarez, M. B. Thomas, I. Garrido-Jurado, and E. Quesada-Moraga, "Comparative effects of temperature and thermoregulation on candidate strains of entomopathogenic fungi for moroccan locust dociostaurus maroccanus control," *BioControl*, vol. 63, no. 6, pp. 819–831, 2018.

[51] G. Dwyer, J. S. Elkinton, and A. E. Hajek, "Spatial scale and the spread of a fungal pathogen of gypsy moth," *The American Naturalist*, vol. 152, no. 3, pp. 485–494, 1998.

[52] H. Malchow, S. V. Petrovskii, and E. Venturino, *Spatiotemporal patterns in ecology and epidemiology: theory, models, and simulation*. CRC Press, 2007.

[53] J. Rajula, A. Rahman, and P. Krutmuang, "Entomopathogenic fungi in southeast asia and africa and their possible adoption in biological control," *Biological Control*, p. 104399, 2020.

[54] F. E. Vega, M. S. Goettel, M. Blackwell, D. Chandler, M. A. Jackson, S. Keller, M. Koike, N. K. Maniania, A. Monzon, B. H. Ownley, *et al.*, "Fungal entomopathogens: new insights on their ecology," *fungal ecology*, vol. 2, no. 4, pp. 149–159, 2009.

[55] J. C. Lord, "From metchnikoff to monsanto and beyond: The path of microbial control," *Journal of invertebrate pathology*, vol. 89, no. 1, pp. 19–29, 2005.

[56] U. Maina, I. Galadima, F. Gambo, and D. Zakaria, "A review on the use of entomopathogenic fungi in the management of insect pests of field crops," *Journal of Entomology and Zoology Studies*, vol. 6, no. 1, pp. 27–32, 2018.

[57] H. T. Gul, S. Saeed, and F. A. Khan, "Entomopathogenic fungi as effective insect pest management tactic: A review," *Applied Sciences and Business Economics*, vol. 1, no. 1, pp. 10–18, 2014.

[58] A. A. Shahid, Q. A. Rao, A. Bakhsh, and T. Husnain, "Entomopathogenic fungi as biological controllers: new insights into their virulence and pathogenicity," *Archives of Biological Sciences*, vol. 64, no. 1, pp. 21–42, 2012.

[59] G. Wallentin, "Spatial simulation: a spatial perspective on individual-based ecology—a review," *Ecological Modelling*, vol. 350, pp. 30–41, 2017.

[60] B. A. Hawkins and H. V. Cornell, *Theoretical approaches to biological control*. Cambridge University Press, 2008.

[61] J. W. Lichstein, T. R. Simons, S. A. Shriner, and K. E. Franzreb, "Spatial autocorrelation and autoregressive models in ecology," *Ecological monographs*, vol. 72, no. 3, pp. 445–463, 2002.

[62] B. D. Elderd, J. Dushoff, and G. Dwyer, "Host-pathogen interactions, insect outbreaks, and natural selection for disease resistance," *The American Naturalist*, vol. 172, no. 6, pp. 829–842, 2008.

[63] A. E. Hajek, T. S. Larkin, R. I. Carruthers, and R. S. Soper, "Modeling the dynamics of entomophaga maimaiga (zygomycetes: Entomophthorales) epizootics in gypsy moth (lepidoptera: Lymantriidae) populations," *Environmental entomology*, vol. 22, no. 5, pp. 1172–1187, 1993.

[64] G. Hess, "Disease in metapopulation models: implications for conservation," *Ecology*, vol. 77, no. 5, pp. 1617–1632, 1996.

[65] S. A. Pedro, S. Abelman, and H. E. Tonnang, "Predicting rift valley fever inter-epidemic activities and outbreak patterns: Insights from a stochastic host-vector model," *PLoS neglected tropical diseases*, vol. 10, no. 12, p. e0005167, 2016.

[66] T. Y. Shin, M. R. Lee, S. E. Park, S. J. Lee, W. J. Kim, and J. S. Kim, "Pathogenesis-related genes of entomopathogenic fungi," *Archives of Insect Biochemistry and Physiology*, p. e21747, 2020.

[67] M. A. Gilchrist, D. L. Sulsky, and A. Pringle, "Identifying fitness and optimal life-history strategies for an asexual filamentous fungus," *Evolution*, vol. 60, no. 5, pp. 970 – 979, 2006.

[68] G. Dwyer, J. Dushoff, J. S. Elkinton, and S. A. Levin, "Pathogen-driven outbreaks in forest defoliators revisited: building models from experimental data," *The American Naturalist*, vol. 156, no. 2, pp. 105–120, 2000.

[69] B. S. Djouda, F. Moukam Kakmeni, P. Guemkam Ghomsi, F. T. Ndjomatchoua, C. Tchawoua, and H. E. Tonnang, "Theoretical analysis of spatial nonhomogeneous patterns of entomopathogenic fungi growth on insect pest," *Chaos: An Interdisciplinary Journal of Nonlinear Science*, vol. 29, no. 5, p. 053134, 2019.

[70] S. Djilali and S. Bentout, "Spatiotemporal patterns in a diffusive predator-prey model with prey social behavior," *Acta Applicandae Mathematicae*, pp. 1–19, 2019.

[71] S. Djilali, B. Ghanbari, S. Bentout, and A. Mezouaghi, "Turing-hopf bifurcation in a diffusive mussel-algae model with time-fractional-order derivative," *Chaos, Solitons & Fractals*, vol. 138, p. 109954, 2020.

[72] F. Souna, A. Lakmeche, and S. Djilali, "The effect of the defensive strategy taken by the prey on predator–prey interaction," *Journal of Applied Mathematics and Computing*, vol. 64, no. 1, pp. 665–690, 2020.

[73] B. Ghanbari and S. Djilali, "Mathematical analysis of a fractional-order predator-prey model with prey social behavior and infection developed in predator population," *Chaos, Solitons & Fractals*, vol. 138, p. 109960, 2020.

[74] F. Souna, A. Lakmeche, and S. Djilali, "Spatiotemporal patterns in a diffusive predator-prey model with protection zone and predator harvesting," *Chaos, Solitons & Fractals*, vol. 140, p. 110180, 2020.

[75] S. Djilali, "Spatiotemporal patterns induced by cross-diffusion in predator–prey model with prey herd shape effect," *International Journal of Biomathematics*, vol. 13, no. 04, p. 2050030, 2020.

[76] S. Djilali, "Pattern formation of a diffusive predator-prey model with herd behavior and nonlocal prey competition," *Mathematical Methods in the Applied Sciences*, vol. 43, no. 5, pp. 2233–2250, 2020.

[77] F. Souna, S. Djilali, and F. Charif, "Mathematical analysis of a diffusive predator-prey model with herd behavior and prey escaping," *Mathematical Modelling of Natural Phenomena*, vol. 15, p. 23, 2020.

[78] J. Dawes and M. Souza, "A derivation of holling's type i, ii and iii functional responses in predator–prey systems," *Journal of theoretical biology*, vol. 327, pp. 11–22, 2013.

[79] C. Tian and L. Zhang, "Hopf bifurcation analysis in a diffusive food-chain model with time delay," *Computers & Mathematics with Applications*, vol. 66, no. 10, pp. 2139–2153, 2013.

[80] A. L. Lloyd, J. Zhang, and A. M. Root, "Stochasticity and heterogeneity in host–vector models," *Journal of the Royal Society Interface*, vol. 4, no. 16, pp. 851–863, 2007.

[81] O. Ovaskainen and B. Meerson, "Stochastic models of population extinction," *Trends in ecology & evolution*, vol. 25, no. 11, pp. 643–652, 2010.

[82] R. M. Anderson and R. M. May, "The population dynamics of microparasites and their invertebrate hosts," *Philosophical Transactions of the Royal Society of London. B, Biological Sciences*, vol. 291, no. 1054, pp. 451–524, 1981.

[83] A. Govindarajan, B. A. Malomed, A. Mahalingam, and A. Uthayakumar, "Modulational instability in linearly coupled asymmetric dual-core fibers," *Applied Sciences*, vol. 7, no. 7, p. 645, 2017.

[84] M. Conforti, F. Copie, A. Mussot, A. Kudlinski, and S. Trillo, "Parametric instabilities in modulated fiber ring cavities," *Optics letters*, vol. 41, no. 21, pp. 5027–5030, 2016.

[85] S. R. Nodari, M. Conforti, G. Dujardin, A. Kudlinski, A. Mussot, S. Trillo, and S. De Bièvre, "Modulational instability in dispersion-kicked optical fibers," *Physical Review A*, vol. 92, no. 1, p. 013810, 2015.

[86] A. Mussot, M. Conforti, S. Trillo, F. Copie, and A. Kudlinski, "Modulation instability in dispersion oscillating fibers," *Advances in Optics and Photonics*, vol. 10, no. 1, pp. 1–42, 2018.

[87] A. J. Black and A. J. McKane, "Stochastic amplification in an epidemic model with seasonal forcing," *Journal of Theoretical Biology*, vol. 267, no. 1, pp. 85–94, 2010.

[88] T. Biancalani, T. Galla, and A. J. McKane, "Stochastic waves in a brusselator model with nonlocal interaction," *Physical Review E*, vol. 84, no. 2, p. 026201, 2011.

[89] D. Alonso, A. J. McKane, and M. Pascual, "Jr soc," *Interface*, vol. 4, pp. 575–582, 2007.

[90] J. Realpe-Gomez, M. Baudena, T. Galla, A. J. McKane, and M. Rietkerk, "Demographic noise and resilience in a semi-arid ecosystem model," *Ecological Complexity*, vol. 15, pp. 97–108, 2013.

[91] R. Marguta and A. Parisi, "Impact of human mobility on the periodicities and mechanisms underlying measles dynamics," *Journal of The Royal Society Interface*, vol. 12, no. 104, p. 20141317, 2015.

[92] M. Asslani, F. Di Patti, and D. Fanelli, "Stochastic turing patterns on a network," *Physical Review E*, vol. 86, no. 4, p. 046105, 2012.

[93] J. Antonovics, A. McKane, and T. Newman, "Spatiotemporal dynamics in marginal populations," *The American Naturalist*, vol. 167, no. 1, pp. 16–27, 2006.

[94] G. Rozhnova, A. Nunes, and A. McKane, "Stochastic oscillations in models of epidemics on a network of cities," *Physical Review E*, vol. 84, no. 5, p. 051919, 2011.

[95] A. J. Black and A. J. McKane, "Stochastic formulation of ecological models and their applications," *Trends in ecology & evolution*, vol. 27, no. 6, pp. 337–345, 2012.

[96] I. Berenstein and J. Carballido-Landeira, "Spatiotemporal chaos involving wave instability," *Chaos: An Interdisciplinary Journal of Nonlinear Science*, vol. 27, no. 1, p. 013116, 2017.

[97] M. C. Cross and P. C. Hohenberg, "Pattern formation outside of equilibrium," *Reviews of modern physics*, vol. 65, no. 3, p. 851, 1993.

[98] A. J. McKane and T. J. Newman, "Stochastic models in population biology and their deterministic analogs," *Physical Review E*, vol. 70, no. 4, p. 041902, 2004.

[99] T. Rogers, W. Clifford-Brown, C. Mills, and T. Galla, "Stochastic oscillations of adaptive networks: application to epidemic modelling," *Journal of Statistical Mechanics: Theory and Experiment*, vol. 2012, no. 08, p. P08018, 2012.

[100] C. Konje, A. Abdulai, A. D. Tange, D. Nsobinenyui, D. Tarla, and M. A. Tita, "Identification and management of pests and diseases of garden crops in santa, cameroon," *Journal of Agriculture and Ecology Research International*, pp. 1–9, 2019.

[101] G. G. Khachatourians and S. S. Qazi, "Entomopathogenic fungi: biochemistry and molecular biology," in *Human and animal relationships*, pp. 33–61, Springer, 2008.

[102] M. Banerjee and Y. Takeuchi, "Maturation delay for the predators can enhance stable coexistence for a class of prey–predator models," *Journal of theoretical biology*, vol. 412, pp. 154–171, 2017.

[103] H. Caswell and M. G. Neubert, "Chaos and closure terms in plankton food chain models," *Journal of Plankton Research*, vol. 20, no. 9, pp. 1837–1845, 1998.

[104] A. Hastings and T. Powell, "Chaos in a three-species food chain," *Ecology*, vol. 72, no. 3, pp. 896–903, 1991.

[105] R. Bhattacharyya and B. Mukhopadhyay, "On a population pathogen model incorporating species dispersal with temporal variation in dispersal rate," *Journal of biological physics*, vol. 37, no. 4, pp. 401–416, 2011.

[106] S. Gourley, N. Britton, M. A. Chaplain, and H. Byrne, "Mechanisms for stabilisation and destabilisation of systems of reaction-diffusion equations," *Journal of Mathematical Biology*, vol. 34, no. 8, pp. 857–877, 1996.

[107] J. A. Sherratt, "Diffusion-driven instability in oscillating environments," *European Journal of Applied Mathematics*, vol. 6, no. 4, pp. 355–372, 1995.

[108] J. A. Sherratt, "Turing bifurcations with a temporally varying diffusion coefficient," *Journal of Mathematical Biology*, vol. 33, no. 3, pp. 295–308, 1995.

[109] S. Webb and J. Sherratt, "Oscillatory reaction-diffusion equations with temporally varying parameters," *Mathematical and computer modelling*, vol. 39, no. 1, pp. 45–60, 2004.

[110] J. T. Mika, A. J. Thompson, M. R. Dent, N. J. Brooks, J. Michiels, J. Hofkens, and M. K. Kuimova, "Measuring the viscosity of the escherichia coli plasma membrane using molecular rotors," *Biophysical journal*, vol. 111, no. 7, pp. 1528–1540, 2016.

[111] D. Lucena, M. Mauri, F. Schmidt, B. Eckhardt, and P. L. Graumann, "Microdomain formation is a general property of bacterial membrane proteins and induces heterogeneity of diffusion patterns," *BMC biology*, vol. 16, no. 1, pp. 1–17, 2018.

[112] R. L. Snyder, "Hand calculating degree days," *Agricultural and forest meteorology*, vol. 35, no. 1-4, pp. 353–358, 1985.

[113] S. P. Worner, "Performance of phenological models under variable temperature regimes: consequences of the kaufmann or rate summation effect," *Environmental entomology*, vol. 21, no. 4, pp. 689–699, 1992.

[114] S. Raychaudhuri, D. Sinha, and J. Chattopadhyay, "Effect of time-varying cross-diffusivity in a two-species lotka-volterra competitive system," *Ecological modelling*, vol. 92, no. 1, pp. 55–64, 1996.

[115] L. A. Segel and J. L. Jackson, "Dissipative structure: an explanation and an ecological example," *Journal of theoretical biology*, vol. 37, no. 3, pp. 545–559, 1972.

[116] M. Bani-Yaghoub, G. Yao, M. Fujiwara, and D. E. Amundsen, "Understanding the interplay between density dependent birth function and maturation time delay using a reaction-diffusion population model," *Ecological Complexity*, vol. 21, pp. 14–26, 2015.

[117] D. Jordan, P. Smith, and P. Smith, *Nonlinear ordinary differential equations: an introduction for scientists and engineers*, vol. 10. Oxford University Press on Demand, 2007.

[118] R. Yamapi and P. Woafo, "Dynamics and synchronization of coupled self-sustained electromechanical devices," *Journal of Sound and Vibration*, vol. 285, no. 4-5, pp. 1151–1170, 2005.

[119] R. Yamapi and P. Woafo, "Synchronized states in a ring of four mutually coupled self-sustained electromechanical devices," *Communications in Nonlinear Science and Numerical Simulation*, vol. 11, no. 2, pp. 186–202, 2006.

[120] Y. C. Kouomou and P. Woafo, "Stability and chaos control in electrostatic transducers," *Physica Scripta*, vol. 62, no. 4, p. 255, 2000.

[121] C. A. Lugo and A. J. McKane, "Quasicycles in a spatial predator-prey model," *Physical Review E*, vol. 78, no. 5, p. 051911, 2008.

[122] J.-P. Laplante, "Inhomogeneous steady state distributions of species in predator-prey systems. a specific example," *Journal of theoretical biology*, vol. 81, no. 1, pp. 29–45, 1979.

[123] M. Minakuchi and S. Nagano, "Stable territory formation in ecology and its potential generality in pattern formations," *Journal of Theoretical Biology*, vol. 350, pp. 17–23, 2014.

[124] T. Reichenbach, M. Mobilia, and E. Frey, "Coexistence versus extinction in the stochastic cyclic lotka-volterra model," *Physical Review E*, vol. 74, no. 5, p. 051907, 2006.

[125] F. Van den Bosch, N. McRoberts, F. Van den Berg, and L. Madden, "The basic reproduction number of plant pathogens: matrix approaches to complex dynamics," *Phytopathology*, vol. 98, no. 2, pp. 239–249, 2008.

[126] P. Van den Driessche and J. Watmough, "Reproduction numbers and sub-threshold endemic equilibria for compartmental models of disease transmission," *Mathematical biosciences*, vol. 180, no. 1-2, pp. 29–48, 2002.

[127] T. Britton, T. House, A. L. Lloyd, D. Mollison, S. Riley, and P. Trapman, "Five challenges for stochastic epidemic models involving global transmission," *Epidemics*, vol. 10, pp. 54–57, 2015.

[128] P. Guemkam Ghomsi, J. Tameh Berinyoh, and F. Moukam Kakmeni, "Ionic wave propagation and collision in an excitable circuit model of microtubules," *Chaos: An Interdisciplinary Journal of Nonlinear Science*, vol. 28, no. 2, p. 023106, 2018.

[129] F. Copie, M. Conforti, A. Kudlinski, A. Mussot, F. Biancalana, and S. Trillo, "Instabilities in passive dispersion oscillating fiber ring cavities," *The European Physical Journal D*, vol. 71, no. 5, pp. 1–11, 2017.

[130] W. Just, M. Bose, S. Bose, H. Engel, and E. Schöll, "Spatiotemporal dynamics near a supercritical turing-hopf bifurcation in a two-dimensional reaction-diffusion system," *Physical Review E*, vol. 64, no. 2, p. 026219, 2001.

[131] M. Meixner, A. De Wit, S. Bose, and E. Schöll, "Generic spatiotemporal dynamics near codimension-two turing-hopf bifurcations," *Physical Review E*, vol. 55, no. 6, p. 6690, 1997.

[132] D. T. Gillespie, "A general method for numerically simulating the stochastic time evolution of coupled chemical reactions," *Journal of computational physics*, vol. 22, no. 4, pp. 403–434, 1976.

[133] V. K. Vanag and I. R. Epstein, "Design and control of patterns in reaction-diffusion systems," *Chaos: An Interdisciplinary Journal of Nonlinear Science*, vol. 18, no. 2, p. 026107, 2008.

[134] V. K. Vanag and I. R. Epstein, "Localized patterns in reaction-diffusion systems," *Chaos: An Interdisciplinary Journal of Nonlinear Science*, vol. 17, no. 3, p. 037110, 2007.

[135] F. Rao and Y. Kang, "The complex dynamics of a diffusive prey–predator model with an allee effect in prey," *Ecological complexity*, vol. 28, pp. 123–144, 2016.

[136] S. Fasani and S. Rinaldi, "Factors promoting or inhibiting turing instability in spatially extended prey–predator systems," *Ecological modelling*, vol. 222, no. 18, pp. 3449–3452, 2011.

[137] J. Roughgarden, "A simple model for population dynamics in stochastic environments," *The American Naturalist*, vol. 109, no. 970, pp. 713–736, 1975.

[138] A. J. McKane and T. J. Newman, "Predator-prey cycles from resonant amplification of demographic stochasticity," *Physical review letters*, vol. 94, no. 21, p. 218102, 2005.

[139] F. Gourbiere, S. Gourbiere, A. Van Maanen, G. Vallet, and P. Auger, "Proportion of needles colonized by one fungal species in coniferous litter: the dispersal hypothesis," *Mycological Research*, vol. 103, no. 3, pp. 353–359, 1999.

[140] B. D. Elderd, B. J. Rehill, K. J. Haynes, and G. Dwyer, "Induced plant defenses, host–pathogen interactions, and forest insect outbreaks," *Proceedings of the National Academy of Sciences*, vol. 110, no. 37, pp. 14978–14983, 2013.

[141] C. Briggs and H. Godfray, "The dynamics of insect-pathogen interactions in stage-structured populations," *The American Naturalist*, vol. 145, no. 6, pp. 855–887, 1995.

[142] Z. Rapti and C. Cáceres, "Effects of intrinsic and extrinsic host mortality on disease spread," *Bulletin of mathematical biology*, vol. 78, no. 2, pp. 235–253, 2016.

[143] J. R. Reilly and B. D. Elderd, "Effects of biological control on long-term population dynamics: identifying unexpected outcomes," *Journal of Applied Ecology*, vol. 51, no. 1, pp. 90–101, 2014.

List of Publications

Published

1. Djouda, B. S., Moukam Kakmeni, F. M., Guemkam Ghomsi, P., Ndjomatchoua, F. T., Tcha-woua, C., Tonnang, H. E. (2019). Theoretical analysis of spatial nonhomogeneous patterns of entomopathogenic fungi growth on insect pest. Chaos: An Interdisciplinary Journal of Nonlinear Science, 29(5), 053134.

2. Djouda, B. S., Ndjomatchoua, F. T., Moukam Kakmeni, F. M., Tchawoua, C., Tonnang, H. E. (2021). Understanding biological control with entomopathogenic fungi—Insights from a stochastic pest–pathogen model. Chaos: An Interdisciplinary Journal of Nonlinear Science, 31(2), 023126.

==

Theoretical analysis of spatial nonhomogeneous patterns of entomopathogenic fungi growth on insect pest

Byliole S. Djouda, F. M. Moukam Kakmeni, P. Guemkam Ghomsi, Frank T. Ndjomatchoua (iD), Clément Tchawoua, and Henri E. Z. Tonnang

View Online   Export Citation   CrossMark

AIP Author Services
English Language Editing

Theoretical analysis of spatial nonhomogeneous patterns of entomopathogenic fungi growth on insect pest

View Online   Export Citation   CrossMark

Byliole S. Djouda,[1] F. M. Moukam Kakmeni,[2,a] P. Guemkam Ghomsi,[1,2] Frank T. Ndjomatchoua,[3] [ID]
Clément Tchawoua,[1] and Henri E. Z. Tonnang[4]

AFFILIATIONS

[1] Laboratory of Mechanics, Materials and Structures, Research and Postgraduate Training Unit for Physics and Applications, Postgraduate School of Science, Technology and Geosciences, Department of Physics, Faculty of Science, University of Yaoundé 1, P.O. Box 812, Ngoa Ekelle, Yaoundé, Cameroon
[2] Complex Systems and Theoretical Biology Group, Laboratory of Research on Advanced Materials and Nonlinear Science (LaRAMaNS), Department of Physics, Faculty of Science, University of Buéa, P. O. Box 63, Buéa, Cameroon
[3] Sustainable Impact Platform, Adaptive Agronomy and Pest Ecology Cluster, International Rice Research Institute (IRRI), DAPO Box 7777-1301, Metro Manila, Philippines
[4] International Institute of Tropical Agriculture (IITA), 08 BP 0932, Tri Postal Abomey Calavi, Cotonou, Benin

[a] Author to whom correspondence should be addressed: moukamkakmeni@gmail.com

ABSTRACT

This paper presents the study of the dynamics of intrahost (insect pests)-pathogen [entomopathogenic fungi (EPF)] interactions. The interaction between the resources from the insect pest and the mycelia of EPF is represented by the Holling and Powell type II functional responses. Because the EPF's growth is related to the instability of the steady state solution of our system, particular attention is given to the stability analysis of this steady state. Initially, the stability of the steady state is investigated without taking into account diffusion and by considering the behavior of the system around its equilibrium states. In addition, considering small perturbation of the stable singular point due to nonlinear diffusion, the conditions for Turing instability occurrence are deduced. It is observed that the absence of the regeneration feature of insect resources prevents the occurrence of such phenomena. The long time evolution of our system enables us to observe both spot and stripe patterns. Moreover, when the diffusion of mycelia is slightly modulated by a weak periodic perturbation, the Floquet theory and numerical simulations allow us to derive the conditions in which diffusion driven instabilities can occur. The relevance of the obtained results is further discussed in the perspective of biological insect pest control.

Published under license by AIP Publishing. https://doi.org/10.1063/1.5043612

A biological control system based on entomopathogenic fungi (EPF) has been developed as an environmentally friendly alternative to the use and application of chemical insecticides against insect pests. However, the dynamics of the entomopathogenic fungi within the insect host, which they eventually kill, is still not well understood. Using a host pathogen model coupled with a nonlinear dependence of the consumption of insect resources by the host, described by the Holling and Powell type II functional responses, this paper shows that the behavior of such a system is rich in dynamics. The model represents a reaction diffusion system of two equations with a cross-diffusion term in the resource consumption. Assuming that the diffusion rate of mycelia depends on the diffusion rate of the insect resource and time, numerical simulations reveal the case where mycelia grow successfully in their host. This work can serve as a tool for understanding the complexity of the fungus developmental processes and growth dynamics that take place in insects and that can be generalized to other hosts.

I. INTRODUCTION

A good number of insects represents a major pest in agriculture.[1–5] They can cause significant damages during their

immature and mature life stages.[6–8] Therefore, it becomes necessary to set up appropriate pest management programs to control these insect pest populations. The harmfulness of chemical insecticides to humans and to the environment has motivated the development of biological mechanisms with pathogenic organisms that only target the insect.[9]

Entomopathogenic fungi (EPF) are organisms that possess the ability to infect the host by ingestion or by simple contact, therefore making insects vulnerable at any of their life stages.[10,11] The penetration process is the most important step in pathogenesis.[12] In contact with the insect's cuticle, conidia (the infectious fungus unit) germinates if conditions of temperature and humidity are favorable (high humidity)[13] and penetrates through the integument of the insect by combining mechanical and enzymatic pressures.[14,15] Furthermore, hyphae proliferate into the insect hemocoel, secrete the toxins to kill the insect, and produce new infective spores, which are ejected toward the insect cuticle for immediate transmission if the environmental conditions are favorable. These infectious spores are subsequently dispersed in the environment by natural phenomena such as wind and rain, which then favor their propagation to noninfected insects. Moreover, this infection can be transmitted by a simple contact between infected and noninfected insects.[2,13,16,17] However, the efficiency of this method is good when the densities of the targeted insect populations are very high, thus enhancing contamination by abundant production and dissemination of spores in the saprophyte phase. Within the insect immune system, the lack of recognition between the host and the pathogen, and the inability of the spores to exploit resources from the insect cuticle can strongly influence the pathogenicity of these natural enemies.[18,19]

The interaction between EPF and their host is very complex. This justifies why most studies have focused on experimental approaches.[17] The successful manipulation of EPF depends on the understanding of their dynamical relationships and the spatiotemporal congruence among the biological control agents and insect pests.[17] As opposed to purely experimental approaches that are limited to the conditions at which the studies are conducted, modeling can be useful to simplify some aspects of the reality and to investigate what are the key characteristics that are primordial to generate the spatial properties of EPF. To illustrate this, models were used in the literature to study the density dependence and spatial structure in the dynamics of insect pathogens.[20] Another study used a model to describe the behavior of infected and noninfected host and predicted the relevant spatial scale during the spread of fungal pathogen.[8] The spread analysis of the contagious disease caused by *Beauveria bassiana* (EPF) in pest (Russian Wheat Aphid) population[2] and the study of the effect of conidial dispersal of fungal pathogen on the survival of its host have been carried out.[13]

A recent study has proposed a model to explain the dynamical evolution of EPF on insects by addressing simple life history questions such as the allocation of resources to either mycelia growth or spore production.[21] The authors assumed that the insect was under a nutritive stress,[21] and their analysis ignored the spatial aspects of the population dynamics and EPF propagation.[21] However, the results of the nonspatial analysis are usually applied to the case of spatially homogeneous and well-mixed populations, which implies that the corresponding habitat is sufficiently small, and the impact of spatial dimensions is, therefore, ignored in a somewhat more exotic case

where the individuals of a given species are assumed to remain fixed in space at any time and in any generation.[8,22] Spatial simulation can overcome such limitations via the link of process and scales.[23] Neglecting the spatial component in such an ecological problem is misleading and thus limits the understanding of ecological relationships which are essential for the occurrence of spatial patterns, and are also inevitable for studying contagious processes.[24,25] In the presence of the enemy, the threatened population moves and forms micro-partition to better fight the threat; thus, the persistence of each population is closely linked to diffusion.[24,26,27] Based on an extension of the model suggested in Ref. 21, a spatial model is developed in this study by explicitly taking into account the diffusion problem between species. Although there are numerous spatial methods like cellular automata, patch model, and network techniques that well describe the spatial interaction between a host and a pathogen, we opted for the reaction–diffusion model, which has already been developed and successfully applied to chemical systems[28] and predator–prey interactions.[29–33] Note that dispersal is the key for the successful formation of spatial structures during the dynamics of insect pest population systems.[24,34,35] This justifies our choice of partial differential equations (PDE) via an addition of spatial diffusion terms in the master equations described in Ref. 21. More specifically, the changes are considered on the dispersion of the species in order to investigate how diffusion affects the spatial and temporal evolutions of fungus in the insects, and also, how instability due to diffusion can be used for practical predictions in the context of EPF contaminating insects.

The formation of spatial and temporal patterns using the Turing stability approach was developed in physics[36–38] and successfully applied in spatial ecology to understand the role of the diffusion rate in the predator–prey population stability and the formation of different spatial structures.[29,31,32,36–40] Experimental studies of mycelium and cell nutrients in hemocoel diffusion and response within the insect immune system, as well as the self-organization of spatial patterns and structures required for fungi development in the biological organism, suggest that the reaction diffusion model, on the one hand, and Turing patterns formation, on the other hand, are more appropriate to describe the mechanisms of evolution of fungi inside the host.[41–47]

It was shown in a previous study that, cross diffusion is necessary for pattern formation, especially in the case where classical diffusion coefficient is not sufficient to favor the occurrence of instability.[48] In certain classes of predator-prey systems, diffusion can be introduced, specifically to capture the gradient of the density of one species that induces the flux of another species. Cross diffusion were employed to model the congregation of preys in order to protect them from the attack of predators.[48–50] They have also been used in chemical reaction and cell division in tumor growth.[49] In the case of insect–fungi interactions,[51] the pest acquires defenses to protect itself against the pathogen infections during host–parasite coevolution. The insect cellular defense system is based on hemocytes circulating in the hemocoel, which are able to distinguish between a self and a nonself cellular organism. In addition, the toxins secreted by hyphal bodies within the insect hemocoel during their propagation have been shown to inhibit the spreading of plasmotocytes. So, the number of circulating hemocytes decreases during the propagation of hyphal bodies,[52] and this could be identified as the inhibition of migration. Such a particularity is introduced in the model developed here by the nonlinear

cross-diffusion term. The theory is applied with the aim of investigating the reasons and conditions that are of capital importance for the success and/or failure of the spatial and temporal biological control using the EPF. This is conducted through the modeling of the within-host pathogen dynamics while focusing on the spores produced by the pathogen and the spores dynamics within the host. It is worth mentioning here that the mechanism of pattern formation of hyphae into the hemocoel has yet to be understood in detail.[2,8,9,13,19,20] The present study tries to unveil this aspect as well.

The text is organized as follows: In Sec. II, the model is described with the underlying hypothesis, and the linear stability analysis is conducted, and, subsequently, the Turing's instability is investigated in Sec. III. Section IV is devoted to the time-dependent diffusivities. A discussion of the results is done in Sec. V, and Sec. VI is devoted to the conclusion.

II. MODEL DESCRIPTION

The model presented by Gilchrist et al.[21] was reformulated by introducing functional responses, logistic growth on resources, and spatial inhomogeneity using the phenomenon of diffusion to characterize the mobility of species. Consideration was given to the most important morphological states of the fungus, which are the mycelia (M) and the spores (S),[53] while taking into account the magnitude and characteristics of the quantity of resources (R) that the insect contains. The system can, thus, be described by the following set of coupled partial differential equations (PDE):

$$
\begin{aligned}
R_t &= D_R \nabla^2 R - F(R) M - \alpha R \left(1 - \frac{R}{K}\right), \\
M_t &= D_M \nabla^2 M + C_1 (1 - q) F(R) M - \gamma M \\
&\quad + D_{MR} \nabla (M \nabla R),
\end{aligned}
\tag{1}
$$

where t is simply the independent time variable and ∇ is the Nabla operator. α corresponds to the linear birth regeneration rate of resources and K is defined to be the carrying capacity.[56] D_R and D_M are the diffusion rates of resources and mycelium, respectively, on the one hand, and on the other hand, D_{MR} is the nonlinear diffusion rate. It is assumed that the density of mycelium (M) can decay naturally at $\gamma \cdot dt$ between the instants t and $t + dt$ and that resources extracted from the insects by fungi are allocated to the mycelium growth and spore production. The coefficient C_1 represents the conversion rate of the resources into mycelium,[21] and $q \cdot dt$ is defined as the probability that the extracted resources are allocated to the sporulation in the presence of the mycelium between the instants t and $t + dt$. The spore production density of the fungus S, is assumed to be proportional to the amount of resources allocated to spore production by the fungus, and can be written as

$$S = C_2 q F(R) M.$$

In this equation, C_2 defines the conversion rate of the resources into spores. The infestation function is represented by Holling and Powell type-II functional responses defined by[27,39,54,55]

$$F(R) = \frac{AR}{B + R}. \tag{2}$$

This function $F(R)$ has been considered to model the nonlinear interaction between species, and more clearly, it is worth the amount of resources extracted per insect's cell per unit time. Here, B is the quantity of resources that leads the functional response to half-saturation, and A is the maximum amount of resources that can be extracted per cell and per unit time. A corresponds also to the value of $F(R)$ when R is very large. In reality, mycelia are switching to resources at different moments with different efficiencies. As most of the mycelia usually switch to resources that are significantly abundant,[57] mycelia pressure is expected to increase more than linearly with resource density over the initial range. Therefore, the nonlinear diffusion term $D_{MR} \nabla (M \nabla R)$ is applied for modeling the tendency of resources congregation (immune system) R to protect itself from the attack of the mycelia M. In order to predict with a good accuracy the behavior of insects during EPFs' infestation or the efficiency of EPF, this switching behavior of the mycelia is modeled by a time-periodic function.[57–60]

It is worth mentioning that, in the case of insect–fungi interaction, daily environmental conditions such as temperature, relative humidity, and solar radiation affect the insect thermoregulation, mycelia growth, and the virulence strategy of fungus entomopathogen.[10,15,17] Thus, it becomes obvious that they equally affect the multiplication and the dispersal of infectious propagules within an insect's body.[10] It has been demonstrated that the diffusion coefficient of cells' biology changes with temperature shifts. Because of our focus on mycelia growth, we neglect the influence of this temperature variation on the resource of insects. A rough analogy with the transmembrane proteins diffusion coefficient in bacteria dynamics shows that diffusion coefficient is proportional to temperature and, consequently, time.[61,62] In view of the fact that living organisms maintain their membranes in a fluid state,[61,62] diffusion coefficient can be made time dependent. To study the effect of fluctuating temperatures on insect development, often some researchers have shown that, diurnal temperature can be approximated by a periodic time dependent function where time is a fractional part of the day.[63,64] Also, in some previous research work, diffusivities have been shown to potentially vary with respect to time. A typical example of this is oceanic diffusion.[65] This important phenomenon has also been taken into account in an ecological model for predator–prey planktonic species, and in a population pathogen model, in order to study the impact of constant and time varying diffusion terms on the disease-dominated ecological population.[57,65] In these studies, a sinusoidal variation of diffusion with respect to time was employed to represent seasonal and daily variation, environmental factors and various intrinsic factors that are inherently internal in nature.[57] In our case, the diffusion coefficient of the resources, D_R, is assumed to be a constant and, D_M and D_{MR} are functions of time t and are given by the expressions

$$
\begin{aligned}
D_M &= D_R (d + b \sin(\omega t)), \\
D_{MR} &= D_R (D_{21} + B_{21} \sin(\omega t + \phi)),
\end{aligned}
\tag{3}
$$

where $d > 1, d > |b|, D_{21} > 1, D_{21} > |B_{21}|$. The model is defined in a bounded fixed domain. The following dimensionless quantities are

introduced in order to simplify the equation:

$$\frac{\partial}{\partial \tau} = \gamma^{-1}\frac{\partial}{\partial t}, \quad M = \gamma\frac{B}{A}m, \quad R = \gamma\frac{B}{C_1 A}r,$$

$$S = \gamma^2\frac{C_2 B}{C_1 A}s, \quad b_{21} = \gamma\frac{B_{21}B}{C_1 A}, \quad \beta = \frac{\alpha}{\gamma}, \tag{4}$$

$$a = \gamma\frac{1}{C_1 A}, \quad d_{21} = \gamma\frac{D_{21}B}{C_1 A}, \quad x = \sqrt{\frac{\gamma}{D_R}}x', \Omega = \frac{\omega}{\gamma}.$$

The master equations (1) become

$$\dot{r} = \beta r\left(1 - \frac{r}{\varepsilon}\right) - \frac{mr}{1+ar} + \nabla'^2 r,$$

$$\dot{m} = (1-q)\frac{mr}{1+ar} - m + (d + b\sin(\Omega\tau))\nabla'^2 m$$

$$+ (d_{21} + b_{21}\sin(\Omega\tau + \phi))\nabla'\left(m\nabla' r\right), \tag{5}$$

with

$$s = q\frac{mr}{1+ar}.$$

The homogeneous Neumann boundary conditions are used, assuming that no external input is imposed on the system.

III. STABILITY ANALYSIS (CASE $b = b_{21} = 0$)

It was considered that there exists a set of stationary, spatially uniform solutions of (5). This allowed us to obtaining three singular points. The only endemic equilibrium point is

$$(r_0, m_0) = \left(\frac{1}{1-q-a}, \frac{(-1+q)\beta\left(\varepsilon(a+q-1)+1\right)}{\varepsilon(a+q-1)^2}\right),$$

which has a biological relevance only if $(q+a) < 1$, $\varepsilon(1-a-q) > 1$, conditions that will be applied throughout the rest of the paper. The color zones of Fig. 1(a) display the instability region of the steady state according to the relevance of the conditions given above. The parameter space (a, q) shows the zone where the steady state is stable and, thus, diffusion-driven instability can develop. To find Turing instability with spatial wavenumber k, we search for the eigenvalues λ of the matrix $\mathbf{A}(k) = \mathbf{J} - k^2\mathbf{D}$ (the expressions of $\mathbf{J}$ and $\mathbf{D}$ are given in Appendix A). When the real part of the dominant eigenvalue λ crosses the imaginary axis for some $k \neq 0$, the spatially homogeneous equilibrium is destabilized by a periodic perturbation of wavelength $2\pi/k$, and the perturbations will exponentially grow with time. If each eigenvalue has a negative real part ($\text{Re}(\lambda_i(k)) < 0, \forall k, i = 1, 2$), the homogeneous state is stable: every perturbation will eventually die out and no pattern will develop. Turing bifurcation happens at the critical value

$$d_{21}^c = \frac{(a+q-1)^2}{(1-q)\det\mathbf{J}}\left(-tr(\mathbf{J})d + 2\sqrt{\det\mathbf{D}\det\mathbf{J}}\right)$$

corresponding to the critical wavenumber

$$k_c^2 = \sqrt{\frac{\det\mathbf{J}}{d}}.$$
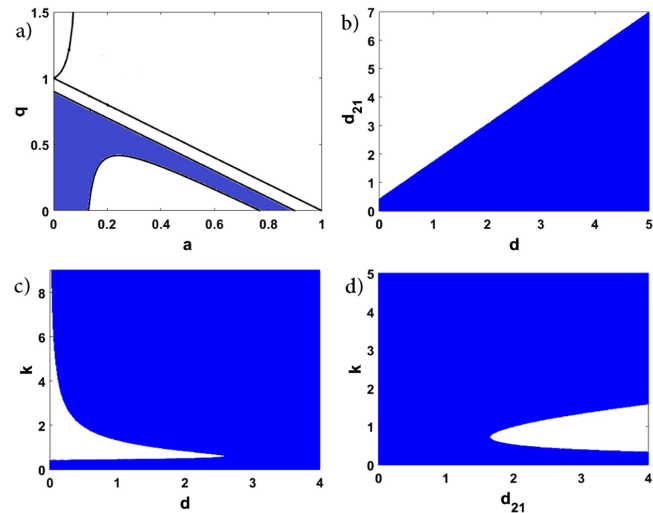
FIG. 1. (a) Stability diagram of the homogeneous steady state. Black line define the boundary of the stable and unstable zones corresponding to $tr(\mathbf{J}) = 0$. The colored areas corresponds to stable region where $tr(\mathbf{J}) < 0$. Turing instability can occur in this region when diffusion is taken into consideration. Others panels [(b) for $k = 1$; (c) for $d_{21} = 2.5$; (d) for $d = 1.2$] show parameter space colored regions are also obtain for couples of points satisfying the stability conditions. The other parameters values are given by $\varepsilon = 10.0$, $\beta = 0.47$, $a = 0.05$; $q = 0.5$; for each case.

Figures 1(b)–1(d) present the Turing instability parameter regions. For $d_{21} > d_{21}^c$, the unstable wavenumber resides between two critical values. This linear analysis of the homogeneous state enables us to determine whether the resulting wave is steady or oscillatory when we look at the imaginary part of the eigenvalues $\text{Im}(\lambda_i(k))$. Steady patterns correspond to $\text{Im}(\lambda_i(k)) = 0$ for all unstable modes k, in which case the instability is called Turing instability [see in Fig. 2(a)]. When $\text{Im}(\lambda_i(k)) \neq 0$ for an unstable mode at a nonzero k, the system is said to undergo wave instability, and the resulting pattern consists of traveling waves, but this behavior does not occur in this system.

A. Spatiotemporal dynamics (1D simulations)

The system was numerically solved using a fully explicit Euler method with a finite-difference approach on space and a temporal step size of 0.01 t.u. (time units). No-flux boundary condition and positive random initial condition with an amplitude of 0.01 over the endemic steady state were employed. The nonlinear diffusion term was approximated by a second-order finite difference algorithm. Spatiotemporal patterns were observed during simulations. The system shows stationary Turing patterns. This behavior is presented in Fig. 2. In panel (a) of this figure, the dispersion relation is plotted and it shows diffusion-driven instability. This behavior is modulated by stationary waves, whereas the space-time structures displayed in Fig. 2(b) are regular stationary stripes. The density of resources oscillates over time and it is reported in Fig. 2(c) at two different points of space. The amplitude of the density of resources oscillates periodically in space [see Fig. 2(d)]. In order to observe the role of the term of

FIG. 2. (a) Stability analysis showing the complex part (red) and the real part (blue) of the eigenvalues. (b) 1D Turing pattern formation, the chosen parameter values are $\varepsilon = 10.0$, $\beta = 0.47$, $a = 0.06$, $q = 0.3$, $d = 1.2$, and $d_{21} = 2.5$(c) blue and red curves are two oscillations located at space $x = 10$ and $x = 12.5$. (d) displays the spatial amplitude modulation at the time given in the legend; (e) and (f) show the influence of the regeneration rate of the EPF during growth ($\beta = 0$ in these cases).
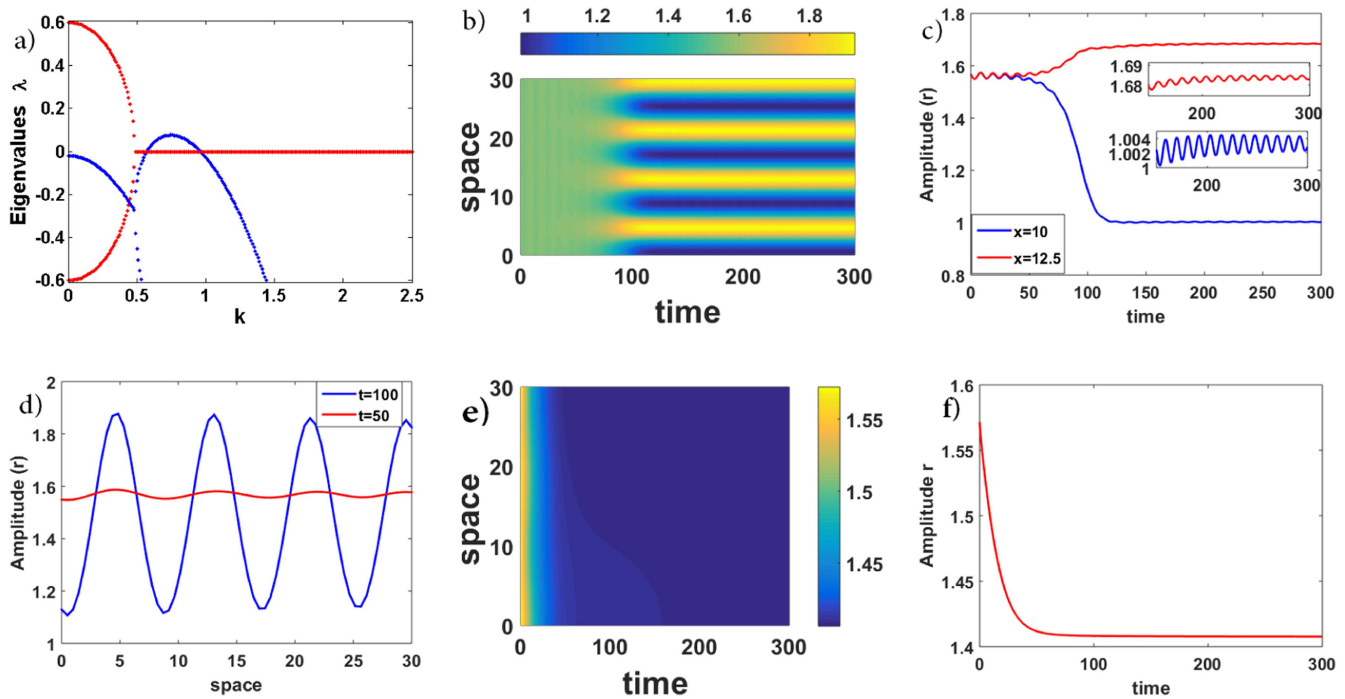
the birth regeneration rate of the resources on the system, the dynamics of the endemic equilibrium point was simulated in the absence of the logistic growth rate of resources. It can be noted that, when $\beta = 0$ [Figs. 2(a), 2(e), and 2(f)], the resource density decreases and there is no pattern formation over time, whereas if $\beta \neq 0$, the species density varies at each site of space as t evolves, as shown in Fig. 2(b).

B. Spatial evolution of fungi within insects hemocoel (2D simulations)

In this section, the dynamics of EPF within their host is explored. The numerical simulations by using the fourth-order Runge–Kutta scheme in a two-dimensional grid with a grid spacing of 0.0625 and a time step of 0.001 were considered. Figure 3 shows the temporal transients of the regular Turing pattern of the mycelia population at different evolution times. In Fig. 3(a), the oscillatory instability seems to emerge after perturbation of the steady state. After a few iterations, the formation of stripes was observed, but hot spots (isolated zones with a high density of mycelia) also occur [Figs. 3(b) and 3(c)]. For a large number of iterations, we observed a formation of interlaced stripes with a high and low density of mycelia population [see Figs. 3(d) and 3(e)]. The panel (f) of Fig. 3 shows more regular patterns with hot spots (isolated zones with a high density of mycelia) and cold stripes (isolated zones with a low population density of mycelia). This means that at a point in space, the density

of species fluctuates in time. It was noticed that when the density of the spores is stationary, the density of mycelia and resources are also stationary but not equal; so the EPF impose their dynamics on the insect.

After discarding the transients subsequent to a long time evolution of their dynamical systems, we could reach some specific Turing structures that are effectively heterogeneous stationary pattern (with permanent or fixed, or nonevolving spatial profiles). Figure 4 shows the stationary spatial pattern of resource density. Figure 4(a) shows double spots connected two by two with stripes, whereas an increase in the cross diffusion coefficient gives in Fig. 4(b) a pattern composed by single spots [see Fig. 4(b)]. But Figs. 4(c) and 4(d) give the Turing pattern of resource density for two different values of probability that the extracted resources are allocated to the sporulation in the presence of the mycelium such that the panel [Fig. 4(c)] has regular structures composed by hot spots showing a hexagonal form. But by increasing the probability q, high stripes connecting cold spots occurs [see Fig. 4(d)].

IV. TIME-DEPENDENT DIFFUSIVITIES (CASE $b \neq 0$ AND $b_{21} \neq 0$)

This section analyzes the time-dependent diffusivities using Eq. (4) that admits a periodic solution. The stability of the system is studied by superimposing a small perturbation of the form
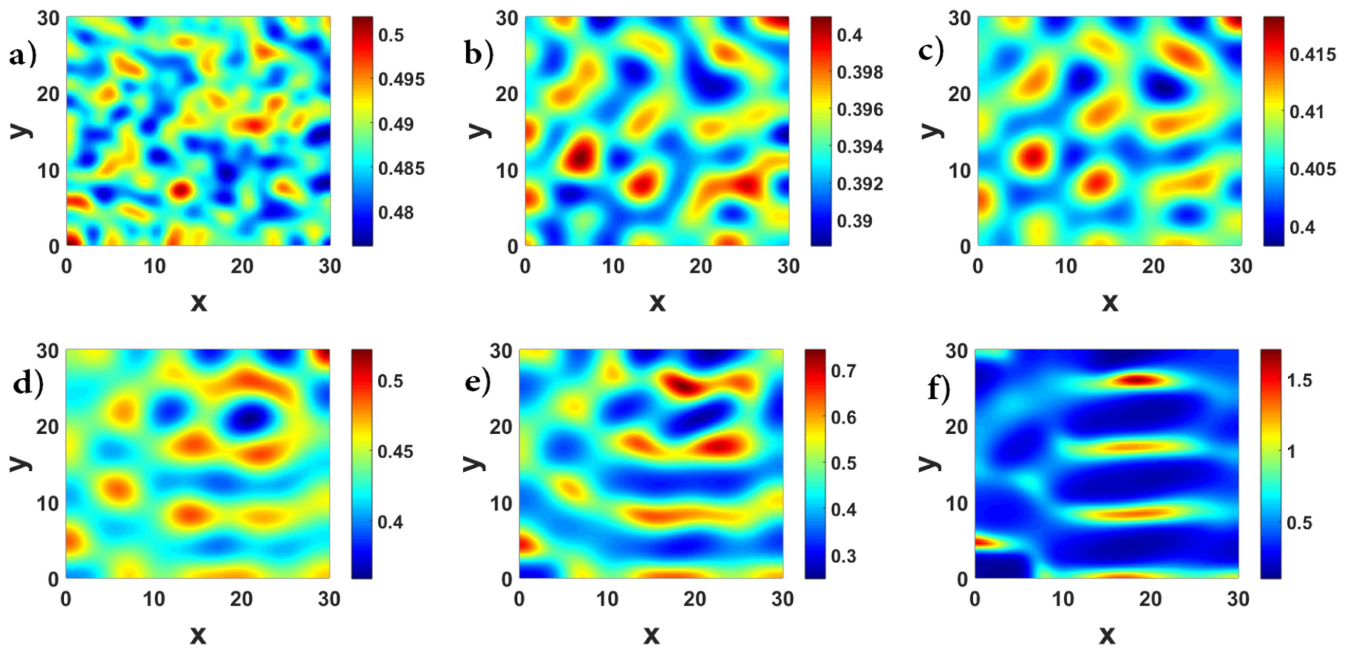
FIG. 3. Temporal transients of regular Turing pattern of the mycelia with the parameter values chosen being identical as in Fig. 2. Time iterations: (a) 100, (b) 500, (c) 1500, (d) 4500, (e) 6500, and (f) 8000. The color bar shows the magnitude of the population density of mycelia.

$a_j(t) \exp(ikx)$, $(j = 1, 2)$ and by then applying the theory of Floquet.[66] In this expression, k corresponds to the wavenumber. By spatially linearizing the inhomogeneous system in the neighborhood of the endemic equilibrium point, we obtained the following first order system:

$$\mathbf{a_t} = A(k,t)\mathbf{a}, \tag{6}$$

where $\mathbf{a} = (a_1, a_2)^T$ represents the amplitude of the perturbation affecting r and m, respectively; $(.)^T$ stands for a transposed vector, $A(k,t)$ is a two-dimensional matrix defined by

$$\mathbf{A}(k,t) = \begin{pmatrix} a_{11} - k^2 & a_{12} \\ a_{21} - m_0 k^2 \left(d_{21} + b_{21} \sin\left(\Omega t + \phi\right)\right) & a_{22} - k^2 \left(d + b \sin\left(\Omega t\right)\right) \end{pmatrix}, \tag{7}$$

where the coefficients a_{ij}, $(i, j = 1, 2)$ are the elements of the Jacobian matrix given above. $A(k,t)$ is periodic, with a minimal period of $2\pi/\Omega$, with Ω being the frequency of the perturbation. The stability of this system is defined by the eigenvalues of the monodromy matrix. According to the Floquet theory,[67] the solutions of this system $\mathbf{a}(t)$ obey the formula

$$\mathbf{a}(t) = \mu \mathbf{a}\left(t + \frac{2\pi}{\Omega}\right),$$

where μ is any eigenvalue of the constant matrix $\mathbf{E}$ transforming a fundamental matrix $\Phi(t)$ of the system into its translate $\Phi\left(t + \frac{2\pi}{\Omega}\right)$. The stability of this system is defined by the eigenvalues of the monodromy matrix $\mathbf{E}$. If $\mu = 1$ then, the system has periodic solutions. For $\mu < 1$, the system has a stable solution; and if any eigenvalue μ is

such that $\mu > 1$, then an unstable behavior appears. It is known that the product of characteristic multipliers is given by

$$\mu_1 \mu_2 = \exp\left(\int_0^{2\pi/\Omega} tr\mathbf{A}(k,t)\, dt\right) = b, \tag{8}$$

with $b = \exp\left\{\frac{2\pi}{\Omega}\left(tr(\mathbf{J}) - k^2(1+d)\right)\right\} < 1$. Considering Cardano's relationship, the characteristic multipliers of the monodromy matrix are solutions of the equation

$$\mu^2 - h(k,\Omega)\mu + b = 0.$$

Based on the fact that $b \in [0, 1]$, the form of $h(k,\Omega)$ is not required, only their interval of variations is needed.[67] A stable behavior occurs in the colored region of Fig. 5(a). However, it exists in the (k,Ω)—plane curves that separate zones where the amplitudes have different qualitative behaviors (see Appendix B). Because the function $h(k,\Omega)$ is not explicitly defined, we searched for the (k,Ω)—couples of values describing these variations by using Fourier series. Let us assume that

$$\begin{pmatrix} a_1 \\ a_2 \end{pmatrix} = \sum_{n=-\infty}^{+\infty} \begin{pmatrix} A_n e^{a_n t} \\ B_n e^{b_n t} \end{pmatrix}, \tag{9}$$

where $a_n = \theta_1 + in\Omega$, $b_n = \theta_2 + in\Omega$, and the quantities θ_1 and θ_2 are two complex numbers.[68–70] By substituting Eq. (B1) into (Eq. 5), and
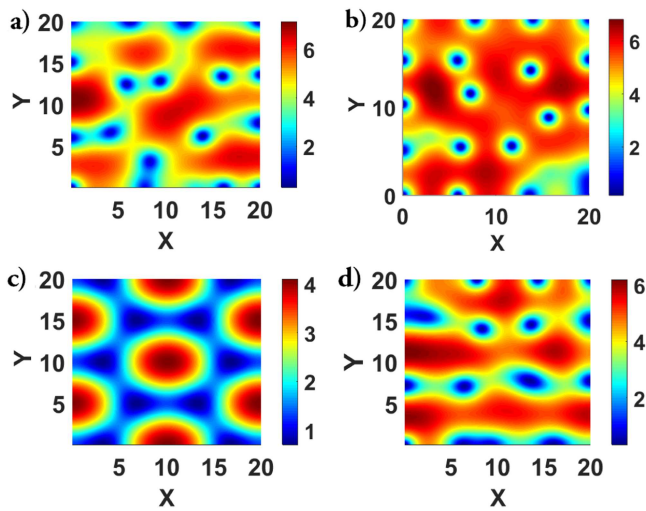
FIG. 4. Stationary spatial Turing patterns of resource density obtained through simulation of model (5) on a squared spatial grid with no-flux boundary conditions for nontemporal diffusion. It shows some pattern formations of resources with parameter values (a) $\varepsilon = 10.0, \beta = 0.47, a = 0.05; q = 0.5; d = 1.2; d_{21} = 2.2$; (b) $\varepsilon = 10.0, \beta = 0.47, a = 0.05; q = 0.5; d = 1.2; d_{21} = 2.35$. Other panels give comparison patterns of the resources between two probabilities q with parameter values: $\varepsilon = 10.0, \beta = 0.47, a = 0.06; d_{21} = 2.25; d = 1.2$. (c) $q = 0.3$, (d) $q = 0.4$. The color bar shows the magnitude of the population density of resources.

FIG. 5. (a) Stability boundary region, (b) transition curve between stability and Turing instability with parameter values: $\varepsilon = 10.0, \beta = 0.47, a = 0.05, q = 0.5, d_{21} = 2.5, b_{21} = 2, d = 1.2, b = 0.8, \theta_1 = \theta_2 = 0$; (c) inhibition of the perturbation (both amplitude of perturbation tending to zero); (d) diffusion driven instability (both amplitudes of perturbation grow).

using the identity $\sin\theta = \left(e^{i\theta} - e^{-i\theta}\right)/2i$, we get

$$\sum_{n=-\infty}^{n=+\infty} \left(k^2 - a_{11} + a_n\right) A_n e^{a_n t} - a_{12} \sum_{n=-\infty}^{n=+\infty} B_n e^{b_n t} = 0,$$

$$(10)$$

$$\sum_{n=-\infty}^{n=+\infty} \left(k^2 d + b_n\right) B_n e^{b_n t} + \sum_{n=-\infty}^{n=+\infty} \left(k^2 m_0 d_{21} - a_{21}\right) A_n e^{a_n t}$$

$$- i\frac{k^2 m_0 b_{21}}{2} e^{i\phi} \sum_{n=-\infty}^{n=+\infty} A_n e^{a_{n+1} t}$$

$$+ i\frac{k^2 m_0 b_{21}}{2} e^{-i\phi} \sum_{n=-\infty}^{n=+\infty} A_n e^{a_{n-1} t} - i\frac{k^2 b}{2} \sum_{n=-\infty}^{n=+\infty} B_n e^{b_{n+1} t}$$

$$+ i\frac{k^2 b}{2} \sum_{n=-\infty}^{n=+\infty} B_n e^{b_{n-1} t} = 0.$$

For nontrivial solutions, the determinant of the matrix obtained from Eq. (C1) must be null. Since the determinant is infinite, the first and second sections of Eq. (C1) are divided by $\left(k^2 - a_{11} - m^2\right)$ and $\left(k^2 d - m^2\right)$, respectively, for the convergence. By considering the lower-order Hill determinant (six rows and six columns) and setting it equal to zero, the nonlinear algebraic equation is obtained (see Appendix C). This equation can be solved numerically by the bisection method or by the Newton–Raphson algorithm, thus leading to

the stability boundaries in the (k, Ω)—plane for the sets of the system parameters represented in Fig. 5(b), where I and III regions are stable domains. At first, the values $k = 0.2, \Omega = 2.0$ were chosen and then, with the same parameter values used to derive Figs. 5(b) and 5(c) shows that the perturbation is inhibited because both amplitudes of perturbation are tending to zero, and modulation by the diffusion periodicity can easily be observed. Second, if $k = 0.6, \Omega = 2.0$ are taken in region II with the same parameter values, there is an increase in the amplitude of the perturbation. The system then exhibits diffusion driven instability [Fig. 5(d)], with the modulation through the periodicity of the diffusive coefficients.

Our main objective here was to indicate via a stability analysis approach that even in the case of our periodically driven system, diffusion-driven instabilities can occur and spatial nonhomogeneous patterns can appear. This study enables us to say that in these conditions, Turing patterns could possibly occur. The occurrence of these patterns is not systematic. However, the diffusion-driven instability conditions, as obtained in Fig. 5(b) provide necessary but not sufficient conditions for these Turing profiles to emerge. A thorough screening of region *II* of Fig. 5(b) may give suitable conditions for these patterns to occur.

V. DISCUSSION

A mathematical model (patch array model) based on the age of the resource allocation matrix to evaluate the effectiveness, in the biological control, of a group of fungi exploiting discrete resource spots in their hosts using the bang-bang resource allocation strategy with the assumption that the insect undergoes a nutritive stress has been developed.[21] By studying the fitness of the spores, it was possible to establish that there is a link between the propagation and the persistence of the entomopathogenic fungus.[21] The study proved that

the success of the employed method depends on the types of fungus and the host species. The literature has revealed some established conditions in which the fungi behave like parasites in their host.[21] However, the study did not account for the interactions between the fitness of components. To improve the model presented in Ref. 21, a functional response, birth regeneration terms, constant, and time-dependent diffusion terms were included in both insect and EPF evolution equations. The proposed model exhibits Turing instability. The nonlinear cross-diffusion term describes the tendency of the mycelia to move in response to a spatially decreasing resource density to maximize resource suppression. As presented in Ref. 48, Turing pattern can occur when cross-diffusion is taken into account. Note that its nonlinear diffusion rate must verify the threshold condition.

In the past, biological control models assumed that either only the spores disperse or the host population (infected and noninfected larvae) change their state.[8,20] However, these studies show that the simplifications underlying the discrepancy between some of their theoretical results and the experimental results were mainly due to the presence of the diffusion coefficient on a certain species.[8,20] To illustrate this, in ecology, when a species invades the territory of another species, the invader interacts with the native species and moves in response to external influences or the medium crowding; there is, therefore, a natural displacement of each species.[24] This is the reason why we asked ourselves the following question: "what would happen if mycelia (m) and the resources (r) are able to disperse simultaneously?" In order to investigate possible outcomes of such a situation, the proposed model took into account not only the reaction between these species but also the dissemination into the insect hemocoel.

In the presence of nonlinear diffusion, the models analyzed here show a destabilization of the homogenous distribution of mycelia and resources, and Turing pattern formation, which have important biological significance. In previous studies, similar phenomena were observed in reaction–diffusion models applied to predator–prey dynamics.[29,31,33,71,72] However, the proposed model presents additional features with three equilibrium points. When the endemic point is stable and the terms of spatial inhomogeneity are introduced, two cases can be distinguished: the case in which the system remains stable, and the situation in which the diffusion drives the instability. Such results corroborate well with what is found in the literature.[28,38,71,73]

Previous studies have shown that varying the key parameters of a system can induce the formation of rich patterns. In predator–prey models, increasing the value of prey growth rate generates similar behavior.[33] This is unlike our case, where PDE [Eq. (C1), $b_i = 0$] exhibits Turing structures only in the presence of a nonzero intrinsic growth rate (of resource) such that the system changes from a stable to an unstable steady state when the regeneration rate (β) passes through zero. A numerical simulation of the system shows the space and space-time plot of density for $\beta = 0$, which indicates a stable behavior of the resource species. For $\beta \neq 0$, the graph exhibits the oscillations of the species populations arising out of instability. It has also been shown that as time evolves, the spatial dynamics of fungus presents more regular structures.

Some studies have shown that temporally periodic perturbations introduced in the diffusion rate have a weak stabilizing effect.

Since such a phenomenon has been observed in predator–prey systems (with two species), it shows that the interval of the dispersal rate in which instability occurs is reduced when the variability is included in the diffusion coefficient.[57,58] On the contrary, the developed model always exhibits stable and unstable regions, but both amplitudes of perturbation do not rapidly tend to zero in the case of stability. Furthermore, it can be noticed that varying the diffusion coefficient has a strong stabilizing effect. The temporal forcing parameters k and Ω in the problem provide a transition zone for the occurrence of Turing instability. It appears that in addition to destabilizing the equilibrium points, a periodic perturbation of the diffusion coefficient provides a better optimization of biological control in the sense that it could be better oriented from this new variation. Therefore, it is possible that the reaction–diffusion models between infected and noninfected larvae and spores[8,20] are insufficient to determine more precisely the conditions for the success of this spatiotemporal biological control, because optimizing the spatial growth of the EPF ensures good control.

Turing instability corresponds to the growth of the EPF and, therefore, to the death of the insect host. Naturally, if the regeneration rate of the insects resources is nil, the density of resources decreases to a threshold, but does not necessarily induce the death of insects. However, the inability of mycelia to use these resources can lead to a failure of biological control,[18] thus explaining why in the situation where the mycelia density decreases, there is no intra-host growth. In the case of the two-dimensional spatial domain, different behaviors of the system are observed at different times when parameters are varied in Turing regions. In particular, it is proved that the presence of the nonlinear diffusion term produces instability in cases only where there is space and time modulation.

VI. CONCLUSION

A study of the dynamics of the pathogen within the host (insect) through the development of a model with the spatial inhomogeneity was conducted. The proposed model differs from others including the functional response to describe nonlinear interactions between the host and the EPF and also by introducing constant and time-dependent diffusion and cross-diffusion terms in both the insect and EPF evolution equations to underscore the influence of the diffusion of a species on another.[8,20,74] In addition, particular attention was given to the intrahost evolution of EPF. The study started by analyzing the stability of the system, establishing conditions for the diffusion driven instability of an inhomogeneous distribution system, and understanding the type of perturbations of the system that lead to equilibrium states and can allow the occurrence of Turing instability. It was observed that cross-diffusion has a remarkable impact on Turing patterns; different structures appear as time evolves. The results showed that the birth regeneration rate is an important parameter that leads to the occurrence of patterns. The Floquet theory permits us to predict and determine the transition curves in the parameter space that demarcate the regions leading to stable and unstable solutions when diffusion and cross-diffusion are described as temporal periodic functions. This work is important for understanding and obtaining the Turing instability in biological control using EPF, which describe the different morphological states of fungus growth

within their host. The obtained outcomes help to better understand the spatial structures of the mycelia relative to the spatial distribution of the insect resources and their persistence while increasing the time related to the physical contact between EPF's population and insect pests. Using a space component, biological control systems are defined as natural systems; therefore, it will be important to study the influence of the Allee effect on resources or on EPF. It is possible that time delay plays an important role in biological control using EPF.

APPENDIX A: CONSTANT DIFFUSION

Linearizing the system in the neighborhood of the steady state (r_0, m_0),[75,76] the following equation is obtained:

$$\mathbf{w}_t = \mathbf{J}\mathbf{w} + \mathbf{D}\nabla^2\mathbf{w}, \tag{A1}$$

where

$$\mathbf{w} = \begin{pmatrix} r - r_0 \\ m - m_0 \end{pmatrix},$$

$$\mathbf{J} = \begin{pmatrix} -\frac{\beta(a^2\varepsilon + (1+\varepsilon(-1+q))a - q + 1)}{((-1+q)\varepsilon(a+q-1))} & \frac{1}{-1+q} \\ -\frac{\beta(\varepsilon(a+q-1)+1)}{\varepsilon} & 0 \end{pmatrix},$$

and

$$\mathbf{D} = \begin{pmatrix} 1 & 0 \\ d_{21}m_0 & d \end{pmatrix}.$$

Since $\det \mathbf{J} = \frac{\beta(\varepsilon(a+q-1)+1)}{\varepsilon(-1+q)}$ is always positive according to the biological relevance conditions, the only way for the endemic singular point to become unstable is $tr(\mathbf{J}) > 0$.

APPENDIX B: TEMPORAL DIFFUSION CASE

The polynomial equation

$$\mu^2 - h(k, \Omega)\mu + \eta = 0$$

have solutions for

$$\mu = \frac{1}{2}\left(h \pm \sqrt{h^2 - 4\eta}\right).$$

For distinct values of μ, Eq. (4) has two linearly independent solutions of the form $\varsigma_i = p_i(\tau)\exp(\rho_i\tau)$ $(i = 1, 2)$, where $\exp(\rho_i T) = \mu_i$ $(i = 1, 2)$ and p_i are functions of period T. The general solution of

Eq. (4) (the first component of ς) is given by

$$a_1 = p_1(\tau)e^{\rho_1\tau} + p_2(\tau)e^{\rho_2\tau}. \tag{B1}$$

The stability or otherwise of the periodic solution of Eq. (4) will be determined by the behavior of $\mathbf{a}$ in Eq. (4). The system is stable if $\text{Re}(\rho_1) < 0$ and $\text{Re}(\rho_2) < 0$. This is equivalent to $\mu_1 < 1$ and $\mu_2 < 1$. The analysis can be split into three cases.

1. $h^2 > 4\eta$, μ_1 and μ_2 are both real and positive, or both real and negative according to the sign of h: in both cases, $\mu_2 < \mu_1$. If they are both positive, then the periodic solution is stable if $\mu_1 = \left(h + \sqrt{h^2 - 4\eta}\right)/2 < 1$ or $h < 1 + \eta$. According to the fact that $\eta \in [0, 1]$, this lower bound is always greater than $2\sqrt{\eta}$. The region between $h = 1 + \eta$ and $h = 2\sqrt{\eta}$ [hatched region in $h > 0$ in Fig. 4(a)] is a stable region. Similarly, if $h < -2\sqrt{\eta}$, then the stability boundaries are $h = -1 - \eta$ and $h = -2\sqrt{\eta}$.

2. If $h^2 = 4\eta$, then there exists a unique double eigenvalue $\mu_1 = \mu_2 = h/2 = \pm\sqrt{\eta}$, stable solution arise and are periodic for the negative eigenvalues.

3. $h^2 < 4\eta$, μ_1 and μ_2 are complex conjugates given by $(h \pm i\theta)/2$, where $\theta = \sqrt{4\eta - h^2}$. The system is therefore stable if $|h| < 2$. In addition to the natural oscillations with frequency Ω, there appear new oscillations. By plotting this boundary region, Fig. 4(a) is obtained, where a stable behavior occurs in a colored region.

APPENDIX C: HILL DETERMINANT

Equating each of the coefficients of the exponential functions to zero yields Eq. (7), the following infinite set of linear, algebraic, homogeneous equations for A_m and B_m is obtained:

$$\left(k^2 - a_{11} + a_m\right)A_m - a_{12}B_m = 0, \tag{C1}$$

$$\begin{aligned}\left(k^2 d + b_m\right)B_m + \left(k^2 m_0 d_{21} - a_{21}\right)A_m - i\frac{k^2 m_0 b_{21}}{2}e^{i\phi}A_{m-1} \\ + i\frac{k^2 m_0 b_{21}}{2}e^{-i\phi}A_{m+1} - i\frac{k^2 b}{2}B_{m-1} + i\frac{k^2 b}{2}B_{m+1} = 0.\end{aligned}$$

For nontrivial solutions, the determinant of the matrix obtained from Eq. (C1) must be nil. Since the determinant is infinite, the first and second sections of Eq. (C1) are divided by $\left(k^2 - a_{11} - 4m^2\right)$ and $\left(k^2 d - 4m^2\right)$, respectively, for the convergence. Thus, the obtained lower Hill determinant is given by

$$\Delta_H = \begin{vmatrix} \Delta_{11} & \Delta_{12} & 0 & 0 & 0 & 0 \\ \Delta_{21} & \Delta_{22} & \Delta_{23} & \Delta_{24} & 0 & 0 \\ 0 & 0 & \Delta_{33} & \Delta_{34} & 0 & 0 \\ \Delta_{41} & \Delta_{42} & \Delta_{43} & \Delta_{44} & \Delta_{45} & \Delta_{46} \\ 0 & 0 & 0 & 0 & \Delta_{55} & \Delta_{56} \\ 0 & 0 & \Delta_{63} & \Delta_{64} & \Delta_{65} & \Delta_{66} \end{vmatrix}, \tag{C2}$$

where

$$\Delta_{11} = \frac{k^2 - a_{11} + \theta_1 - i\Omega}{k^2 - a_{11} - 4}, \quad \Delta_{12} = -\frac{a_{12}}{k^2 - a_{11} - 4}, \quad \Delta_{21} = -\frac{-m_0 k^2 d_{21} + a_{21}}{k^2 d - 4}, \quad \Delta_{22} = \frac{k^2 d + \theta_2 - i\Omega}{k^2 d - 4},$$

$$\Delta_{23} = i\frac{k^2 m_0 b_{21} e^{(-i\phi)}}{2k^2 d - 8}, \quad \Delta_{24} = i\frac{k^2 b}{2k^2 d - 8}, \quad \Delta_{33} = \frac{k^2 - a_{11} + \theta_1}{k^2 - a_{11}}, \quad \Delta_{34} = -\frac{a_{12}}{k^2 - a_{11}}, \quad \Delta_{41} = -i\frac{m_0 b_{21} e^{(i\phi)}}{2d},$$

$$\Delta_{42} = -i\frac{b}{2d}, \quad \Delta_{43} = -\frac{-m_0 k^2 d_{21} + a_{21}}{k^2 d}, \quad \Delta_{44} = \frac{k^2 d + \theta_2}{k^2 d}, \quad \Delta_{45} = i\frac{m_0 b_{21} e^{(-i\phi)}}{2d}, \quad \Delta_{46} = i\frac{b}{2d},$$

$$\Delta_{55} = \frac{k^2 - a_{11} + \theta_1 + i\Omega}{k^2 - a_{11} - 4}, \quad \Delta_{56} = -\frac{a_{12}}{k^2 - a_{11} - 4}, \quad \Delta_{63} = -i\frac{k^2 m_0 b_{21} e^{(i\phi)}}{2k^2 d - 8}, \quad \Delta_{64} = -i\frac{k^2 b}{2k^2 d - 8},$$

$$\Delta_{65} = -\frac{-m_0 k^2 d_{21} + a_{21}}{k^2 d - 4}, \quad \Delta_{66} = \frac{k^2 d + \theta_2 + i\Omega}{k^2 d - 4}.$$

By rearranging this determinant, the following equation is obtained:

$$\Delta_H = F_4(k)\Omega^4 + F_3(k)\Omega^3 + F_2(k)\Omega^2 + F_1(k)\Omega + F_0(k), \tag{C3}$$

with $F_i(k)$ $(i = 0, \ldots, 4)$ defined by

$$F_4 = \frac{1}{(k^2 - a_{11} - 4)^2 (k^2 d - 4)^2 (k^2 - a_{11}) k^2 d} \left(dk^4 + ((-a_{11} + \theta_1) d + d_{21} m_0 a_{12} + \theta_2) k^2 - a_{11}\theta_2 - a_{12}a_{21} + \theta_1\theta_2 \right),$$

$$F_3 = -\frac{1}{2(k^2 - a_{11} - 4)^2 (k^2 d - 4)^2 (k^2 - a_{11}) d} \left(a_{12} b k^2 m_0 b_{21} \sin(\varphi) \right),$$

$$F_2 = \frac{1}{2(k^2 - a_{11} - 4)^2 (k^2 d - 4)^2 (k^2 - a_{11}) k^2 d} (m_0 b a_{12} k^4 b_{21} ((-d+1)k^2 + \theta_1 - \theta_2 - a_{11}) \cos(\varphi)$$

$$+ (-b^2 d + 2d^3 + 2d) k^8 + \left(2 d_{21} m_0 (d-1)^2 a_{12} + (2\theta_1 - 2a_{11}) d^3 + 6\theta_2 d^2 - (b^2 - 6)(\theta_1 - a_{11}) d + (-b^2 + 2)\theta_2\right) k^6$$

$$+ (m_0^2 (-4d_{21}^2 + b_{21}^2) a_{12}^2 - (4d - 4) \left(-d_{21} m_0 a_{11} + \theta_1 d_{21} m_0 - \theta_2 d_{21} m_0 + \frac{1}{2} da_{21} - \frac{1}{2} a_{21}\right) a_{12} + 6\theta_2 (\theta_1 - a_{11}) d^2$$

$$+ \left(6\theta_2^2 + 6(\theta_1 - a_{11})^2\right) d - \theta_2 \left(b^2 - 6\right)(\theta_1 - a_{11}))k^4 + (8 d_{21} m_0 a_{21} a_{12}^2 + (2\theta_1 - 2\theta_2 - 2a_{11})(-d_{21} m_0 a_{11}$$

$$+ \theta_1 d_{21} m_0 - \theta_2 d_{21} m_0 + 2da_{21} - 2a_{21})a_{12} + (2\theta_1 - 2a_{11})\left(3\theta_2^2 + (\theta_1 - a_{11})^2\right) d + \left(2\theta_2^2 + 6(\theta_1 - a_{11})^2\right)\theta_2)k^2$$

$$+ \left(4 a_{12} a_{21} + 2\theta_2^2 + 2(\theta_1 - a_{11})^2\right)(-a_{12} a_{21} + \theta_2 (\theta_1 - a_{11}))),$$

$$F_1 = \frac{\sin(\varphi) b_{21} b m_0 k^2 a_{12}}{2(k^2 - a_{11} - 4)^2 (k^2 d - 4)^2 (k^2 - a_{11}) d} \left(dk^4 + ((-a_{11} + \theta_1) d + d_{21} m_0 a_{12} + \theta_2) k^2 - a_{11}\theta_2 - a_{12}a_{21} + \theta_1\theta_2 \right),$$

$$F_0 = -\frac{1}{2(k^2 - a_{11} - 4)^2 (k^2 d - 4)^2 (k^2 - a_{11}) k^2 d} \left(k^4 d + ((\theta_1 - a_{11}) d + d_{21} a_{12} m_0 + \theta_2) k^2 + \theta_2 (\theta_1 - a_{11}) - a_{12}a_{21} \right)$$

$$\times (2 b b_{21} k^4 m_0 a_{12} \left(k^2 - a_{11} + \theta_1\right) \cos(\varphi) + \left(b^2 - 2d^2\right) k^8 + \left((-4\theta_1 + 4a_{11}) d^2 + (-4 d_{21} a_{12} m_0 - 4\theta_2) d + 2b^2 (\theta_1 - a_{11})\right) k^6$$

$$\times (-2(\theta_1 - a_{11})^2 d^2 + ((-8\theta_1 + 8a_{11})\theta_2 - 4a_{12}(-d_{21} m_0 a_{11} + \theta_1 d_{21} m_0 - a_{21})) d - 2\theta_2^2 - 4\theta_2 d_{21} m_0 a_{12} + b^2 a_{11}^2 - 2b^2\theta_1 a_{11}$$

$$+ m_0^2 \left(-2 d_{21}^2 + b_{21}^2\right) a_{12}^2 + b^2\theta_1^2)k^4 - (-4 a_{12} a_{21} + 4\theta_2 (\theta_1 - a_{11}))((\theta_1 - a_{11}) d + d_{21} a_{12} m_0 + \theta_2) k^2$$

$$- 2(-a_{12} a_{21} + \theta_2 (\theta_1 - a_{11}))^2). \tag{C4}$$

REFERENCES

[1] S. J. Risch, D. A. Andow, and M. A. Altieri, "Agroecosystem diversity and pest control: Data, tentative conclusions, and new research directions," Environ. Entomol. **12**, 625–629 (1983).

[2] G. R. Knudsen and D. J. Schotzko, "Spatial simulation of epizootics caused by *Beauveria bassiana* in Russian wheat aphid populations," Biol. Control **326**, 318–326 (1999).

[3] E. Scholte, K. Ng, and J. Kihonda, An entomopathogenic fungus for control of adult African Malaria mosquitoes," Science **308**, 1641 (2014).

[4] H. Ranson *et al.*, "Pyrethroid resistance in African anopheline mosquitoes: What are the implications for malaria control?," Trends Parasitol. **27**, 91–98 (2011).

[5] B. Ouafa, "Evaluation de Metarhizium anisopliae titre dagent de lutte biologique contre les larves de moustiques," thesis (University Constantine 1, 2015).

[6] L. S. Osborne and Z. Landa, "Biological control of whiteflies with entomopathogenic fungi," Florida Entomol. Soc. **75**, 456–471 (2012).

[7]N. V. Meyling and J. Eilenberg, "Ecology of the entomopathogenic fungi *Beauveria bassiana* and *Metarhizium anisopliae* in temperate agroecosystems: Potential for conservation biological control," Biol. Control **43**, 145–155 (2007).

[8]G. Dwyer, J. S. Elkinton, and A. E. Hajek, "Spatial scale and the spread of a fungal pathogen of gypsy moth," Am. Soc. Nat. **152**, 485–494 (1998).

[9]A. Hajek, "Interactions between fungal pathogens and insect hosts," Annu. Rev. Entomol. **39**, 293–322 (1994).

[10]H. Roy *et al.*, *The Ecology of Fungal Entomopathogens* (Springer, 2010).

[11]R. A. Samson, H. C. Evans, and J.-P. Latge, *Atlas of Entomopathogenic Fungi* (Springer, Berlin, 1988).

[12]P. Ferron, J. Fargues, and G. Riba, "Les champignons agents de lutte microbiologique contre les ravageurs," in *Handbook of Applied Mycology* (1993), Vol. **2**, 65–92.

[13]R. M. Weseloh, "Effect of conidial dispersal of the fungal pathogen *Entomophaga maimaiga* (Zygomycetes: Entomophthorales) on survival of its gypsy moth (Lepidoptera: Lymantriidae) host," Biol. Control **29**, 138–144 (2004).

[14]D. G. Boucias, J. C. Pendland, and J. P. Latge, "Nonspecific factors involved in attachment of entomopathogenic deuteromycetes to host insect cuticle," Appl. Environ. Microbiol. **54**, 1795–1805 (1988).

[15]R. J. Leger St., "Biology and mechanisms of insect-cuticle invation by deuteromycete fungal pathogens," in *Parasites and Pathogens of Insects* (Academic Press Inc., New York, 1993).

[16]J. Baverstock, H. E. Roy, and J. K. Pell, "Entomopathogenic fungi and insect behaviour: From unsuspecting hosts to targeted vectors," BioControl **55**, 89–102 (2010).

[17]H. Hesketh, H. E. Roy, J. Eilenberg, J. K. Pell, and R. S. Hails, "Challenges in modelling complexity of fungal entomopathogens in semi-natural populations of insects," Ecol. Fungal Entomopathog. **55**, 55–73 (2010).

[18]R. J. Leger St., "Integument as a bamer to microbial infections," in *The Physiology of Insect Epidermis*, edited by A. Retnakaran and K. Binnington (CSIRO, Australia, 1991), pp. 286–308.

[19]R. I. Carruthers, Z. Feng, M. E. Ramos, and R. S. Soper, "The effect of solar radiation on the survival of *Entomophaga grylli* (entomophthorales: Entomophthoraceae) conidia," J. Invertebr. Pathol. **52**, 154–162 (1988).

[20]G. Dwyer, "Density dependence and spatial structure in the dynamics of insect pathogens," Am. Nat. **143**, 533–562 (1994).

[21]M. A. Gilchrist, D. L. Sulsky, and A. Pringle, "Identifying fitness and optimal life-history strategies for an asexual filamentous fungus," Evolution **60**, 970–979 (2006).

[22]H. Malchow, S. V Petrovskii, and E. Venturino, in *Spatiotemporal Patterns in Ecology and Epidemiology*, Chapman Hall/CRC Mathematical and Computational Biology (Chapman Hall/CRC, 2008).

[23]G. Wallentin, "Spatial simulation: A spatial perspective on individual-based ecology—A review," Ecol. Modell. **350**, 30–41 (2017).

[24]H. A. Bradford and H. V. Cornell, *Theoretical Approaches to Biological Control* (Cambridge University Press, 1999).

[25]S. Appalachian, "Spatial autocorrelation and autoregressive models in ecology," Ecosyst. Coop. Unit Stud. **72**, 445–463 (2002).

[26]Y. V. Tyutyunov, L. I. Titova, and I. N. Senina, "Prey-taxis destabilizes homogeneous stationary state in spatial gause Kolmogorov-type model for predatorprey system," Ecol. Complex **31**, 170–180 (2017).

[27]A. Morozov, S. Petrovskii, and B. Li, "Spatiotemporal complexity of patchy invasion in a predator-prey system with the Allee effect," J. Theor. Biol. **238**, 18–35 (2006).

[28]I. Berenstein and J. Carballido-Landeira, "Spatiotemporal chaos involving wave instability," Chaos **27**, 13116 (2017).

[29]M. Baurmann, T. Gross, and U. Feudel, "Instabilities in spatially extended predator-prey systems: Spatio-temporal patterns in the neighborhood of Turing-Hopf bifurcations," J. Theor. Biol. **245**, 220–229 (2007).

[30]S. Chakraborty, B. W. Kooi, B. Biswas, and J. Chattopadhyay, "Revealing the role of predator interference in a predator prey system with disease in prey population," Ecol. Complex. **21**, 100–111 (2015).

[31]S. Fasani and S. Rinaldi, "Factors promoting or inhibiting turing instability in spatially extended prey predator systems," Ecol. Modell. **222**, 3449–3452 (2011).

[32]C. V. Pao, "Global asymptotic stability of Lotka–Volterra 3-species reaction diffusion systems with time delays," J. Math. Anal. Appl. **281**, 186–204 (2003).

[33]F. Rao and Y. Kang, "The complex dynamics of a diffusive preypredator model with an Allee effect in prey," Ecol. Complex. **28**, 123–144 (2016).

[34]J.-P. Laplante, "Inhomogeneous steady state distributions species in predator-prey systems: A specific example," J. Theor. Biol. **91**, 29–45 (1979).

[35]M. Minakuchi and S. Nagano, "Stable territory formation in ecology and its potential generality in pattern formations," J. Theor. Biol. **350**, 17–23 (2014).

[36]M. Banerjee and V. Volpert, "Prey-predator model with a nonlocal consumption of prey," Chaos **26**, 83120 (2016).

[37]M. C. Cross and P. C. Hohenberg, "Pattern formation outside of equilibrium," Rev. Mod. Phys. **65**, 851–1112 (1993).

[38]J. Li *et al.*, "Square turing patterns in reaction-diffusion systems with coupled layers square turing patterns in reaction-diffusion systems with coupled layers," Chaos **24**, 23115 (2014).

[39]H. Caswell and M. G. Neubert, "Chaos and closure terms in plankton food chain models," J. Plankton Res. **20**, 1837–1845 (1998).

[40]P. Gramlich, S. J. Plitzko, L. Rudolf, B. Drossel, and T. Gross, "The influence of dispersal on a predator–prey system with two habitats," J. Theor. Biol. **398**, 150–160 (2016).

[41]J. P. C. Cuadros, A. S. Aponte, and M. X. R. Bocanegra, "In vitro interaction of *Metarhizium anisopliae* Ma9236 and *Beauveria bassiana* Bb9205 with heterorhabditis bacteriophora HNI0100 for the control of *Plutella xylostella*," Springerplus **5**, 2068 (2016).

[42]A. Gabarty, H. M. Salem, M. A. Fouda, A. A. Abas, and A. A. Ibrahim, "Pathogencity induced by the entomopathogenic fungi *Beauveria bassiana* and *Metarhizium anisopliae* in *Agrotis ipsilon* (Hufn.)," J. Radiat. Res. Appl. Sci. **7**, 5–10 (2014).

[43]A. Hussain and M. Tian, "Germination pattern and inoculum transfer of entomopathogenic fungi and their role in disease resistance among coptotermes formosanus (Isoptera: Rhinotermitidae)," Int. J. Agric. Biol. **15**, 319–324 (2014).

[44]T. J. Kurtti and N. O. Keyhani, "Intracellular infection of tick cell lines by the entomopathogenic fungus *Metarhizium anisopliae*," Microbiology **154**, 1700–1709 (2008).

[45]L. Diambra, V. R. Senthivel, D. B. Menendez, and M. Isalan, "Cooperativity to increase turing pattern space for synthetic biology," Am. Chem. Soc. **4**, 177–186 (2014).

[46]L. G. Harrison, S. Wehner, and D. M. Holloway, "Complex morphogenesis of surfaces: Theory and experiment on coupling of reaction diffusion patterning to growth," J. R. Soc. Chem. **120**, 277–294 (2001).

[47]L. Yang *et al.*, "Turing patterns beyond hexagons and stripes," Chaos **16**(3), 037114 (2006).

[48]G. Gambino and M. C. Lombardo, "Cross-diffusion-induced subharmonic spatial resonances in a predator-prey system," Phys. Rev. E **97**, 012220 (2018).

[49]E. Tulumello, M. C. Lombardo, and M. Sammartino, "Cross-diffusion driven instability in a predator-prey system with cross-diffusion," Acta Appl. Math. **132**, 621–633 (2014).

[50]R. Han and B. Dai, "Cross-diffusion-driven turing instability and weakly nonlinear analysis of turing patterns in a uni-directional consumer-resource system," Boundary Value Probl. **2017**, 125 (2017).

[51]I. M. Dubovskiy *et al.*, "More than a colour change: Insect melanism, disease resistance and fecundity," Proc. R. Soc. B **280**, 20130584 (2013).

[52]A. Vilcinskas and P. Glitz, *Parasitic Fungi and Their Interactions with the Insect Immune System* (Academic Press, 1999). Vol. 43.

[53]G. Khachatourians, "Entomopathogenic fungi: Biochemistry and molecular biology," in *Human and Animal Relationships. The Mycota (A Comprehensive Treatise on Fungi as Experimental Systems for Basic and Applied Research)*, edited by A. A. Brakhage and P. F. Zipfel (Springer, Berlin, Heidelberg, 2008), Vol. 6.

[54]J. H. P. Dawes and M. O. Souza, "A derivation of Hollings type I, II and III functional responses in predator prey systems," J. Theor. Biol. **327**, 11–22 (2013).

[55]A Hastings and T. Powell, "Chaos in a three species food chain," Ecology **72**, 896–903 (1991).

[56]M. Banerjee and Y. Takeuchi, "Maturation delay for the predators can enhance stable coexistence for a class of prey–predator models," J. Theor. Biol. **412**, 154–171 (2017).

[57] R. Bhattacharyya and B. Mukhopadhyay, "On a population pathogen model incorporating species dispersal with temporal variation in dispersal rate," J. Biol. Phys. **37**, 401–416 (2011).

[58] S. A. Gourley, N. F. Britton, M. A. J. Chaplain, and H. M. Byrne, "Mechanisms for stabilisation and destabilisation of systems of reaction-diffusion equations," J. Math. Biol. **34**, 857–877 (1996).

[59] J. A. Sherratt, "Oscillatory reaction-diffusion equations with temporally varying parameters," Math. Comput. Model. **39**, 7177 (2004).

[60] J. A. Sherratt, "Turing bifurcations with a temporally varying diffusion coefficient," J. Math. Biol. **33**, 295–308 (1995).

[61] J. T. Mika *et al.*, "Measuring the viscosity of the *Escherichia coli* plasma membrane using molecular rotors," Biophys. J. **111**, 1528–1540 (2016).

[62] D. Lucena, M. Mauri, F. Schmidt, B. Eckhardt, and P. L. Graumann, "Microdomain formation is a general property of bacterial membrane proteins and induces heterogeneity of diffusion patterns," BMC Biol. **16**, 1–17 (2018).

[63] R. L. Snyder and M. A. X. Min, "Hand calculating degree days," Agric. For. Meterol. **35**, 353–358 (1985).

[64] S. P. Worner, "Performance of phenological models under variable temperature regimes: Consequences of the Kaufmann or rate summation effect," Entomol. Soc. Am. **21**, 689–699 (1992).

[65] S. Raychaudhuri and K. Sinha, "Effect of time-varying cross-diffusivity in a two-species Lotka-Volterra competitive system," Ecol. Modell. **92**, 55–64 (1996).

[66] J. A Sherratt, "Diffusion-driven instability in oscillating environments," Eur. J. Appl. Math. **6**, 355–372 (1995).

[67] D. W. Jordan and P. Smith, *Nonlinear Ordinary Differential Equations* (Oxford University Press Inc., New York, 2007).

[68] R. A. Yamapi and P. Woafo, "Dynamics and synchronization of coupled self-sustained electromechanical devices," J. Sound Vib. **285**, 1151–1170 (2005).

[69] R. Yamapi and P. Woafo, "Synchronized states in a ring of four mutually coupled self-sustained electromechanical devices," Commun. Nonlinear Sci. Numer. Simul. **11**, 186–202 (2006).

[70] Y. C. Kouomou and P. Woafo, "Stability and chaos control in electrostatic transducers," Phys. Scr. **62**, 255 (2000).

[71] V. K. Vanag and I. R. Epstein, "Design and control of patterns in reaction-diffusion systems," Chaos **18**, 1–11 (2008).

[72] V. K. Vanag, "Localized patterns in reaction-diffusion systems," Chaos **17**, 37110 (2007).

[73] N. M. St. Clair, "Pattern formation in partial differential equations," Department of Mathematics, Scripps College (Women's College, Claremont, CA, 2006).

[74] N. J. J. Mills and W. M. M. Getz, "Modelling the biological control of insect pests: A review of host-parasitoid models," Ecol. Modell. **92**, 121–143 (1996).

[75] L. A. Segel and J. L. Jackson, "Dissipative structure: An explanation and an ecological example," J. Theor. Biol. **37**, 545–559 (1972).

[76] M. Bani-Yaghoub, G. Yao, M. Fujiwara, and D. E. Amundsen, "Understanding the interplay between density dependent birth function and maturation time delay using a reaction-diffusion population model," Ecol. Complex **21**, 14–26 (2015).

Byliole S. Djouda, Frank T. Ndjomatchoua, F. M. Moukam Kakmeni, Clément Tchawoua, and Henri E. Z. Tonnang

View Online

Export Citation

CrossMark

Understanding biological control with entomopathogenic fungi—Insights from a stochastic pest–pathogen model

Byliole S. Djouda,[1,2] (ID) Frank T. Ndjomatchoua,[3] (ID) F. M. Moukam Kakmeni,[2,a)] (ID) Clément Tchawoua,[1] and Henri E. Z. Tonnang[4]

AFFILIATIONS

[1]Laboratory of Mechanics, Materials and Structures, Research and Postgraduate Training Unit for Physics and Applications, Postgraduate School of Science, Technology and Geosciences, Department of Physics, Faculty of Science, University of Yaoundé 1, P.O. Box 812, Ngoa Ekelle, Yaoundé, Cameroon
[2]Complex Systems and Theoretical Biology Group, Laboratory of Research on Advanced Materials and Nonlinear Science (LaRAMaNS), Department of Physics, Faculty of Science, University of Buéa, P.O. Box 63, Buéa, Cameroon
[3]Sustainable Impact Platform, Adaptive Agronomy and Pest Ecology Cluster, International Rice Research Institute (IRRI), DAPO Box 7777-1301, Metro Manila, Philippines
[4]International Institute of Tropical Agriculture (IITA), 08 BP 0932 Tri Postal Abomey Calavi, Cotonou, Benin

[a)]**Author to whom correspondence should be addressed:** moukamkakmeni@gmail.com

ABSTRACT

In this study, an individual-based model is proposed to investigate the effect of demographic stochasticity on biological control using entomopathogenic fungi. The model is formulated as a continuous time Markov process, which is then decomposed into a deterministic dynamics using stochastic corrections and system size expansion. The stability and bifurcation analysis shows that the system dynamic is strongly affected by the contagion rate and the basic reproduction number. However, sensitivity analysis of the extinction probability shows that the persistence of a biological control agent depends to the proportion of spores collected from insect cadavers as well as their ability to be reactivated and infect insects. When considering the migration of each species within a set of patches, the dispersion relation shows a Hopf-damped Turing mode for a threshold contagion rate. A large size population led to a spatial and temporal resonant stochasticity and also induces an amplification effect on power spectrum density.

Published under license by AIP Publishing. https://doi.org/10.1063/5.0019971

Entomopathogenic fungi (EPF) are more used as a biological control agent, with long and irregular periods between outbreaks. However, the EPF outbreaks are strongly influenced by environmental factors such as temperature and humidity. The ability of EPF to persist in the insect habitat plays an important role in fungi disease transmission. The first sequence of analyses consists of the construction of the mathematical models [individual-based model (IBM) and its corresponding deterministic model called the population level model (PLM)]. The IBM that is inherently stochastic is formulated as a continuous time Markov process, which is then decomposed into a deterministic dynamics using stochastic corrections and system size expansion; we deduce the mechanisms behind the dynamics of the system in order to understand the interplay between deterministic and stochastic forces, and we compare the obtained models. This study suggests that the persistence of EPF depends on the density of conidia, which becomes resting and can be reactivated in favorable conditions. Our results show that the contagious processes between susceptible and infected insects and the maximum number of species a patch may contain are more responsible factors of EPF persistence and outbreaks. This study well describes EPF outbreaks and disease transmission between insects and thus can be served to understand the epidemiological characteristic of fungal infections and to characterize the density species fluctuations that are simply a result of an interaction between demographic parameters.

I. INTRODUCTION

A wide spectrum of animals, weeds, and diseases can be a burden for agriculture and human health.[1] As an alternative to chemical control that is dangerous for the environment and for non-targeted living organisms, the biological control is often preferred.[1] This particular type of control consists of using living organisms to reduce population density of another organism.[2] Biological control schemes use microbial agents (bacteria, viruses, and fungi), and predatory insects and mites that parasite and kill other arthropods, weeds, or nematodes.[2]

In order to address important issues about the biological control and pest eradication problems in applied ecology, numerous mathematical models were suggested.[1–17] However, the question of how to study complex host-pathogen dynamics remains contentious with several competing paradigms available.[3,18] An important approach is individual-based models [or individual-level models (ILMs)], which include demographic noise effects associated with birth, death, immigration, and emigration assuming the physical environment constant.[4,19] The stochastic demography (often called demographic noise) is defined as a random variation originating from the discrete nature of individuals and stochastic character of these events, where birth/death rates are not affected by external forcing.[4,19] This is a useful approach to understand how biological and ecological systems evolve over time while considering the behavior and interactions among species and deduct the associated emerging patterns when the population is well mixed.[4,19] This approach was successfully applied in predicting rift valley fever inter-epidemic activities and outbreak patterns,[5] predator–prey cycles from resonant amplification from demographic stochasticity,[20–23] stochastic amplification in epidemics,[24] demographic noise and resilience in a semi-arid ecosystem,[6] impact of human mobility on the periodicity and mechanisms underlying diseases dynamics,[7] demographic stochasticity and heterogeneity in transmission of infection,[25] and stochastic Turing's patterns.[26,27] The approach is promising, and it was hypothesized that it can provide good insight when applied in the context of biological control modeling.

In this paper, the interaction between susceptible and infected insects, and spores of EPF is modeled. The role of stochasticity in the dynamic between the both species is investigated by studying the resilience and stochastic amplification. The spatial aspect of this system was also explicitly considered in order to explain the dynamics, which take place between individuals from different patches.

A considerable challenge for controlling pest via a biological control is to understand how the parasite or the pathogen can persist within the pest population without an external reservoir.[1–4] However, most of the existing biological control models operating at an individual level included the stochasticity mostly by random functions/parameters.[3,8–11] The effect of individual variability on pathogen persistence is still undervalued in biological control studies. The present study brings novelty by starting with an individual-based model for biological control (BC), which is *inherently* stochastic. Considering the case study of BC using entomopathogenic fungi (EPF) already investigated in the deterministic and non-ILM approach,[12–14] we moved forward and designed a stochastic ILM model for BC and EPF to find how to optimize insect pest extinction or a major outbreak of pathogen? Note that despite

the development of numerous mathematical models that have examined the use of micro-organisms and parasitoids as control agents, the role of entomopathogenic fungi and the mechanisms underlying host–pathogen relations that result from epizootics are not fully investigated.[3,15,18] Entomopathogenic Fungi (EPF) are convenient for use in biological control (BC) and in integrated pest management to reduce crop devastator damages because it can generate a secondary infection after the initial spray via the production of spores by first infected individuals during their interactions depending on temperature, humidity degree, and dispersion by natural phenomenon (such as wind, rain).[16,17] The number of secondary infection also known as the measurement of the disease transmission has been investigated in the previous mathematical models.[25] Previous researchers have shown their role on the interplay between species and/or their habitat and predicted the dynamics, the extinction, and the persistence of individuals by using bifurcation and stability analysis theory.[28–35] The underlying theories demonstrated relevant results in the context of predator–prey models,[20,21,28–37] in the context of disease transmission,[5,25] in population dynamics,[4] and so on.

The infection of a pest occurs in two ways: (1) direct contamination by spores[38] and (2) contamination by infected insects (contagious phenomenon) usually called horizontal transmission.[38] However, the number of conidia resulting from the infectious insects or cadavers is important to evaluate the persistence of EPF in the field and sustain a resilience of the BC.[17] In general, three factors were highlighted as major determinants in the long-term dynamics of the pathogen in the population: (1) the intrinsic biological properties of EPF, (2) the life history traits and population parameters of pests, and (3) spatial evolution of EPF within crop devastator's population. Thus, a very important property of spore causing long-term infectiousness and persistence of a BC agent underlined in this study is its ability to be rested on mummified insects and upon reactivation causing pests to become infectious.[39] The pathogen spread during the ongoing epidemics is enhanced by a simple contact between infected and susceptible insects during their reproduction, their foraging, and intra/interspecific competition.[15] It is noteworthy to mention that for certain classes of EPF, spores emerged on their host cuticle only after death.[3,15] Note that parameters such as social group size, recruitment rate, and mobility can also affect the persistence of pathogen.[19,23,40]

This study is organized as follows: In Sec. II, the model is described with the underlying hypothesis following by the stability and bifurcation analysis. Other analyses such as the role of stochasticity in the dynamics of the system and the condition at which population coexists or goes to extinction are also investigated in the same section. In Sec. III, the results obtained are discussed. The conclusion is done in Sec. IV.

II. MATERIALS AND METHODS

A. Dynamical model

In this section, an individual-based stochastic model that considers all essential features of the interactions between EPF and insect pests is formulated. This model investigates a biological control using entomopathogenic fungi to target insect pest's population when their size is large but finite. This work focused solely on

the pathogen particle populations, assuming that they are implicitly dispersed in the environment by natural phenomena such as wind or rain. An additional transmission pathway is simple contacts between infected and susceptible insects depending on the species of entomopathogenic fungi,[15,38] assuming this can be ignored in the particular case where spores are produced by insect cadavers. It is assumed that insect individuals exist in two discrete states: susceptible or infected. To simplify the analyses, it was supposed that for the same species, every individual has an identical probability for birth, death, migration, or acquiring infection.

New insects produced at a birth rate b_1 are susceptible to be infected. They undergo natural death at the rate d_1. A susceptible insect is infected by a previous infected insect or by a pathogen particle at probabilities I_1 and I_2, respectively.[41] Infected insects die and produce either more infective conidia with the probability b_2. If environmental conditions are not favorable, spores become inactivated at the rate d_3.[15] The carrying capacity N, defined as the maximum number of individuals allowed per site, is kept constant. In this framework, n denotes the number of insects susceptible to be infected S, m the number of infected insect species I, and l the number of pathogen particle species C. A fourth class E denoting empty (describes the possibility to receive a new individual in the patch) is introduced. It is supposed that the population dynamics of the system can be essentially described by four processes:

1. Infection.
   A spore species may come into contact with a susceptible insect giving rise to one infected pests. This is assumed to take place at a rate I_2. A susceptible insect may also be infected by an infected (that is, from the environment, reproduction) for a certain species of entomopathogenic fungi at the rate I_1 giving rise to two infected pests. Therefore, to generalize this study, there are two mechanisms written as $CS \rightarrow CI$ and $IS \rightarrow II$. The case where spores emerge on their host cuticle only after insect death corresponds to the case where the second mechanism does not exist.
2. Death.
   To describe a more realistic epidemiological model, it is assumed that each of the three types of individuals has its specific death rate. These are represented by $S \rightarrow E$ and $C \rightarrow E$ at the rate d_1 and d_3, respectively. The death of a spore means the resting process (inactive stage). The death of an infected insect is affected to case 4.
3. Birth.
   In regard to the potential of EPF to rapidly kill their host, it is assumed here that there is no offspring for infected insects. They only give rise to the new spore generation. Thus, the mechanisms $SE \rightarrow SS$ occur for susceptible insects at the rate b_1.
4. Death/conidia production.
   Each death of infected insects gives rise to the sporulation. This transition is represented by $I \rightarrow C$ and occurs at the rate b_2.

1. Small population size

The transition probability per unit time step of the local system of individuals from state $\sigma = (n, m, l)$ to the state $\sigma' = (n', m', l')$

is noted $T(\sigma'|\sigma)$. The process occurring in this framework is conceptualized by the following events:

1. Infection

$$T(n-1, m+1, l\,|\,n, m, l) = \frac{2I_1 nm}{N} + \frac{2I_2 nl}{N}. \quad (1)$$

2. Birth

$$T(n+1, m, l\,|\,n, m, l) = 2b_1 \frac{n}{N}(N-n-m-l). \quad (2)$$

3. Death

$$T(n-1, m, l\,|\,n, m, l) = d_1 n,$$
$$T(n, m, l-1\,|\,n, m, l) = d_3 l. \quad (3)$$

4. Death/conidia production

$$T(n, m-1, l+1\,|\,n, m, l) = b_2 m. \quad (4)$$

The factor of 2 comes from the fact that the choices AB and BA are identical. A and B illustrate different species. The rate of occurrence (transition rate) depends only on the present state and could be for a species A defined as the number of this type at the time t divided by the total number of possibility to draw individuals. Thus, the coefficients b_1 and I_i (with $i = 1, 2$) are scaled by a factor $(N-1)$ and b_2 and d_i by a factor N. The system (1)–(3) is simulated using the Gillespie algorithm.[42]

2. System size expansion

The master equation describing the time evolution of the system is defined to be a sum of transition probabilities giving rise to a change in the probability distribution function $P(n, m, l, t) = P(\sigma, t)$ with time and takes the following form:[5,21,23]

$$dP(\sigma, t)/dt = \sum_{\sigma \neq \sigma'} \left(T(\sigma|\sigma') P(\sigma', t) - T(\sigma'|\sigma) P(\sigma, t) \right), \quad (5)$$

where t represents the time since the first infection; for more details, the reader is referred to Appendix A. This equation is too complicated to solve exactly, and as proposed in previous research,[19,22,43] it can be analyzed in the limit of a large system size. Van Kampen's approximation transforms the system to deterministic equations associated with its stochastic corrections.[19,22,43] Defined in terms of the populations $\phi = \lim_{N \to \infty} n/N$, $\varphi = \lim_{N \to \infty} m/N$, $\psi = \lim_{N \to \infty} l/N$, these equations are explicitly given by

$$\dot{\phi} = r\phi\left(1 - \frac{\phi}{k}\right) - \alpha_1 \phi\varphi - \beta_1 \phi\psi,$$
$$\dot{\varphi} = \alpha_2 \phi\varphi + \theta\phi\psi - b_2\varphi, \quad (6)$$
$$\dot{\psi} = b_2\varphi - d_3\psi.$$

The details about the mean-field theory are provided in Appendix A. The dot above the average state variable represents the first order derivative with respect to the time, and the coefficients are given by $r = 2b_1 - d_1$, $k = 1 - \frac{d_1}{2b_1}$, $\alpha_1 = 2(b_1 + I_1)$, $\beta_1 = 2(b_1 + I_2)$, $\alpha_2 = 2I_1$, and $\theta = 2I_2$.

B. Stability and bifurcation analysis

It was considered that there exists a set of stationary, spatially uniform solutions of (6). This allowed us to obtaining three singular points. The only endemic equilibrium point is $E^{SIC} = (\phi^s, \varphi^s, \psi^s)$, which has a biological relevance only if $k\left(\theta b_2 + \alpha_2 d_3\right) - b_2 d_3 > 0$, the condition that will be applied throughout the rest of this study. To make this analysis more easy, the basic reproduction number R_0 defining the expected number of secondary infections caused by a single infected case is introduced from the relevance biological conditions (see details in Appendix A). In our model, when $R_0 < 1$, the endemic equilibrium point does not have a biological relevance, and the EPF population density will die out with time and cannot reduce the pest population; whereas for $R_0 > 1$, the introduction of EPF can lead to a targeted spread, and the endemic equilibrium point exists and can be stable/unstable. The color zones of Fig. 1(a) display the stability region of the steady state according to the relevance of the conditions given above. The parameter space (R_0, I_1) shows the zone where the steady state exists and is unstable so that EPF can invade insect pest population. Figure 1(c) shows that the transcritical bifurcation occurs at $R_0 = 1$ and changes the stability from the trivial steady state (disease free equilibrium E^1) to the endemic equilibrium. More clearly, E^1 is stable when $R_0 < 1$. The underlying steady state becomes unstable for $R_0 > 1$. At the same time, the endemic point is stable for the contagious rate corresponding to the black colored area of Fig. 1(a). At the threshold basic reproduction number $R_0 = 1$, the infected insect population can invade the susceptible population, and the resulting free-disease equilibrium system becomes unstable. Because R_0 and I_1 are proportional, R_0 can be sufficient to describe dynamics of the systems.[44] Therefore, the fundamental question here is *How to maintain R_0 always greater than one?* To answer this question, the sensitivity analysis of the basic reproduction number R_0 is conducted by a Latin hypercube sampling (LHS) in combination with a partial rank correlation coefficient (PRCC).[45] This method is useful to identify parameters that affect the quantity R_0. The input model parameters k, θ, α_2 or I_1, b_2, d_3 from which R_0 depends are randomly and uniformly distributed between their lower and higher values into Q equal probability intervals and subsequently used to compute the LHS matrix of five (number of input parameters) columns with Q lines. The basic reproduction number R_0 is evaluated as a corresponding output matrix. These matrices are rank-transformed to calculate the partial rank correlation coefficient (PRCC), which gives the sensitive index of R_0 associated with each parameter.[45] The parameters that have the sensitivity indexes closer to ± 1 should significantly affect R_0. The more a parameter is tending to minus one, the more it has a reductive effect on R_0, and the parameters for which the PRCC is close to one increase the basic reproduction number. Therefore, the resting rate of spore d_3 decreases the basic reproduction number [Fig. 3(a)]. It is also easy to see that the carrying capacity and the fraction of a susceptible insect pest have the most important augmentative effect on the basic reproduction number. This affects the logistic growth of other species in these BC systems. This is in agreement with the investigation,[3] where it is shown that in the BC, using entomopathogenic against nematode pests can be efficiently used to control the host population only if the host's reproductive rate is also regulated in a density-dependent manner. A comparison between ILM and deterministic system equations obtained in van Kampen approximation, shown through a numerical simulation, sustained oscillations of all species (Fig. 2, red line), whereas the deterministic equation models showed damped oscillations [see Fig. 2 (dark and blue dotted lines)], a similar result was observed.[4,5,21,46] It is the expected long-term behavior for host–vector models.[5]

C. Population extinction, coexistence, and stochastic amplification

1. Probability of extinction and coexistence

In epidemic models, the main concern is to find conditions under which a pathogen agent introduced into a community will
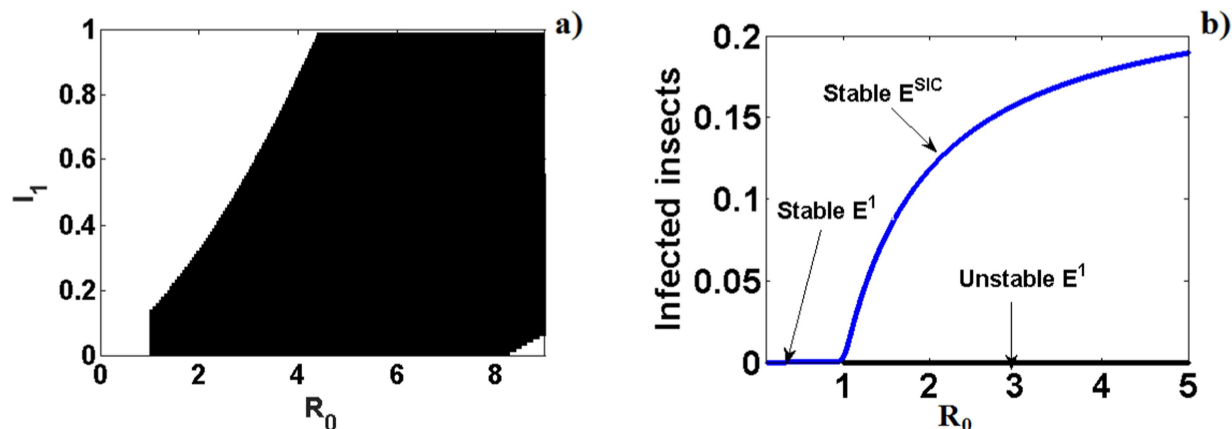

FIG. 1. Stability diagram of the endemic steady state. The colored zone corresponds to the stable region according to the biological relevance conditions and the coupled point satisfies the stability condition in the parameter spaces. (b) Transcritical bifurcation at R_0. Parameter values are $d_1 = 0.05, b_1 = 0.25, b_2 = 0.15, d_3 = 0.1,$ and $l_2 = 0.05$ for each case.
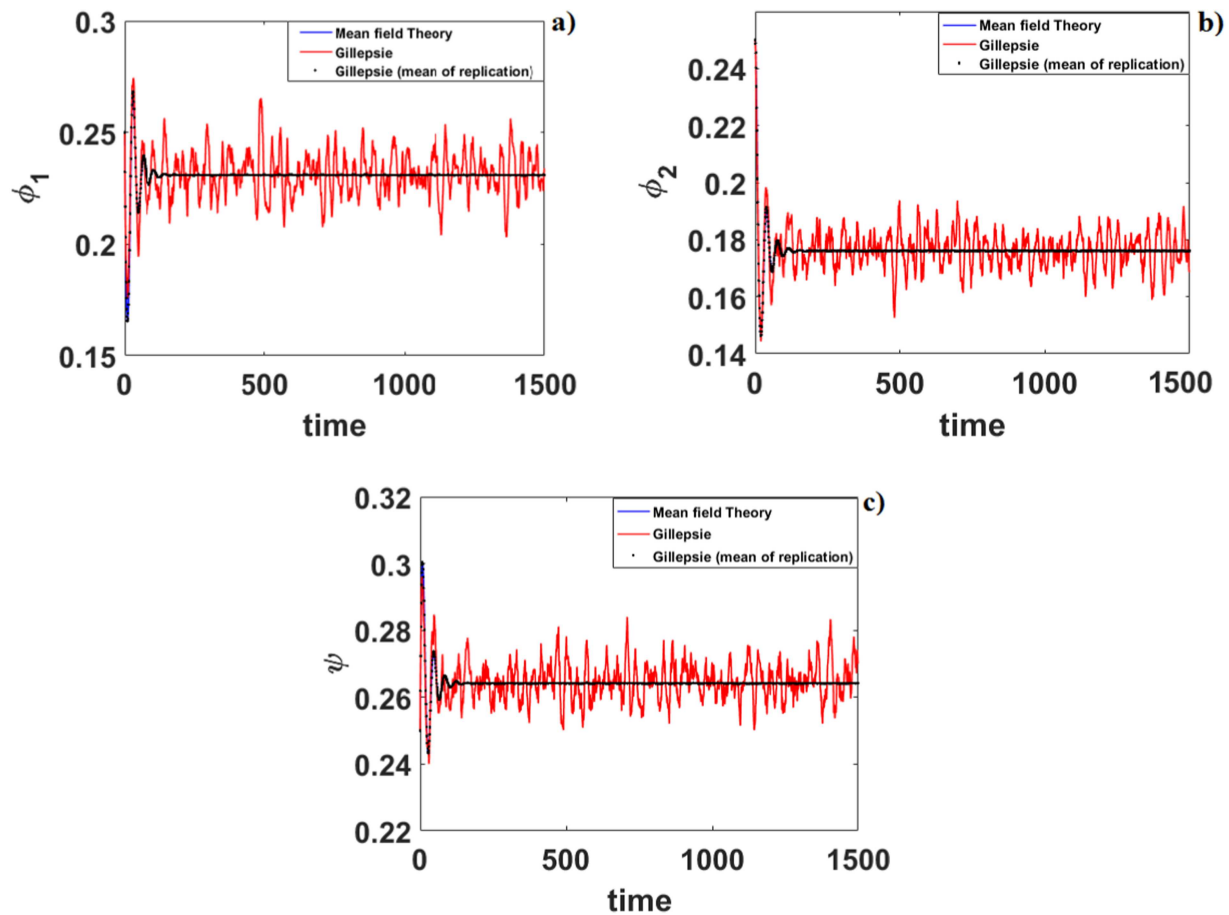
FIG. 2. These panels show susceptible (ϕ), infected pest (φ), and pathogen (ψ) population densities as a function of time [(a), (b), and (c), respectively] for $N = 10\,000$. The red line is the average of time series of 100 replications generated from the ILM [Eqs. (1)–(3)] using the Gillespie algorithm,[43] and the dashed dark line is the average of the species density time series from 10 000 replicates generated from the ILM and is almost indistinguishable with the continuous blue line that corresponds to the deterministic equations from mean-field approximation simulated with a classical Runge–Kutta algorithm. The parameters used in the simulations are $b_2 = 0.15$, $d_3 = 0.1$, $l_1 = 0.25$, $d_1 = 0.05$, $b_1 = 0.25$, and $l_2 = 0.05$.

develop into a large outbreak, while coexistence of populations was never observed.[47] Therefore, the question asked here is *Under which conducive conditions the EPF may become endemic in a susceptible insect pest population?* It has been shown that the epidemic outbreak is not always guaranteed by having R_0 greater than one: stochastic extinction can occur during the period immediately following the introduction when there are a few infectious individuals within the system.[25,48] Rather than the major outbreak that would be expected based on the behavior of the deterministic model, only a minor outbreak might occur. During this early period after EPF introduction, little depletion of a susceptible insect will have occurred; therefore, invasion probabilities can be derived using the linear model that arises by assuming that the populations are entirely susceptible.[5,25] A more challenging question is to calculate the probability that the infection persists or extinct through the trough that follows the initial epidemic.[48] It is noteworthy to mention that the infection of the

insect pest occurs in two range: one is the transmission of infection by a direct contact between infected and susceptible insects[38] and the other refers to the transmission from the pathogen particle (spore) to susceptible individuals. In many disease models, it is assumed that a constant rate of death for the hosts and a constant death rate for a resting spore, leading to the duration of infection, for both hosts and pathogens are being exponentially distributed.[25] Assuming the secondary infections arise independently at a constant rate over these infectious periods,[25,48] extinctions probabilities taken as s_1 and s_2 for host and EPF, respectively, start from a single individual of the same type, are found by calculating the smallest positive root of the equation $G_1(G_2(s_1)) = s_1$ and $G_2(G_1(s_2)) = s_2$, respectively, where G_i (*with i=1,2*) denotes the probability generating functions (PGFs) using subscript 1 for insect species and subscript 2 for a pathogen particle. The sensitivity analysis of the probability of pest extinction is given in Fig. 2(b). In contrast to other parameters, the sensitivity
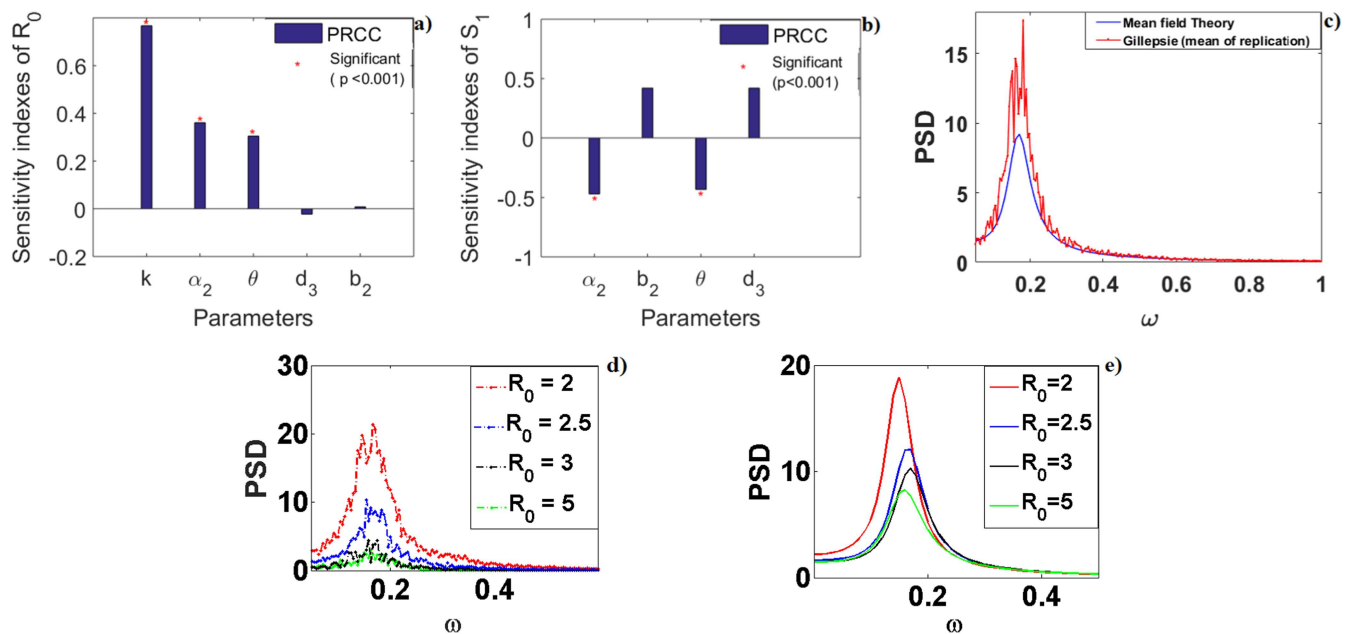
FIG. 3. (a) Sensitivity analysis of the number of secondary infection (R_0) results. (b) Sensitivity analysis of the number of secondary infection (S_1) results. Sample size $Q = 1000$. The symbol ($*$) denotes PRCCs that the p-values are significantly different from zero. (c) Numerical and theoretical predictions of the power spectral density of infected insects [Eq. (A11)] for a total number of species. (d) and (e) Numerical and analytic predictions of the impact of the basic reproduction number on the power spectral density of infected insects [Eq. (A11)] for a total number of species using the same parameter values of five in Fig. 2.

indexes for α_2, θ are negative, meaning that they have a decreasing effect on s_1. It is easy to remark that the proportion of infected pest's death b_2 followed by the rate d_3 of a spore becoming a resting stage has a large effect on increasing extinction probability because these spores have the ability to be reactivated when conditions are favorable.

2. Periodicity and stochastic amplification

As mentioned previously, the ILM model discussed here leads to the existence of stochastic cycles (also called quasi-cycles) because it does not have a single period, but a distribution of period centered around an average value corresponding to the maximal amplitude of fluctuations. Therefore, a power spectrum density of the frequency distribution is essential to adequately capture the quasi-periodicity. A description of the stochastic fluctuations of the system requires consideration of higher-order terms in the Van Kampen expansion. In particular, a very good approximation is obtained only if the next-to-leading order is considered. In this way, we obtain linear Fokker–Planck equations, which have their natural equivalent to a set of Langevin's equations for the temporal evolution of the normalized fluctuations of susceptible, infectious individuals and a pathogen particle around equilibrium values (ξ, η, ϑ, respectively). By Fourier's transformation of these equations, we are able to analytically calculate the power spectral densities (PSDs)

corresponding to the normalized fluctuations, which is no longer dependent on the community size N. After averaging, the three expected forms of these PSDs of susceptible pests, infected pests, and spores around the endemic equilibrium are given by (A11). The complete derivations of these PSDs and detailed descriptions about the functions $\kappa_i, b_{ij}, \Gamma_i$, and $D(\omega)$ depend on model parameters (see Appendix A). In Fig. 3(c), the very large amplification of these fluctuations is remarkable and almost exceptionally important for the infected host species. The system has a tendency to oscillate at a greater amplitude at some frequencies rather than at others. Internal noise arises from demographic stochasticity contained in the individual's processes and leads to the resonant effect. By using the expression for the PSD for the infected insects, the basic reproduction number effects on the periodicity of the pest's outbreaks are examined. Figures 3(d) and 3(e) show that as R_0 moves from unity, the amplitude of PSD decreases, whereas the width increases. The width is important as it shows how coherent the cycles are: the smaller the width is, the longer the cycles remain in phase. Therefore, for R_0 tending to one, the power spectra present a large peak at a preferred frequency different from zero, which corresponds to the irregular dynamics. This increases stochasticity in the smaller systems but also the fade-out boundary, where extinction and re-colonization events start to have an impact on the dynamics.[46] However, the PSD of the deterministic case shows that when R_0 increases, the amplitude of the power spectral

density decreases. Also, a light shift of the resonant frequency is observed.

D. Spatial dynamic

1. Small population size

In this section, we proposed a spatial stochastic version of the model. The mechanisms corresponding to birth, death, and infections described above are assumed to be local meaning that it is only involved in a local site. Here, the possibility of migration between nearest-neighbor patches is taken into consideration. It is also assumed that the inhabited patches, labeled by $i = 1, \ldots, \Omega$, are located at the sites of a d-dimensional hypercubic lattice.[23] For applications, we are interested in the case of a square lattice in two dimensions, but we prefer to work with general d. One reason is that it is not any more complicated to do so. Another justification is because our stochastic simulations have been carried out in $d = 1$ in order to achieve a higher accuracy. Each patch possesses a finite carrying capacity, N, which is the maximum number of individuals allowed per site. The number of susceptible pests, infected pests, and spores in the patch i will be denoted by n_i, m_i, and l_i, respectively. There are, therefore, $(N - n_i - m_i - l_i)$ empty or vacant "spaces," E, in the patch i. These are necessary to allow the number of S, I, and C individuals in patch i to independently vary with time. The transition rate is given in two groups: locally, it corresponds to the transition probability described in (1), (2), (3), and (4) adding a subscription i and scaled by Ω. In addition to processes described in the local model, an individual is moved from the patch i to another patch label j at a constant rate as

- Susceptible pest: $S_i E_j \rightarrow E_i S_j$, $E_i S_j \rightarrow S_i E_j$ at the rate μ_1.
- Infected pest: $I_i E_j \rightarrow E_i I_j$, $E_i I_j \rightarrow I_i E_j$ at the rate μ_2.
- A given spore can be displaced by rain, wind, or spray by another insect or animal: $C_i E_j \rightarrow E_i C_j$, $E_i C_j \rightarrow C_i E_j$ at the rate μ_3.

To summarize, the migratory transition rate is given by

$$
\begin{aligned}
T\left(n_i + 1, n_j - 1 \mid n_i, n_j\right) &= \frac{\mu_1 n_j \left(N - n_i - m_i - l_i\right)}{z \Omega N}, \\
T\left(n_i - 1, n_j + 1 \mid n_i, n_j\right) &= \frac{\mu_1 n_i \left(N - n_j - m_j - l_j\right)}{z \Omega N}, \\
T\left(m_i + 1, m_j - 1 \mid m_i, m_j\right) &= \frac{\mu_2 m_j \left(N - n_i - m_i - l_i\right)}{z \Omega N}, \\
T\left(m_i - 1, m_j + 1 \mid m_i, m_j\right) &= \frac{\mu_2 m_i \left(N - n_j - m_j - l_j\right)}{z \Omega N}, \\
T\left(l_i + 1, l_j - 1 \mid l_i, l_j\right) &= \frac{\mu_3 l_j \left(N - n_i - m_i - l_i\right)}{z \Omega N}, \\
T\left(l_i - 1, l_j + 1 \mid l_i, l_j\right) &= \frac{\mu_3 l_i \left(N - n_j - m_j - l_j\right)}{z \Omega N}.
\end{aligned}
\tag{7}
$$

Here, z denotes the coordination number of the lattice that is the number of nearest neighbors of any given site. It needs to be included since it represents the choice of nearest neighbor j once a patch i has been chosen.

2. Stability analysis

The master equation is rewritten in two main contributions: the first part defined local mechanisms that correspond to the form given in a non-spatial case adding a subscript i with a scaled Ω calling T_i^{loc} and the second one takes migration into consideration T_{ij}^{mig}.[23] Therefore (see Appendix B),

$$
\frac{dP_{n,m}(t)}{dt} = \sum_{i=1}^{\Omega} \left(T_i^{loc} P_{n,m}(t) + \sum_{j \in i} T_{ij}^{mig} P_{n,m}(t) \right),
\tag{8}
$$

where the notation $j \in i$ means that j is the nearest neighbor of i. The deterministic models are written as the 3Ω macroscopic equations given by

$$
\begin{aligned}
\dot{\phi}_i &= r\phi_i(1 - \frac{\phi_i}{k}) - \alpha_1 \phi_i \varphi_i - \beta_1 \phi_i \psi_i \\
&\quad + \mu_1 \left(\Delta\phi_i + \phi_i \Delta\varphi_i - \varphi_i \Delta\phi_i + \phi_i \Delta\psi_i - \psi_i \Delta\phi_i \right), \\
\dot{\varphi}_i &= \alpha_2 \phi_i \varphi_i + \theta \phi_i \psi_i - b_2 \varphi_i \\
&\quad + \mu_2 \left(\Delta\varphi_i + \varphi_i \Delta\phi_i - \phi_i \Delta\varphi_i + \varphi_i \Delta\psi_i - \psi_i \Delta\varphi_i \right), \\
\dot{\psi}_i &= b_2 \varphi_i - d_3 \psi_i \\
&\quad + \mu_3 \left(\Delta\psi_i + \psi_i \Delta\phi_i - \phi_i \Delta\psi_i + \psi_i \Delta\varphi_i - \varphi_i \Delta\psi_i \right),
\end{aligned}
\tag{9}
$$

where $i = 1, \ldots, \Omega$ and the symbols (.) and Δ denote the time derivation (scaled $\tau = t/\Omega$) and the discrete Laplacian operator $\Delta f_i = (2/z) \sum_{j \in i} \left(f_j - f_i\right)$, respectively.[23] In this sum, z corresponds to the total number of first neighbors. The limit $\Omega \rightarrow \infty$ corresponds to shrinking the lattice spacing d to zero and so leading to the continuum mean-field description. In this limit, the system (9) converges to

$$
\begin{aligned}
\dot{\phi} &= r\phi(1 - \frac{\phi}{k}) - \alpha_1 \phi\varphi - \beta_1 \phi\psi \\
&\quad + \mu_1 \left(\nabla^2\phi + \phi\nabla^2\varphi - \varphi\nabla^2\phi + \phi\nabla^2\psi - \psi\nabla^2\phi \right), \\
\dot{\varphi} &= \alpha_2 \phi\varphi + \theta\phi\psi - b_2 \varphi \\
&\quad + \mu_2 \left(\nabla^2\varphi + \varphi\nabla^2\phi - \phi\nabla^2\varphi + \varphi\nabla^2\psi - \psi\nabla^2\varphi \right), \\
\dot{\psi} &= b_2 \varphi - d_3 \psi \\
&\quad + \mu_3 \left(\nabla^2\psi + \psi\nabla^2\phi - \phi\nabla^2\psi + \psi\nabla^2\varphi - \varphi\nabla^2\psi \right).
\end{aligned}
\tag{10}
$$

The eigenvalues of the associated Jacobian matrix defined by Eq. (B19) in Appendix B give information about whether perturbing the homogeneous solution leads to instability. If each eigenvalue has a negative real part $\operatorname{Re}\left(\lambda_i(q)\right) < 0 \forall q$, $(i = 1, 2, 3)$, the homogeneous state is stable: Every perturbation will eventually die out and no pattern will develop. If, on the other hand, there is an eigenvalue at a nonzero q with a positive real part, then a spatially modulated instability occurs: A perturbation will grow in magnitude, taking the system from the homogeneous state to one with the wave number defined by q. This growth will eventually be saturated by the nonlinear terms leading to a spatial perturbation with a characteristic wave number q. This linear analysis of the homogeneous state is also able to determine whether the resulting wave is steady or oscillatory by looking at the imaginary part of the eigenvalues $\operatorname{Im}\left(\lambda_i(q)\right)$. Steady patterns correspond to $\operatorname{Im}\left(\lambda_i(q)\right) = 0$ for

all unstable modes q, the case in which the instability is called a Turing instability. When $\text{Im}\left(\lambda_i\left(q\right)\right) \neq 0$ for an unstable mode at a nonzero q, the system exhibits a wave instability as the resulting pattern will consist of traveling waves or at the zero q, this condition leads to bifurcation.[27,49] The present study also suggests that the total size of the population can have a relevant effect on the oscillation features. The dispersion relation is shown in Fig. 4. Figure 4(a) shows that adding the migration processes leads the systems to go over three possible dynamics. Region (I), at zero wave number, the eigenvalues are positive and thus are above the threshold $\text{Re}\left(\lambda\left(q=0\right)\right)=0$. The system exhibits a Hopf bifurcation mode. In region II, the real part of the dominant eigenvalues is negative and defined a stable dynamics, with the oscillation frequency defined by $\text{Im}\left(\lambda\left(q\right)\right) \neq 0$. Region III describes damped Turing modes since $\text{Re}\left(\lambda\left(q\right)\right) < 0$ and $\text{Im}\left(\lambda\left(q\right)\right) = 0$ for $q \neq 0$. From region I to II, there is a bifurcation point satisfying the condition $\text{Re}\left(\lambda\left(q\right)\right) = 0$ and $\text{Im}\left(\lambda\left(q\right)\right) \neq 0$ with $q \neq 0$. The latter condition

gives the threshold of the Hopf–Turing bifurcation. These unstable modes occur for the selected parameter values [see Fig. 4(b)]. Unlike the temporal model (6), Hopf-damped Turing bifurcation dynamics occurs for the contagion rate threshold $I_1 = 0.305$. By using the Gillespie algorithm mentioned above and the fully explicit Euler method with a three-point approximation with no-flux boundary conditions, we compare numerically the stochastic model (1)–(4) and (8) and the deterministic model (10). As shown in Fig. 5, the same phenomenon of sustained oscillations and damped oscillations observed above in local dynamics occurs here; from a mathematical perspective, a similar behavior appears in Ref. 6. The discrete version seems to exhibit slower dynamic compared to its continuous analog. These space components also have a large influence on the power spectral density. It is clear that the migration contributions make a significant difference in both spectra since $\alpha_{q,ij} \neq a_{ij}$ and $B_{q,ij} \neq b_{ij}$. The analytic expressions of PSD are obtained by replacing a_{ij} by $\alpha_{q,ij}$ and b_{ij} by $B_{q,ij}$ in Eq. (A11). It is observed that in

FIG. 4. Linear stability analysis showing (a) the complex part (red) and the real part (blue) of the eigenvalues. H: Hopf-bifurcation with $\text{Re}\left(\lambda\left(q\right)\right) > 0$ and $\text{Im}\left(\lambda\left(q\right)\right) > 0$ at $q = 0$, DT: damped Turing with $\text{Re}\left(\lambda\left(q\right)\right) < 0$ and $\text{Im}\left(\lambda\left(q\right)\right) = 0$ at $q \neq 0$. (b) The real part of the eigenvalues for five different values of I_1. (c) Linear stability analysis around the endemic steady state. (d) Linear stability analysis around the free-disease steady state. Using the same parameter values: $\Omega = 500$, $N = 15\,000$, $b_2 = 0.15\Omega$, $d_3 = 0.1\Omega$, $l_1 = 0.31\Omega$, $l_2 = 0.05\Omega$, $d_1 = 0.05\Omega$, $b_1 = 0.25\Omega$, $\mu_1 = 0.6\Omega$, $\mu_2 = 0.4\Omega$, and $\mu_3 = 0.2\Omega$.

FIG. 5. Comparison of the spatiotemporal dynamics of the species density in the stochastic model [panel (b)] with that in the corresponding deterministic approximation [panel (a)] for the line patches defined as a conti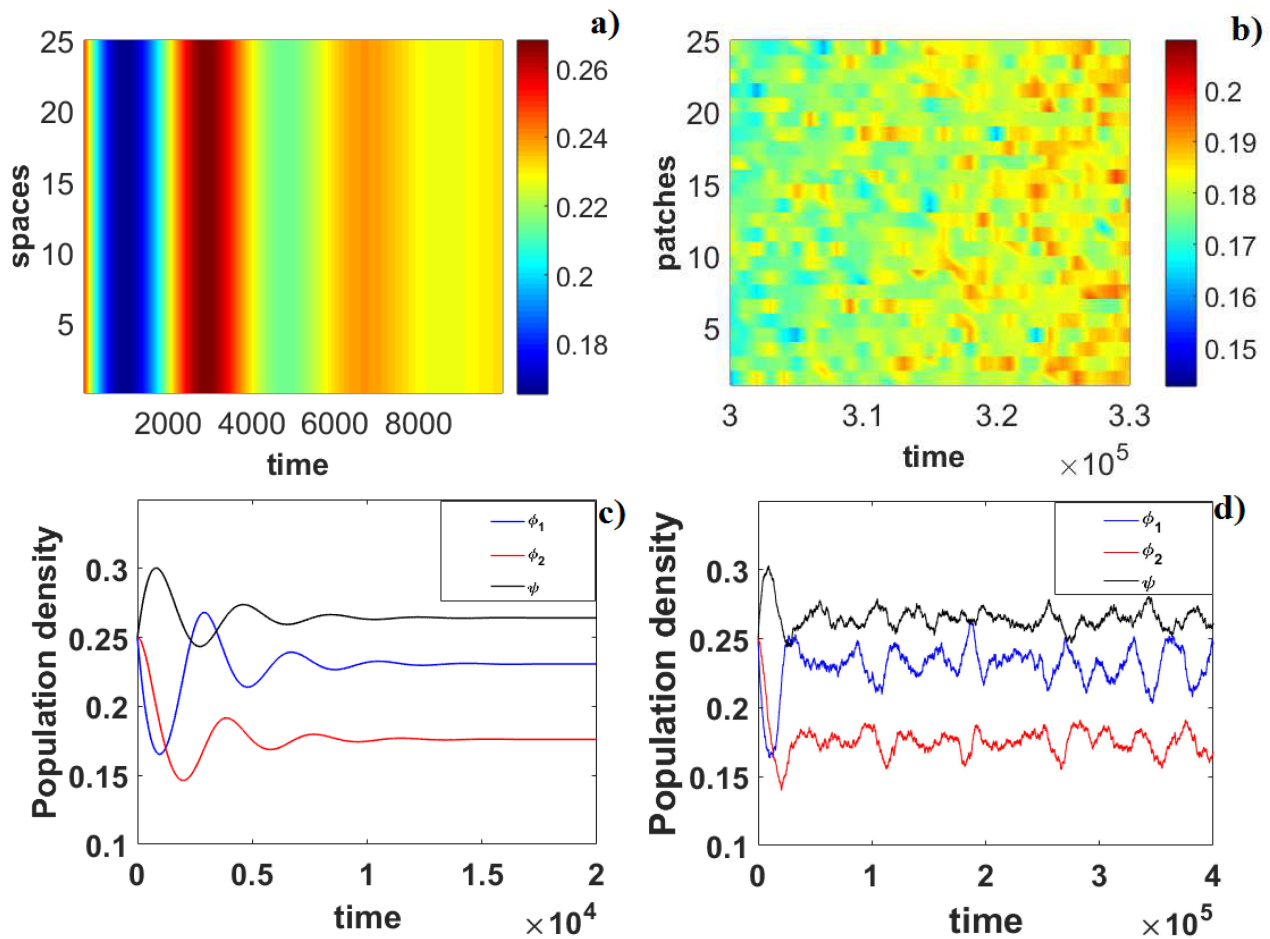nuous space in mean-field approximation. A comparison of the temporal dynamics of the species density in the stochastic model [panel (d)] with that in the corresponding deterministic approximation [panel (c)] at the same selected patch. The uninfected insect pest (ϕ), the infected pest (φ), and the pathogen (ψ) are plotted in green, blue, and red, respectively. The zoomed curves are purposely displayed for highlighting the persistence of oscillations. While the deterministic approximation leads to stabilization, the full stochastic model recovers. The color bar gives the density of infected insects. The capacity and the number of patches were $N = 10\,000$ and $\Omega = 100$. The parameters used in the simulations are $b_2 = 0.15\Omega$, $d_3 = 0.1\Omega$, $l_1 = 0.25\Omega$, $l_2 = 0.05\Omega$, $d_1 = 0.05\Omega$, $b_1 = 0.25\Omega$, $\mu_1 = 0.6\Omega$, $\mu_2 = 0.4\Omega$, and $\mu_3 = 0.2\Omega$.

infected insect pest's spectra especially, there is a large peak at a nonzero value of ω depending on the q-values as shown in Fig. 6. Therefore, resonant behavior still occurs in this spatial model just as it did in the non-spatial case. The more the q increases, the peak increases, although the migration rate differs among all the three species.

The results presented in Figs. 7 and 8 aim to show the effect of the total population size on the power spectra and its spatial distribution, respectively. These figures show the PSD of infected insect pests obtained from direct analytic calculations with $N = 500, 1000, 5000$, and $15\,000$. The population size has an effect on the power spectra in two ways: first, the existence of a spatial amplification and second, when the population size increases, the pathogenic period is shifted to lower central frequencies. This means

that the frequency of the oscillation depends on the total number of individuals.

III. DISCUSSION

This study proposed a model to understand the entomopathogenic fungi outbreak within an insect population. Based on the fact that demographic processes are inherently random, an individual-level model is proposed. The obtained results are compared to its corresponding deterministic model in order to determine the most appropriate or useful approach, which better mimics that the dynamic occurs between species. In addition, because the outbreak of EPF is related to the instability and the persistence of
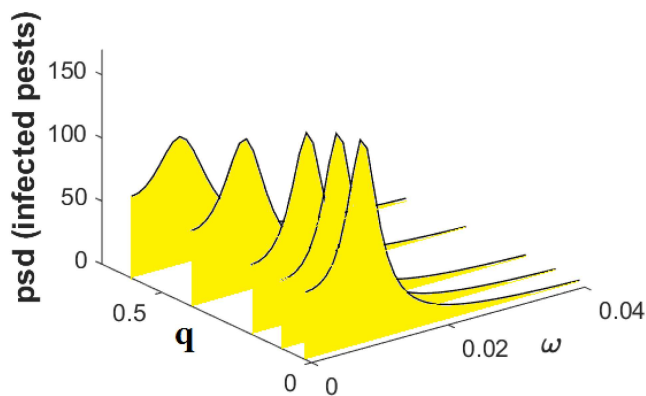
FIG. 6. Theoretical predictions of the power spectral density (PSD) for a system composed of $\Omega = 500$ sites occupied by $N = 15\,000$ species for different size populations using the same parameters values: $b_2 = 0.15\,\Omega$, $d_3 = 0.1\,\Omega$, $l_1 = 0.25\,\Omega$, $l_2 = 0.05\,\Omega$, $d_1 = 0.05\,\Omega$, $b_1 = 0.25\,\Omega$, $\mu_1 = 0.6\,\Omega$, $\mu_2 = 0.4\,\Omega$, and $\mu_3 = 0.2\,\Omega$.

EPF within the insect habitat, stability conditions and the extinction probability are investigated.

A. Non-spatial

Natural population dynamic is controlled by random fluctuations. These fluctuations among individuals within populations are often caused by birth and death events and usually called demographic stochasticity.[50,51] The latter occurs independently among individuals and leads to the population growth in large populations or to reduce in size. Understanding the processes that influence demographic stochasticity and its potential effect of the pathogen is, therefore, important when attempting to explain patterns of extinction of pest and success of the biological control method.

A large body of biological research was devoted to the biological control using EPF to target crop devastators.[3,18] The mechanism identified as most important in this interaction is the contagiousness among pest individuals, which permits propagation of the EPF within the insect population. In order to understand this mechanism, we begin by the investigation of the dynamics between EPF and insect pests in the local patch, followed by the interaction on a larger collection of patches. The approach is totally different from what is found in the literature as majority of studies focused only on either an individual level[3,8–10] or on well-mixed populations.[3,18] Most existing models on the population dynamics of the host–parasitoid or predator–prey include a type II functional response.[52–55] It used experimental data to describe the relationship between the host density and the number of host attacked per natural enemy per unit of time and showed that the parasitoid/pathogen does not really create a stable pest's enemy equilibrium during the growing season of a crop, but that it suppresses the insect population and subsequently prevent the pest from causing yield losses.[3,8–10,52] However, the same phenomena are observed here without any functional response. A number of models described

how insects and their fungal pathogens could be used in a framework to exploring metapopulation theory;[15] in addition, they lack realism because all ecological and biological phenomena are inherently random.[4,19,56] The challenge in modeling the complexity of fungal entomopathogens in populations of insects is thoroughly discussed in Ref. 15; these authors emphasize that the heterogeneity of individuals should be incorporated; they further demonstrated that the explicit consideration of stochastic demography is crucial. In order to provide a framework for evaluating different ensembles of life history and demographic properties favoring the success of biological control based EPF, the present study complements experimental and theoretical approaches through the use and application of an individual-level model (ILM). The model assumed that insect hosts do not acquire immunity to their pathogens and, therefore, do not include a resistant class of hosts immune to further infection,[15] the insect is also assumed to be infected only by a single spore, and multiple infections are not considered in this model.

By comparing the IBM and its corresponding population level model (PLM), it is observed that most of the existing models for EPF–pest interactions are mean-fields and they failed to adequately capture the resilience and oscillation sustainability of the pathogenesis without any external reservoir.[13,57–59] Our analytical results pertain to self-maintenance of species (pest and the pathogen population) dynamics in the absence of seasonality, thus reflecting the role of individual (discrete) behaviors of EPF in regulating the population of insect's pests and vice versa.

In previous studies, external infectious stages ensured that the fungi persist during periods of low host population density when the horizontal transmission is insufficient to maintain the prevalence in the host population.[15] It was hypothesized that EPF could potentially regulate and cause cycles in each species,[15] which corroborates the quasi-cycle persistence predicted by our model. By assuming that natural selections drive the rates of transmission through altered host susceptibility,[60–63] it was found that stochasticity induces cycles even at a high rate of heterogeneity during transmission. By considering natural selection as a pure demographic stochasticity, we were able to characterize the quasi-cycle amplitudes and the frequency distribution, which is not the case in the literature.[60–63] It was demonstrated that the control ability of EPF is strongly dependent on the average number of secondary infections produced by a single infectious unit of EPF (conidia).[3] With the aim to maintain R_0 greater than one, a sensitivity analysis is performed in order to determine which parameters can make the basic reproductive number growth. We also assess the relative importance of different factors responsible for pests and EPF growth to better determine how to reduce the harmfulness of insect devastator. In contrast to the present study, the basic reproduction number reported in previous epidemiological research studies describing insect-EPF dynamics but did not highlight the relevance on the degree self-limitation of the susceptible insects on the proportion of spores entering the inactive stage and their important effects on EPF invasion.[12,14] If the population grows according to a birth and death process, then BC agents might survive forever and the number of spores increases at a slower speed than the population does; therefore, the fraction of the infected individuals goes to zero.[48] It is also possible that the pest population and
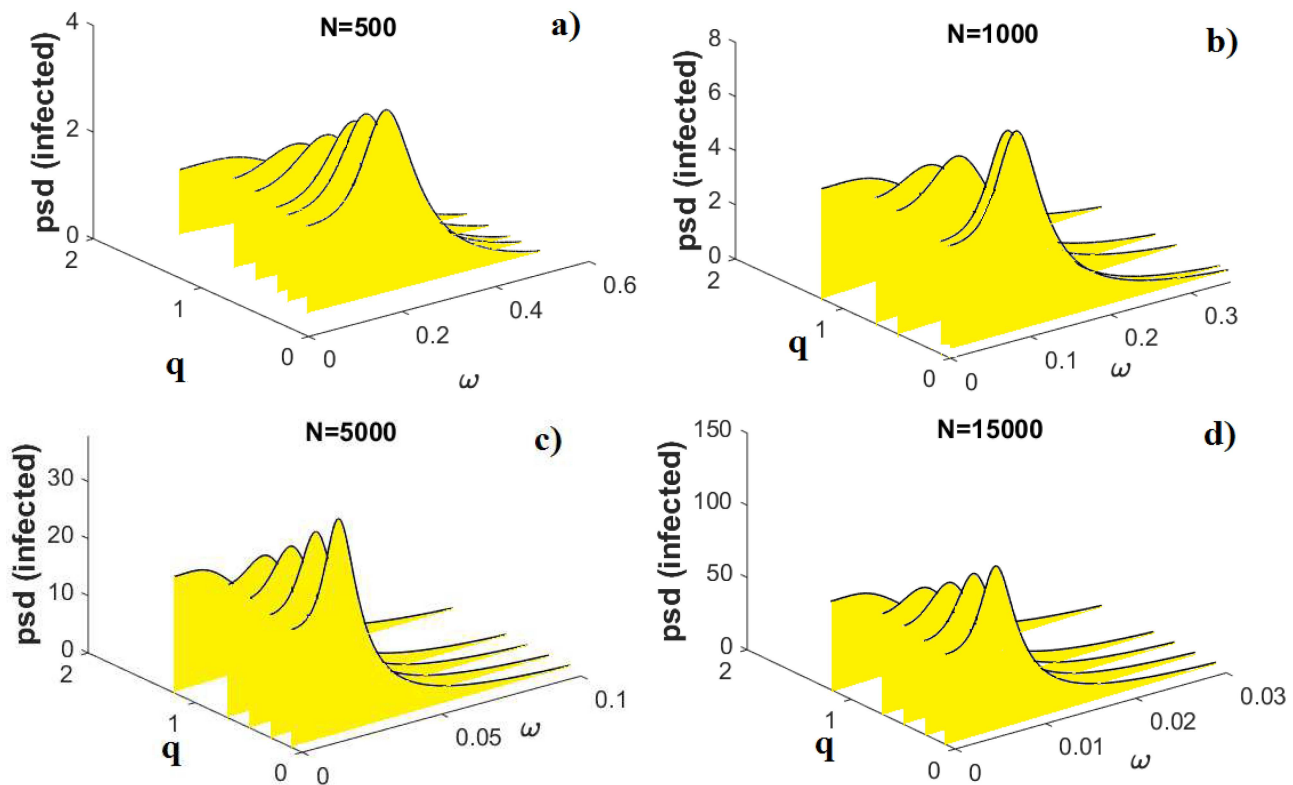
FIG. 7. Theoretical predictions of the power spectral density (PSD) for a system composed of $\Omega = 500$ sites occupied by (a) $N = 500$, (b) $N = 1000$, (c) $N = 5000$, and (d) $N = 15\,000$ species for different size populations using the same parameter values: $b_2 = 0.15\Omega$, $d_3 = 0.1\Omega$, $l_1 = 0.25\Omega$, $l_2 = 0.05\Omega$, $d_1 = 0.05\Omega$, $b_1 = 0.25\Omega$, $\mu_1 = 0.6\Omega$, $\mu_2 = 0.4\Omega$, and $\mu_3 = 0.2\Omega$.

conidia reach equilibrium and the fraction of infectious individuals converges to a constant as defined by BC. However, although EPF may suppress a pest below its carrying capacity, most systems could show prolonged oscillations.[48] The fraction of the susceptible insect exposed is contaminated by infected insects; therefore, the contagious event is primordial.[58] Therefore, in this study where the desired result is to obtain an important number of infected pests for a successful BC (increase in the basic reproductive number), the suggested strategy must be to increase the carrying capacity and apply the EPF in a large area to optimize the chance for infecting a large number of insect pest host. Some models are proposed to investigate this density dependence and spatial pattern dynamics of EPF[57] and to investigate the spread of infections through dispersion of conidia by considering the behavior of susceptible and infected host.[41,58,64] The potential of fungi to regulate insect populations will depend on their abundance in the host population (prevalence) as well as their abundance and persistence in the surrounding environment.[3,15] Because this abundance is strongly controlled by the contagion phenomenon, another suggested strategy would be to develop a control method by increasing the host individual to get the propensity of having more physical contacts.

However, one of the most powerful tools for analyzing such oscillations is the power spectrum. This determines how the periodicity of the stochastic system that makes up the time series is distributed. We derived the PSD of the fluctuations around an equilibrium using a large N expansion method due to Van Kampen.

In the case where the pest was not influenced by any external regulation, pathogens could be responsible for population cycles.[15,61] However, the largely sustained oscillations, which replace the deterministic predictions of damped oscillation behavior, have a single preferred frequency at which resonant stochasticity occurs.

The results obtained show that coexistence or extinction probabilities of species can have a complex relationship when spreading parameters are varied. It is demonstrated that the extinction probability of the host is strongly susceptible to be amplified by the death rate of the insect pest during the infectious period. Furthermore, the proportion of spores entering an inactivated stage reduces the number of susceptible hosts by their potential to survive in the soil and on the dormant or mummified pest.[65] These spores control the persistence of BC by their ability to be reactivated and alternatively infect hosts, and produce another conidium.[3] Unfortunately, EPF takes a lot of time to suppress pest populations, whereas chemical pesticides provide immediate results.[40] Moreover, this BC agent is used to
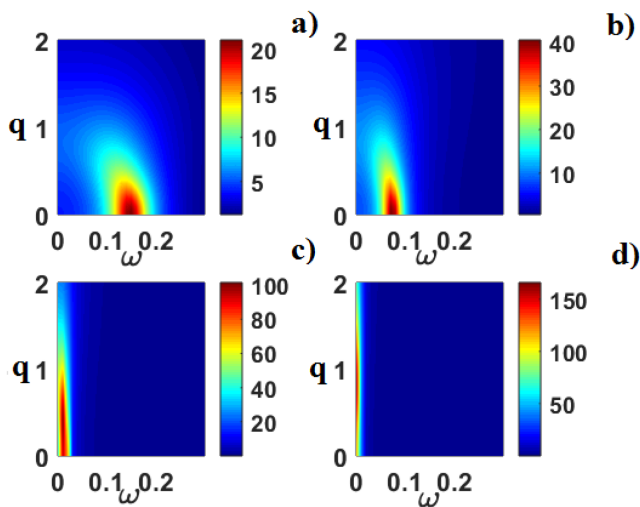
FIG. 8. Spatial distributions of the power spectral density (PSD) for a system composed of $\Omega = 500$ sites occupied by (a) $N = 500$, (b) $N = 1000$, (c) $N = 5000$, and (d) $N = 15\,000$ species for different size populations using the same parameter values: $b_2 = 0.15\Omega$, $d_3 = 0.1\Omega$, $l_1 = 0.25\Omega$, $l_2 = 0.05\Omega$, $d_1 = 0.05\Omega$, $b_1 = 0.25\Omega$, $\mu_1 = 0.6\Omega$, $\mu_2 = 0.4\Omega$, and $\mu_3 = 0.2\Omega$.

reduce the population density but not often gives rise to total extinction. Another limit is that sometimes it needs to be sprayed more than one time in the field.[2]

B. Spatial

Entomopathogenic fungi are relatively immobile compared to hosts but could be migrated by water, wind, rain, and so on; thus, any spatial refuge may be vital in allowing hosts to escape parasitism.[15] Therefore, populations may regularly pass through a series of localized extinctions and re-colonize from neighboring populations, which show that increasing the spatial wavelength of perturbation gives rise to the large possible oscillation frequency that increases the maximal infectious period. In order to illustrate the role of the nonlocal interaction term, the temporal evolution of each species is computed at a single patch for the stochastic and determinist approach; this model verifies as assumed in our previous study that a nonlinear diffusion is well appropriate to describe biological systems.[66] It is observed that the diffusion coefficient system starts to exhibit Hopf modes when increasing the contagions rate. The phenomenon of sustained oscillations observed in the stochastic approach remains when patches interact. Many researchers compared the stochastic model and the deterministic analog in spatiotemporal dynamics and show in a certain case that the deterministic system predicts an extinction;[6] here, it is observed that the discrete behavior slows evolution of dynamics and predicts self-maintained oscillations.

Reilly and Elderd[63] showed that depending on the threshold of the insect population size and the amount of biocontrol, the system may display large-amplitude cycles, steady states, or a range of intermediate behaviors. The present study further complements

previous results by illustrating that an increase of the possibility of having a contact between host populations reduces the width of the PSD and consequently extends the infection period leading the EPF to persist for large periods. The interest in this result stems from observed epidemic oscillations in EPF and insect pests. Despite sustained oscillations could be produced in deterministic models by introducing various complications (external seasonal forcing or nonlinear dissipation, for instance), in contrast to what is reported in the literature on insect pest BC interactions,[60–63] here, it is shown that cycles result from the coherence between random variations and damped oscillations.[46] The oscillations of the stochastic model presented here have a frequency distribution, evidenced by the power spectral density of the process of infective and stochastically varying amplitude. This phenomenon, in which random fluctuations sustain nearly periodic oscillations in a system that has a stable constant equilibrium in the deterministic limit, has been called coherence resonance or autonomous stochastic resonance.[24]

From a numerical study, we can understand that the mobility of the species within their habitat increases the possibility of disease transmission by leading to a rich behavior. When increasing the infection rate, the magnitude of the onset of instability through Hopf bifurcation increases. In addition, stability analysis around the trivial equilibrium, for example, shows that the species migration has a stabilizing effect on the system dynamics.

A wide spectrum of theoretical models describing the fungal dispersal and/or outbreaks within a given host insect population based on the mechanism of reaction and reaction–diffusion has been proposed.[57,58,61,62] They concluded that diffusion of species between habitats ensures the spread of the disease and could potentially lead to insect's extinction, which is translated mathematically by the instability of the pest–pathogen interaction.[39] However, many studies proved that the presence of diffusion is sufficient to induce a rich dynamics through Hopf bifurcation, Turing patterns, and Turing–Hopf bifurcation.[28–35,66] Furthermore, the underlying dynamics has been well applied in the context of population dynamics of predator–prey models[28–35] and intra-host growth of entomopathogenic fungi.[66] A rough analogy with these research studies shows that Hopf bifurcation, Turing instability, and Turing–Hopf bifurcation promise good description of the EPF outbreaks within a pest population. However, our analysis shows a transcritical bifurcation for local dynamics and a Hopf-damped Turing bifurcation in a spatial case. Similar results have been obtained in the predator–prey model[34,35] and in the Brusselator model describing the competition of two chemical species in a chemical reaction.[67] To the best of our knowledge, this specific bifurcation has not yet been obtained from an individual-based model, particularly in biological control (BC).

IV. CONCLUSION

A model describing biological control developed in order to understand the EPF persistence mechanism in a pest's population by taking into consideration the carrying capacity and the random variation of the demographic parameter is proposed. A similar approach has been applied in the predator–prey system and in nonlocal models in other areas, such as epidemic spread or social dynamics, and the authors obtained no Turing patterns and stochastic Turing patterns, respectively.[23,27] Here, using the same approach in epidemic

spread, the deterministic spatial system exhibits Hopf-damped Turing bifurcation when increasing the infection parameters, whereas the local dynamics exhibits transcritical bifurcation at the threshold of the number of secondary infection. However, the optimal control strategy depends on the success of establishing more contact between the host and the relationship between the inoculum size and the probability of spore entering in a resting stage. The model predicted the existence of multiple endemic equilibria when the basic reproduction number is greater than unity. The present study leads us to conclude that R_0 should be maintained above this threshold to guarantee fungi invasion into the insect host population. The cost-effective strategy for performing the spread of the infection unit is also determined. By the application of Van Kampen approximation, the deterministic analysis of the proposed model is performed. It allowed examining the period of the cycle occurrence in the biological system by the power spectrum in both non-spatial and spatial considerations. Four control variables to be handled in order to maximize the number of infected hosts and the total number of pathogen unit population are (1) carrying capacity on the host population, (2) the number of uninfected, which could be contaminated by infected pests, (3) the number of pest death, and (4) the number of resting conidia.

APPENDIX A: LOCAL MODEL

1. Mean-field theory

At the beginning of this appendix, details of the mean-field versions of the stochastic models are given. In the second part, the stability analysis of the equilibrium state is derived from the deterministic model. The details of the calculation of the power spectral density are from a stochastic Fokker–Planck equation.[5,22] The master equation that completely defined the time evolution of the non-spatial system is given by

$$\frac{dP(n,m,l,t)}{dt} = T\left(n,m,l|n-1,m+1,l\right) P(n-1,m+1,l,t)$$
$$+ T\left(n,m,l|n-1,m,l\right) P(n-1,m,l,t)$$
$$+ T\left(n,m,l|n+1,m,l\right) P(n+1,m,l,t)$$
$$+ T\left(n,m,l|n,m-1,l+1\right) P(n,m-1,l+1,t)$$
$$+ T\left(n,m,l|n,m,l-1\right) P(n,m,l-1,t)$$
$$- [T\left(n-1,m+1,l|n,m,l\right) + T\left(n-1,m,l|n,m,l\right)$$
$$+ T\left(n+1,m,l|n,m,l\right) + T\left(n,m-1,l+1|n,m,l\right)$$
$$+ T\left(n,m,l-1|n,m,l\right)]P(n,m,l,t), \tag{A1}$$

using step operators $\varepsilon_x^{\pm 1}, \varepsilon_y^{\pm 1}$, and $\varepsilon_z^{\pm 1}$ defined in function of n, m, and l such that

$$\varepsilon_x^{\pm 1} f(n,m,l) = f(n \pm 1, m, l),$$
$$\varepsilon_y^{\pm 1} f(n,m,l) = f(n, m \pm 1, l), \tag{A2}$$
$$\varepsilon_z^{\pm 1} f(n,m,l) = f(n, m, l \pm 1).$$

Equation (A1) can be rewritten as follows:

$$\frac{dP(n,m,l,t)}{dt} = \left(\left(\varepsilon_x \varepsilon_y^{-1} - 1\right) T\left(n-1, m+1, l|n,m,l\right)\right.$$
$$+ (\varepsilon_x - 1) T\left(n-1, m, l|n,m,l\right)$$
$$+ \left(\varepsilon_x^{-1} - 1\right) T\left(n+1, m, l|n,m,l\right)$$
$$+ \left(\varepsilon_y \varepsilon_z^{-1} - 1\right) T\left(n, m-1, l+1|n,m,l\right)$$
$$\left. + (\varepsilon_z - 1) T\left(n, m, l-1|n,m,l\right)\right) P(n,m,l,t). \tag{A3}$$

By transforming stochastic variables $\sigma = (n,m,l)$ to a new stochastic variable $\zeta = (\xi, \eta, \vartheta)$, we found that

$$n = N\phi(t) + N^{1/2}\xi,$$
$$m = N\varphi(t) + N^{1/2}\eta, \tag{A4}$$
$$l = N\psi(t) + N^{1/2}\vartheta.$$

The probability distribution function defined by $P(n,m,l,t) = \Pi(\xi, \eta, \vartheta, t)$ is written as

$$\frac{dP}{dt} = \frac{\partial \Pi}{\partial t} - N^{1/2}\frac{d\phi}{dt}\frac{\partial \Pi}{\partial \xi} - N^{1/2}\frac{d\varphi}{dt}\frac{\partial \Pi}{\partial \eta} - N^{1/2}\frac{d\psi}{dt}\frac{\partial \Pi}{\partial \vartheta}, \tag{A5}$$

with $\phi = \lim_{N\to\infty} n/N, \varphi = \lim_{N\to\infty} m/N, and \psi = \lim_{N\to\infty} l/N$. The step operators defined in Eq. (A2) in terms of involving the new variables are given by

$$\varepsilon_x^{\pm 1} = 1 \pm N^{-1/2}\frac{\partial}{\partial \xi} + \frac{1}{2}N^{-1}\frac{\partial^2}{\partial \xi^2} + \cdots,$$

$$\varepsilon_y^{\pm 1} = 1 \pm N^{-1/2}\frac{\partial}{\partial \eta} + \frac{1}{2}N^{-1}\frac{\partial^2}{\partial \eta^2} + \cdots,$$

$$\varepsilon_z^{\pm 1} = 1 \pm N^{-1/2}\frac{\partial}{\partial \vartheta} + \frac{1}{2}N^{-1}\frac{\partial^2}{\partial \vartheta^2} + \cdots,$$

$$\varepsilon_x \varepsilon_y^{-1} = 1 + N^{-1/2}\left(\frac{\partial}{\partial \xi} - \frac{\partial}{\partial \eta}\right) + \frac{1}{2}N^{-1}\left(\frac{\partial}{\partial \xi} - \frac{\partial}{\partial \eta}\right)^2 + \cdots,$$

$$\varepsilon_y \varepsilon_z^{-1} = 1 + N^{-1/2}\left(\frac{\partial}{\partial \eta} - \frac{\partial}{\partial \vartheta}\right) + \frac{1}{2}N^{-1}\left(\frac{\partial}{\partial \eta} - \frac{\partial}{\partial \vartheta}\right)^2 + \cdots. \tag{A6}$$

Replacing these expressions and transition rates in Eq. (A3), the following list with given contributions at the order of N^0 and N^2 is obtained:

1. $\left(\varepsilon_x \varepsilon_y^{-1} - 1\right) \left(\frac{2I_1 nm}{N} + \frac{2I_2 nl}{N}\right),$
   $N^0 : (I_1\phi\varphi + I_2\phi\psi) \frac{\partial^2}{\partial \xi^2}, (I_1\phi\varphi + I_2\phi\psi) \frac{\partial^2}{\partial \eta^2},$
   $-2 (I_1\phi\varphi + I_2\phi\psi) \frac{\partial^2}{\partial \xi \partial \eta}, 2I_1\phi\frac{\partial}{\partial \xi}\eta, -2I_1\phi\frac{\partial}{\partial \eta}\eta,$

$(2I_1\varphi + 2I_2\psi)\frac{\partial}{\partial\xi}\xi, -(2I_1\varphi + 2I_2\psi)\frac{\partial}{\partial\eta}\xi, 2I_2\phi\frac{\partial}{\partial\xi}\vartheta$,
$-2I_2\phi\frac{\partial}{\partial\eta}\vartheta$.
$N^{1/2} : 2(I_1\phi\varphi + I_2\phi\psi)\frac{\partial}{\partial\xi}\xi, -2(I_1\phi\varphi + I_2\phi\psi)\frac{\partial}{\partial\eta}$.

2. $(\varepsilon_x - 1)d_1 n$,
$N^0 : d_1\frac{\partial}{\partial\xi}\xi, \frac{d_1}{2}\phi\frac{\partial^2}{\partial\xi^2}$,
$N^{1/2} : d_1\phi\frac{\partial}{\partial\xi}$.

3. $(\varepsilon_z - 1)d_3 l$,
$N^0 : d_3\frac{\partial}{\partial\vartheta}\vartheta, \frac{d_3}{2}\psi\frac{\partial^2}{\partial\vartheta^2}$,
$N^{1/2} : d_3\psi\frac{\partial}{\partial\vartheta}$.

4. $(\varepsilon_x^{-1} - 1)2b_1\frac{n}{N}(N - n - m - l)$,
$N^0 : 2b_1\phi\frac{\partial}{\partial\xi}\xi, 2b_1\phi\frac{\partial}{\partial\xi}\eta, 2b_1\phi\frac{\partial}{\partial\xi}\vartheta$,
$-2b_1(1 - \phi - \varphi - \psi)\frac{\partial}{\partial\xi}\xi, b_1\phi(1 - \phi - \varphi - \psi)\frac{\partial^2}{\partial\xi^2}$,
$N^{1/2} : -2b_1\phi(1 - \phi - \varphi - \psi)\frac{\partial}{\partial\xi}$.

5. $((\varepsilon_y\varepsilon_z^{-1} - 1)b_2 m$,
$N^0 : b_2\varphi\frac{\partial^2}{\partial\eta^2}, b_2\varphi\frac{\partial^2}{\partial\vartheta^2}, -2b_2\varphi\frac{\partial^2}{\partial\vartheta\partial\eta}$,
$b_2\frac{\partial}{\partial\eta}\eta, -b_2\frac{\partial}{\partial\vartheta}\eta$,
$N^{1/2} : b_2\varphi\frac{\partial}{\partial\eta}, -b_2\varphi\frac{\partial}{\partial\vartheta}$.

Substituting these terms in Eq. (A3) and identifying the terms of order $N^{1/2}$ on the resulting equation to Eq. (A5), we obtained the macroscopic equation given by Eq. (6). The terms of order N^0 lead to a Fokker–Planck equation for fluctuation variables $\zeta = (\xi, \eta, \vartheta)$,

$$\frac{\partial\Pi}{\partial t} = -\sum_{i,j=1}^{3} a_{ij}\frac{\partial(\zeta_j\Pi)}{\partial\zeta_i} + \frac{1}{2}\sum_{i,j=1}^{3} b_{ij}\frac{\partial^2\Pi}{\partial\zeta_i\partial\zeta_j}; \qquad (A7)$$

the coefficients a_{ij} and b_{ij} are given by

$$\begin{aligned}
a_{11} &= -2b_1\phi^s - d_1 + 2b_1(1 - \phi^s - \varphi^s - \psi^s) \\
&\quad - (2I_1\varphi^s + 2I_2\psi^s), \\
a_{12} &= -2(b_1 + I_1)\phi^s, a_{13} = -2(b_1 + I_2)\phi^s, \\
a_{21} &= 2(I_1\varphi^s + I_2\psi^s), a_{22} = (-b_2 + 2I_1\phi^s), \\
a_{23} &= 2I_2\phi^s, a_{31} = 0, a_{32} = b_2, a_{33} = -d_3, \\
b_{11} &= 2I_1\phi^s\varphi^s + 2I_2\phi^s\psi^s + d_1\phi^s \\
&\quad + 2b_1\phi^s(1 - \phi^s - \varphi^s - \psi^s), b_{23} = -2b_2\varphi^s, \\
b_{22} &= 2I_1\phi^s\varphi^s + 2I_2\phi^s\psi^s + 2b_2\varphi^s, \\
b_{33} &= 2b_2\varphi^s + d_3\psi^s, \\
b_{12} &= -4I_1\phi^s\varphi^s - 4I_2\phi^s\psi^s
\end{aligned} \qquad (A8)$$

at the non-trivial steady state.

2. The basic reproduction number

According to previous research studies, there exist many analytical methods for evaluating the basic reproduction number such as the next generation method,[5,68] the survival function,[68] the eigenvalues of the Jacobian matrix around the free-disease equilibrium,[5,68] the constant term of the characteristic polynomial of the free-disease equilibrium,[68] the existence of the endemic equilibrium,[68–70] the number of susceptible at the endemic steady state, the average age

of infection, the final size equation, and the intrinsic growth rate.[25] In this study, we have used the existence of the endemic equilibrium method. However, the same results can be obtained when using the constant term of the characteristic polynomial around the free-disease equilibrium and the average lifetime. By using the latter method, the basic reproduction number can be decomposed as follows:

$$R_0 = R_0^{in\sec ts} + R_0^{spores}, \qquad (A9)$$

where $R_0^{in\sec ts}$ is the number of secondary infections from an infected insect and R_0^{spores} corresponds to the number of secondary infections caused by a single spore. The average number of insects that can be infected by a single infected insect during its life period $(1/b_2)$ is $\alpha_2 k$. Therefore, a single infected insect will give rise to an average $R_0^{in\sec ts} = \alpha_2 k/b_2$. Similarly, a new generated spore will give rise to average new infections $R_0^{spores} = \theta k/d_3$ during its life period $(1/d_3)$ time units. By adding both expressions, we obtained

$$R_0 = \frac{k(\alpha_2 d_3 + \theta b_2)}{b_2 d_3}. \qquad (A10)$$

3. Stability and bifurcation analysis of the equilibrium state

System (6) has to be analyzed with the set of initial conditions $\phi > 0$, $\varphi > 0$, and $\psi > 0$. This systems possesses three different equilibrium points: (i) $E^0 = (\phi = 0, \varphi = 0, \psi = 0)$ species free equilibrium, (ii) $E^1 = (\phi = k, \varphi = 0, \psi = 0)$ infected insects and spores free equilibrium, and (iii) the coexistence equilibrium of the pest, the infected insect, and the uninfected insect $E^{SIC} = (\phi^s, \varphi^s, \psi^s)$, which has a biological relevance if and only if $k(\theta b_2 + \alpha_2 d_3) - b_2 d_3 > 0$. This biological relevance condition is thus giving the threshold for the basic reproduction number defined as the expected number of secondary infections caused by a single infection such that $R_0 - 1 > 0$ where R_0 is defined by Eq. (A9) Therefore, the equilibrium E^{SIC} can be rewritten as $\phi^s = \frac{k}{R_0}$, $\varphi^s = \frac{d_3 r(R_0-1)}{R_0(\alpha_1 d_3 + b_2\beta_1)}, \psi^s = \frac{b_2 r(R_0-1)}{R_0(\alpha_1 d_3 + b_2\beta_1)}$.

- The species free equilibrium point E^0: The Jacobian matrix is a triangular matrix with eigenvalues $(r, -d_3, -b_2)$. Because $(r > 0, d_3 > 0, b_2 > 0)$, E^0 is always a saddle point; therefore, its stability does not change.
- The infected insects and conidia free equilibrium E^s: This point is stable if and only if $0 < -r(k\theta b_2 + k\alpha_2 d_3 - b_2 d_3), 0 < -k\alpha_2 + b_2 + d_3 + r$, and $0 < -r(k\alpha_2 - b_2 - d_3) - k\theta b_2 - k\alpha_2 d_3 + b_2 d_3 + r(k\theta b_2 + k\alpha_2 d_3 - b_2 d_3)/(-k\alpha_2 + b_2 + d_3 + r)$, or we restrict the analysis here to the case where $0 < (k\theta b_2 + k\alpha_2 d_3 - b_2 d_3)$ $(R_0 > 1)$ holds true in condition to the property that all parameter values are positive. Because $r > 0$, the first condition cannot be satisfied, and then, E^s is also a saddle point for the three dimensional equilibrium point. However, the characteristic polynomial obtained from the Jacobian matrix around the free-disease steady state is a cubic polynomial with coefficient $1, A, B, C$, where $A = -k\alpha_2 + b_2 + d_3 + r, B = (A - r)r - (R_0 - 1), and C = -(R_0 - 1)rb_2 d_3$. Therefore, for $C = 0$ meaning that $R_0 = 1$, the system exhibits transcritical bifurcation and is stable for $R_0 < 1$.

- The epidemic equilibrium: the characteristic polynomial obtained from the Jacobian matrix around the endemic steady state is a cubic polynomial with coefficient $1, A, B, C$. Therefore, for $A > 0$, $B > 0$, and $C > 0$ for $R_0 > 1$, the steady state exists. Thus, the polynomial equation has no root, which is positive or zero (Descartes' rule of sign). This equation will only have negative roots or complex roots with a negative real part if and only if $AB - C > 0$ according to the Routh–Hurwitz criteria. Thus, the system is stable about the infectious equilibrium point E^{SIC} whenever it exists and $AB - C > 0$ (under the condition, we plot to obtain the stability diagram), with $A = d_3 + \frac{k\theta b_2 + d_3 r}{d_3 R_0} > 0$ for $R_0 > 1$, $B = \frac{r}{R_0}\left(\frac{\alpha_1 b_2 d_3 (R_0 - 1)}{\alpha_1 d_3 + b_2 \beta_1} - \frac{b_2 d_3 \alpha_2}{\theta b_2 + \alpha_2 d_3} + b_2 + d_3\right)$, and $C = \frac{r b_2 d_3 (R_0 - 1)}{R_0}$ for $R_0 > 1$. If $C = 0$, thus, $R_0 = 1$; the system exhibits transcritical bifurcation and is stable for $R_0 > 1$ in addition to $AB - C > 0$.

4. Power spectral analysis

The power spectra of the fluctuations in the neighborhood of the equilibrium state are evaluated from the temporal Fourier transform of the Langevin equation, which describes fluently the stochastic behavior of the system.[5,22,23] The latter corresponding to the Fokker–Planck equation [Eq. (A7)] is

$$\frac{d\zeta_i}{dt} = \sum_{j=1}^{3} a_{ij}\zeta_j + \lambda_i(t), \ (i, j = 1, 2, 3), \quad \text{(A11)}$$

where $\zeta_i \ (i = 1, 2, 3)$ denotes the random deviation of the system from the mean fields and $\lambda_i(t) \ (i = 1, 2, 3)$ is the Gaussian white noise with zero mean and a correlation function given by $\langle \lambda_i(t)\lambda_j(t')\rangle = b_{ij}\delta(t - t')$. Taking the temporal Fourier transform $\tilde{\zeta}_i(\omega) = \int_{-\infty}^{+\infty} e^{-i\omega t}\zeta_i(t)\,dt$ of Eq. (A11) leads to

$$-i\omega\tilde{\zeta}_i(\omega) = \sum_{j=1}^{3} a_{ij}\tilde{\zeta}_j(\omega) + \tilde{\lambda}_i(\omega), \quad \text{(A12)}$$

with $\left\langle\tilde{\lambda}_i(\omega)\tilde{\lambda}_j(\omega')\right\rangle = b_{ij}(2\pi)\delta(\omega + \omega')$. The obtained system corresponds now to three coupled linear algebraic equations, which can be used to derive a closed form expression for the power spectra. Therefore, by solving equation [Eq. (A11)], we obtain $\tilde{\xi}(\omega) = ((a_{23}a_{32} - a_{22}a_{33})\tilde{\lambda}_1 + (a_{12}a_{33} - a_{13}a_{32})\tilde{\lambda}_2 + (a_{13}a_{22} - a_{12}a_{23})\tilde{\lambda}_3 + \tilde{\lambda}_1\omega^2 + i\omega\left(-(a_{33} + a_{22})\tilde{\lambda}_1 + \tilde{\lambda}_2 a_{12} + \tilde{\lambda}_3 a_{13}\right))/D(\omega)$, $\tilde{\eta}(\omega) = ((a_{21}a_{33} - a_{23}a_{31})\tilde{\lambda}_1 + (a_{31}a_{13} - a_{11}a_{33})\tilde{\lambda}_2 + (a_{11}a_{23} - a_{13}a_{21})\tilde{\lambda}_3 + \tilde{\lambda}_2\omega^2 + i\omega\left(a_{21}\tilde{\lambda}_1 - (a_{11} + a_{33})\tilde{\lambda}_2 + \tilde{\lambda}_3 a_{23}\right))/D(\omega)$, $\tilde{\vartheta}(\omega) = ((a_{22}a_{31} - a_{21}a_{32})\tilde{\lambda}_1 + (a_{32}a_{11} - a_{12}a_{31})\tilde{\lambda}_2 + (a_{12}a_{21} - a_{11}a_{22})\tilde{\lambda}_3 + \tilde{\lambda}_3\omega^2 + i\omega\left(a_{31}\tilde{\lambda}_1 + a_{32}\tilde{\lambda}_2 - (a_{11} + a_{22})\tilde{\lambda}_3\right))/D(\omega)$, where the denominator is given by $D(\omega) = (i\omega)^3 + tr\mathbf{a}(i\omega)^2 + \Theta(i\omega) + \det\mathbf{a}$, with $tr\mathbf{a} = a_{11} + a_{22} + a_{33}$, $\Theta = a_{11}a_{22} + a_{11}a_{33} - a_{12}a_{21} + a_{22}a_{33} - a_{23}a_{32} - a_{13}a_{31}$, and $\det\mathbf{a} = a_{11}a_{22}a_{33} - a_{11}a_{23}a_{32} - a_{12}a_{21}a_{33} + a_{13}a_{21}a_{32} + a_{31}a_{12}a_{23} - a_{13}a_{22}a_{31}$. We recall that the power spectra correspond to the squared moduli average $\tilde{\zeta}_i(\omega)$. Using the expression $\left\langle\tilde{\lambda}_i(\omega)\tilde{\lambda}_j(\omega')\right\rangle$

$= b_{ij}(2\pi)\delta(\omega + \omega')$, we obtained

$$P_\phi(\omega) = \left\langle|\xi(\omega)|^2\right\rangle = \frac{b_{11}\omega^4 + \Gamma_\phi\omega^2 + \kappa_\phi}{|D(\omega)|^2},$$

$$P_\varphi(\omega) = \left\langle|\eta(\omega)|^2\right\rangle = \frac{b_{22}\omega^4 + \Gamma_\varphi\omega^2 + \kappa_\varphi}{|D(\omega)|^2}, \quad \text{(A13)}$$

and

$$P_\psi(\omega) = \left\langle|\vartheta(\omega)|^2\right\rangle = \frac{b_{33}\omega^4 + \Gamma_\psi\omega^2 + \kappa_\psi}{|D(\omega)|^2},$$

where

$$|D(\omega)|^2 = \left(\omega^3 - \Theta\omega\right)^2 + \left(\det\mathbf{a} - tr\mathbf{a}\omega^2\right)^2,$$

$$\Gamma_\phi = a_{12}{}^2 b_{22} + 2a_{12}a_{13}b_{23} - 2a_{12}a_{22}b_{12} - 2a_{13}a_{32}b_{12}$$
$$\quad - 2a_{12}a_{23}b_{13} + a_{13}{}^2 b_{33} - 2a_{13}a_{33}b_{13} + a_{22}{}^2 b_{11}$$
$$\quad + 2a_{23}a_{32}b_{11} + a_{33}{}^2 b_{11},$$

$$\kappa_\phi = a_{12}{}^2 a_{23}{}^2 b_{33} - 2a_{12}{}^2 a_{23}a_{33}b_{23} + a_{12}{}^2 a_{33}{}^2 b_{22}$$
$$\quad - 2a_{12}a_{13}a_{22}a_{23}b_{33} + 2a_{12}a_{13}a_{22}a_{33}b_{23}$$
$$\quad + 2a_{12}a_{13}a_{23}a_{32}b_{23} - 2a_{12}a_{13}a_{32}a_{33}b_{22}$$
$$\quad + 2a_{12}a_{22}a_{23}a_{33}b_{13} - 2a_{12}a_{22}a_{33}{}^2 b_{12}$$
$$\quad - 2a_{12}a_{23}{}^2 a_{32}b_{13} + 2a_{12}a_{23}a_{32}a_{33}b_{12}$$
$$\quad + a_{13}{}^2 a_{22}{}^2 b_{33} - 2a_{13}{}^2 a_{22}a_{32}b_{23} + a_{13}{}^2 a_{32}{}^2 b_{22}$$
$$\quad - 2a_{13}a_{22}{}^2 a_{33}b_{13} + 2a_{13}a_{22}a_{23}a_{32}b_{13}$$
$$\quad + 2a_{13}a_{22}a_{32}a_{33}b_{12} - 2a_{13}a_{23}a_{32}{}^2 b_{12} + a_{22}{}^2 a_{33}{}^2 b_{11}$$
$$\quad - 2a_{22}a_{23}a_{32}a_{33}b_{11} + a_{23}{}^2 a_{32}{}^2 b_{11},$$

$$\Gamma_\varphi = a_{11}{}^2 b_{22} - 2a_{11}a_{21}b_{12} - 2a_{13}a_{21}b_{23} + 2a_{31}a_{13}b_{22}$$
$$\quad + a_{21}{}^2 b_{11} + 2a_{21}a_{23}b_{13} + a_{23}{}^2 b_{33}$$
$$\quad - 2a_{23}a_{31}b_{12} - 2a_{23}a_{33}b_{23} + a_{23}{}^2 b_{22},$$

$$\kappa_\varphi = a_{11}{}^2 a_{23}{}^2 b_{33} - 2a_{11}{}^2 a_{23}a_{33}b_{23} + a_{11}{}^2 a_{33}{}^2 b_{22}$$
$$\quad - 2a_{11}a_{13}a_{21}a_{23}b_{33} + 2a_{11}a_{13}a_{21}a_{33}b_{23}$$
$$\quad + 2a_{11}a_{13}a_{23}a_{31}b_{23} - 2a_{11}a_{13}a_{33}a_{31}b_{22}$$
$$\quad + 2a_{11}a_{21}a_{23}a_{33}b_{13} - 2a_{11}a_{21}a_{33}{}^2 b_{12}$$
$$\quad - 2a_{11}a_{23}{}^2 a_{31}b_{13} + 2a_{11}a_{23}a_{31}a_{33}b_{12} + a_{13}{}^2 a_{21}{}^2 b_{33}$$
$$\quad - 2a_{13}{}^2 a_{21}a_{31}b_{23} + a_{13}{}^2 a_{31}{}^2 b_{22}$$
$$\quad - 2a_{13}a_{21}{}^2 a_{33}b_{13} + 2a_{21}a_{13}a_{23}a_{31}b_{13}$$
$$\quad + 2a_{21}a_{13}a_{31}a_{33}b_{12} - 2a_{13}a_{23}a_{31}{}^2 b_{12}$$
$$\quad + a_{21}{}^2 a_{33}{}^2 b_{11} - 2a_{21}a_{23}a_{31}a_{33}b_{11} + a_{23}{}^2 a_{31}{}^2 b_{11}, \quad \text{(A14)}$$

$$
\begin{aligned}
\kappa_\psi =\ & a_{11}{}^2 a_{22}{}^2 b_{33} - 2 a_{11}{}^2 a_{22} a_{32} b_{23} + a_{11}{}^2 a_{32}{}^2 b_{22} \\
& - 2 a_{11} a_{12} a_{21} a_{22} b_{33} + 2 a_{11} a_{12} a_{21} a_{32} b_{23} \\
& + 2 a_{11} a_{21} a_{22} a_{32} b_{13} + 2 a_{11} a_{12} a_{21} a_{32} b_{23} \\
& + 2 a_{11} a_{12} a_{22} a_{31} b_{23} - 2 a_{11} a_{12} a_{31} a_{32} b_{22} \\
& - 2 a_{11} a_{21} a_{32}{}^2 b_{12} - 2 a_{11} a_{22}{}^2 a_{31} b_{13} \\
& + 2 a_{11} a_{22} a_{31} a_{32} b_{12} + a_{12}{}^2 a_{21}{}^2 b_{33} - 2 a_{12} a_{21}{}^2 a_{32} b_{13} \\
& - 2 a_{12}{}^2 a_{21} a_{31} b_{23} + a_{12}{}^2 a_{31}{}^2 b_{22} + 2 a_{21} a_{12} a_{22} a_{31} b_{13} \\
& + 2 a_{21} a_{12} a_{31} a_{32} b_{12} - 2 a_{12} a_{22} a_{31}{}^2 b_{12} \\
& - 2 a_{21} a_{22} a_{31} a_{32} b_{11} + a_{22}{}^2 a_{31}{}^2 b_{11} + a_{21}{}^2 a_{32}{}^2 b_{11}, \\[4pt]
\Gamma_\psi =\ & a_{11}{}^2 b_{33} - 2 a_{11} a_{31} b_{13} + 2 a_{12} a_{21} b_{33} \\
& - 2 a_{12} a_{31} b_{23} - 2 a_{21} a_{32} b_{13} + a_{22}{}^2 b_{33} \\
& - 2 a_{22} a_{32} b_{23} + a_{31}{}^2 b_{11} + 2 a_{31} a_{32} b_{12} + a_{32}{}^2 b_{22}. \quad \text{(A15)}
\end{aligned}
$$

5. Extinction probability

We label types of individuals as 1 (for insects) and 2 (EPF); their distributions of secondary infections of each type can be summarized by the two generating functions,[4] $G_i(s_1, s_2) = \sum_{k_1, k_2} s_1^{k_1} s_2^{k_2} P(X_{i1} = k_1, X_{i2} = k_2)$. Here, i is equal to 1 or 2 and X_{ij} is the random variable giving the number of secondary infections of the type j that arise from an individual of type i.

Assuming that the number of spores is very small, thus, $l = 1$; a spore only infects healthy insects according to a Poisson process with the intensity θ during their on life period $1/d_3$ in which it is exponentially distributed. In this case, the probability of generating function offspring produced by a single spore during an infectious period t is estimated as $G_2(s_1, s_2) = \sum_{k_1, k_2} s_1^{k_1} s_2^0 P(X_{21} = k_1, X_{22} = 0)$ since there is no transmission between spores. This is given as
$G_2(s_1) = \sum_{k_1} s_1^{k_1} P(X_{21} = k_1) = \sum_{k_1} s_1^{k_1} \int_0^{+\infty} d_3 e^{-d_3 t}$
$\left(\frac{(\theta t)^{k_1} e^{-\theta t}}{k_1!} \right) = d_3 \int_0^{+\infty} e^{-(d_3 + \theta) t} \left(\sum_{k_1 = 0}^{+\infty} \frac{(s_1 \theta t)^{k_1}}{k_1!} \right) dt = d_3$
$\int_0^{+\infty} e^{-(d_3 + \theta - s_1 \theta) t} dt$,

$$
G_2(s_1) = \frac{1}{1 + R_{12}(1 - s_1)}, \quad \text{(A16)}
$$

with $R_{12} = \frac{\theta}{d_3}$

In addition, an infected pest infects a susceptible and also give rise to new propagules according to a Poisson process at the intensity α_2 and b_2, respectively, within an infectious period $1/b_2$. Take a single infected insect in their exponential distributions, we have found the probability of generating function as $G_1(s_1, s_2) = \sum_{k_1, k_2} s_1^0 s_2^{k_2} P(X_{11} = 0, X_{12} = k_2)$; rearranging the latter, we obtained

$$
G_1(s_2) = \frac{1}{1 + R_{21}(1 - s_2)}, \quad \text{(A17)}
$$

where $R_{21} = \frac{b_2 + \alpha_2}{b_2}$.

In stochastic models, the terms R_{12} and R_{21} denote the distributions of secondary infections for EPF-to-insect and insect-to-EPF

transmission, respectively. The probability of extinction following introduction of a single spore is found by calculating the positive roof of equation $G_1(G_2(s_1)) = s_1$, which corresponds to

$$
s_1 = \frac{1}{1 + R_{21}\left(1 - \frac{1}{1 + R_{12}(1 - s_1)}\right)}, \quad \text{(A18)}
$$

which leads to $(1 - s_1)[1 + R_{12} - R_{12}(1 + R_{21})s_1] = 0$, which is a square polynomial in s_1; note that $s_1 = 1$ is always a solution. The other solutions are given by
$s_1 = \frac{1 + R_{12}}{R_{12}(1 + R_{21})}$.

It is shown that this solution is always positive and is smaller than 1 if and only if $R_{12}R_{21}$ is greater than 1. Estimation of the extinction probability following the introduction of a single spore required to find the smallest non-negative root[5] of $G_1(G_2(s_1)) = s_1$ after rearranging the above equation and solving, we obtained two positive solutions; $s_1 = 1$ is always a solution. The other solution is given by
par $s_1 = \frac{1 + R_{12}}{R_{12}(1 + R_{21})}$.

APPENDIX B: SPATIAL MODEL

1. Mean-field theory

The master equation is written in two contributions: the first part defined local mechanisms that correspond to the form given in a non-spatial case adding a subscript with a scaled Ω calling T_i^{loc} and the second takes migration into account T_{ij}^{mig}. The latter is given by

$$
\begin{aligned}
T_{ij}^{mig} =\ & \left(\varepsilon_{x_i}^{-1} \varepsilon_{x_j} - 1\right) T\left(n_i + 1, n_j - 1 \,|\, n_i, n_j\right) \\
& + \left(\varepsilon_{x_i} \varepsilon_{x_j}^{-1} - 1\right) T\left(n_i - 1, n_j + 1 \,|\, n_i, n_j\right) \\
& + \left(\varepsilon_{y_i}^{-1} \varepsilon_{y_j} - 1\right) T\left(m_i + 1, m_j - 1 \,|\, m_i, m_j\right) \\
& + \left(\varepsilon_{y_i} \varepsilon_{y_j}^{-1} - 1\right) T\left(m_i - 1, m_j + 1 \,|\, m_i, m_j\right) \\
& + \left(\varepsilon_{z_i}^{-1} \varepsilon_{z_j} - 1\right) T\left(l_i + 1, l_j - 1 \,|\, l_i, l_j\right) \\
& + \left(\varepsilon_{z_i} \varepsilon_{z_j}^{-1} - 1\right) T\left(l_i - 1, l_j + 1 \,|\, l_i, l_j\right). \quad \text{(B1)}
\end{aligned}
$$

To obtain its contribution on the master equation, we carry out the same procedures doing on the local contribution. Therefore, the operator expressions listed below are required for the other parameters change $u = (x, y, z)$ and $\zeta = (\xi, \eta, \vartheta)$,

$$
\varepsilon_{u_i}^{-1} \varepsilon_{u_j} - 1 = N^{-1/2}\left(\frac{\partial}{\partial \zeta_j} - \frac{\partial}{\partial \zeta_i}\right) + \frac{1}{2} N^{-1}\left(\frac{\partial}{\partial \zeta_i} - \frac{\partial}{\partial \zeta_j}\right)^2 + \cdots,
$$

$$
\varepsilon_{u_i} \varepsilon_{u_j}^{-1} - 1 = N^{-1/2}\left(\frac{\partial}{\partial \zeta_i} - \frac{\partial}{\partial \zeta_j}\right) + \frac{1}{2} N^{-1}\left(\frac{\partial}{\partial \zeta_i} - \frac{\partial}{\partial \zeta_j}\right)^2 + \cdots.
$$
$$\text{(B2)}$$

Replacing these expressions and transition rates in T_{ij}^{mig}, the following list gives contributions at the order N^0 and $N^{1/2}$

$$\left(\varepsilon_{x_i}^{-1}\varepsilon_{x_j}-1\right)T\left(n_i+1,n_j-1\,|n_i,n_j\right):$$

$$N^0:$$

$$-\phi_j\left(\frac{\partial}{\partial\xi_j}-\frac{\partial}{\partial\xi_i}\right)(\xi_i+\eta_i+\vartheta_i),$$

$$(1-\phi_i-\varphi_i-\psi_i)\left(\frac{\partial}{\partial\xi_j}-\frac{\partial}{\partial\xi_i}\right)\xi_j,$$

$$\frac{1}{2}\phi_j\left(1-\phi_i-\varphi_i-\psi_i\right)\left(\frac{\partial}{\partial\xi_j}-\frac{\partial}{\partial\xi_i}\right)^2, \tag{B3}$$

$$N^{1/2}:$$

$$\phi_j\left(1-\phi_i-\varphi_i-\psi_i\right)\left(\frac{\partial}{\partial\xi_j}-\frac{\partial}{\partial\xi_i}\right). \tag{B4}$$

The contributions of the terms are $\left(\varepsilon_{x_i}\varepsilon_{x_j}^{-1}-1\right)T\left(n_i-1,n_j+1\,|n_i,n_j\right)$ obtained by interchanging i and j. Therefore, adding the terms in order $N^{1/2}$ together and identified $\partial\Pi/\partial\xi_i$ for each i with the corresponding term on the left-hand side of the master equation lead to $-\frac{2\mu_1}{z\Omega}\left(\sum_j\left(\phi_j-\phi_i\right)+\sum_j\left(\phi_i\varphi_j-\phi_j\varphi_i\right)+\sum_j\left(\phi_i\psi_j-\phi_j\psi_i\right)\right)$.

Using the discrete Laplacian operator $\Delta f_i=(2/z)\sum_{j\in i}\left(f_j-f_i\right)$, the following equation is obtained:

$$-\frac{\mu_1}{\Omega}\left(\Delta\phi_i+\phi_i\Delta\varphi_i-\varphi_i\Delta\phi_i+\phi_i\Delta\psi_i-\psi_i\Delta\phi_i\right). \tag{B5}$$

A similar analysis may be carried out for the terms $\left(\varepsilon_{y_i}^{-1}\varepsilon_{y_j}-1\right)$ $T\left(m_i+1,m_j-1\,|m_i,m_j\right)$, $\left(\varepsilon_{y_i}\varepsilon_{y_j}^{-1}-1\right)T\left(m_i-1,m_j+1\,|m_i,m_j\right)$, and $\left(\varepsilon_{z_i}^{-1}\varepsilon_{z_j}-1\right)T\left(l_i+1,l_j-1\,|l_i,l_j\right)$, $\left(\varepsilon_{z_i}\varepsilon_{z_j}^{-1}-1\right)$ $T\left(l_i-1,l_j+1\,|l_i,l_j\right)$ to obtain

$$-\frac{\mu_2}{\Omega}\left(\Delta\varphi_i+\varphi_i\Delta\phi_i-\phi_i\Delta\varphi_i+\varphi_i\Delta\psi_i-\psi_i\Delta\varphi_i\right) \tag{B6}$$

and

$$-\frac{\mu_3}{\Omega}\left(\Delta\psi_i+\psi_i\Delta\varphi_i-\varphi_i\Delta\psi_i+\psi_i\Delta\phi_i-\phi_i\Delta\psi_i\right), \tag{B7}$$

respectively. Identifying Eqs. (B5)–(B7) to the left-hand side of the master equation leads to deterministic equations defined by Eq. (10).

The stochastic contributions of the terms $\left(\varepsilon_{x_i}^{-1}\varepsilon_{x_j}-1\right)T$ $\left(n_i+1,n_j-1\,|n_i,n_j\right)$ are given by the two first terms of N^0,

$$\frac{\mu_1}{z\Omega}\sum_{i,j}\left(\frac{\partial}{\partial\xi_j}-\frac{\partial}{\partial\xi_i}\right)\left(-\phi_j\left(\xi_i+\eta_i+\vartheta_i\right)\right.$$

$$\left.+\left(1-\phi_i-\varphi_i-\psi_i\right)\xi_j\right). \tag{B8}$$

Adding with the contributions from $\left(\varepsilon_{x_i}\varepsilon_{x_j}^{-1}-1\right)T$ $\left(n_i-1,n_j+1\,|n_i,n_j\right)$ leads to

$$-\frac{\mu_1}{\Omega}\sum_i\frac{\partial}{\partial\xi_i}\left(D_{i,11}\xi_i+D_{i,12}\eta_i+D_{i,13}\vartheta_i\right)\Pi, \tag{B9}$$

where

$$D_{i,11}=\Delta-\left(\varphi_i+\psi_i\right)\Delta+\left(\Delta\left(\varphi_i+\psi_i\right)\right),$$
$$D_{i,12}=D_{i,13}=\phi_i\Delta-\left(\Delta\phi_i\right). \tag{B10}$$

To obtain the stochastic contributions given from the terms concerning the migration of infected pests and spores just interchanging,

For infected pest: $\mu_1\to\mu_2$, $\phi_i\to\varphi_i$, and $\xi_i\to\eta_i$
For spore: $\mu_1\to\mu_3$, $\phi_i\to\psi_i$, and $\xi_i\to\vartheta_i$.
Therefore, this gives, respectively,

$$-\frac{\mu_2}{\Omega}\sum_i\frac{\partial}{\partial\eta_i}\left(D_{i,21}\xi_i+D_{i,22}\eta_i+D_{i,23}\vartheta_i\right)\Pi \tag{B11}$$

and

$$-\frac{\mu_3}{\Omega}\sum_i\frac{\partial}{\partial\vartheta_i}\left(D_{i,31}\xi_i+D_{i,32}\eta_i+D_{i,33}\vartheta_i\right)\Pi, \tag{B12}$$

with

$$D_{i,21}=D_{i,23}=\varphi_i\Delta-\left(\Delta\varphi_i\right),$$
$$D_{i,22}=\Delta-\left(\phi_i+\psi_i\right)\Delta+\left(\Delta\left(\phi_i+\psi_i\right)\right),$$
$$D_{i,33}=\Delta-\left(\varphi_i+\phi_i\right)\Delta+\left(\Delta\left(\varphi_i+\phi_i\right)\right),$$
$$D_{i,31}=D_{i,32}=\psi_i\Delta-\left(\Delta\psi_i\right). \tag{B13}$$

These terms are the diffusion contribution of the first terms of Fokker–Planck equations such that it can be defined by

$$\frac{\partial\Pi}{\partial t}=-\sum_{i=1}^{\Omega}\frac{\partial\left(A_i\left[\zeta\left(t\right)\right]\Pi\right)}{\partial\zeta_i}+\frac{1}{2}\sum_{i,j}\frac{\partial^2\left[B_{ij}\left(t\right)\Pi\right]}{\partial\zeta_i\partial\zeta_j}, \tag{B14}$$

where fluctuation variables $\zeta_i=\left(\xi_i,\eta_i,\vartheta_i\right)$ are introduced. The function $A_i\left(\zeta\right)$ is given by

$$A_{i,1}=\alpha_{i,11}\xi_i+\alpha_{i,12}\eta_i+\alpha_{i,13}\vartheta_i,$$
$$A_{i,2}=\alpha_{i,21}\xi_i+\alpha_{i,22}\eta_i+\alpha_{i,23}\vartheta_i, \tag{B15}$$
$$A_{i,3}=\alpha_{i,31}\xi_i+\alpha_{i,32}\eta_i+\alpha_{i,33}\vartheta_i,$$

where $\alpha_{i,jk}$ $\left(j,k=1,2,3\right)$ are exactly the coefficients found adding element a_{ij} given in Eq. (A9) of Appendix A with subscript i with diffusion terms defined by Eqs. (B10) and (B13) at an equilibrium state and can also be deduced from stability analysis of the spatial equation given by Eq. (10) in the main paper. The matrix B_{ij}

is defined as follows:

$$
\begin{aligned}
B_{ij,11} &= \big(2I_1\phi^s\varphi^s + 2I_2\phi^s\psi^s + d_1\phi^s \\
&\quad + 2b_1\phi^s\,(1-\phi^s-\varphi^s-\psi^s) \\
&\quad + 4\mu_1\phi^s\,(1-\phi^s-\varphi^s-\psi^s)\big)\,\delta_{ij} \\
&\quad - \frac{4\mu_1}{z}\phi^s\,(1-\phi^s-\varphi^s-\psi^s)\,J_{\langle ij\rangle},
\end{aligned}
$$

$$
B_{ij,23} = B_{ij,32} = -2b_2\varphi^s,
$$

$$
\begin{aligned}
B_{ij,22} &= \big(2I_1\phi^s\varphi^s + 2I_2\phi^s\psi^s + 2b_2\varphi^s \\
&\quad + 4\mu_1\varphi^s\,(1-\phi^s-\varphi^s-\psi^s)\big)\,\delta_{ij} \\
&\quad - \frac{4\mu_2}{z}\varphi^s\,(1-\phi^s-\varphi^s-\psi^s)\,J_{\langle ij\rangle},
\end{aligned}
$$

$$
B_{ij,13} = B_{ij,31} = 0, \tag{B16}
$$

$$
B_{ij,12} = B_{ij,21} = -4I_1\phi^s\varphi^s - 4I_2\phi^s\psi^s,
$$

$$
\begin{aligned}
B_{ij,33} &= \big(2b_2\varphi^s + d_3\psi^s + 4\mu_1\phi^s\,(1-\phi^s-\varphi^s-\psi^s)\big)\,\delta_{ij} \\
&\quad - \frac{4\mu_1}{z}\phi^s\,(1-\phi^s-\varphi^s-\psi^s)\,J_{\langle ij\rangle}.
\end{aligned}
$$

This term is found by using the elements defined in equations [Eq. (A9)] and the third terms of Eq. (B3). See Ref. 23 for more details and background.

2. Stability and bifurcation analysis of a heterogeneous system

To study the stability of the heterogeneous steady state, we consider a small perturbation of the initial homogeneous stationary state in the formula: $\phi_j = u_j + \phi^s, \varphi_i = v_i + \varphi^s, \psi_i = w_i + \psi^s$. Equation (10) can be rewritten in a unified form as

$$
\dot{\mathbf{u}}_j = \mathbf{A}\mathbf{u}_j, \tag{B17}
$$

with $\mathbf{u}_j = (u_j, v_j, w_j)^T$ and $\mathbf{A}$ being a square 3×3 matrix of elements $\alpha_{q,ij}\,(i,j=1,2,3)$ (defining the linearized matrix). By considering the solutions, we form $\mathbf{u}_j(\tau) \propto \exp(\lambda\tau + ia\mathbf{q.j})$, with a defined a lattice, where $\mathbf{q}$ corresponds to the vector of wave numbers and λ denoted the frequency at which the perturbation occurs. These two parameters defined the conditions

$$
\det(\lambda\mathbf{I} - \mathbf{A}) = 0. \tag{B18}
$$

$\mathbf{I}$ is an identity 3×3 matrix, and $\mathbf{A}$ is defined by the elements

$$
\begin{aligned}
&\alpha_{q,11} = a_{11} + \mu_1\,(1-\varphi^s-\psi^s)\,\Delta_q,\quad \alpha_{q,12} = a_{12} + \mu_1\phi^s\Delta_q, \\
&\alpha_{q,13} = a_{13} + \mu_1\phi^s\Delta_q,\quad \alpha_{q,21} = a_{21} + \mu_2\varphi^s\Delta_q, \\
&\alpha_{q,22} = a_{22} + \mu_2\,(1-\phi^s-\psi^s)\,\Delta_q,\quad \alpha_{q,23} = a_{23} + \mu_1\varphi^s\Delta_q, \\
&\alpha_{q,31} = a_{31} + \mu_3\psi^s\Delta_q,\quad \alpha_{q,32} = a_{32} + \mu_3\psi^s\Delta_q, \\
&\alpha_{q,33} = a_{33} + \mu_3\,(1-\phi^s-\varphi^s)\,\Delta_q,
\end{aligned} \tag{B19}
$$

where

$$
\Delta_k = \frac{2}{d}\sum_{\gamma=1}^{d}\big[\cos\,(k_\gamma a) - 1\big] \tag{B20}
$$

corresponds to the discrete Laplacian for a d-dimensional hyper-cubic lattice; see Ref. 23. In the continuum limit $\Delta_q \approx -q^2$, therefore, by using the continuum mean-field equation, the same results are obtained. Instability could occur in this system if one of the eigenvalues verify the conditions $Re(\lambda\,(q)) > 0$. More clearly,

- The species free equilibrium point E^0: Eq. (B20) has three solutions $\lambda_1 = -q^2k + r$, $\lambda_2 = -q^2k - d_3$, and $\lambda_3 = -q^2k - b_2$. The system is unstable for $q^2k < r$ and becomes stable when the wave number becomes sufficiently high.
- The infected insects and conidia free equilibrium E^s: the linearized matrix A is given by

$$
\mathrm{A}_{E^s} = \begin{pmatrix} a_{11} & a_{12} & a_{13} \\ 0 & a_{22} & a_{23} \\ 0 & a_{32} & a_{33} \end{pmatrix}, \tag{B21}
$$

with $a_{11} = -q^2\mu_1 - r, a_{12} = -k\,(q^2\mu_1 + \alpha_1), a_{13} = -k\,(q^2\mu_1 + \beta_1), a_{32} = b_2, a_{22} = \alpha_2 k - b_2 - \mu_2(1-k)q^2, a_{23} = \theta k, a_{33} = -d_3 - \mu_3(1-k)q^2$. According to Routh–Hurwitz criteria, this point is stable if $-(a_{11} + a_{22} + a_{33}) > 0, -a_{11}a_{22}a_{33} + a_{11}a_{23}a_{32} > 0, a_{11}a_{22} + a_{11}a_{33} + a_{33}a_{22} - a_{32}a_{23} + (-a_{11}a_{22}a_{33} + a_{11}a_{23}a_{32})\,/a_{11} + a_{22} + a_{33} > 0$, corresponding to the colored zone of Fig. 4(d).
- The epidemic equilibrium: the eigenvalues are very large and, therefore, are not reported here. However, the analysis has been numerically computed. However, Eq. (B20) is a cubic polynomial with coefficients 1, $A\,(q)$, $B\,(q)$, and $C\,(q)$, respectively. The system is stable if and only if $A\,(q) > 0, C\,(q) > 0$, and $A\,(q)\,B\,(q) - C\,(q) > 0$. These conditions are satisfied in the colored zone of Fig. 4(c).

The bifurcation analysis of these steady states is well described by the eigenvalues obtained from the dispersion relation given by Eq. (B20). The sign of the real and imaginary parts of the dominant eigenvalue (function of wavenumber q) derived from the underlying equation defined the dynamics of the system. The positive $Re\,(\lambda\,(q))$ defined the unstable dynamics, whereas the imaginary part gives the frequency of oscillations.

DATA AVAILABILITY

Data sharing is not applicable to this article as no new data were created or analyzed in this study.

REFERENCES

[1] A. Hajek, Ecol. Entomol. **25**, 91 (2004).
[2] J. Bale, J. van Lenteren, and F. Bigler, Trans. R. Soc. **363**, 761 (2008).
[3] B. A. Hawkins and H. V. Cornell, *Theoretical Approaches to Biological Control* (Cambridge University Press, 2008).
[4] O. Ovaskainen and B. Meerson, Trends Ecol. Evol. **25**, 643 (2010).
[5] S. A. Pedro, S. Abelman, and H. E. Tonnang, PLoS Negl. Trop. Dis. **10**, e0005167 (2016).
[6] J. Realpe-Gomez, M. Baudena, T. Galla, A. J. McKane, and M. Rietkerk, Ecol. Complexity **15**, 97 (2013).
[7] R. Marguta and A. Parisi, J. R. Soc. Interface **12**, 20141317 (2015).
[8] F. Parise, J. Lygeros, and J. Ruess, Front. Environ. Sci. **3**, 42 (2015).
[9] J. Baveco and R. Lingeman, Ecol. Modell. **61**, 267 (1992).
[10] J. Babin-Fenske and M. Anand, Ecol. Modell. **222**, 2561 (2011).

[11]F. Vinatier, M. Gosme, and M. Valantin-Morison, Landsc. Ecol. **27**, 1421 (2012).

[12]C. Briggs and H. Godfray, Am. Nat. **145**, 855 (1995).

[13]M. A. Gilchrist, D. L. Sulsky, and A. Pringle, Evolution **60**, 970 (2006).

[14]Z. Rapti and C. Cáceres, Bull. Math. Biol. **78**, 235 (2016).

[15]H. E. Roy, F. E. Vega, D. Chandler, M. S. Goettel, J. Pell, E. Wajnberg *et al.*, *The Ecology of Fungal Entomopathogens* (Springer, 2010).

[16]P. Shah and J. Pell, Appl. Microbiol. Biotechnol. **61**, 413 (2003).

[17]D. W. Long, E. Groden, F. A. Drummond *et al.*, Agric. For. Entomol. **2**, 11 (2000).

[18]G. Gurr and S. Wratten, *Biological Control: Measures of Success* (Kluwer Academic Publishers, Dordrecht, 2000), ISBN 978-0-412-84280-1.

[19]A. J. Black and A. J. McKane, Trends Ecol. Evol. **27**, 337 (2012).

[20]J. Dawes and M. Souza, J. Theor. Biol. **327**, 11 (2013).

[21]A. J. McKane and T. J. Newman, Phys. Rev. Lett. **94**, 218102 (2005).

[22]A. J. McKane and T. J. Newman, Phys. Rev. E **70**, 041902 (2004).

[23]C. A. Lugo and A. J. McKane, Phys. Rev. E **78**, 051911 (2008).

[24]D. Alonso, A. J. McKane, and M. Pascual, J. R. Soc., Interface **4**, 575 (2007).

[25]A. L. Lloyd, J. Zhang, and A. M. Root, J. R. Soc. Interface **4**, 851 (2007).

[26]M. Asslani, F. Di Patti, and D. Fanelli, Phys. Rev. E **86**, 046105 (2012).

[27]T. Biancalani, T. Galla, and A. J. McKane, Phys. Rev. E **84**, 026201 (2011).

[28]S. Djilali and S. Bentout, Acta Appl. Math. **169**, 125–143 (2020).

[29]S. Djilali, B. Ghanbari, S. Bentout, and A. Mezouaghi, Chaos Solitons Fractals **138**, 109954 (2020).

[30]F. Souna, A. Lakmeche, and S. Djilali, J. Appl. Math. Comput. **64**, 665 (2020).

[31]B. Ghanbari and S. Djilali, Chaos Solitons Fractals **138**, 109960 (2020).

[32]F. Souna, A. Lakmeche, and S. Djilali, Chaos Solitons Fractals **140**, 110180 (2020).

[33]S. Djilali, Int. J. Biomath. **13**, 2050030 (2020).

[34]S. Djilali, Math. Methods Appl. Sci. **43**, 2233 (2020).

[35]F. Souna, S. Djilali, and F. Charif, Math. Model. Nat. Phenom. **15**, 23 (2020).

[36]C. Tian and L. Zhang, Comput. Math. Appl. **66**, 2139 (2013).

[37]M. Baurmann, T. Gross, and U. Feudel, J. Theor. Biol. **245**, 220 (2007).

[38]J. Baverstock, H. E. Roy, and J. K. Pell, in *The Ecology of Fungal Entomopathogens* (Springer, 2009), pp. 89–102.

[39]H. Hesketh, H. Roy, J. Eilenberg, J. Pell, and R. Hails, BioControl **55**, 55 (2010).

[40]A. Fenton, R. Norman, J. P. Fairbairn, and P. J. Hudson, J. Appl. Ecol. **37**, 309 (2000).

[41]R. M. Weseloh, Biol. Control **29**, 138 (2004).

[42]D. T. Gillespie, J. Phys. Chem. **81**, 2340 (1977).

[43]R. P. Boland, T. Galla, and A. J. McKane, Phys. Rev. E **79**, 051131 (2009).

[44]A. A. Lashari, K. Hattaf, G. Zaman, and X.-Z. Li, Appl. Math. Inf. Sci. **7**, 301 (2013).

[45]S. Marino, I. B. Hogue, C. J. Ray, and D. E. Kirschner, J. Theor. Biol. **254**, 178 (2008).

[46]A. J. Black and A. J. McKane, J. Theor. Biol. **267**, 85 (2010).

[47]T. Reichenbach, M. Mobilia, and E. Frey, Phys. Rev. E **74**, 051907 (2006).

[48]T. Britton, T. House, A. L. Lloyd, D. Mollison, S. Riley, and P. Trapman, Epidemics **10**, 54 (2015).

[49]M. Cross and H. Greenside, *Pattern Formation and Dynamics in Nonequilibrium Systems* (Cambridge University Press, 2009).

[50]J. Roughgarden, Am. Nat. **109**, 713 (1975).

[51]A. M. Lee, B.-E. Sæther, and S. Engen, Am. Nat. **177**, 301 (2011).

[52]P. Gramlich, S. J. Plitzko, L. Rudolf, B. Drossel, and T. Gross, J. Theor. Biol. **398**, 150 (2016).

[53]C. Pao, J. Math. Anal. Appl. **281**, 186 (2003).

[54]S. Fasani and S. Rinaldi, Ecol. Model. **222**, 3449 (2011).

[55]H. Caswell and M. G. Neubert, J. Plankton Res. **20**, 1837 (1998).

[56]J. Antonovics, A. McKane, and T. Newman, Am. Nat. **167**, 16 (2006).

[57]G. Dwyer, Am. Nat. **143**, 533 (1994).

[58]G. Dwyer, J. Dushoff, and A. E. Hajek, Am. Nat. **152**, 485 (1998).

[59]F. Gourbiere, S. Gourbiere, A. Van Maanen, G. Vallet, and P. Auger, Mycol. Res. **103**, 353 (1999).

[60]G. Dwyer, J. Dushoff, J. S. Elkinton, and S. A. Levin, Am. Nat. **156**, 105 (2000).

[61]B. D. Elderd, B. J. Rehill, K. J. Haynes, and G. Dwyer, Proc. Natl. Acad. Sci. U.S.A. **110**, 14978 (2013).

[62]B. D. Elderd, J. Dushoff, and G. Dwyer, Am. Nat. **172**, 829 (2008).

[63]J. R. Reilly and B. D. Elderd, J. Appl. Ecol. **51**, 90 (2014).

[64]G. Knudsen and D. Schotzko, Biol. Control **16**, 318 (1999).

[65]N. V. Meyling, K. Thorup-Kristensen, and J. Eilenberg, Biol. Control **59**, 180 (2011).

[66]B. S. Djouda, F. Moukam Kakmeni, P. Guemkam Ghomsi, F. T. Ndjomatchoua, C. Tchawoua, and H. E. Tonnang, Chaos **29**, 053134 (2019).

[67]K. Wang, M. L. Steyn-Ross, D. A. Steyn-Ross, M. T. Wilson, J. W. Sleigh, and Y. Shiraishi, BMC Syst. Biol. **8**, 45 (2014).

[68]J. Li, D. Blakeley *et al.*, Comput. Math. Methods Med. **2011**, 527610 (2011).

[69]F. Van den Bosch, N. McRoberts, F. Van den Berg, and L. Madden, Phytopathology **98**, 239 (2008).

[70]P. Van den Driessche and J. Watmough, Math. Biosci. **180**, 29 (2002).